Bedload sediment transport regimes of urban gravel-bed rivers under different management scenarios

by

Elli Papangelakis

A thesis
presented to the University of Waterloo
in fulfillment of the
thesis requirement for the degree of
Doctor of Philosophy
in
Civil Engineering - Water

Waterloo, Ontario, Canada, 2019

©Elli Papangelakis 2019

Examining Committee Membership

The following served on the Examining Committee for this thesis. The decision of the Examining Committee is by a majority vote.

External Examiner	Dr. Peter Downs
Supervisor	Dr. Bruce MacVicar Associate Professor
Internal Member	Dr. William K. Annable Associate Professor
Internal Member	Dr. John Quilty Assistant Professor
Internal-external Member	Dr. Mike Stone Professor

Author's Declaration

This thesis consists of material all of which I authored or co-authored: see Statement of Contributions included in the thesis. This is a true copy of the thesis, including any required final revisions, as accepted by my examiners.

I understand that my thesis may be made electronically available to the public.

Statement of Contributions

Important contributions were made towards this thesis by my supervisor Dr. Bruce MacVicar, and by Dr. Peter Ashmore (University of Western Ontario) through their inputs towards the overall study design and by providing guidance on analysis and interpretation of results.

Study site selection and set-up for data presented in Chapters 3-5 were led by Julian Krick, including the installation of gauges and tracer seeding.

Chapter 4 was prepared in collaboration with Asal Montakhab. Asal developed the MATLAB code to calculate the flow metrics from raw water level data.

Tracer stones in the 2013 dataset presented in Chapter 5 (Wave 1) were created, seeded, and recovered (up until 2015) by a team led by Margot Chapuis.

Chapter 6 was prepared in collaboration with Chris Muirhead and Adam Schneider. Chris contributed to the development of the second Wobblestone prototype and created the plastic injection mould and assembly procedure. Adam contributed to early lab tests to finalize synthetic tracer material mixture and the assembly procedure of the first prototype.

I certify, with the above qualifications, that this thesis and the research to which it refers is the product of my own work.

Abstract

Watershed urbanization profoundly alters the hydrologic characteristics of urban rivers compared to their rural counterparts. This change in hydrologic conditions in combination with alterations to the sediment supply regime in urban watersheds leads to adjustments to channel form and the widespread degradation of urban rivers. Urban river management increasingly attempts to balance the societal needs of flood and erosion control, while simultaneously improving the ecological health or waterways. Two common types of river management include stormwater management (SWM), which focuses on the attenuation of urban floods, and in-stream restoration, which attempts to reconstruct stable and ecologically favourable channels. However, current urban river management designs lack consideration of the key process responsible for channel stability and habitat availability: bedload sediment transport. Two reasons for this shortcoming are the lack of bedload sediment data in urban watersheds and the consequent gap in understanding of the bedload transport dynamics of urban rivers. Consequently, the degradation of urban rivers persists.

This project investigates bedload transport dynamics in urban rivers with different management scenarios to focus on four themes: (1) how urbanization affects bedload transport dynamics and its relationship to channel morphology, (2) how to best predict bedload transport dynamics in urban rivers, (3) how current urban river management strategies change the transport dynamics of rivers, and (4) how to improve bedload sediment monitoring technology. This project focuses on the grain-scale bedload transport dynamics of coarse material because it links to the morphodynamics and ecological processes of channels, it provides insights on the exact controls and spatial variability of bedload transport, and the responses to individual flood events can be directly measured. The overarching goal of this study is to contribute to improved urban river management strategies that focus on adaptive management and interdisciplinary approaches.

Bedload sediment transport was monitored using RFID tracer stones in three streams with different hydrologic settings: rural, urban with no SWM, and urban with SWM. High-resolution water level data confirmed the hydrologic differences expected from the three watershed conditions, as well as channel enlargement characteristic of urban rivers. Results demonstrate that the morphologic differences between the study streams can be linked to changes in the grain-scale bedload transport dynamics of the streams. Bedload transport is accelerated in the urban stream due to an increase in the frequency of bedload mobilization, particularly of coarse sediment sizes. In contrast, SWM has

decreased the bedload transport to an immobile and armoured state indicative of a competence-limit transport regime. Results are used to make recommendations for improved urban river management.

Results from the bedload tracking were used to build predictive models of tracer displacements. A new variable that captures both the mobility and travel length of bed particles is introduced. Several flow metrics developed in the literature in rural and laboratory settings are calculated, and their ability to predict tracer displacements in the three streams is tested. Scaling tracer travel lengths by mean channel width collapses the data into a single, strong relationship with cumulative energy expenditure, providing a single model that can be used across systems with different watershed conditions.

To assess the impact of an in-stream riffle-pool channel reconstruction on bedload sediment dynamics, bedload transport and morphologic change was monitored in adjacent unrestored and restored reaches of an urban channel. Results reveal that the restored reach is stable and self-maintaining, mirroring bedform maintenance processes in natural riffle-pool streams. However, the construction is more successful at slowing down the transport of coarse sediment more than fine sediment, leading to a coarse sediment discontinuity that may be contributing to accelerated channel adjustment beyond the limits of the constructed riffle-pool sequences. This project highlights the importance of considering the entire channel corridor when designing and monitoring restoration projects.

A large limitation of bedload sediment tracking technology is the inability to determine the vertical position of tracers, which hinders the ability to study vertical mixing and translate tracer data into bedload transport rates. A new Radio Frequency Identification (RFID) bedload tracer stone is presented, along with results of laboratory performance tests. This new bedload tracer improves upon existing bedload sediment monitoring technology by providing the ability to measure the burial depth of tracers without disturbing the bed.

An important contribution of this study is the extensive dataset of bedload transport collected in urban rivers. This study attempts to move away from descriptive differences in the characteristics of urban rivers compared to rural streams, and towards a process-level understanding of the anthropogenic effects on river systems. Grain-scale bedload transport theory, developed in rural and laboratory settings, is applied to urban settings to gain insights into the effects of urbanization and common river management strategies on the geomorphic processes of urban rivers. Recommendations for improved urban river management are developed from the results of this thesis.

Acknowledgements

First and foremost, I would like to thank my supervisor Dr. Bruce MacVicar for his guidance and support over the past four years. I would also like to thank Dr. Peter Ashmore for providing valuable insights and feedback during all stages of this project. This thesis would not have been possible without them.

I would like to thank the community at the University of Waterloo and the Department of Civil and Environmental Engineering for providing resources needed to complete this thesis. NSERC provided financial support to make this project possible.

I would like to acknowledge the individuals who worked on selecting, setting up, and seeding the field sites used in this project long before my arrival to Waterloo, particularly Vernon Bevan and Margot Chapuis.

Terry Ridgeway and Julian Krick deserve special recognition, as their help with site instrumentation, fixing equipment, and teaching me how to survey were vital to the success of this thesis.

The data collection for this project was long and painstaking, requiring early mornings, suffering through GTA traffic, and many hours in less-than-favourable weather and/or bug conditions. I want to thank the long list of graduate students and co-op students who helped with chasing stones and frustrating surveys: Thomas Raso, Patricia Huynh, Aryn Cain, Chris Muirhead, Kayla Goguen, Asal Montakhab, Matthew Iannetta, Adam Schneider, Allen Chen, Kayleanna Giesinger, Lukas Mueller, Sadegh Arshari, and Jackie Wintermeyer. Thank you for helping turn those long days into amazing memories.

To my family and friends who volunteered their time to help me in the field, your support on those desperate days is appreciated. Thank you to my brothers, Panos and George Papangelakis, Sarah Peirce, and Krystalia Hatzinakos.

I would not have been able to complete this degree without the encouragement of my family and friends. Thank you for challenging me to reach high and for your unconditional support at every step. I am grateful for every coffee break, pot-luck, hike, and overnight-stay.

Finally, to Adam: your patience and unwavering belief in me have been paramount to my success – thank you.

Table of Contents

List of Figures

List of Tables

List of Abbreviations

Abbreviation	Description
AIC	Akaike information criterion
CDI	cumulative dimensionless impulse (-)
CEDSS	cumulative excess dimensionless shear stress (-)
CEQ	cumulative excess discharge (m^3)
CESP	cumulative excess stream power (N/m)
CESS	cumulative excess stream power (Pa·s)
CEV	cumulative excess velocity (m)
CI	cumulative impulse (m)
DA	drainage area
DEM	digital elevation model
DOD	DEM of difference
FDX	full-duplex
GPS	global positioning system
HDX	half-duplex
LID	low impact development
PIT	passive integrated transponder
RFID	radio frequency identification
RSE	residual standard error
SE	standard error
SWM	stormwater management
TIN	triangular interpolation network
TE	time of exceedance (h)
TOB	top of bank
VIF	variance inflation factor
WI	work index (J/m^2)

List of Symbols

Symbol	Description
A	cross-sectional area (m^2)
B	mean channel bed width (m)
CI_{95}	95% confidence interval
D_i	b-axis diameter of the i^{th} percentile particle size (m)
E_i	i^{th} mobilizing event in recovery period
F_m	fraction of all tracers that moved over the entire duration of the study
F_{mi}	fraction of tracers in size class *i* that moved over the entire duration of the study
f_m	fraction of all tracers that moved over a given recovery period
f_{mi}	fraction of tracers in size class *i* that moved over a given recovery period
g	gravitational acceleration (m/s^2)
h	mean water depth (m)
h_{ci}	critical flow depth to mobilize size class *i* (m)
k_s'	roughness parameter (-)
L	geometric mean travel length of all tracers (m)
L_i	geometric mean travel length of tracers in size class *i* (m)
$\tilde{L}$	weighted mean travel length of all tracers (m)
$\tilde{L}_i$	weighted mean travel length of tracers in size class *i* (m)
n	total number of tracers that moved since previous recovery
m_i	total number of tracers in size class *i* that moved since previous recovery
n	number of tracers found in both given recovery and previous recovery
n_i	number of tracers in size class *i* found in both given recovery and previous recovery
P	wetted perimeter (m)
P_{ex}	probability of exceedance
Q	flow discharge (m^3/s)
Q_b	bedload transport rate (m^3)
Q_{ci}	critical discharge to mobilize size class *i* (m^3/s)
Q_p	peak discharge (m^3/s)
q_b	specific bedload transport rate (m^2)
R_h	hydraulic radius (m)

r	Pearson correlation coefficient
S	mean bed slope (-)
t_s	start time of mobilizing event
t_e	end time of mobilizing event
u_*	shear velocity (m/s)
u_{*ci}	critical shear velocity to mobilize size class *i* (m/s)
V	mean flow velocity (m/s)
V_{ci}	critical flow velocity to mobilize size class *i* (m/s)
λ	tracer travel length (m)
ρ_w	mass density of water (kg/m^3)
ρ_s	mass density of tracer stones (kg/m^3)
α	confidence interval
σ	standard deviation
τ	shear stress (Pa)
τ_{ci}	critical shear stress to mobilize size class *i* (Pa)
τ_{ci}^*	dimensionless critical shear stress to mobilize size class *i* (-)
τ_p^*	peak dimensionless critical shear stress (-)
ϕ	phi class (= $\log_2 D_i$)
ψ	psi class (= – ϕ)
Ω	cumulative excess energy expenditure (N)
ω	specific stream power (N/m)
ω_{ci}	critical stream power to mobilize the i^{th} size class (N/m)
ω_p	peak stream power (N/m)
ω_p^*	peak dimensionless stream power (-)

Ποταμοῖσι τοῖσιν αὐτοῖσιν ἐμβαίνουσιν, ἕτερα καὶ ἕτερα ὕδατα ἐπιρρεῖ.

On those who enter the same rivers, ever different waters flow.

– *Heraclitus (535–475 BC)*

Chapter 1
Introduction

Urbanization is a global trend, with an increasing proportion of the world population living in urban areas (Chin, 2006; Chin et al., 2013; Poff et al., 2006). The process of converting natural or agricultural land to urban use involves substantial modifications to the landscape that in turn alter biophysical processes. Fluvial systems are particularly vulnerable to land-use changes due to their position within the landscape (Walsh et al., 2005), and river systems are more drastically affected by urbanization than any other human activity (Chin et al., 2013). Urbanizing watersheds experience changes such as the replacement of natural land cover with impermeable surfaces, direct modifications to rivers (e.g. channelization and straightening), and the introduction of drainage networks and flood control infrastructure (Chin et al., 2013). These modifications alter the hydrologic, geomorphologic, chemical, and ecological processes of rivers (Ladson et al., 2006), resulting in rapid shifts in channel structure, changes in flood characteristics, and deterioration of river ecology. The degradation of urban river systems is so ubiquitous that consistently observed responses to urbanization have been collectively named the 'urban stream syndrome' (Walsh et al., 2005).

Urban river management increasingly focuses on treating symptoms of the urban stream syndrome (Bernhardt et al., 2007). The goals of urban river management are twofold: firstly, management projects aim to address the needs of urban development, such as effective stormwater management and erosion control. Second, projects treating degrading urban rivers attempt to shift the ecological conditions of the streams to more closely match those of un-urbanized streams (Palmer and Bernhardt, 2006; Walsh et al., 2005). Management strategies are focused either on stressors at the local stream scale, such as constructing artificial habitat structures or introducing woody debris, or through changes in the watershed-scale hydrology, such as stormwater retention ponds (Ladson et al., 2006). However, although the science of river systems from both a physical and ecological standpoint has advanced significantly, tools to successfully translate the knowledge to strategies that address management goals remain inadequate (MacVicar et al., 2015; Wohl et al., 2015b; Wilcock, 2012). Consequently, the ecological deterioration of urban rivers persists (Violin et al., 2011).

Our understanding of how urbanization and current river management strategies affect urban streams remains largely through studies aimed at *effects* rather than *processes.* A substantial body of literature focuses on changes in river dimensions or ecological markers pre- and post-watershed

urbanization or channel modification (Chin, 2006; Gregory et al., 1992; Hawley et al., 2013), while much less is known about the mechanisms that drive these changes (Downs & Piégay, 2019; Wilcock, 2012). Bedload sediment transport is an important geomorphic process that links hydrology, channel morphology, and ecology (Hawley & Vietz, 2016; Wohl et al., 2015a). Despite its importance, bedload sediment transport is often neglected in current urbanization and stream restoration studies (MacVicar et al., 2015; Shields, 2009). This gap is at least in part due to the lack of data that directly captures bedload transport in these environments (MacVicar et al., 2015; Russell et al., 2017; Shields, 2009). Consequently, despite consensus on the importance of incorporating geomorphic process into urban river management (e.g. Grabowski et al., 2014; Newson, 2002; Sear, 1994, Chin & Gregory, 2005), the scientific understanding of how urbanization and current management practices affect bedload transport remains limited. A process-based understanding of how urbanization and current river management practices affect bedload transport and its relationship to other river processes is imperative for improved urban river management (Booth & Jackson, 1997; Hawley et al., 2013; Vietz et al., 2015; Wohl et al., 2015a).

1.1 Objectives

The goal of this project is to address key gaps in the understanding of bedload sediment dynamics in the context of watershed urbanization and urban river management. The specific objectives of this thesis are to answer the following questions:

(1) How do the changes in hydrologic conditions resulting from watershed urbanization and stormwater management impact the bedload transport dynamics of rivers?

(2) How can bedload transport responses be predicted in rivers with hydrology modified by urbanization and stormwater management?

(3) How are current river restoration designs impacting bedload sediment transport processes and how do they relate to the success or failure of these projects?

(4) How can the limitations of current bedload transport monitoring technology be improved?

Addressing these research questions will advance the field of sediment transport, and produce new tools useful for urban river management. First, answering research questions (1) – (3) will provide much-needed sediment transport data in urban environments. Second, high resolution hydrologic and bedload transport data will allow for a new process-based perspective on the effect of urbanization on river systems through answering question (1). Third, question (2) moves from

explanatory to predictive abilities to understanding bedload transport in urban rivers. The intent is that predictive models can be used for improving decisions for urban river management and restoration and inform evidence-based policy around water. Answering question (3) will lead to recommendations for improved restoration designs and monitoring techniques that aim to restore processes. Finally, answering question (4) will provide a new tool to further advance research in the field of sediment transport and improve project monitoring techniques.

This project is part of a larger collaborative effort to understand the effects of land-use change on river systems and improve urban river management. Raso (2017) modelled the effects of the SWM infrastructure the hydrology and discharges of a small urban stream that is also used in this study. A parallel project on the effects of urbanization and river management projects on benthic macroinvertebrates is being conducted on overlapping study sites through the School of Environment, Resources and Sustainability at the University of Waterloo. Related studies of the effects of wood and the dynamics of semi-alluvial cover development are being done through the Department of Geography at Western University. These complementary studies focus on the same field sites and locations as this study, allowing for direct comparison and linking of different river processes. Recommendations for improved urban river management strategies informed on the results of this collaborative effort can help move river management towards adaptive management. Adaptive management strategies can be successful for river management because they allow for modifications to occur as the dynamics of the river system change, rather than be fixed in time. Such interdisciplinary perspectives are crucial for effective for the successful management of urban river systems (Wohl et al., 2005).

1.2 Thesis organization

This thesis is organized into chapters that address each of the research questioned outlined above. Each chapter is written as a stand-alone manuscript that either been already, or will be in the future, submitted for publication in scientific journals. Modifications to the original manuscripts have been done to minimize the repetition of methods sections between chapters, although some repetition exists to keep the logical flow of the Chapters intact. Transition paragraphs between chapters 3 – 6 are included to provide links between topics.

Chapter 2 provides a literature review of important background information on urban hydrology and geomorphology, river management, bedload transport theory, and bedload monitoring technology.

Chapter 3 focuses on research question (1). Bedload transport is monitored in three streams with different hydrologic settings (rural, urban with no SWM, and urban with SWM) to describe differences in the grain-scale bedload transport dynamics of the systems and assess whether they can explain differences in the channel evolution of each stream. Recommendations for improved urban river management strategies are discussed.

Chapter 4 focuses on research question (2). Bedload transport data collected from tracers in Chapter 4 are used to build predictive models of tracer displacement from hydrographs. The calibration and performance of these models are examined, and their implications to urban river management are presented.

Chapter 5 focuses on research question (3). Bedload transport and morphologic change are monitored in adjacent restored and un-resorted reaches of an urban stream to explore how the designed riffle-pool channel affects the bedload transport dynamics and its relationship to channel morphology. Implications for assessing project 'success' from a process-based perspective are presented.

Chapter 6 focuses on research question (4) by introducing a new tracer stone technology for sediment tracking applications in riverine environments. The design, two prototypes, and results from a series of performance tests of the new tracer stone are presented.

Chapter 7 summarizes the key conclusions of this thesis and provides directions for future research.

Chapter 2

Literature Review

2.1 The 'Urban Stream Syndrome'

Rivers are heavily impacted by human activities, including land-use change from urbanization (Chin, 2006; Paul & Meyer, 2001). The position of rivers as low-lying areas of the landscape makes them particularly vulnerable to impacts associated with land-use change (Bernhardt & Palmer, 2007; Walsh et al., 2005). In fact, watershed urbanization is a primary driver of hydrologic and geomorphic change in streams (Hawley & Bledsoe, 2013). Four key features of river systems are impacted by urbanization: hydrology, geomorphology, water quality and stream ecology (Ladson et al., 2006). Table 2.1 outlines both the consistently and inconsistently observed responses of these river features with urbanization (Walsh et al., 2005). This project focuses on bedload transport dynamics in urban streams making the focus of this literature review the hydrologic and geomorphic responses of channels to urbanization.

Table 2.1. Summary of consistently and inconsistently observed changes in the hydrology, geomorphology, water quality and ecology of urban rives. Modified from Walsh et al. (2005).

Feature	Consistent Response	Inconsistent Response
Hydrology	↑ Frequency of overland flow	Baseflow magnitude
	↑ Frequency of erosive flow	
	↑ Magnitude of peak flow	
	↓ Lag time to peak flow	
Geomorphology	↑ Channel width	Sedimentation
	↑ Pool depth	
	↑ Scour	
	↓ Sinuosity	
	↓ Channel complexity	
Water Quality	↑ Nutrients (N, P)	
	↑ Contaminants	
	↑ Temperature	
Ecology	↑ Tolerant invertebrates	Algal biomass
	↓ Sensitive invertebrates and fishes	Leaf decomposition
	↓ Oligotrophic diatoms	Fish abundance/biomass

The term 'urban stream syndrome' was first coined by Meyer et al. (2005) to describe the consistently observed patterns of degradation in streams draining urban areas (Walsh et al., 2005). Despite the consistency in observed effects of urbanization on stream hydrology, structure and ecology, the mechanisms that drive these changes are yet to be fully understood (Downs & Piégay, 2019). This lack of understanding is propagated by the lack of experimental evidence and empirical data to directly measure mechanisms of change (Walsh et al., 2005). Furthermore, a paradigm shift from treating the symptoms to treating the causes of the urban stream syndrome is occurring throughout the literature (Anim et al., 2019b; Beechie et al., 2010; Diaz-Redondo et al., 2018; Elosegi et al., 2010; Formann et al., 2014; Grabowski et al., 2014; Poppe et al., 2016; Vaughan et al., 2009; Whipple & Viers, 2019). Successfully restoring the hydrologic and geomorphic processes of rivers requires further research into the processes that link hydrology, geomorphology and ecology in these systems (Vietz et al., 2016).

2.2 Urban hydrology

The primary driver of hydrologic change in urban river systems is the increase of impervious land cover that increases surface runoff and results in a flashier hydrologic regime characterized by short lag times to peak flows and larger peak flows (Bledsoe & Watson, 2001; Chin, 2006; Konrad et al., 2005; Ladson et al., 2006; Poff, et al., 2006). Stormwater infrastructure such as gutters, drains, and storm sewers convey runoff rapidly and efficiently to channels, contributing to the shift towards a flashier regime (Booth et al., 2004; Hammer, 1972). Watersheds are sensitive to the introduction of impervious surfaces; increases of 10-20% in watershed imperviousness have been documented to lead to doubled or tripled peak flows of flows with recurrence of 0.5 – 2 years (Hammer, 1972; Hollis, 1975). Furthermore, the frequency of bankfull or larger flows, as well as the number of shorter duration events increase with urbanization (Annable et al., 2011; Doyle et al., 2000; Plumb et al., 2017). Despite these general trends, the magnitude of hydrologic response to urbanization is highly variable and sensitive to factors such as watershed context, connectivity to floodplains, vegetation, amongst others (Annable et al., 2011; Bledsoe & Watson, 2001).

The effects of urban development on the flow regime of streams have been primarily described in terms of simple streamflow metrics that have social significance (e.g. peak discharge, lag time to peak flow, recession rate etc.) but do not necessarily carry geomorphic or ecological significance (Konrad et al., 2005). Moreover, given the complexities of river systems, relationships between urbanization and these simple hydrologic variables are unlikely, and a detailed analysis of

the entire hydrograph allows for a more complete investigation of the hydrologic changes caused by urbanization (Booth, 1990). Specifically, since both the frequency and duration of hydrologic events can have important effects on the channel processes, such parameters can offer more nuanced insights into the response of rivers to urbanization (Doyle et al., 2000).

A large body of literature aims to characterize hydrologic records and analyze the effects of land-use changes on both the magnitude and frequency of hydrologic events by distinguishing the effects of urbanization on high-frequency low-magnitude versus low-frequency, high-magnitude events. Urban streams have been shown to display low variability in annual maximum flows between years, as well as shorter durations of high flows (Konrad et al., 2005). It has been consistently shown that urbanization has the greatest impact on small, frequent events so that the peak flow of small, frequent events increases by a larger percentage than large infrequent floods (Booth, 1991; Konrad et al., 2005; McClintock & Harbor, 2013). Furthermore, the frequency of high flows in urban streams is likely to increase more than the cumulative duration of those flows through the combination of an increased peak flow and more rapid storm falling limbs (Konrad et al., 2005). Annable et al. (2012) suggest that the annual cumulative volume of all bankfull or larger events show no difference between urban and rural catchments (Figure 2.1). However, the annual cumulative volume of flow only exceeding bankfull discharge was larger in urban streams, suggesting that urban streams convey more water in flows above bankfull than their rural counterparts (Annable et al., 2012). In a recent study, Plumb et al. (2017) demonstrated through hydrologic models that watershed urbanization increased the frequency of flows that exceed the bedload transport threshold, bankfull flow, and effective flow.

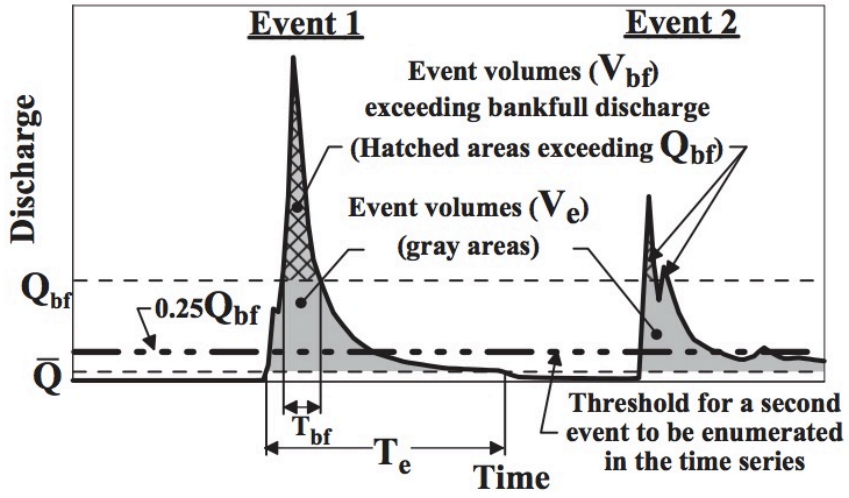

Figure 2.1. Conceptual hydrograph showing the distinction between 'event volume' and 'event volume only exceeding bankfull'. From Annable et al. (2012).

In summary, the effects of urbanization on the hydrology of streams is complicated and involves both the magnitude and duration of flows. Often, the consequences of the hydromodification of urban streams does not directly affect engineering designs because such designs are based on large floods (i.e. 10-year return flood) that are less impacted by urbanization than small events, but these hydromodifications can have important consequences for channel form and stability (Doyle et al., 2000). The sensitivity of rivers to changes in small-to-medium magnitude events is further highlighted by evidence that suggests that the geomorphic significance of these events increases with urbanization (Plumb et al., 2017). It is therefore important to fully understand how urbanization modifies events of all magnitudes and the importance of all magnitude events on bedload transport and stream stability. A review of the literature suggests the need for higher resolution hydrologic data capable of capturing detailed changes in hydrographs over long periods. Such data can be used to capture the full extent of hydromodification both at event-scale and at the long timescale, such as changes to the distribution and duration of flows.

2.3 Channel form and stability

The determinants of channel form have been theorized throughout many decades. Mackin first introduced the idea of the graded river in 1948, referring to a river that has adjusted its slope to provide the flow velocity needed to transport the sediment load supplied, given the available discharge and the prevailing channel characteristics (Mackin, 1948). In other words, a graded river has self-adjusted over some time to fit the flow and sediment regime provided by the watershed. Later, Lane (1955) refined the idea by positing that there exists a between sediment supply, sediment size, discharge and slope, and that a change in one of these factors will lead to channel aggradation or degradation (Figure 2.2). Streams respond to watershed changes by adjusting their form over time to satisfy the balance between sediment input and water input.

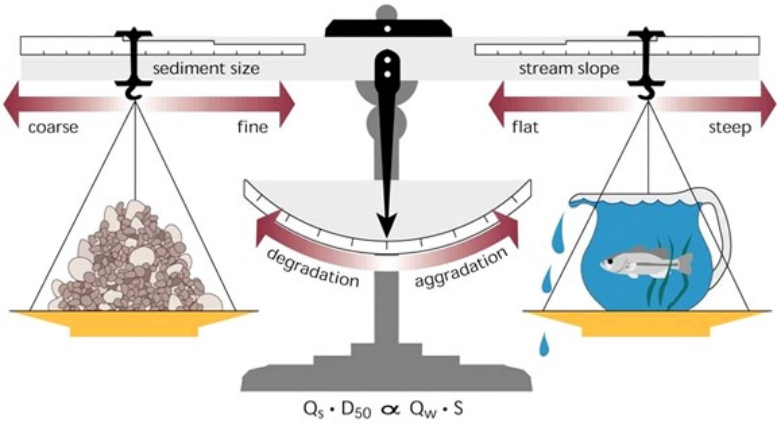

Figure 2.2. Visual representation of the Lane (1955) relationship. From Rosgen (1996).

The combination of a new flow regime and the reduction in sediment supply characteristic of watershed urbanization leads to an imbalance in the river system (Bledsoe & Watson, 2000; Booth, 1990; Schumm, 1977). Additionally, direct channel modifications such as straightening also increase the channel slope (Booth & Fischenich, 2015). Following from the Lane relationship, this imbalance is expected to lead to channel degradation (Booth & Fischenich, 2015; Simon & Rinaldi, 2006). In the new urban regime, the amount of sediment readily available for transport during a particular hydrologic event does not match the ideal input needed to maintain the equilibrium state, leading to destabilization (Bledsoe & Watson, 2000; Booth, 1990; Chapius et al., 2014; Simon & Rinaldi, 2006). The increased runoff produced by urbanization coupled with a decline in sediment delivery results in channel enlargement through incision and bank erosion (Bledsoe, 2002; Booth, 1990; Pizzuto et al., 2000; Trimble, 1997). Changes to the channel dimensions of urban channels, in turn, affects the hydraulic forcing on the channel bed. Recent modelling studies of the interplay between hydrologic, morphologic and hydraulic conditions have revealed the complexity in the links between different river processes (Anim et al., 2018, 2019a, 2019c). As shear stress is directly linked to the cross-sectional geometry of a channel, changes to the channel form will consequently alter how discharge is translated to the force available to transport bedload. Despite the complexity and feedback mechanisms present between channel form and hydraulics, these links are important for efforts that attempt to remediate degraded river systems.

2.3.1 Conceptual models of channel response to urbanization

Several conceptual models of channel morphologic adjustments in response to watershed urbanization have been developed. Simon and Hupp (1986) developed a six-stage channel evolution model (CEM)

for channels responding to channel construction and land-use change (Figure 2.3). Stage I represents the channel before modifications and Stage II represents the channel immediately after the disturbance that introduces an imbalance between sediment supply, discharge and slope. In Stage III, the channel experiences rapid vertical degradation increased bank heights and steeper bank angles that lead to failure of the banks near the base of the banks (Simon & Hupp, 1986). Once the critical shear strength of the channel bank material is reached, the destabilization of the channel banks leads to channel widening by bank failure (Stage IV). As channel gradients decrease during Stages III and IV, channel degradation migrates upstream and the channel eventually reaches Stage V, which is characterized by aggradation (Simon & Hupp, 1986). The establishment of vegetation on the banks further helps sediment deposition, and the channel gradient continues to decrease through meander elongation. Finally, the channel reaches a new quasi-equilibrium state (Stage VI) (Simon & Rinaldi, 2006). The Simon and Hupp CEM has been largely adopted both in the interpretation of channel responses to disturbances and to predictive applications for channel management.

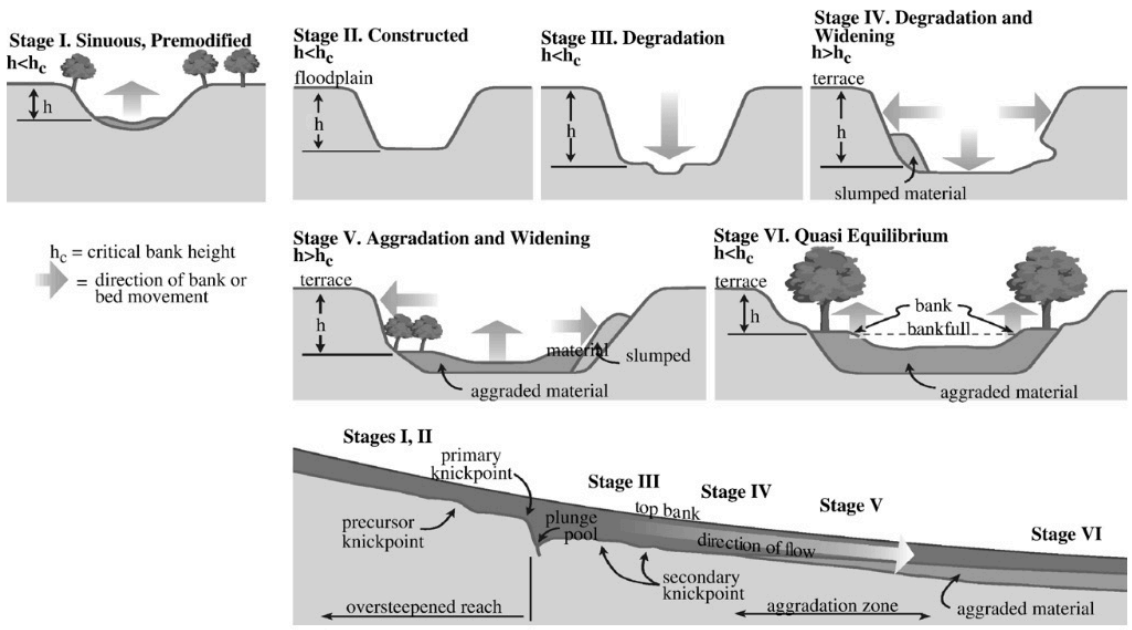

Figure 2.3. Simon and Hupp (1986) channel evolution model. From Simon and Rinaldi (2006).

The development of CEM models has largely focused on alluvial channels, while less emphasis has been placed on non-alluvial channels or channels with human modifications such as bank stabilization. To address this gap, Booth and Fischenich (2015) expanded the Simon and Hupp CEM to include a broader range of channel contexts (Figure 2.4). In this model, the Simon and Hupp

CEM is used as a basis, and various channel contexts and disturbance trajectories are considered, providing a more comprehensive view of channel evolution for the purpose of channel management. The models presented by Booth and Fischenich (2013) have not been extensively validated through field observation in diverse settings. Bevan et al. (2018) used a combination of historical and recent channel surveys to propose a CEM for a semi-alluvial river in response to urbanization. The study was focused on a small river whose bed consisted of a thin layer of gravel cover over a highly erodible compact clay till layer. In the proposed CEM model, channel widening followed by avulsions at meander bends acts as the primary processes of morphological adjustment (Bevan et al., 2018) (Figure 2.4). Following the avulsions, the channel deepens following a more typical pattern of channel enlargement (Bevan et al., 2018).

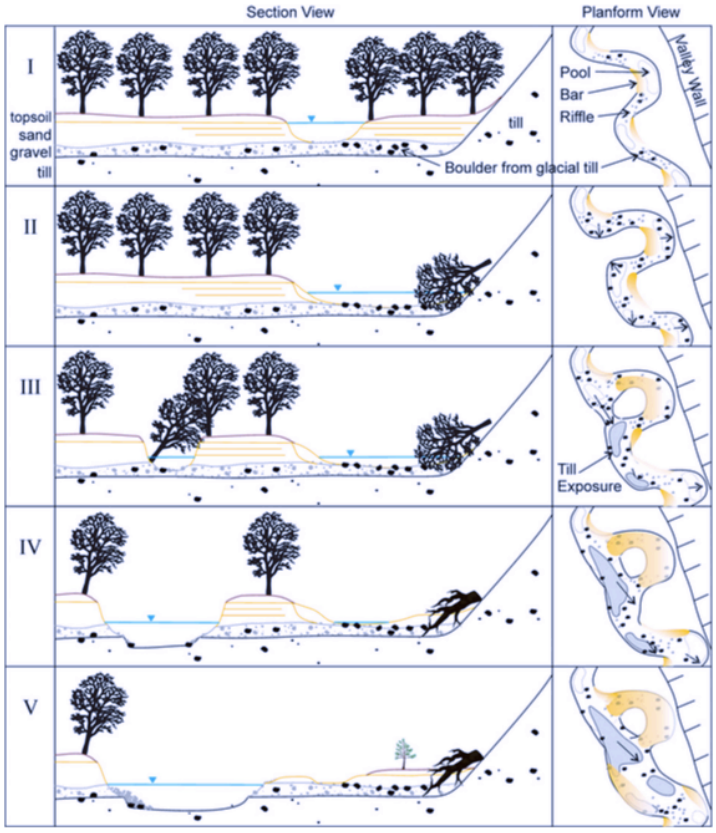

Figure 2.4. CEM model in response to urbanization in a small semi-alluvial river. From Bevan et al. (2018).

2.3.2 Trends of channel change in response to urbanization

There exists a relationship between increased imperviousness and both channel geometries such as width, depth and slope, and morphological characteristics such as pool length, riffle length and pool-riffle ratios. Many studies have demonstrated that urban streams display enlarged channel dimensions (Bevan et al., 2018; Bledsoe & Watson, 2001; Galster et al., 2008; Gregory et al., 1992; Hawley et al., 2013; Pizzuto et al., 2000; Trimble, 1997) and reduced channel complexity (Walsh et al., 2005). A consequence of channel incision disconnection of the channel from its floodplains (Bernhardt and Palmer, 2007; Booth, 1990; Hammer, 1972; MacVicar et al., 2015; Segura and Booth, 2010). This disconnection further accelerates the imbalance between increased flow and decreased sediment supply (Chapuis et al., 2014a), further amplifying the increase in shear stresses and transport capacity with increasing discharge (Bledsoe and Watson, 2000). This positive feedback mechanism can result in significant channel enlargement. In one example, Bevan et al. (2018) measured a 75% increase in channel width and a 50% increase in channel depth of a small semi-alluvial river in Southern Ontario between a pre-urban survey in 1958 and 2016.Comparable magnitudes of channel enlargement have been documented elsewhere. For example, Hawley et al. (2013) measured a 47% increase in bankfull cross-sectional area following urbanization in northern Kentucky, while in North Carolina, O'Driscoll et al., (2009) found cross-sectional areas were on average 1.78 times greater for urban channels, while full-channel capacities were 3.4 times greater. In a detailed study, Gregory et al., (1992) found channel widths were enlarged 2.2 times in urban streams in southern England, and incision depths of up to 0.4 m were measured.

Some debate exists in the literature over the time it takes for a new quasi-equilibrium state to be reached and whether a quasi-equilibrium state is at all possible. The answer to these questions depends heavily on the spatial scale studied and on the time during watershed adjustment that it is asked (Chin, 2006). Depending on when measurements are conducted during urbanization and channel evolution, the magnitudes of impacts can be small or large, and direction can change (aggrading versus eroding). Therefore, the timeframe in which measurements are made must be carefully examined (Chin, 2006). Timescales for channel enlargement are also variable (several years to decades) depending on watershed-scale variables such as geology, groundwater interactions and the rate of urbanization (Chin, 2006). Some studies have demonstrated that urbanized channels can spontaneously stabilize their banks over 1-2 decades given a constant watershed land use, although the results are only observed in some channels (Henshaw & Booth, 2000). Some argue that alluvial channels with limited sediment supply, such as those found in urban environments, are more likely to experience frequent and extensive bed disturbance not just during their evolution from rural to urban,

but even after long periods (Konrad et al., 2005). The increase in the frequency of bed disturbances means that although streams widen and the size of bed material coarsens, responses may be insufficient to reestablish a new equilibrium (Konrad et al., 2005).

2.4 River management strategies

Management efforts to address the 'urban stream syndrome' usually aim to shift the ecological conditions of the stream closer to that of un-urbanized streams (Walsh et al., 2005). Management of urban rivers can be summarized in two broad strategies: mitigating negative impacts at the instream scale through river restoration projects, and mitigating stressors within the watershed that lead to these negative effects. The second strategy includes changes to hydrology through the introduction of stormwater management (SWM), or changes to sediment supply (Ladson et al., 2006). Recent studies using catchment-scale models suggest that the most successful strategies for preserving or improving the ecological integrity of urban streams likely involved a combination of managing both the channel form and the hydrology (Anim et al., 2019c).

2.4.1 River restoration

'River restoration' is a term used to describe a large variety of manipulations of streams channels in an attempt to improve the condition of the river relative to some degraded state (MacVicar et al., 2015). River restoration is becoming an increasingly common undertaking globally and is a significant economic activity (Bernhardt et al., 2005; Pasternack, 2013). Instream restoration involves reconstructing channels or introducing structures to existing channels to recreate a specific morphology, protect banks, provide grade control, promote flow deflection etc. The main goal of such activities is to create a channel that mimics a stable channel morphology and provides the needed aquatic habitat for riverine ecosystems (Niezgoda & Johnson, 2005). Instream structures such as constructed pools and riffles are popular due to their perceived benefits for both ecology and channel stability (MacVicar et al., 2015; Wohl et al., 2005; Bernhardt et al., 2005).

A large shortcoming of restoration projects is the strong focus on stability that leads to designs that do not allow for dynamic river processes to occur. Such strategies go against geomorphic principles of dynamic equilibrium (Sear, 1994). Thompson (2002) concluded that the rigid nature of most in-stream structures does not allow them to respond to the long-term dynamic adjustment of the system and studied cases did not succeed in maintaining the design channel form in the long term (Thompson, 2002). Furthermore, stream stability alone is not sufficient to improve the ecological

condition of rivers (Henshaw & Booth, 2000). Rigid river restoration designs are not successful in improving channel complexity needed for ecological health (Lub et al., 2012). These shortcomings highlight the need for designing more dynamic instream restoration projects. Much of the challenge in achieving such designs is that we know little about the sediment dynamics in urban streams and how restoration affects it (Shields, 2009).

There continue to be many challenges surrounding restoration practices. Firstly, most restoration projects lack scientific context (Beechie et al., 2010; Pasternack, 2013; Shields, 2009; Wohl et al., 2005, 2015) and the empirical basis for restoration of urbanized channels is unclear (Pizzuto et al., 2000). Second, although there is growing acknowledgment of the need to move towards designs of dynamic systems that can accommodate a wide range of hydrologic conditions (Annable et al., 2012; Baker et al., 2008; Palmer et al., 2010), methods that would allow for dynamic designs of rivers are lacking. Finally, there is lack of consideration of key river processes in current restoration efforts, including sediment dynamics (Beechie et al., 2010; Chapuis et al., 2014a; Pasternack, 2013; Shields, 2009; Vietz et al., 2015), contributing to failings of river restoration projects.

2.4.2 Project success and monitoring

Despite the increasing number of river restoration projects, little is known about their effectiveness, particularly in the long-term (Bernhardt et al., 2005; Palmer & Bernhardt, 2006; Roni et al., 2008). A large issue is that although there is increasing consensus on the importance of urban river restoration, no agreement exists on what successful restoration is (Dufour and Piégay, 2009; Palmer et al., 2005). From a physical standpoint, restoration success/failure is often evaluated by measuring bed topography or geometry to assess the structural integrity of constructed features (Bouska et al., 2015; Miller & Kochel, 2009; Roni et al., 2008; Buchanan et al., 2014). Results from monitoring projects and success/failure measures are difficult to interpret and compare due to the variable length of time it takes for 'success' or 'failure' to manifest (Buchanan et al., 2014; Morandi et al., 2014). Furthermore, sometimes both negative or positive effects of restoration projects manifest that were not part of the initial design (Buchanan et al., 2014). Some have argued to move away from designs that attempt to restore stream conditions to their pre-disturbance state and towards a focus on improving the ecosystem services provided by streams (Dufour & Piégay, 2009; Palmer et al., 2014). These points highlight the challenges associated with the development of consistency in evaluating the effectiveness of restoration, particularly the cumulative effects of many small projects (Palmer and Bernhardt, 2006). Despite these challenges and lack of consensus, sources often cite high failure rates

of restoration projects (e.g. Booth et al., 2004) and little is known about whether restoration is successful at restoring ecological function (Palmer et al., 2007).

Contributing to the problem is that most restoration projects do not have adequate monitoring post-construction. In a survey of 317 restoration projects across the U.S.A., less than 50% of projects set measurable outcomes for their designs, but two-thirds report project success (Bernhardt et al., 2007). Although part of this lack of monitoring is due to the challenges associated with restoration evaluation outlined previously, another main reason for lack of monitoring is reported to be the lack of resources (time/money) (Bernhardt et al., 2007). When monitoring is undertaken, it is often ineffective because it misses the potential impacts of rare hydrologic events (Bernhardt et al., 2007; Miller & Kochel, 2009; Morandi et al., 2014; Shields, 2009). For example, projects are typically designed for 10 years but often monitored for only 5 (Niezgoda & Johnson, 2005). There is an urgent need for the development of better monitoring techniques to assess the effects of restoration projects on sediment transport (Schwartz et al., 2009; Wilcock, 2012).

2.4.3 Stormwater management

The role of flow regimes in sustaining healthy river ecology is increasingly recognized (Poff et al., 2006). SWM attempts to alter the hydrology of urban streams to reduce adverse effects on river form and ecology. This management method is, therefore, an attempt to mitigate the root causes of urban river degradation rather than to fix symptoms of degraded streams (Vietz et al., 2015). The most common SWM strategy is 'peak shaving', which attempts to alter peak flows to match pre-development magnitudes and is commonly achieved through the use of stormwater detention ponds. However, management of stormwater often occurs on an ad hoc basis with little consideration of geomorphic processes (Bledsoe & Watson, 2000; Rohrer & Roesner, 2006; Tillinghast et al., 2011).

Since SWM is usually designed with flood control in mind, it tends to focus on low-frequency high-duration events rather than the flows that transport most sediment or the duration of flows (Booth, 1990). The conventional peak-shaving approach typically increases the magnitudes, durations, and frequency of erosive discharges (Bledsoe, 2002; Bledsoe & Watson, 2001; Nehrke & Roesner, 2004; Pomeroy et al., 2008; Rohrer & Roesner, 2006). This occurs because often the rate at which detention ponds release overflow exceeds the critical shear stress of the sediment (Tillinghast et al., 2012). Studies show that peak shaving of the 2-year return interval flood increase erosion due to an increase in the sediment transport potential (MacRae, 1997; 1991; McCuen & Molgen, 1988). Furthermore, SWM ponds trap fine sediment thereby altering the sediment delivery to the stream and further exacerbating the problem (Baker et al., 2008). Consequently, simply limiting peak flows may

not be enough to maintain pre-development channel stability levels because the duration of flow can affect the channel stability as much as the magnitude of flow (Baker et al., 2008). Some studies have demonstrated that traditional detention ponds lead to morphologic inactivity in downstream reaches (e.g. Badelt, 1996). Little empirical data exists in streams with peak-shaving SWM to fully assess the effects of the altered hydrologic regime on bedload transport processes.

As an alternative strategy to peak-shaving approaches, McCuen and Moglen (1988) suggested 'erosion control detention', where SWM is designed so that the cumulative post-development bedload transport volume does not exceed the volume for 2-year recurrence interval (Figure 2.5). Erosion control detention has been found to control urbanization-induced erosion, but that this design comes at a cost: the required detention volume is much larger (Booth & Jackson, 1997). Modelling by Bledsoe (2002) using various bedload transport equations found that that detention design for erosion control requires a storage volume 61% larger than peak-shaving. More recently, there has been increasing attention paid to catchment-scale SWM strategies, such as increasing watershed infiltration rates (Pomeroy et al., 2008; Rohrer & Roesner, 2006), or stormwater control measures located at or near the runoff source (Amin et al., 2019; Li et al., 2017). Although the effectiveness of these SWM strategies on reducing bedload transport has been modelled (e.g. Amin et al., 2019), little empirical evidence to verify its effects on geomorphic processes of streams.

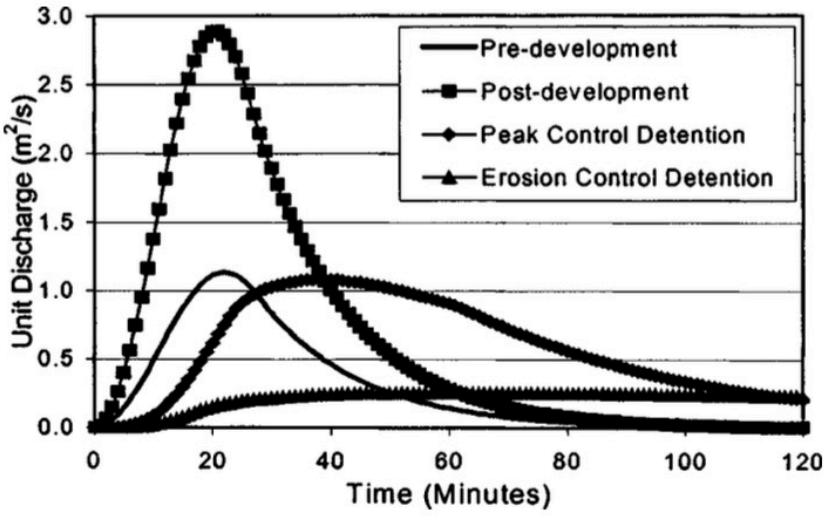

Figure 2.5. Comparison of measured pre-development and post-development hydrographs and modelled peak control and erosion control SWM hydrographs. From Bledsoe (2002).

2.5 Bedload sediment transport

The morphologic adjustments in response to watershed urbanization outlined in Section 2.3 are driven by the transport of bedload sediment through processes of erosion and deposition. Understanding the mechanisms by which altered flow regimes and human modifications affect the transport of bedload sediment can lead to better predictions of the responses of rivers to watershed urbanization. Bedload transport is also an important river process from an ecological perspective because it provides a link between hydrologic and biological responses (Booth et al., 2004). Therefore, an improved understanding of the bedload transport dynamics in urban rivers could improve urban river restoration and management efforts (Bledsoe & Watson, 2001; Hawley et al., 2013; Vietz et al., 2015).

Historically, sediment transport studies have measured bulk sediment transport rates and related them to large-scale channel characteristics such as slope, discharge, sediment size and shape, and sediment budget (Hassan et al., 2013). This approach has led to the development of many bedload transport equations that calculate bulk bedload transport rates. Bedload transport rate equations are developed upon the hypothesis of a critical shear stress threshold, beyond which the sediment of a given size class is entrained from the bed and transported downstream. This idea was first developed by Shields (1936), who derived a relationship between sediment size and critical shear stress. Bedload transport formulae such as the Meyer-Peter-Muller (1948) formula assumes the critical shear stress and uses experimentally-derived empirical constants to relate shear stress to a transport rate. Wilcock and Crowe (2003) improved the Meyer-Peter-Muller formula to make it applicable to mixed-size sediment through the introduction of a hiding function. The hiding function takes into consideration that although small grains have less mass and therefore require less force to entrain, they may become shielded by larger particles that may be more exposed to the flow (Andrews, 1983; Brayshaw, 1985). Although useful, these equations do not provide detailed information on the controls of bedload transport and assume a spatially-uniform transport rate across the bed for a given flow.

Since bulk bedload transport is the cumulative result of the transport of individual particles, an alternative approach is to study and characterize the movement of individual particles to obtain a more detailed view of bedload transport processes (Church & Hassan, 1992). Such an approach can provide insights into the exact controls and spatial variability of bedload transport that can lead to improvements in predictions of channel adjustments in streams (Haschenburger & Church, 1998; Hassan et al., 2013). This perspective on bedload dynamics was first introduced by Einstein (1950), who posited that, given the complexity of the geometry of mixed sediment beds and flow turbulence, the exact flow for which a given grain will move cannot be known. Rather, only the probability of entrainment can be calculated based on the sediment characteristics and the flow (Buffington &

Montgomery, 1997; Paintal, 1971). The distance a grain will travel once entrained is also a random variable that can be described through probability distributions (Einstein, 1950). Although much of Einstein's work remained theoretical and experimental, studies in the field have demonstrated the validity and usefulness of his framework in understanding bedload transport processes.

2.5.1 Particle mobility

When studying the behaviour of individual particles on the streambed, a useful metric is the mobility or the fraction of sediment that is entrained and transported during a flood. 'Partial mobility' refers to the condition where only a fraction of the bed is mobile while the remaining particles remain static (Wilcock & McArdell, 1997). Studies of gravel river beds in both flume and field settings have demonstrated that the majority of bedload transport occurs under partial mobility, while full mobility, the condition where all bed particles are mobile, occurs only during the most extreme events (e.g. Church & Hassan, 2002; Haschenburger & Wilcock, 2003; Wilcock & McArdell, 1997). The mobility of bed sediment has been shown to be a factor of both the flow conditions, and the particle size. Bed mobility has been shown in both flume and field studies to increase with flow variables such as shear stress (Ashworth & Ferguson, 1989; Phillips & Jerolmack, 2014; Wilcock & McArdell, 1997; Wong et al., 2007), peak discharge (Haschenburger & Wilcock, 2003; Papangelakis & Hassan, 2016), and excess stream power (Gintz et al., 1996; Hassan et al., 1992; Lenzi, 2004). The relationship between sediment mobility and grain size has been the focus of many studies. Although it is accepted that mobility is a 'size-selective' process, the relationship between particle size and mobility is not simple because non-uniform size mixtures complicate the problem (Church & Hassan, 1992; Yager & Schott, 2013). It has been consistently measured both in lab settings and field studies that for a given discharge, small particles experience similar mobility values, but larger particles have rapidly decreasing mobility with grain size (Church & Hassan, 1992; Ferguson & Wathen, 1998; Lenzi, 2004; Wilcock & McArdell, 1993). Lab experiments have documented that for a given flow condition, fine sediment up to a certain size experience almost equal transport rates, and the values quickly collapse for larger particles (Wilcock and McArdell, 1993) (Figure 2.6). Differences in the mobility of particles of different sizes decreased with increasing flow conditions, approaching a state of 'equal mobility' is approached (Wilcock & McArdell, 1993).

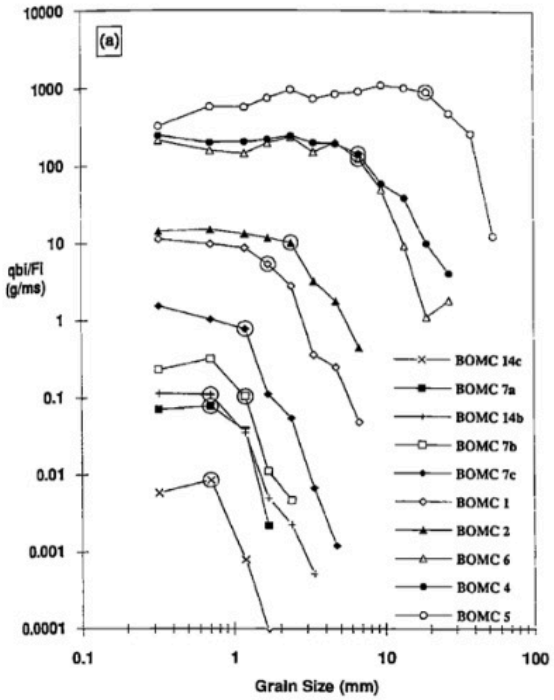

Figure 2.6. Fractional transport rates of various sized particles from a mixed-size bed. From Wilcock and McArdell (1993).

2.5.2 Particle travel lengths

The distribution of tracer travel distances has been shown to be positively skewed. Field-based studies have found that travel distances follow distributions follow exponential or gamma distributions (e.g. Bradley & Tucker, 2012; Papangelakis & Hassan, 2016), power laws (e.g Liébault et al., 2012) or the Einstein-Hubbell-Sayre (compound Poisson) distribution (Hubbell & Sayre, 1964). Particle travel distances, however, do not always fit these distributions, highlighting the complexity of controls on particle dispersion (Hassan et al., 1991), including channel morphology, tracer burial, and flow magnitude (Hassan et al., 2013). Distributions of particle travel lengths may also be categorized by the characteristics of the tail of the distribution as thin-tailed, where the tail collapses quickly, or heavy-tailed, where the presence of a small number of frontrunners elongates the tail (Hassan et al., 2013). The determination of thin- very heavy-tailed distributions is important for bedload transport modelling because the characteristic of the tail determines which types of mathematical models best describe bedload transport. Classical advection-diffusion models have been used to model the dispersion of sediment as a diffusion process, but the presence of heavy-tailed travel length

distributions requires the use of sub- or super-diffusive models must be considered (Ganti et al., 2009; Hill et al., 2010).

Similar to bed mobility, tracer travel distances increase with increasing flow magnitude. Mean travel distances have been found to scale as a power law to flow metrics including shear stress (Wong et al., 2007), excess stream power (Gintz et al., 1996; Schneider et al., 2014), cumulative excess stream power (Hassan et al., 1992; Lamarre & Roy, 2008; Schneider et al., 2014), dimensionless peak stream power (Vazquez-Tarrio et al., 2019), and total excess flow energy expenditure (Haschenburger, 2013; Papangelakis & Hassan, 2016). Phillips et al. (2013) developed a hydrologic metric based on the time integration of shear velocity for the time the velocity exceeded the critical value for transport. This variable, named dimensionless impulse, was found to have a strong correlation with travel distance (Phillips et al., 2013).

The travel distance of bed grains is also influenced by sediment size, and has been consistently shown to decrease with increasing grain size following a relationship between scaled distance and scaled grain size developed empirically by Church and Hassan (1992):

$$\frac{L}{L_{D50}} = 1.77\left(1 - \log\frac{D}{D_{50}}\right)^{1.35} \quad (2.1)$$

where L is the mean travel distance of particles of size D, and D_{50} is the median particle size class. Although this relationship has been confirmed by a large number of other particle tracking studies (Ferguson & Wathen, 1998; Habersack, 2001; Lenzi, 2004; Liedermann et al., 2013; MacVicar & Roy, 2011; Schneider et al., 2014), it is not universally found in all settings, and large scatter in the data exists, further demonstrating the complex controls on bedload transport listed previously (Figure 2.7). For example, larger particles have been documented to travel further distances if the channel slope is steep enough and for particular sediment size mixtures (Hill et al., 2010; Solari & Parker, 2000). Furthermore, equation (2.1) is applicable only where the largest size fractions are only partially mobile (Wilcock, 1997), while different relationships have been found for unconstrained sediment (MacVicar & Roy, 2011). More recently, researchers have compiled data from several studies to propose a modified relationship to better fit the data across a larger range of settings (Vazquez-Tarrio et al., 2019) (Figure 2.7).

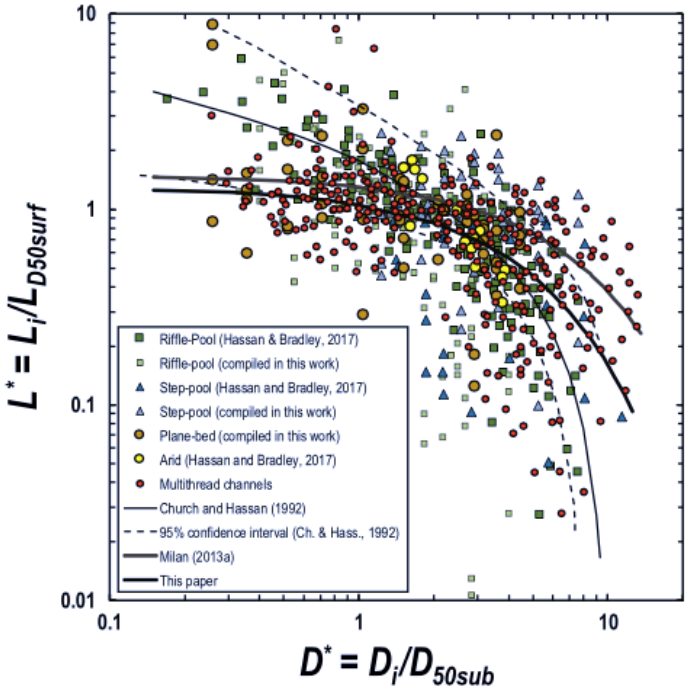

Figure 2.7. Relationship of scaled tracer travel length (L^*) and scaled grain size (D^*). From Vazquez-Tarrio et al. (2019) using data compiled from several previous studies.

2.5.3 Virtual velocity

The fraction of mobile tracers and their travel distance can be used to scale up the motion of individual particles on the bed to estimate long-term bedload dispersion and bedload transport rates (Wilcock, 1997). 'Virtual velocity' is a measure of the average rate of dispersion of sediment in units of length per time, and has been defined in two ways. The first is the event-based virtual velocity, or the velocity of bed particles during a given mobilization event, calculated as the mean travel distance of particles in a given size class, divided by the length of competent flow (Hassan et al., 1992). This definition of virtual velocity can be used to estimate the bedload flux (or rate) when the depth of the active layer is known (Brenna et al., 2019; Mao et al., 2017; Haschenburger & Church, 1998; Wilcock, 1997). Several researchers shown that event-based virtual velocity increases with flow metrics such as cumulative unit stream power (Hassan et al., 1992), dimensionless peak stream power (Vazquez-Tarrio et al., 2019), reach average shear stress (Ferguson & Wathen, 1998), and cumulative shear velocity (Klösch et al., 2017). The effects of grain size on virtual velocity are more complex, with studies showing event-based virtual velocity to both decrease (Ferguson & Wathen, 1998), and increase (Milan, 2013b) with grain size. The second definition of virtual velocity is focused on longer

timescales and is defined as the mean travel distance of particles per year, usually calculated over at least 2 years (Houbrechts et al., 2015). Although this method cannot be used to directly calculate bedload transport rates, it is a useful metric for comparing long-term bedload displacement between systems (Houbrechts et al., 2015).

2.5.4 Bedload dynamics and channel morphology

The relationships between mobility and sediment size are not always straightforward, and partial mobility rates are not uniform across the bed even during a given flow event (Haschenburger & Wilcock, 2003; Papangelakis & Hassan, 2016). The lack of spatially-uniform mobility suggests that sediment size and flow are not the only controls on sediment transport, and bed morphology must also be important. The idea that morphology plays a role in grain mobility is intuitive; if bedforms are created and evolve through the processes of bedload transport then they must both influence and, in turn, depend on individual grain movements. In other words, grains must be displaced in patterns that lead to the development and maintenance of the bed morphology (Hassan, 1992; Kasprak et al., 2015; Pyrce & Ashmore, 2003a). Indeed, it has been observed that in cases where flow approaches or exceeds channel-forming floods travel distances of grains are associated with the length scale of the dominant bed morphology (Bradley & Tucker, 2012; Chuch & Hassan, 1992; Kasprak et al., 2015; Lamarre & Roy, 2008; Pyrce & Ashmore 2003b, 2005). Furthermore, the relationship between travel distances of bedload particles and flow has been shown to differ in reaches with different morphologies and channel dimensions (e.g. Hassan & Bradley, 2017; Papangelakis & Hassan, 2016; Vazquez-Tarrio et al., 2019).

Patterns of transport associated with morphology have been linked to morphology evolution and maintenance. In flume experiments, Pyrce and Ashmore (2003a, 2005) linked preferential areas of erosion, deposition and storage of individual bedload particles to the growth and evolution of bars. The distribution of particle travel distances was also shown to evolve as bars formed over time, further reflecting the feedback relationship between bedload transport and morphology (Figure 2.8) (Pyrce & Ashmore, 2005, 2003a). Milan et al. (2013a) similarly used patterns of grain displacement through riffle-pool units to develop a hypothesis for riffle-pool maintenance. These studies highlight how understanding the relationship between bedload transport at a small scale can allow for better prediction of channel response and morphological evolution. Such an understanding can, therefore, be powerful for successful river management and improved restoration design. Very few studies have explored the relationship of morphology and bedload transport in urban streams, and even fewer in

the context of restoration and how constructed morphologies constrain or enhance the transport of bedload sediment.

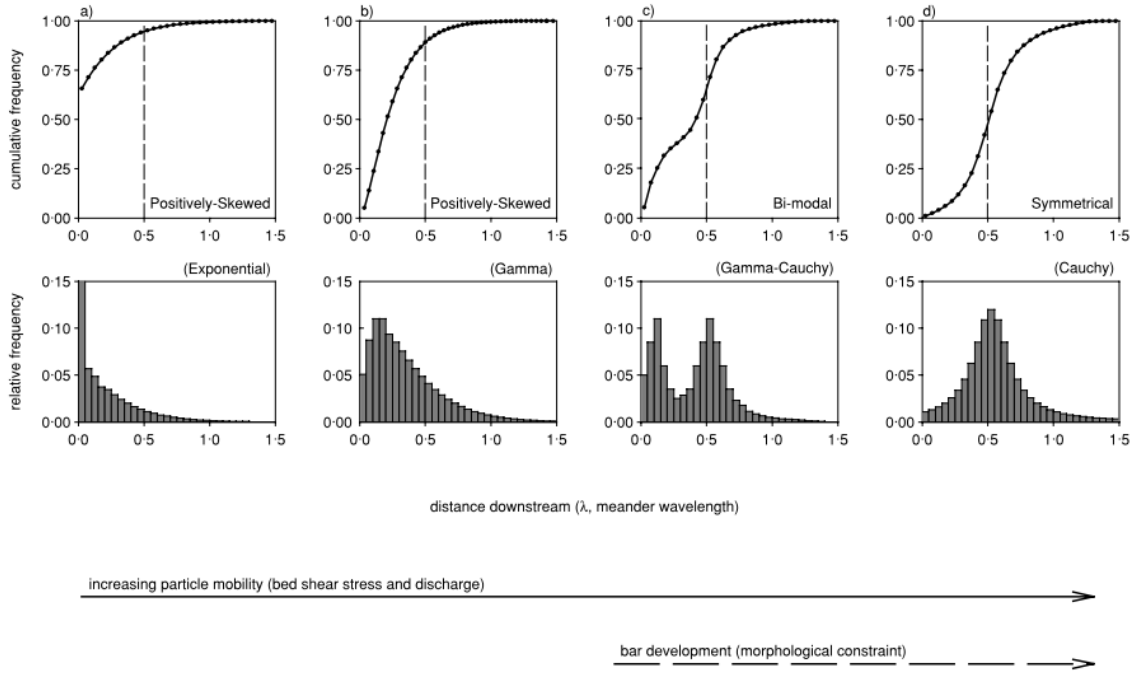

Figure 2.8. Relationship between travel distance of particles and morphology. From Pyrce and Ashmore (2003a).

2.5.5 Bedload transport in urban rivers

Research into the effects of urbanization on rivers predominantly focuses on the effects of varying degrees of watershed urbanization on channel form, with little consideration of how the altered hydrologic and sediment supply regimes affect the sediment transport dynamics of urban rivers. The key process that is responsible for morphologic adjustment in rivers is bedload sediment transport (Mackenzie et al., 2018), and is, therefore, a key piece in understanding how altered hydrologic conditions result in morphological adjustments. At the grain scale, alluvial stream channels will stabilize under flows that persist for a long enough duration, provided there are a sufficient fraction of immobile particles to cover the bed (Lane, 1955) and a limited upstream supply of mobile particles (Little & Mayer, 1976). Bed stabilization occurs when during high and long duration flows, small particles move to more stable positions between larger particles and under eddies along channel margins. This process eventually exhausts the in-channel supply of sediment available for transport for that flow, leading to bed armouring and a stable channel (Konrad et al., 2005; Laronne & Carson,

1976; Yager & Schott, 2013). The consequences of this mechanism for urban streams is that as the magnitude, frequency and duration of mobilizing flows changes, these flows will be able to entrain much more of the bed surface and produce high transport rates because there is not sufficient time to exhaust the in-channel sediment supply available for transport (Reid & Laronne, 1995). Studies using hydraulic models have demonstrated how shifts in the hydrologic conditions of urban watersheds and those with SWM change the distribution of hydraulic forces in channels, which result in alterations to the frequency of bed sediment mobilization (Anim et al., 2018). Although the theory behind the mechanisms of bedload sediment transport regime shifts resulting from urbanization is well established, little empirical data exists to describe the bedload transport dynamics of urban rivers.

A recent study in an urban river in Southern Ontario used bedload transport models to demonstrate an increase of 150% in average bedload yield pre- and post-development that was attributed to a shift in the frequency and geomorphic significance of flood events (Plumb et al., 2017). An increase in the bulk sediment yield of rivers in urbanizing watersheds has been measured in a variety of environments (Russell et al., 2018; Russel et al., 2017), and sediment budgets of urban rivers been successfully used to investigate historical shifts in sediment transport (Downs et al., 2018). Few studies apply bedload tracking as a means to measure the bedload transport dynamics of urban rivers and as a tool to measure the performance of urban stream management strategies. Plumb et al. (2017) employed bedload tracer stones in an urban stream, showing decreased travel distances as a result of decreased flood durations. A direct comparison of results to rivers with different levels of watershed urbanization and SWM remains to be done. MacVicar et al. (2015) studied bedload transport in a heavily urbanized creek and compared bedload transport dynamics between a restored and unrestored reach. Results showed that there as a decrease in mobility in the restored reach as compared to the control reach but only for particles in the D_{50} and D_{84} size classes, and not for particles larger or smaller (MacVicar et al., 2015). Bedload monitoring over longer timescales is required to verify observed trends, while a better methodological design to improve the statistical power of the results is needed (MacVicar et al., 2015). Furthermore, the complex relationships between bedload transport and the restored morphology captured by MacVicar et al. (2015) warrant further investigation.

2.5.6 Bedload transport in semi-alluvial rivers

Much of the bedload transport research in gravel-bed rivers is focused on alluvial rivers, while less emphasis is placed on semi-alluvial settings. Semi-alluvial rivers are those whose bed cover is comprised of both alluvial and non-alluvial material, the latter of which can be either bedrock or

sediment of a different origin. In North America, many semi-alluvial rivers are eroding into glacial sediments (Ashmore & Church, 2001; Ebisa Fola, 2010; Phillips & Desloges, 2015b; Thayer et al., 2016). In Southern Ontario in particular, these glacial sediments comprise of dense and compact silt or clay containing varying amounts of coarse gravel (Sharpe et al., 1997). The lack of high tomography to introduce colluvial inputs into the channel means that coarse material is sourced directly from the underlying till layers in (Figure 2.9). These glacially-conditioned semi-alluvial rivers have unique geomorphic characteristics. The channel profiles of these streams have a characteristic convex shape that may be scalloped as the channel erodes through different layers of glacial deposits (Bevan et al., 2018; Thayer et al., 2016). The floodplain morphology has been shown to be very sensitive to the characteristics of the underlying glacial material (Phillips & Desloges, 2015b), and floodplain materials are relatively thin (Thayer & Ashmore, 2016). Hydraulic geometry relationships have also shown to differ from those in alluvial gravel-bed rivers, with clay-dominated semi-alluvial streams having greater width-to-depth ratios than alluvial sand-bed or gravel-bed rivers (Ebisa Fola & Rennie, 2010). Finally, many of these differences lead to unique distributions of stream power along the channel networks that are highly dependent on the underlying glacial surficial geology in the watershed (Phillips & Desloges, 2014).

The semi-alluvial nature of the bed cover of these rivers is also likely to affect the sediment supply and resulting grain size distribution of these rivers. The high erodibility of the till layers may be further exacerbated by the presence of the thin gravel cover (Pike et al., 2018). Furthermore, a higher fraction of fine sediments on the bed may decrease the critical shear stress for gravel mobilization (Miwa & Parker, 2017; Venditti et al., 2010), thereby altering the bedload transport dynamics of beds with a wide range of particle sizes. These unique aspects of semi-alluvial rivers suggest that bedload transport dynamics in these rivers will be different than in alluvial gravel-bed rivers. The distribution of shear stress, channel morphology, and unique sediment supply regimes of these rivers are likely to have an effect on the displacement of bed sediment at the grain scale. However, extensive bedload transport research in semi-alluvial rivers has not been done, and the bedload transport dynamics of these systems are poorly understood, particularly as it relates to the morphology and evolution of these systems.

Figure 2.9. Example of exposed till layer in two rivers in Southern Ontario, Canada. From Pike et al. (2018).

2.6 Bedload tracking techniques

Throughout the decades, techniques for bedload tracking have advanced from painted sediment to magnetic tracer stones, and most recently to radio-tracking technologies (Hassan & Ergenzinger, 2005). Radio frequency identification (RFID) tracking technology is becoming increasingly popular in river research due to advantages such as individualized particle displacement information, low cost, battery-free and robust nature (Cassel et al., 2016; Lamarre et al., 2005; Tsakiris et al., 2015). RFID technology has been employed successfully in a large variety of riverine environments (e.g. Bradley & Tucker, 2012; Hassan et al., 2013; Lamarre et al., 2005; Liébault et al., 2012; Olinde & Johnson, 2015; Schneider et al., 2014). RFID sediment tracking technology requires three components: a passive integrated transponder (PIT) that emits a unique radio frequency signal when activated through electromagnetic induction, an antenna that activates the transponder, and a reader that controls the antenna and receives the emitted signal from the transponder (Tsakiris et al., 2015). Limitations of current RFID tracking technology for bedload tracking applications are:

1) the assumption that tracer movement can be extrapolated to provide information on the movement of the entire bed (Hassan & Ergenzinger, 2005)
2) the decrease in data accuracy over time due to burial, tracer breakage or loss of tracers from the study reach (Ferguson et al., 2002, Haschenburger, 2011; Lamarre & Roy, 2008; Liébault et al., 2012)
3) the lack of continuous movement information (Hassan & Ergenzinger, 2005; Papangelakis & Hassan, 2016)

4) limitations on sediment sizes that can be embedded with a PIT tag and therefore monitored using RFID technology
5) errors associated with detection ranges including burial, tag orientation, and tag clustering (Cassel et al., 2016; Chapuis et al., 2014b)
6) the lack of information on vertical tracer position (i.e. burial) (Haschenburger, 2011; Hassan & Ergenzinger, 2005; Tsakiris et al., 2015).

Limitations (1) - (3) are fundamental limitations of tracer methodologies and are difficult to correct through improvements to the RFID tracking technique. Recovery rates of tracer stones using RFID tracking are high and remain above 80% per recovery even over long timescales (Ferguson et al., 2002; Haschenburger, 2013; Papangelakis & Hassan, 2016). However, over long timescales particles become trapped and reworked into less active parts of the channel, meaning data from tracers may no longer reflect the sediment dynamics of the entire bed (Ferguson et al., 2002). Broken tracers or those transported out of the study reach also reduce recovery rates of tracers over the course of long studies (Lamarre et al., 2005; Liébault et al., 2012). Finally, no information can be gathered about the precise movements of particles (i.e. when they moved and how far) in between recoveries (Hassan & Ergenzinger, 2005). Since multiple mobilizing events may occur between recoveries, this gap can cause further complexities in data processing and analysis (Papangelakis & Hassan, 2016). To address limitation (4), fabricated stones have allowed for the creation of the minimum size of tracer particles possible given a PIT tag size, and have shown success in application (e.g. Cassel et al., 2016; Eaton et al., 2008). The lack of transport data of smaller size classes can be supplemented with bulk sediment measurements (e.g. Plumb et al., 2017). These limitations should be considered in the analysis and conclusions drawn from studies that rely on it. Careful attention should be paid to sample sizes and seeding strategies to maximize the ability of the sediment tracking to capture sediment dynamics (Ferguson & Hoey, 2002; MacVicar et al., 2015).

Limitations (5) and (6) are based upon the technology of RFID tracking itself and can be improved with new methodological advancements. Improvements can come through optimization of tag detection ranges so that particles may be detected from a larger distance and in a more accurate spatial location. The main controls on the transponder detection range are the size of the transponder and the orientation of the transponder relative to the antenna (Chapuis et al., 2014b). Figure 2.10 shows the theoretical detection zones of PIT tags. Ensuring that tags are oriented vertically with respect to the antenna would, therefore, increase the distance from which a tag can be detected while minimizing spatial error (Chapuis et al., 2014b). If the orientation of the tag relative to the antenna is

known, the voltage of the signal can be used to calculate the distance between the tag the antenna (Tsakiris et al., 2015). An application of such a voltage analysis to field experiments would allow the determination of burial depths of tracers during recovery and lead to improved understanding of bed dynamics in addition to more accurate predictions of mobility.

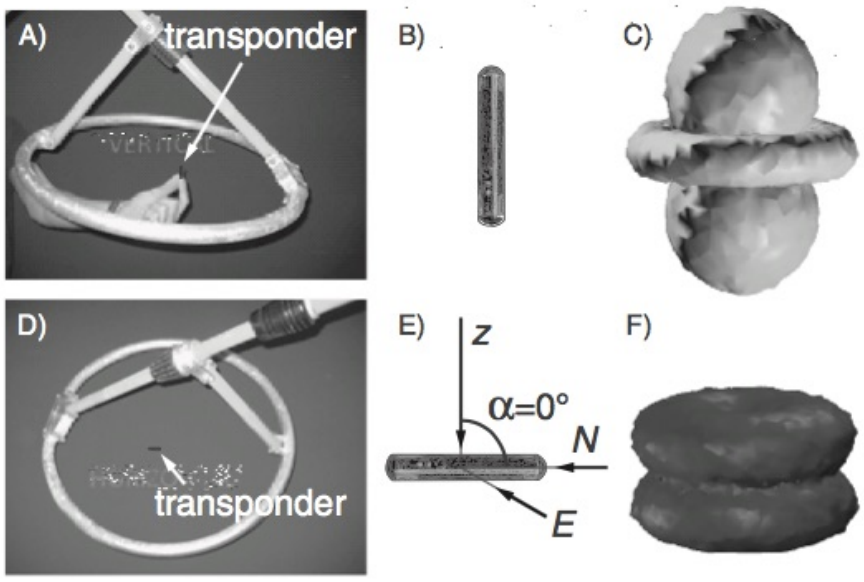

Figure 2.10. Theoretical detection ranges for a 23 mm PIT tag based on transponder orientation relative to a loop antenna with a 0.5 m detection radius. From Chapuis et al. (2014b).

2.7 Summary of research gaps

The literature presented here highlights research gaps in understanding and remediating the urban stream syndrome from the perspective of bedload sediment transport. Despite the growing literature on bedload dynamics, most studies have been conducted in flume or undisturbed river settings. Since flow, sediment supply, and bed morphology are important controls on bedload transport, it can be expected that bedload transport dynamics will change in response to urban hydromodification and both restoration and SWM infrastructure. Nevertheless, bedload dynamics in the urban context remains a significant research gap, propagated by a lack of bedload sediment transport data in urban environments (Russell et al., 2017; Shields, 2009), and the opportunity remains to apply bedload transport theory to urban rivers and those with in-stream restoration and SWM projects. An improved understanding of the bedload transport dynamics of urban rivers is imperative for improved management practices and more scientifically grounded SWM and restoration project design with a

greater probability of positively affecting urban rivers (Pasternack, 2013; Hawley et al., 2013; Hawley & Vietz, 2016; Vietz et al., 2016). Finally, the unique glacially-conditioned semi-alluvial nature of rivers in Southern Ontario presents a unique setting in which to explore differences in bedload transport dynamics in these systems as compared to alluvial gravel-bed rivers.

Transition A

Chapter 3 focuses on answering the second research question of this thesis: How do the altered in hydrologic conditions resulting from watershed urbanization and stormwater management impact the bedload transport dynamics of rivers? The aim is to move away from comparative studies that document trends between channel dimensions and other geomorphological markers between streams with different land-use scenarios, and towards measuring the processes that drive morphological responses in urban rivers – bedload transport. Bedload sediment data is scarce, and even more so in urban environments (Wohl et al., 2015a). Although recent studies have documented or modelled changes in bulk sediment transport rates in urban rivers (e.g. Russell et al., 2018; Plumb et al., 2017), few have described the grain-scale dynamics of urban rivers in detail. Plumb et al. (2017) and MacVicar et al., (2015) employed bedload tracking in urban rivers, but no studies have directly compared bedload transport dynamics at the grain scale among rivers with different land-use and SWM characteristics. In Chapter 4 we use a space-for-time substitution to investigate how the grain-scale bedload transport dynamics change with urbanization and SWM, and whether these differences can explain the observed morphologic adjustments. The bedload sediment transport regime of three rivers with different watershed settings is characterized: rural, urban with no SWM, and urban with SWM. Chapter 3 presents empirical evidence of the effects of watershed urbanization and SWM on bedload transport and bed morphology, and provides recommendations for process-based urban river management strategies.

Chapter 3

Bedload Sediment Transport Regimes of Semi-Alluvial Rivers Conditioned by Urbanization and Stormwater Management

This chapter is based on the following published manuscript:

Papangelakis, E., MacVicar, B., & Ashmore, P. (2019). Bedload sediment transport regimes of semi-alluvial rivers conditioned by urbanization and stormwater management. *Water Resources Research.*DOI:10.1029/2019WR025126

Data presented in this chapter can be found at:

Papangelakis, E., MacVicar, B., Ashmore, P. (2019). Bedload sediment transport and morphologic data in semi-alluvial rivers conditioned by urbanization and stormwater management [Dataset]. https://dx.doi.org/10.20383/101.0172

3.1 Introduction

Watershed urbanization alters the hydrologic and geomorphic processes of rivers (Ladson et al., 2006), leading to the widespread degradation of urban river ecosystems (Booth et al., 2015; Walsh et al., 2005). The combination of increased runoff, efficient stormwater systems, and decreased sediment supply characteristic of urban watersheds results in channel instability and adjustments to river morphology (Bledsoe & Watson, 2000; Booth, 1990; Simon & Rinaldi, 2006). Consistent trends between pre- and post- urbanization include channel enlargement through widening and incision (Bevan et al., 2018; Bledsoe & Watson, 2001; Galster et al., 2008; Gregory et al., 1992; Hawley et al., 2013; Pizzuto et al., 2000; Trimble, 1997), decreased riffle lengths (Hawley et al., 2013), and bed coarsening (Chin, 2006; Pizzuto et al., 2000). Stormwater management (SWM) has become ubiquitous in urban watersheds to combat increased flows from urbanization. The most common SWM strategy is the 'peak shaving' approach, in which retention ponds are used to store excess runoff and release it over time. This approach successfully reduces flow magnitudes but extends the duration of erosive discharges (Bledsoe, 2002; Bledsoe & Watson, 2001; Nehrke & Roesner, 2004; Pomeroy et al., 2008; Rohrer & Roesner, 2006). Although sediment transport is recognized as an important process in the physical and ecological function of urban rivers (Hawley & Vietz, 2016; Wohl et al., 2015a), bedload sediment transport in urban settings remains a research gap (Russell et

al., 2017), particularly as a means to assess the success or failure of measures meant to mitigate river degradation.

Dating back to Leopold (1956), land-use change has been connected to changes to sediment yield and channel adjustment (Chin, 2006). The imbalance between decreasing sediment supply and increasing erosive forces has been used to explain urban channel enlargement (Bledsoe and Watson, 2000; Booth, 1990; Schumm, 1977). Recent studies aim to quantify links between degrees of urbanization and watershed-scale hydrologic variables, and increases in total bedload yield through bulk sediment measurements (e.g. Russell et al., 2018) or sediment transport models (e.g. Plumb et al., 2017). However, despite advancements in grain-scale bedload transport theory in flume and rural settings, its application to urban rivers remains limited. The importance of flow and sediment supply to grain mobilization and dispersion means the grain-scale transport dynamics of urban rivers can be expected to differ from those in undeveloped watersheds. Plumb et al. (2017) applied particle tracking to characterize grain-scale dynamics in an urban gravel-bed river and found that despite increased peak flows, particles travelled shorter distances compared to non-urban streams, which was explained by shortened event durations. Opportunity remains to directly compare bedload transport dynamics in rivers with different hydrologic settings and their relationship to channel morphology and evolution. Furthermore, bedload transport regimes of rivers with retention ponds is likely driven by the increased duration of flows above the threshold for mobilization (Booth, 1990; Bledsoe, 2002; Rohrer & Roesner, 2006; Tillinghast et al., 2011; Tillinghast et al., 2012). Little empirical data exists, however, to quantify bedload transport in rivers with SWM and establish its relationship to channel morphology (Baker et al., 2008).

Tracking the movement of individual particles provides insights into the controlling parameters of bedload transport (Haschenburger & Church, 1998) as it allows direct comparison of responses to flood events, captures the speed of bed sediment dispersion (Bradley & Tucker, 2012), and is more sensitive to spatial variability in bedload transport (Haschenburger & Wilcock, 2003) compared to bulk samples. It has been established that bedload transport predominantly occurs as partial transport, where only a fraction of particles on the bed surface are mobile, and that mobility increases with flow towards a condition of full mobility (Wilcock & McArdell, 1997). The displacement of bedload sediment is also dependent on grain size so that transport is size-selective; mobility and travel lengths decrease with increasing grain size, and the difference among grain sizes diminishes with increasing flow (Ashworth & Ferguson, 1989; Church & Hassan, 1992; Ferguson & Wathen, 1998; Parker & Klingeman, 1982; Parker & Toro-Escobar, 2002; Wilcock & McArdell, 1997). Relationships have also been found between tracer travel lengths, and flow variables including

shear stress (Ashworth & Ferguson, 1989; Phillips & Jerolmack, 2014; Wilcock & McArdell, 1997; Wong et al., 2007), peak discharge (Haschenburger & Wilcock, 2003), and excess stream power (Gintz et al., 1996; Hassan et al. 1991, 1992; Lenzi, 2004; Schneider et al., 2014), allowing tracers to be used as a method to assess the effects of hydrologic change on sediment transport. Bedload tracers can also be used to directly link bedload transport to morphologic change, as the tracer dynamics are related to reach-scale channel morphology (Hassan & Bradley, 2017; Papangelakis & Hassan, 2016; Vazquez-Tarrio et al., 2019), as well as the maintenance and evolution of bedforms (MacVicar & Roy, 2011; Milan, 2013a; Pyrce & Ashmore, 2003a; 2005).

The nature of the bed cover is also expected to influence bedload transport. Glacially-conditioned rivers in Southern Ontario have been referred to as 'semi-alluvial' in that they are characterized by a thin and transient cover of alluvial material over a cohesive glacial till layer (Ashmore & Church, 2001). The alluvial cover is sourced from the erosion of the underlying till layers, and varies in extent, thickness, and grain size (Pike et al., 2018; Thayer & Ashmore, 2016). Research in bedrock-alluvial channels has shown size-independent transport of the alluvial material, as well as lower threshold shear stresses for sediment mobilization and higher rates of dispersion compared to alluvial gravel-bed rivers (Hodge et al., 2011). Although the floodplain morphology (Phillips & Desloges, 2015b; Thayer & Ashmore, 2016) and channel evolution (Bevan et al., 2018) of glacially-conditioned semi-alluvial rivers have been explored, little is known about the transport dynamics of the alluvial cover, its relationship to channel morphology, and how it may change in response to urbanization or SWM.

The goal of this study is to assess the effect of different hydrologic conditions resulting from watershed urbanization and SWM on the bedload sediment transport regimes of glacially-conditioned semi-alluvial rivers. Three streams were chosen to represent a rural watershed, an urban watershed with no SWM, and an urban watershed with SWM. Specific objectives are to: (1) characterize the grain-scale bedload sediment dynamics in a rural stream with a semi-alluvial bed; (2) assess whether differences in sediment transport dynamics in an urban river can explain trends of channel enlargement and degradation; and (3) evaluate the degree to which SWM offers protection from changes to bedload transport dynamics that result from urbanization. By focusing on the grain-scale, this study provides a process-based perspective on the morphologic changes that occur in rivers because of urbanization and common SWM strategies. The intent is that this research will lead to management strategies that, rather than trying to arrest common symptoms such as channel enlargement, are informed by fluvial process.

3.2 Study sites

Three streams in the Greater Toronto Area of Southern Ontario, Canada, were selected for this study (Figure 3.1). The study streams differ in watershed land-use characteristics and presence of SWM infrastructure (Table 3.1) but to facilitate direct comparisons, sites were selected to minimize differences in surficial geology, bed slope, drainage area (DA), and grain size distributions (Table 4.1; Figure 3.2). A study reach of 15–20 channel widths long was chosen in each stream to adequately capture the channel morphology (Montgomery and Buffington, 1997). All three streams are semi-alluvial, which in this geologic context means they have a layer of alluvial gravel cover overtop of cohesive glacial till that is exposed intermittently in areas of the bank and bed. The till layer is Newmarket Till (Sharpe et al., 1997), which is a dense silty diamicton containing > 5% gravel and the source of coarse sediment inputs to the channels through erosion (Pike et al., 2018; Sharpe et al., 1997). The study reaches are located within glaciolacustrine valley complexes (up to 40 m deep) that formed due to a downstream decrease in base level when glacial Lake Iroquois drained and the modern Lake Ontario was formed (Thayer et al., 2016).

Figure 3.1. Location of study sites representing three watershed conditions: undeveloped (Ganastekaigon Creek), urban with no SWM (Wilket Creek), and urban with SWM (Morningside)

Table 3.1. Study creek characteristics and mean channel dimensions. TOB stands for 'top-of-bank'.

Creek	Total DA (km^2)	DA at Reach (km^2)	Reach Slope	Mean TOB Width (m)	Mean TOB Depth (m)	% Watershed Developed[a]	% Watershed Impervious[a]
Ganatsekaigon	13.6	12.6	0.012	9.9	1.0	12	4
Wilket	14.9	13.0	0.010	12.5	1.4	96	68
Morningside	18.8	15.3	0.011	6.2	0.6	76	46

[a]Calculated from satellite data

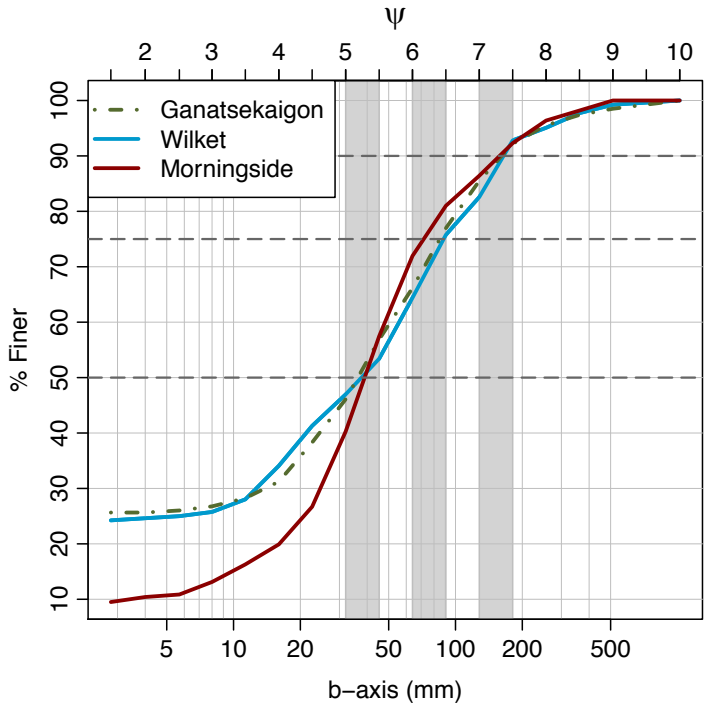

Figure 3.2. Surface grain size distributions of the study sites. The size classes of the D_{50}, D_{75}, and D_{90} are highlighted in grey.

Ganatsekaigon Creek was chosen to represent a watershed with a rural hydrologic condition. Land-cover in the watershed is primarily agriculture and forest (Table 3.1). The channel is well connected to the floodplain and large amounts of wood debris are supplied to the channel, resulting in channel-spanning log jams throughout the stream network. Beavers further introduce wood to the channel and contribute to the intermittent damming of the stream. The chosen study reach begins downstream of a channel-spanning log jam and has minimal in-stream wood. Fine sediment in the stream is primarily sand (20%), with a smaller amount of silt (3%). The site has a well-defined riffle-pool morphology, with an average riffle spacing of approximately 3 bankfull widths (Figure 3.3a).

Wilket Creek was chosen to represent a watershed with an urban hydrologic condition that is unmodified by SWM. Land-cover in this watershed is primarily residential housing of mixed density and some areas of dense mixed-use commercial development. Development occurred in the 1950s and 60s, and there is no significant SWM infrastructure in the watershed (TRCA, 2015). Watershed connectivity is high because road networks and roof leaders/foundation drains are typically connected to storm sewers (D'andrea et al., 2004). All tributaries to the creek and most of the main stem were replaced with underground sewers as a part of land use change. Currently only ~6 km of the main stem remains as an open channel. At the study site, the channel is well connected to the floodplain, with only local constraints at the apex of some meanders due to the high valley walls. Extensive channel stabilization and restoration efforts have been undertaken throughout the channel (Barr, 2017; TRCA, 2015), but the study site was selected because it has minimal in-stream engineering, although one section is locally constrained (Segura & Booth, 2010) where it is narrowed with reinforced banks and bed to protect a sanitary sewer (beneath the river) and a footbridge. Large wood is added to the creek due to erosion of the floodplain, but is periodically removed from the channel by city staff. Fine sediment in the stream is mostly sand (19%), with some silt (5%). The study site has a riffle-pool morphology, with an average riffle spacing of 3 bankfull widths (Figure 3.3b). Over the past sixty years, Wilket Creek has undergone significant channel enlargement, with the channel 75% wider (10.5 to 18.4 m) and 50% deeper (0.87 to 1.30 m) in 2016 relative to a 1958 survey of the creek (Bevan et al., 2018). Historic dimensions are close to the current dimensions of Ganatsekaigon Creek. Channel evolution has not followed the classic model developed by Schumm et al. (1984) and Simon (1989) due to the influence of the semi-alluvial bed (Booth and Fischenich, 2015). Instead, the system has been characterized by channel widening and deepening, increased exposure of the till bed, and an increased tendency for channel avulsions (Bevan et al., 2018).

Morningside Creek was chosen to represent an urbanized watershed where the hydrology is further conditioned by SWM. Land cover in this watershed is primarily low-density residential with some industrial uses (Table 4.1). Development occurred within the last 30 years, and SWM infrastructure planned and implemented alongside the land-use change (Badelt, 1999; Raso, 2017). Currently, seven offline retention ponds, one online pond, and a high flow diversion weir operate within the watershed. An active beaver population intermittently dams the stream, further complicating storm hydrographs. At the study site, the channel is well connected to the floodplain and free of channel-spanning log jams with minimal influence of in-stream wood. Morningside Creek has a smaller fraction of fine sediments (Figure 3.2); sand and silt fractions are reduced to 9% and < 1%, respectively, due to retention of fine sediment in the SWM ponds (Badelt, 1999). Channel

morphology is a plane bed, characterized by a lack of bars and long stretches of relatively featureless runs (Figure 3.3c). Where pools and riffles exist, they are less defined than in the other two streams. Morningside Creek is narrower and shallower than Ganatsekaigon Creek (Table 4.1), which suggests that it has evolved into a narrower channel with an armoured bed and fewer bedforms, though no pre-urbanization surveys from near the study site are available. A previous geomorphic assessment of a headwater reach of Morningside Creek found the channel downstream of the retention ponds did evolve into a morphologically inactive state in response to the decreased flood magnitudes and lack of sediment supply (Badelt, 1999).

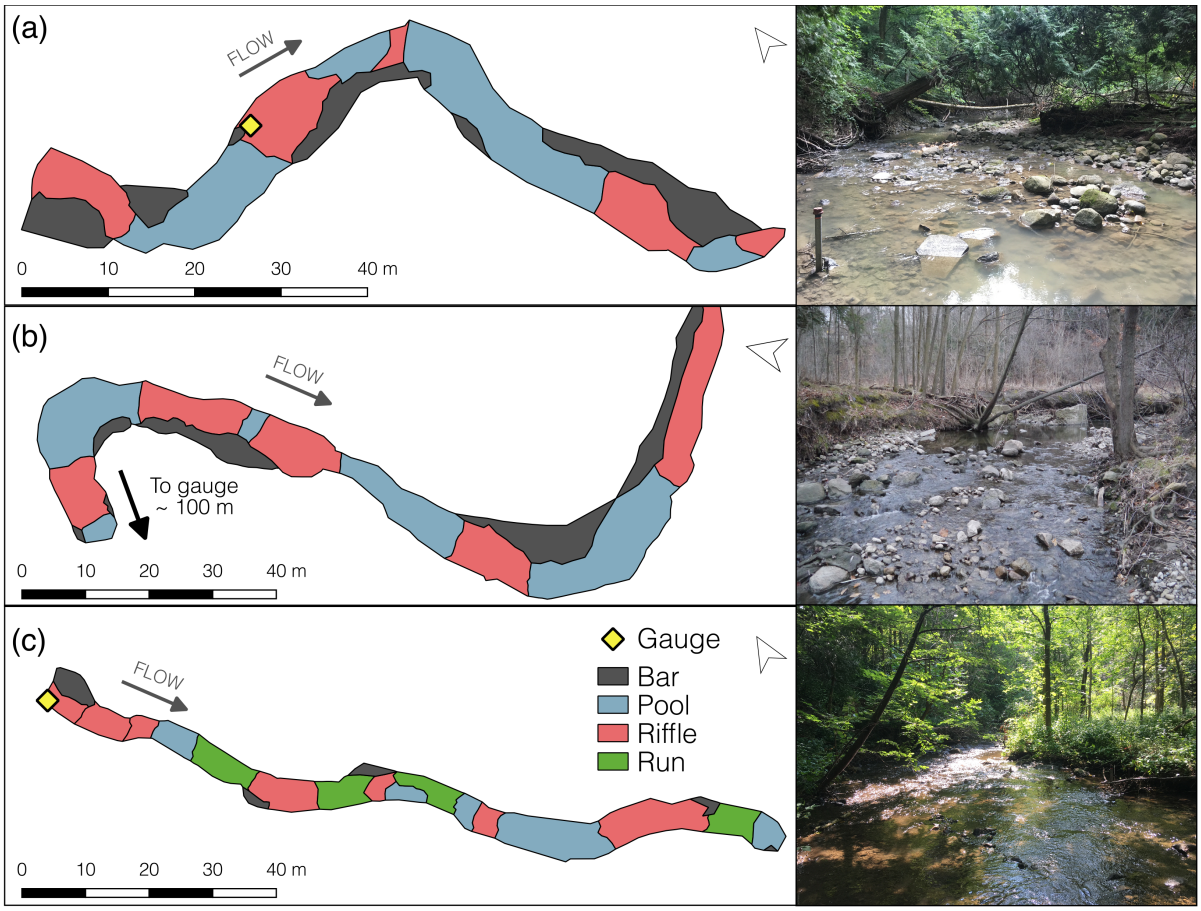

Figure 3.3. Map of study reaches shoring morphological units and photo of (a): Ganatsekaigon Creek, (b): Wilket Creek, and (c): Morningside Creek. Morphological units were based on visual field assessment following Montgomery & Buffington (1997).

As part of the site investigation stage, preliminary measurements of water level variation during floods were used to give a rapid assessment of hydrologic differences among the streams (Figure 3.4). A sample of three floods from 2015 shows that Wilket Creek typically has a higher

flood peak flow depth than Ganatsekaigon Creek, with more rapidly rising and falling limbs on the storm hydrographs (Figure 3.4). These observations match what has been found in other studies of hydrologic change in urban watersheds both locally (Barr, 2017; Trudeau & Richardson, 2015; Trudeau & Richardson, 2016) and around the world (Bledsoe and Watson, 2001; Walsh et al 2005; Chin, 2006). Wilket Creek also shows signs of a daily flow cycle, with higher flows in the daytime likely linked with cross-connected sanitary sewers or other urban activities such as lawn watering. Hydrographs in Morningside Creek show increased flow depths relative to Ganatsekaigon Creek and elongated falling limbs. Relative to Wilket Creek the flood peaks are reduced and lagged in time. A detailed hydrologic model of the Morningside watershed was used to demonstrate up to 87% reduction of peak flows due to routing of flows through the existing SWM infrastructure (Raso, 2017), which matches what is expected from SWM infrastructure designed for flood peak control (Bledsoe, 2002).

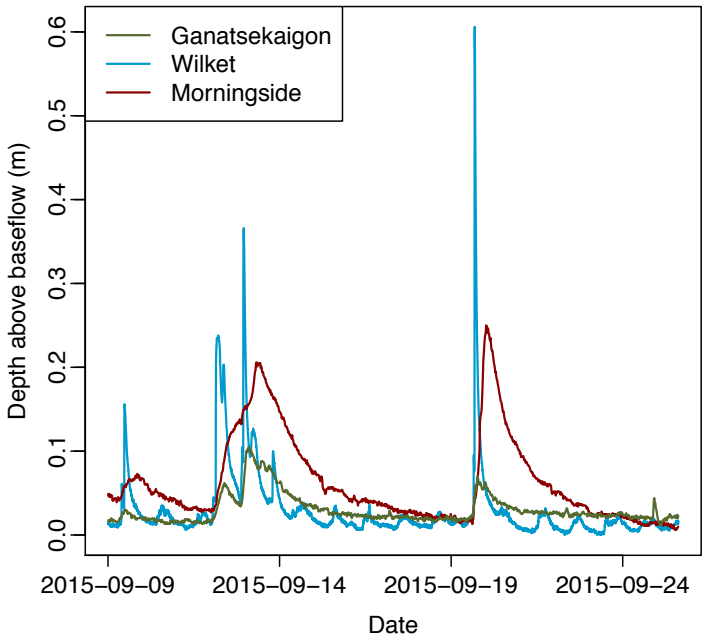

Figure 3.4. Examples of typical hydrographs in each study stream.

3.3 Methods

3.3.1 Hydrology

Water level was recorded using pressure transducer gauges (HOBO-U20 Water Level Data Logger, Onset) from a gauge at each reach. Logging intervals were set to 1–2 minutes during the active field

season (April–November), and 7 minutes during the winter season (December–March) to ensure that the data did not have to be downloaded when the streams were frozen. Raw pressure was converted to mean water depth (h) through barometric compensation using atmospheric pressure data collected at each site. Depth was converted to discharge in Wilket Creek using a stage-discharge rating curve based on velocity measurements from a handheld radar gun (Surface Velocity Radar, Decatur Electronics Inc.). The curve was calibrated for flows between 1.6–12 m^3/s but was extrapolated for higher discharges following a Keulegan-type flow resistance equation. The Toronto and Region Conservation Authority (TRCA) operates gauges with established stage-discharge rating curves in Ganatsekaigon Creek and Morningside Creek, so discharge was calculated at each stage in these creeks by applying a local drainage area weighting relationship from Phillips and Desloges (2014):

$$Q_1 = Q_2 \left(\frac{DA_1}{DA_2}\right)^{0.863} \tag{3.1}$$

where Q_i and DA_i are the discharge and drainage area at each gauging location.

3.3.2 Morphology

To capture morphologic change in the three study sites over the duration of the study, detailed topographic surveys were conducted using a total station ($\pm$ 2mm error) and benchmarks with known coordinates. Two surveys were conducted in each site during the summers of 2016 and 2018 with a point density of 0.81–1.79 points/m^2. A Digital Elevation Model (DEM) of the channel bed was created using a Triangular Interpolation Network (TIN). Surveys were 'morphologically based' so that changes in bedform slopes were captured, providing an accurate representation of the bed surface after interpolation (Chapuis et al., 2015; Heritage et al., 2009). DEM of difference (DoD) maps were then created by subtracting the 2016 DEM from the 2018 DEM in each stream. Survey errors in the raw DEMs were estimated from repeated surveys of the known benchmarks giving a mean standard error of 0.01 m for distance and 0.008 m for elevation.

3.3.3 Sediment tracking

Bedload sediment transport was monitored using tracer stones equipped with Radio Frequency Identification (RFID) passive integrated transponder (PIT) tags. This technology has been widely applied for assessing the sediment transport regime of gravel-sized particles because it offers high recovery rates, battery-free hardware that is robust, and unique identification codes (Lamarre et al., 2005). Decisions about the number and size of tracers in the river require a consideration of competing needs to maintain large samples sizes, which maximize the statistical precision of results

(Ferguson & Hoey, 2002; MacVicar et al 2015), while not overcrowding the tracers on the bed, which can lead to RFID signal 'collision' where tracers cannot be detected because they are too close together (Chapuis et al, 2014b). Three size classes of tracers were seeded in each site with median b-axis diameters corresponding to the half-phi size classes of the D_{50}, D_{75} and D_{90} particles of the field sites, equal to 5–5.5, 6–6.5, and 7–7.5 ψ, respectively ($\psi = -\phi = -\log_2 D$, where D is the particle b-axis in mm) (Figure 3.5). Coarse particles are the focus of this study due to their importance in controlling channel dynamics (MacKenzie et al., 2018). These coarser particle sizes are predominant on the surface of riffles and the comparison between sites and size classes allowed us to assess differences in the size selectivity of sediment transport. A larger number of smaller tracers were seeded to counteract the effect of smaller tracers having higher loss rates (Ferguson and Hoey, 2002). A total of 300 tracers were seeded in each stream, with approximately 150 tracers in the 5–6 ψ class, 100 tracers in the 6–7 ψ class, and 50 tracers in the 7–8 ψ size class (Figure 3.5b). Slight discrepancies in the number of tracers in each reach are due to some tracers falling outside the targeted size classes.

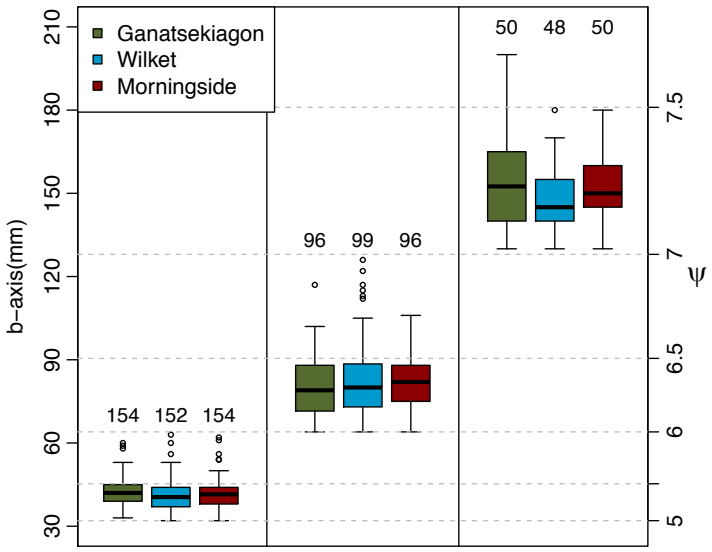

Figure 3.5. Boxplot of tracer b-axis diameters in each of the three tracer size classes. Numbers above each boxplot are the number of tracers in that size class.

Tracers were created from stones randomly sampled from each stream to preserve the natural distribution of particle shape and density. Stones were returned to the lab where they were drilled, embedded with a 23 mm tag (HDX PIT tag; ISO 11784/11785), and sealed with silicone. Once tagged, tracer stones were returned to the site from which they were taken and seeded in groups of

150 tracers on two sequential riffles. The tracers were randomized based on size and placed across the entire width of channel in a series of lines perpendicular to the flow. Tracers were separated by approximately 1 m to reduce the risk of signal collision. A replacement method was used where an in-situ stone was removed from the bed and a tracer of similar size was placed in the empty spot to mimic the natural structural arrangement of the bed (Bradley & Tucker, 2012; Chapuis et al., 2015; Gintz et al., 1996; Liébault et al., 2012). This method attempts to minimize the effects of surface tracers being readily available for transport during early flow events (Hassan et al., 1991).

Tracers were monitored from August 2015 until the end of July 2018. An attempt was made to locate the positions of the tracers following each mobilizing flow event. No recoveries took place during the winter season due to difficult tracking conditions. In the summer the rapid succession of floods made it impossible isolate all events. A loop antenna with a 0.5 m detection radius (pole antenna and LF HDX Backpack Reader, OregonRFID Inc.) was used to locate tracers in areas where they were sparsely distributed, while a stick antenna with a 0.2 m detection radius (AEA580 antenna with DataTracer II Reader, OregonRFID Inc.) was used to locate tracers where they were closer together. The stick antenna was also used to improve the precision of tracer locations first detected with the loop antenna, though this was not always possible due to the lower detection range. Tracer positions were surveyed using a total station.

Tracers recovered on at least ten occasions between August 2015 and July 2018. More surveys were completed for Wilket (12) and Morningside Creeks (13) due to more frequent floods at these sites. The total length of the study exceeds the 2-year minimum recommended by Houbrechts et al. (2015) to minimize flood variability. Mean recovery rates of tracer surveys were between 95 and 97%, which is exceptionally high in comparison with past studies and other tracer techniques (see Chapuis et al. 2014b for a review). Recovery rates include tracers that were not found in the field but whose positions could be inferred based on subsequent surveys because they had not moved. Recovery rates decreased over time, but the recovery rates of the final surveys remained high at 80–93%. A complete summary of the tracer recovery dates and recovery rates can be found in the Appendix (Table A.1).

3.3.4 Analysis

The analysis for the current study is based on a comparison of shear stress (τ) and specific stream power (ω) with the fraction of tracers that are moved each flood, the travel length of mobile tracers, and the 'virtual velocity' of the tracers, defined as the average rate (m/year) at which particles are moved downstream. The flow metrics are for peak flood values, which are thought to exert a

dominant control on tracer displacement (Hassan et al., 1992). Peak metrics have been used in many previous tracer studies of sediment transport (e.g. Gintz et al., 1996; Haschenburger & Wilcock, 2003; Hassan et al., 1991; Lenzi, 2004; Schneider et al., 2014), which can be used for comparison and an assessment on the limitations of this approach for the characterization of systems with different shaped hydrographs. A summary of river characteristics from other tracking studies used for comparison can be found in the Appendix (Table A.2).

Shear stress is the force of friction induced by the flow on the channel bed. Depth measurements were converted to shear stress (τ, Pa) following the definition:

$$\tau = \rho_w g R_h S \tag{3.2}$$

where $\rho_w$is the density of water (1000 kg/m^3), g is the acceleration due to gravity (9.81 m/s^2), R_h is the hydraulic radius (m), and S is the reach-averaged slope (from Table 4.1). Shields (1936) showed that sediment mobility occurs when the shear stress exceeds a critical value (τ_c):

$$\tau_{ci} = \tau^*_{ci}(\rho_s - \rho_w) g D_i \tag{3.3}$$

where ρ_s is the stone density (2700 kg/m^3 based on the mean of samples (n = 900) from the field sites), and τ^*_{ci} is the critical dimensionless Shields parameter that was chosen using the tracer data.

The specific stream power (ω, W/m^2) is the rate of energy dissipation per unit area of the channel bed (Bagnold, 1966). Stream power is an important flow metric for hydraulic research and has been used to model river morphology (Phillips & Desloges, 2014; van den Berg, 1995), bedrock incision (Lague, 2014), and sediment transport (Ferguson, 2005; Hassan et al., 1992). Peak specific stream power (ω_p) was calculated as:

$$\omega_p = \frac{\rho_w g Q_p S}{B} \tag{3.4}$$

where Q_p is the peak discharge of a flood, and B is the channel bed width (m). The critical stream power of the D_{50} grain size (ω_{cD50}) was calculated by determining the discharge corresponding to the shear stress threshold (Q_{cD50}) using the calibrated rating curves.

Tracers were classified as 'moved' or 'unmoved' for each flood period. A stone was considered to have moved if the distance between two recorded locations was greater than two times the precision of the technique (i.e. > 0.5 m for stones found with the stick antenna, and >1 m for stones found with the loop antenna). These thresholds minimize false classification of particle movement. The fraction of tracers that moved over the entire duration of the study was calculated for the entire tracer population (F_m), as well as by size class (F_{mi}) as:

$$F_{m(i)} = \frac{m_{(i)}}{n_{(i)}} \tag{3.5}$$

where $m_{(i)}$ is the number of stones that moved since the last recovery and $n_{(i)}$ is the total number of stones that were found in both that recovery and the previous recovery. The fraction of tracers that moved each recovery was also calculated for the entire tracer population (f_m) and for each size class (f_{mi}). The 95% confidence intervals were calculated as the binomial proportion confidence interval (CI_{Fm}):

$$CI_{95} = z\sqrt{\frac{F_{m(i)}(1-F_{m(i)})}{n_{(i)}}} \tag{3.6}$$

where $z = 1 - \frac{\alpha}{2}$ with a significance level set to $\alpha = 0.05$.

The mean travel length of mobile tracers for each recovery period was also calculated for the entire tracer population (L), as well as by size class (L_i). Due to the skewness in travel length distributions, the geometric mean was used for a more representative measure of the central tendency of tracer travel length (MacVicar et al., 2015). The 95% confidence intervals for $L_{(i)}$ values were calculated as:

$$CI_{95} = 10^{z\frac{\sigma_{\log(\lambda)}}{\sqrt{n_{(i)}}}} \tag{3.7}$$

where $\sigma_{\log(\lambda)}$ is the standard deviation of the log-transformed travel lengths (λ).

Virtual velocity has been defined as the rate of downstream travel of tracer stones either over single events (following Hassan et al., 1992), or over several years (Houbrechts et al., 2015). This study used the latter method to quantify the long-term downstream travel rate of sediment (in m/year) and assess the influence of urbanization and SWM on sediment displacement. Virtual velocity was calculated for each size class as the mean cumulative travel length over the entire duration of the study (including immobile tracers), divided by the total length of study (2.75 years in Ganatsekaigon Creek and Wilket Creek, and 2.92 years in Morningside Creek).

3.4 Results

3.4.1 Shear stress thresholds

Shear stress thresholds were used to assess entrainment conditions and compare between reaches. The fraction of stones that moved each recovery was used to identify events with low mobility, and the peak shear stress from these events was assumed to represent the critical shear stress (see table A.1 for values). One tracer recovery in Morningside Creek was excluded from this analysis because the flow hydrograph corresponding to the maximum precipitation event was not recorded due to a

pressure transducer malfunction (see Table A.1). Sediment entrainment shear stress thresholds are similar for the three field sites, both in terms of shear stress and water depth (Table 3.2). This result verifies the experimental strategy of the study because it demonstrates that the similar slopes and median grain sizes of the study sites translate to similar entrainment thresholds. A dimensionless critical shear stress of the D_{50} size class τ^*_{cD50} = 0.047 was a good fit for all sites. This value agrees with results from other studies of gravel-bed rivers (Buffington & Montgomery, 1997). To account for the effects of pocket geometry resulting from a wide grain size distribution on the critical shear stress, a hiding function (Egiazaroff, 1965) was required to adequately calibrate the τ^*_{ci} value of tracer sizes classes larger or smaller than the median particle size of the bed (D_i):

$$\frac{\tau^*_{ci}}{\tau^*_{cD50}} = \left[\frac{\log(19)}{\log\left(19\frac{D_i}{D_{50}}\right)}\right]^2 \tag{3.8}$$

Critical shear stress values obtained through the hiding function were similarly verified by comparison with peak shear stresses during recoveries when tracer mobility of these size classes was very low (Raso, 2017). Overall, the consistent shear stress thresholds for the three systems and the alignment of the dimensionless thresholds with values from the literature show that the unique semi-alluvial nature of the bed does not fundamentally alter the entrainment mechanics of these rivers.

The study sites experienced different magnitudes and frequencies of mobilizing events. Due to the larger size of the channel, Wilket Creek has a critical discharge over three times what is required to move D_{50} size class in the other channels (Table 3.2). Despite this high threshold, this urban channel experienced more than four times the number of events exceeding the threshold, and the peak discharge recorded during the study was estimated to be double that of the rural channel (Table 3.2). However, the mean event peak shear stress was slightly higher in the rural creek, which is explained by the narrower width of the channel. In contrast, many trends are reversed in Morningside Creek so that the peak discharge is an order of magnitude less, and the peak stress is about 75% lower than in the rural channel. Events above the threshold are fewer, but the durations were over double than in the rural channel and over 7 times longer than in the urban system without SWM. The differences in mobilizing events are consistent with what is expected from urbanization and SWM. Increases in the frequency of bed mobilization is documented in other urban rivers (Anim et al., 2018; Hawley & Bledsoe, 2011), while over 50% increases in the duration of mobilizing flows due to peak-shaving SWM approaches has been previously demonstrated through hydraulic modelling (Bledsoe, 2002).

Table 3.2. Summary of frequency, magnitude and duration of flow events over the duration of the study.

	Ganatsekaigon	Wilket	Morningside
Critical shear stress (τ_{cD50}) (Pa)	32.9	31.4	32.1
Critical depth (h_{cD50}) (m)	0.49	0.40	0.45
Critical discharge (Q_{cD50}) (m^3/s)	1.5	4.7	1.1
Number of events > τ_{cD50}	18	81	16
Mean duration > τ_{cD50}	6.7	2.1	15.0
Mean event peak discharge (m^3/s)	4.6	9.5	1.5
Mean event peak shear stress (Pa)	49.3	45.2	41.6
Maximum discharge (m^3/s)	19.2	39.7	3.0
Maximum shear stress (Pa)	95.8	103.7	71.7

Cumulative distribution functions of shear stresses exceeding the τ_{cD50} in each stream show that Ganatsekaigon and Wilket Creek were subject to similar distributions of excess shear stress, while the distribution of shear stresses in Morningside Creek was clearly modified by the SWM 'peak-shaving' infrastructure. As shown in Figure 3.6, excess shear stresses were never more than ~35 Pa in Morningside Creek. In contrast, approximately 5% of excess shear stress values measured in the other two systems exceeded this value, with maximum excess shear stresses reaching 60-70 Pa. For these rare floods, the urban Wilket Creek values slightly exceed those of the rural Ganatsekaigon Creek, but overall the distributions in these two systems are similar in shape despite the differences in land use between the two watersheds. This somewhat surprising result may be because of the low water infiltration capacity of the regional soils and tile draining from agricultural fields, which likely lead to high runoff values during intense storms even before urbanization. At lower excess shear stresses, the trends are reversed so that Morningside Creek experiences an excess shear stress of 25 Pa approximately 20% of the time during floods, while this level of stress occurred < 10% of the time during floods in the other systems. This level of excess stress is close to the threshold of the D_{90} so that this coarse fraction was subject to mobilizing stress for a total of 16.8 hours in Morningside Creek during the study, which occurred over a single event. This duration far exceeds that measured in the rural stream (5.6 hours), and exceeds that in the urban system without SWM (12.1 hours), despite the urban stream experiencing 13 events > τ_{cD90}.

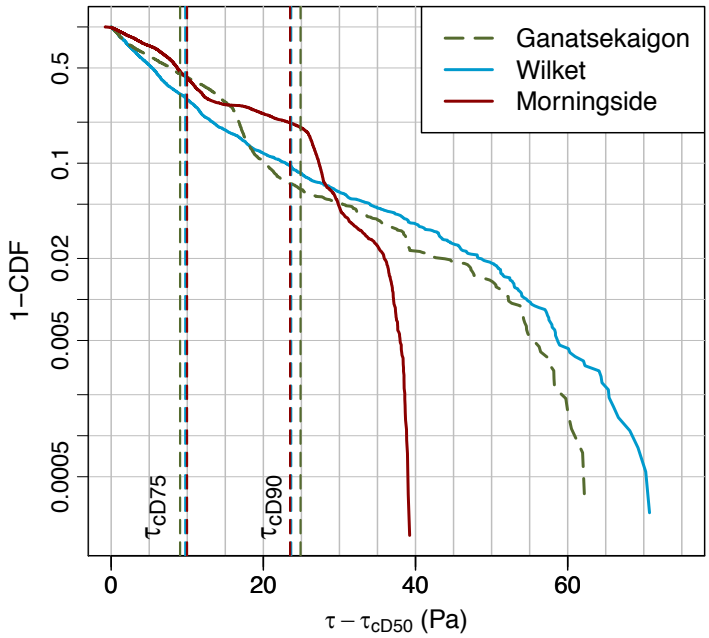

Figure 3.6. Cumulative distribution curves of shear stresses exceeding the τ_{cD50} in each study stream.

3.4.2 Morphologic change

Changes in bed morphology between 2016 and 2018 were mapped to provide context for the relationship between tracer displacement and morphologic change. The DODs demonstrate differences in the magnitude and spatial location of morphologic change among the three streams (Figure 3.7). Ganatsekaigon Creek experienced the largest changes over the study period. Two high flow events on June 23 and July 17 of 2017 resulted in a small avulsion at the upstream bend, reflected as erosion at the upstream bar and deposition at the subsequent bar downstream in the DOD (Figure 3.7a). Photographs of the avulsion can be found in the Appendix (Figure A.1). The lack of sediment to replace eroded sediment at the upstream bend may be due to the channel-spanning log jam at the upstream limit of the study reach trapping sediment and disrupts sediment delivery. The DOD of Wilket Creek shows less drastic changes to morphology compared to Ganatsekaigon Creek, with an overall trend of deposition and isolated pockets of erosion (Figure 3.7b). This trend is counter to the channel enlargement that has occurred (Bevan et al., 2018), but may be explained by local effects of wood. The most notable area of change is the downstream pool showing aggradation of > 30 cm, which can be attributed to the accumulation of fine woody debris that trapped fine sediment (Figure A.2). Furthermore, the DODs presented here are only between two topographical surveys, providing limited information on possible scour and fill cycles occurring (e.g. MacVicar and Roy,

2011). Morningside Creek experienced the least morphologic change over the duration of the study (Figure 3.7c). Only one significant area of scouring is evident at the downstream end, which coincides with where a log jam was dislodged over the winter season of 2017–2018.

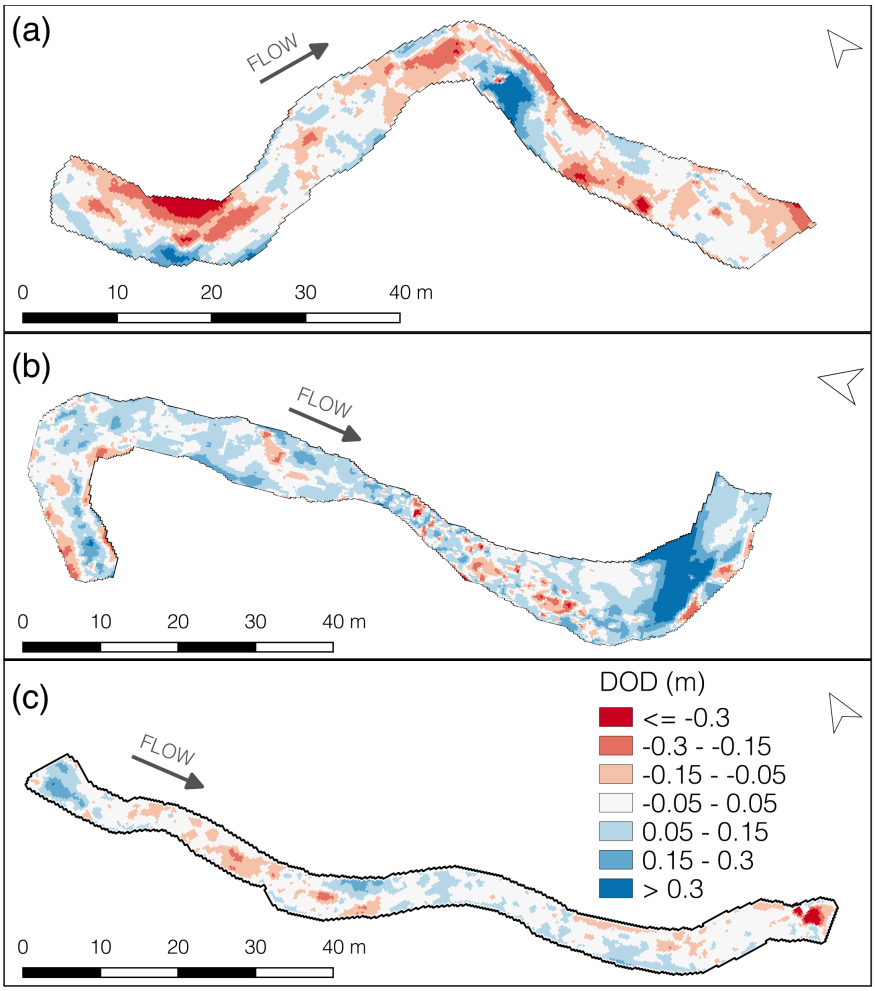

Figure 3.7. DODs between 2016 and 2018 in (a): Ganatsekaigon Creek, (b): Wilket Creek, and (c): Morningside Creek.

3.4.3 Tracer mobility

A comparison of the total tracer mobility (f_m) to the peak excess shear stress ratio ($\frac{\tau_p}{\tau_{cD50}}$) each recovery shows that mobility increases with peak shear stress in all systems. The distribution of event magnitudes differs between streams, with Wilket Creek exhibiting more frequent events with significant mobility. The majority of tracking periods in Ganatsekaigon Creek had low f_m (< 0.2), with only two tracking periods reaching f_m > 0.4 (Figure 3.8). These periods correspond to two large

floods that reached peak excess shear stress of almost 3 times the τ_{cD50}. In contrast, half of the tracking periods in Wilket Creek had f_m = 0.2–0.4 and only three periods had f_m < 0.2. The large variability in peak excess shear stresses corresponding to f_m = 0.2–0.4 may be the consequence of tracer slowdown that occurs over several mobilizing events (Ferguson & Hoey, 2002), supported by the lower f_m values for periods later in the study (see Table A.1). Three tracking periods in Wilket Creek had f_m > 0.4 that correspond to peak excess shear stress 2.7– 3 times the τ_{cD50}, which are similar to values observed in Ganatsekaigon Creek. This similarity in the flow magnitude driving sediment mobilization suggests urbanization does not alter the control of peak flow magnitude on bed mobility, only the frequency of bed mobilization. One outlier to this trend is the largest f_m value (0.67) corresponding to a high-flow event that occurred the day following seeding, and may therefore be unrepresentatively high. In Morningside Creek, most tracking periods had f_m < 0.2, three had f_m = 0.2–0 .4, and only one had f_m > 0.4. The reduction in the frequency of events with f_m > 0.2 compared to Wilket Creek suggest that the SWM is successful at reducing the frequency of bed sediment mobilization. The relation between peak excess shear stresses and f_m is weaker at Morningside Creek, with nearly identical $\frac{\tau_p}{\tau_{cD50}}$ values resulting in f_m ranging between 0.05–0.35. This weaker relation suggests flow parameters other than those relating to peak flow are important for bedload transport in this system.

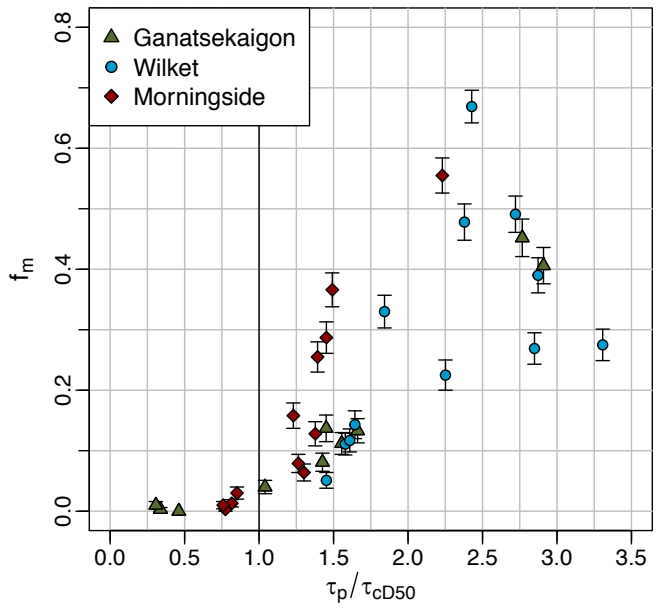

Figure 3.8. Fraction of entire tracer population that moved each recovery (f_m) by excess shear stress expressed as a ratio of the peak shear stress to the critical shear stress of the D_{50}. One tracer recovery in Morningside Creek excluded because of missing flow data (see Table A.1).

A key difference in the bedload transport regime of Wilket Creek is shown by a comparison of mobility by particle size class in Figure 3.9. Over the entire study period (F_{mi}), the mobility of the largest tracer size class is significantly lower in Ganatsekaigon Creek and Morningside Creek than in Wilket Creek (Figure 3.9); over 80% of particles in the 7–8 ψ class (i.e. the D_{90} size class) moved in Wilket Creek, while less than 50% moved in the other two systems. Wilket Creek, in fact, shows no significant difference in the mobility of the three tracer size classes, which means that the D_{90} moves as often as the D_{50} in this system. This result confirms preliminary results from a shorter study that showed a similar lack of sensitivity to particle size (MacVicar et al 2015). In contrast, transport in the other two creeks is size-selective, with larger grains less mobile than smaller grains. Size-selective transport is more commonly observed in the coarse fractions of bed sediment in gravel rivers (Hassan & Church, 2005), which suggests that the urbanization in Wilket Creek has changed the nature of transport in the creek, while the SWM in Morningside Creek is helping to maintain size-selective bed mobility post-urbanization.

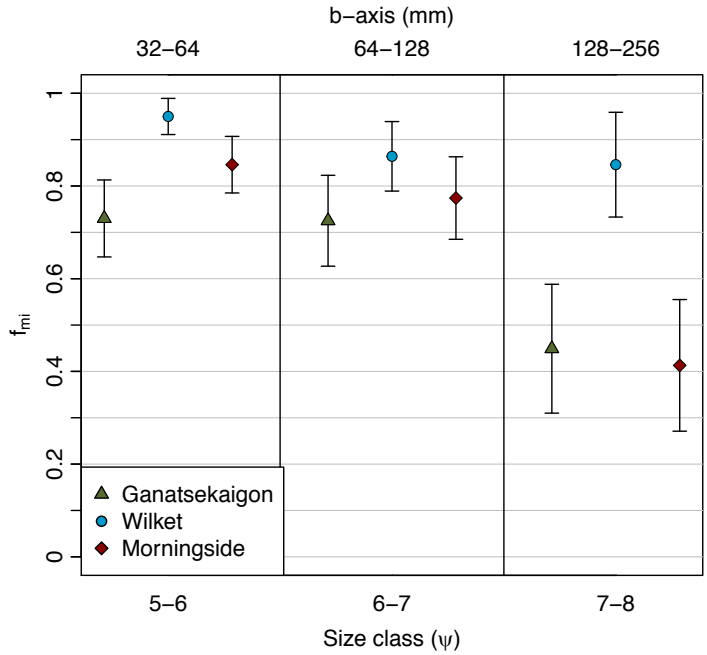

Figure 3.9. Mobility over the entire study period for each tracer size class.

The patterns observed for the overall tracer mobility by particle class are also observed for discrete mobilization events. Four tracking periods with $f_m \approx 0.05$, $f_m \approx 0.13$, $f_m \approx 0.40$ and the largest f_m at each stream (≥ 0.45) were compared (Figure 3.10). Recovery periods considered in this

analysis are listed in Table A.1. In Ganatsekaigon Creek, the largest tracer size class has lower mobility than the smaller size classes for all tracking periods, a difference that is significant in all tracking periods except $f_m \approx 0.40$ (Figure 3.10c). In contrast, Wilket Creek shows no significant differences in mobility among size classes except for the smallest magnitude event ($f_m \approx 0.05$), in which the largest sizes did not move (Figure 3.10a). The similar mobility of particles in the D_{50}, D_{75}, and D_{90} size classes for this urbanized system again stands in contrast to what is observed in other gravel-bed rivers, from where it is expected that size-selective mobility is more common, especially during smaller magnitude floods (Church & Hassan, 2002). Hydrologic conditioning by SWM again appears to prevent this type of high mobility from occurring in Morningside Creek, as the mobility of the largest tracer size class is only higher than 0.10 for the highest magnitude event (Figure 3.10d), and the D_{90} is less likely to move than the D_{50} for all tracking periods.

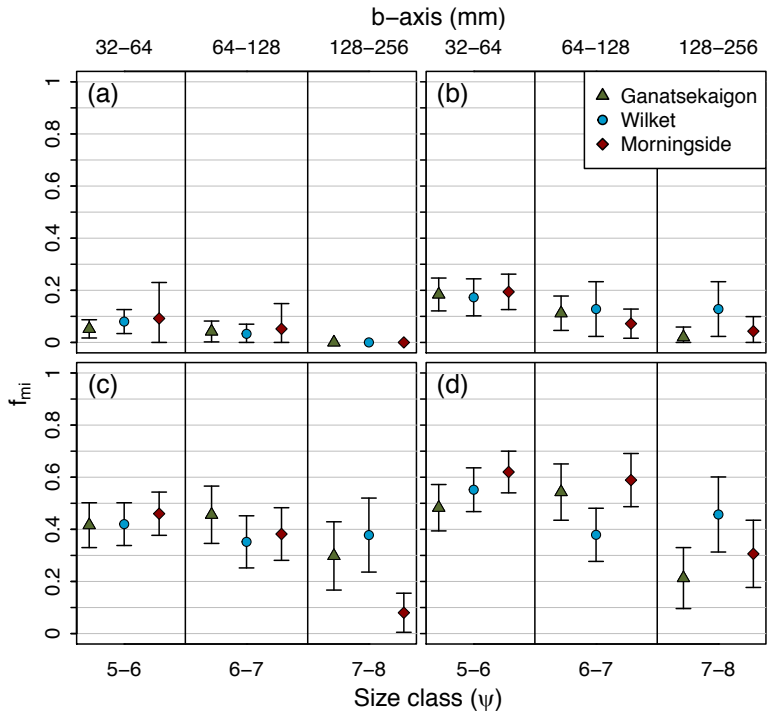

Figure 3.10. Mobility by tracer size class for recoveries with (a): $f_m \approx 0.05$, (b): $f_m \approx 0.13$, (c): $f_m \approx 0.40$, and (c): the largest f_m at each stream (≥ 0.45).

3.4.4 Travel lengths

Overall travel lengths of tracers over the entire study duration follow expected probability distributions, with tracers in the urban stream travelling farther. Tracer travel lengths in all streams

follow an exponential distribution (Kolmogorov-Smirnov test; p-value < 0.01) (Figure 3.11), fitting with the highly positively-skewed distributions observed in other settings (Bradley & Tucker, 2012; Liébault et al., 2012; Papangelakis & Hassan, 2016). More tracers travelled farther in Wilket Creek, while the distribution of travel lengths in Ganatsekaigon Creek and Morningside Creek overlap. The travel length distributions of all three streams decrease faster than the fitted distributions up to an exceedance probability of ~ 0.3, highlighting the skewness of travel lengths towards small values. Between exceedance probability of 0.05–0.3, travel lengths are greater than the fitted exponential distribution in all three streams. These travel lengths of greater probability suggest a secondary mode in the frequency of travel lengths.

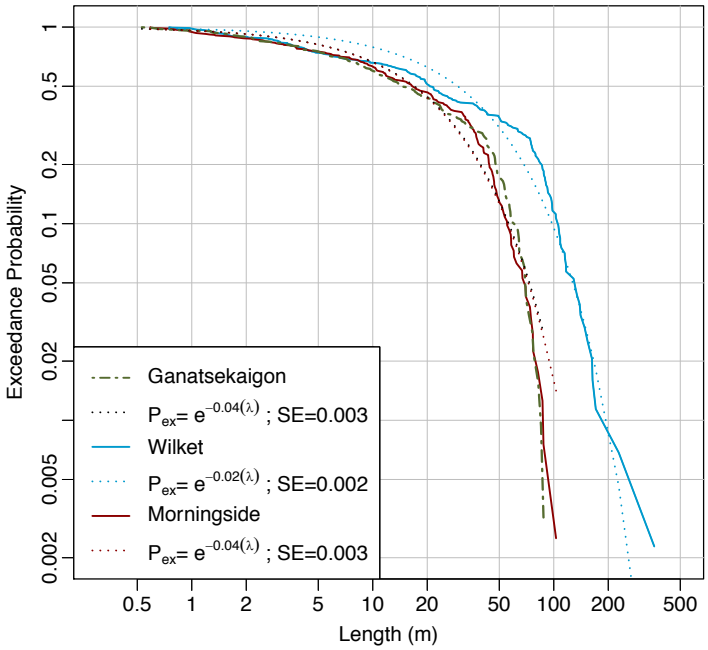

Figure 3.11. Exceedance probability (P_{ex}) distributions of tracer stone travel lengths (λ) with fitted exponential distributions and residual standard errors (RSE).

Separation of travel lengths by size and tracking period reveals the driver of the increased travel lengths observed in Wilket Creek. For the $f_m \approx 0.05$ events (Figure 3.12a), no tracers of the largest size class moved in any of the three study streams, while tracers in the 5–6 ψ and 6–7 ψ size classes have generally short travel lengths of < 5 m. A small number of outliers in Wilket Creek and Morningside Creek travelled > 10 m. During the $f_m \approx 0.13$ events (Figure 3.12b), Wilket Creek shows consistently longer travel lengths than the other two streams for all size classes, with even some of the largest tracers moving > 5 m. However, travel lengths during the $f_m \approx 0.40$ and $f_m \geq 0.45$

events are similar between Ganatsekaigon and Wilket Creeks for the 5–6 ψ and 6–7 ψ size classes (Figure 3.12c-d). Tracers in the largest size class, in fact, travelled farther in Ganatsekaigon Creek during these high magnitude transport events, suggesting that the higher overall travel lengths in Wilket Creek are explained by the increase in the frequency of bed mobilization. The travel lengths in Morningside Creek are shorter than the other two streams during the $f_m \approx 0.40$ events, showing that the SWM is effective at reducing travel distances as well as mobility. Another important observation is that the inflection point in the distributions seen in the overall travel length distributions (Figure 3.11) is also present in the 5–6 ψ size class in Ganatsekaigon and Morningside Creek, indicating secondary modes in travel lengths appearing even over single events. The lack of a secondary mode during high mobility events in Wilket Creek suggests that the secondary mode in the overall travel length distribution only emerges as a cumulative effect of several mobilizing events.

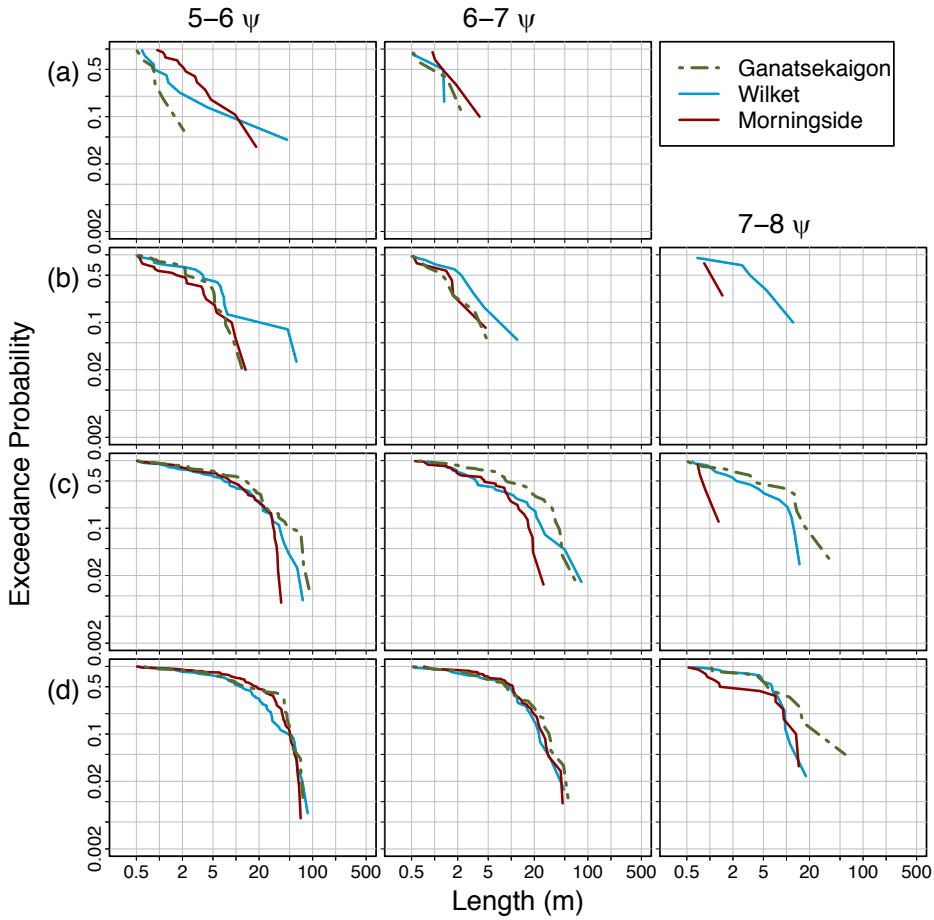

Figure 3.12. Exceedance probability distributions of tracer stones separated by size class and for events with (a): $f_m \approx 0.05$, (b): $f_m \approx 0.13$, (c): $f_m \approx 0.40$, and (c): the largest f_m at each stream ($\geq$ 0.45).

To assess the influence of bed morphology on bedload sediment transport in each stream, the distribution of tracer travel lengths were compared to morphological length-scales. Pyrce and Ashmore (2003b) proposed that morphological units act as preferential sediment deposition sites, so that secondary modes in particle travel length distributions coincide with multiples of channel width during channel-forming flows. Travel lengths over the entire duration of the study were scaled by mean channel width to determine if the location of secondary modes observed in Figures 3.11 and 3.12 coincide with consistent multiples of channel width. All tracer sizes have skewed distributions with a primary mode at 0–1 channel widths, consistent with the overall exponential distribution (Figure 3.13). The 5–6 ψ size class shows a secondary mode in all three streams that persists into the 6–7 ψ size class in Ganatsekaigon and Wilket Creeks. No clear secondary mode is seen for the 6–7 ψ size class at Morningside Creek, which suggests either an absence of morphological influence on the travel of these tracers, or that travel distances are too short to be limited by the bedform morphology of the channel. In both cases, the relatively large riffle spacing, lack of point bars, and presence of long runs in Morningside Creek result in a decreased influence of morphology on the dispersion of tracers larger than the 5–6 ψ size class. The largest tracer size class shows no secondary mode in all three streams, explained by short overall travel lengths that do not reach the secondary mode.

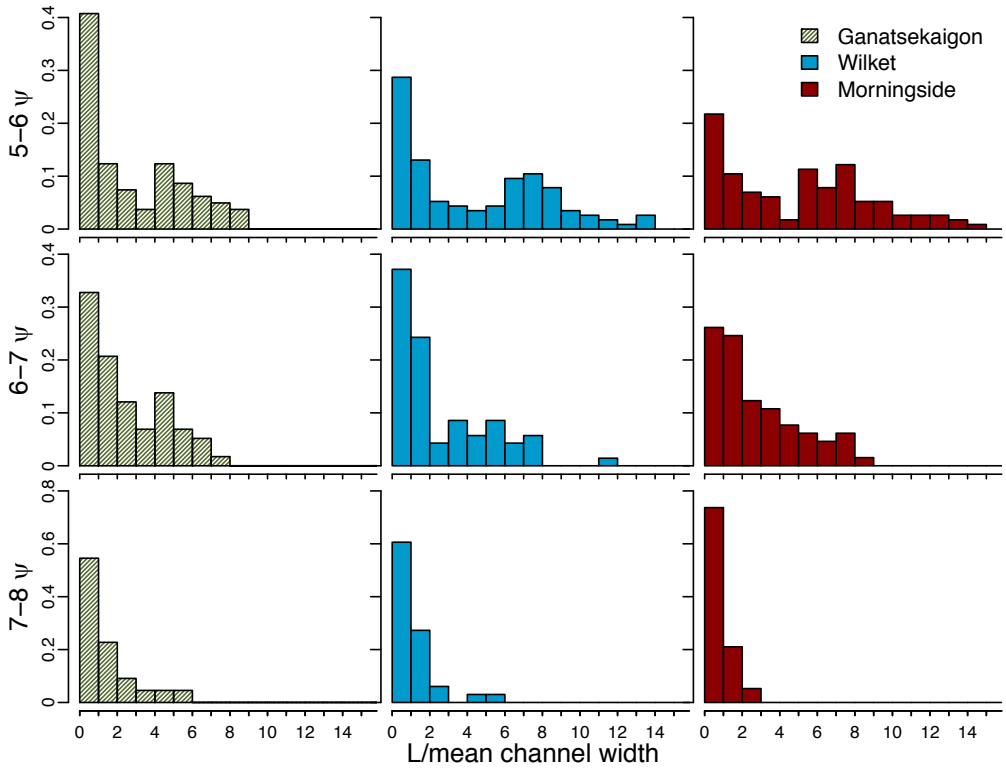

Figure 3.13. Density histograms of tracer travel lengths scaled by the mean channel width.

3.4.5 Virtual velocity

Significant differences among the three streams emerge in terms of the virtual velocity of tracer stones (Figure 3.14). In Ganatsekaigon Creek, the infrequent bedload transport results in low (< 2 m/year) virtual velocities for all sizes. Wilket Creek has significantly higher virtual velocities for all three size classes, and particularly for tracers in the D_{50} size class, which has a virtual velocity of more than 5 times that of Ganatsekaigon Creek. This is true despite tracer travel lengths in Ganatsekaigon Creek that are similar or longer than those in Wilket Creek (Figure 3.12), which means that higher virtual velocities are the cumulative effect of frequent bed mobilization rather than an increase in travel lengths. In Morningside Creek, the virtual velocity of the D50 is about twice that in Ganatsekaigon Creek, but smaller than in Wilket Creek. There is no significant difference in the virtual velocity of the D_{50} and D_{75} size classes between Ganatsekaigon and Morningside Creeks. Taken together, these results suggest that watershed urbanization significantly increases the long-term dispersion of bedload sediment, that SWM helps to decrease the dispersion rate of bed sediment, and that SWM reduces the dispersion rates of larger particles (>D_{50}) to match pre-urban rates.

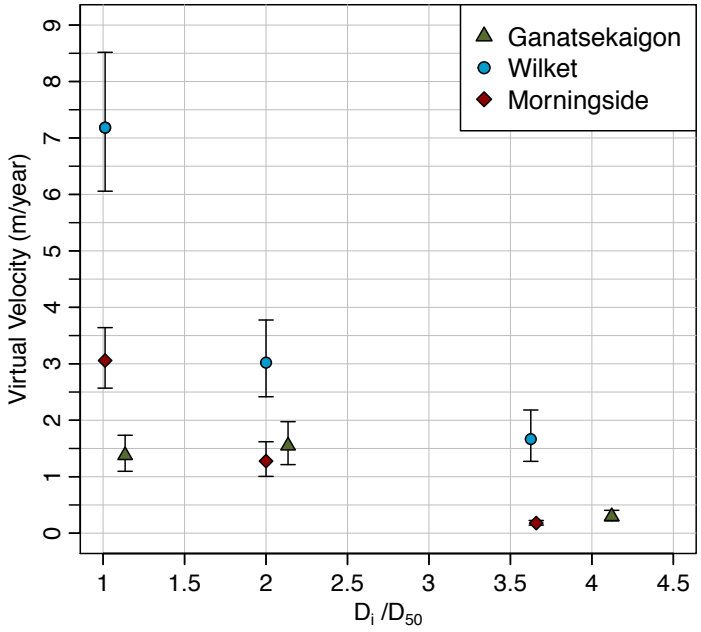

Figure 3.14. Virtual velocity of tracers by normalized size.

3.4.6 Comparison with alluvial rivers

Scaled travel lengths were compared to the relation proposed by Church and Hassan (1992) and modified by MacVicar and Roy (2011):

$$\frac{L_i}{L_{D50}} = (1 - \log\frac{D_i}{D_{50}})^{1.35} \quad (3.9)$$

where L_{D50} is the mean travel length of the tracer size class containing the D_{50} of the surface material. A second relation developed using a large number of tracer studies by Vazquez-Tarrio et al. (2019) was also compared:

$$\log\left(\frac{L_i}{L_{D50}}\right) = -0.26\left(\frac{D_i}{D_{50}}\right) + 0.26 \quad (3.10)$$

The two larger tracer size classes travelled farther than predicted by both the Church and Hassan (1992) and Vazquez-Tarrio et al. (2019) relations in Ganatsekaigon Creek over the entire duration of the study (Figure 3.15). Travel lengths in Wilket Creek follow the Church and Hassan (1992) relation well, while the largest size class travelled farther than predicted by the Vazquez-Tarrio et al. (2019) relation. These results suggest the relationship between travel lengths and grain size is similar to other gravel-bed rivers, although coarse particles travel longer distances relative to their size in the semi-alluvial stream than in other settings. The largest size classes travelled significantly shorter distances than predicted in Morningside Creek, consistent with the short distances observed in this size class during high mobility tracking events (Figure 3.12b-d).

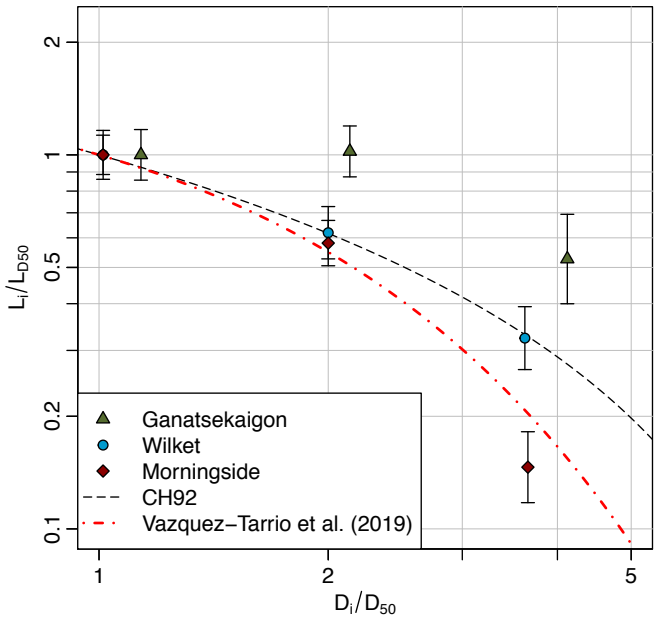

Figure 3.15. Scaled mean travel lengths compared to the Church & Hassan (1992) relation (CH92), and the relation from Vazquez-Tarrio et al. (2019).

The power relationships between event-based travel lengths scaled by mean channel width and peak excess stream power from this study were compared to 7 alluvial gravel-bed rivers (see Table A.2). Travel lengths measured in this study fall within the range measured in alluvial rivers (Figure 3.16). An overall relation combing data from all rivers was developed:

$$\frac{L}{b} = 0.123(\omega_p - \omega_{cD50})^{0.59} \qquad p < 0.01;\ R^2 = 0.47 \tag{3.11}$$

This relation is much stronger than that produced without scaling by channel width (R^2 = 0.26), suggesting that much of the variability in tracer travel lengths between systems can be reduced with width scaling. Relationships between channel width and tracer travel lengths have been established (Pyrce & Ashmore, 200b; Vazquez-Tarrio & Batalla, 2019), while channel width as an important morphologic scale has been proposed for many decades (e.g Keller & Melhorn, 1978; Leopold et al., 1964).

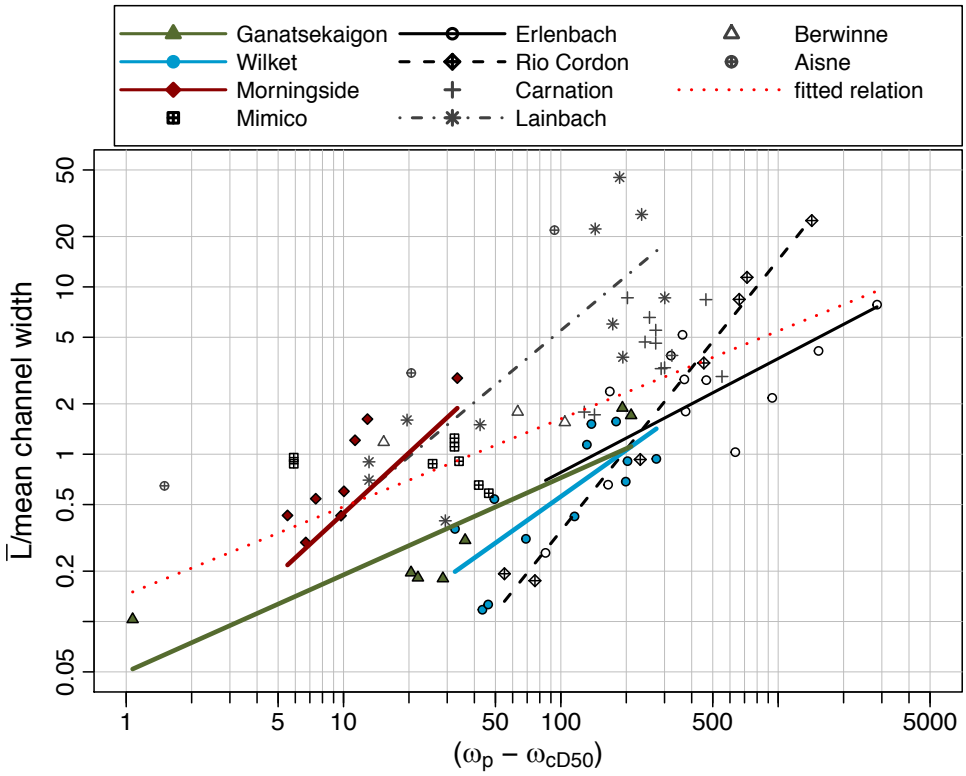

Figure 3.16. Scaled mean travel length versus peak excess unit stream power for channels in this study, Mimico Creek (Plumb et al., 2017), the Erlenbach (Schneider et al., 2014), Rio Cordon (Lenzi, 2004), Carnation Creek (Haschenburger & Church, 1998), the Lainbach (Gintz et al., 1996), and the Berwinne and Aisne rivers (Houbrechts et al., 2012). The arithmetic mean (rather than the geometric mean) of the tracer travel lengths was used in this figure.

The rivers can be broken into two groups based on whether the relationship between peak excess unit stream power and mean travel length is significant or not ($p \leq 0.05$). A significant relationship, in this case, suggests that flow magnitude is a dominant control on particle dispersion (Hassan et al., 1991). The group with a significant relationship includes Wilket Creek and Ganatsekaigon Creek, as well as steep mountain step-pool channels the Lainbach (Gintz et al., 1996), Erlenbach (Schneider et al., 2014), and Rio Cordon (Lenzi, 2004). The largest transport events in these rivers are produced by extreme summer rainfall events characteristic of summer convective storms in both Southern Ontario, and the Swiss pre-Alps (Schneider et al., 2014). The rate of increase in mean travel length with peak excess stream power in Ganatsekaigon and the Erlenbach appears to match the overall relation, although travel lengths are shorter. Wilket Creek, the Rio Cordon and the Lainbach appear to have a steeper relationship than the overall relation. However, a Student-Newman-Keuls (SNK) test performed on the regressions indicated that the fitted relationships of Wilket Creek and Ganatsekaigon Creek are statistically the same ($\alpha = 0.05$). The fitted relationships of these rivers suggest that bedload transport in the semi-alluvial rivers of this study is controlled by event magnitude like high energy, step-pool mountain streams, and that the urbanization of the catchment does not fundamentally change this dynamic.

Rivers without a significant relationship between peak excess unit stream power and mean travel lengths include Morningside Creek, Mimico Creek from the urban area around Toronto, the Berwinne and Aisne Rivers from the Ardenne area of Belgium, and Carnation Creek. The Belgian rivers have larger drainage areas and milder slopes than the rivers in this study (see Table A.2), while Carnation is dominated by long-duration rainfall events (Haschenburger & Church, 1998). Mimico and Morningside Creeks do not fit with these types of systems based on their watershed properties, but both have modified hydrology due to SWM infrastructure in the watershed (Plumb et al., 2017). Comparing streams from this study, travel lengths in Morningside Creek plot near those in Wilket Creek, but the range in mean travel lengths is much larger for a narrower range of excess stream power (Figure 3.16). The lack of relationship between peak excess unit stream power and travel length in these systems likely indicates that other flow characteristics are important controls on bedload dispersion, such as flood duration or hydrograph shape.

3.5 Discussion

The goal of this study is to assess the effects of urbanization and SWM on the bedload sediment transport regimes of semi-alluvial gravel-bed rivers. Similar to other studies, sediment transport in

gravel rivers is a complex process, with hydrologic controls modified significantly by morphologic and sedimentological differences between the channels (Vazquez-Tarrio et al., 2019). As much as possible, this study has controlled for differences between the sites by finding reaches with similar drainage area, slope, and particle size distributions. Despite these similarities, hydrologic differences stemming from land-use characteristics have led to significant differences between the channels. A summary of the effects of the semi-alluvial bed cover, urbanization, and SWM on the hydrology, morphology and bedload transport of the streams are presented in Table 3.3. Differences in the number, magnitude and duration of mobilizing events match what is expected of urbanization and SWM, as do the observed changes in morphology. As a consequence of near-complete urbanization over 50 years ago, Wilket Creek has undergone significant enlargement (Bevan et al., 2018), while multi-layered SWM in Morningside Creek has led to channel narrowing immediately after (Badelt, 1999) and in the 20 years since urbanization. Morphologic adjustment may continue in the future, particularly in Morningside Creek due to the relatively recent urbanization, but here we characterize the bedload transport dynamics of the three sites based on their existing condition. We compare and contrast between them and with other alluvial systems in the literature to understand how the semi-alluvial bed affects sediment dynamics and propose conceptual models for how those dynamics are modified by urbanization both with and without SWM.

Table 3.3. Summary of differences in hydrology, channel morphology, and coarse bedload transport dynamics. The rural semi-alluvial stream is compared to alluvial gravel-bed rivers. The urban with no SWM and urban with SWM are compared to the rural stream. NC = no change.

	Rural	Urban no SWM	Urban with SWM
Hydrology & Morphology			
# of events		+	NC
Event peak		+	-
Event duration		-	+
Channel dimensions		+	-
Bedload Transport			
Threshold shear stress	NC	NC	NC
Bedload mobility (F_m)		+	NC
Event travel lengths (L)		NC	-
Overall travel lengths relative to D_{50} (L_i/L_{D50})	+	-	-
Control of peak flow	+	NC	-
Virtual velocity (m/year)		+	+ for D_{50} NC for > D_{50}

Bedload transport in the rural semi-alluvial stream shares several important characteristics with alluvial gravel-bed rivers. First, the threshold for mobilization of coarse sediment (≥ D_{50})

matches that in other gravel-bed rivers (Table 3.3), suggesting the unique cover does not fundamentally alter bedload entrainment processes. This result is counter to studies in laboratory settings that show decreased entrainment thresholds of gravel when fine materials are introduced (Ahmad et al., 2017; Miwa & Parker, 2017; Venditti et al., 2010, Wilcock & Kenworthy, 2002). Second, most flood events mobilize only small fractions of the bed and the transport is size-selective, with particles transported over a largely stable bed (Ashworth & Ferguson, 1989, Hassan and Church, 2002). Significant transport and morphological change occur only during infrequent high-magnitude events, which is typical of gravel-bed rivers (Reid et al., 1985). Anecdotally, watershed managers were surprised by the amount of transport and erosion during the floods of 2017, and there is no indication of regular channel migration and adjustment, suggesting they occur even more rarely than the rate of twice in three years that was observed in this study. Overall, the rural semi-alluvial stream can be characterized as a relatively stable headwater stream that fits with many expectations of alluvial gravel-bed systems.

Despite the similarities, there are a few differences between the semi-alluvial streams in this study and alluvial gravel-bed rivers that may affect bedload transport. The first is the patches of exposed cohesive till on the channel bed. These areas are sparse and primarily located along the outside bank of bends, which are not common deposition sites for coarse particles (Milan, 2013a; MacVicar & Roy, 2011), and therefore likely do not impact the behaviour of tracers. The second difference is the low infiltration capacity of the local soils, which may increase runoff during intense precipitation. The high runoff may alter the hydrologic controls on bedload transport such that the magnitude of flows is the primary driver (Table 3.3) while the duration is less important, in contrast with what has been found in other systems (Papangelakis & Hassan, 2016; Phillips et al., 2013; Schneider et al., 2014). Finally, coarse sediment is sourced directly from erosion of the underlying till layer (Pike et al., 2018; Thayer & Ashmore, 2016) and the indications are that this leads to several key differences in the sediment dynamics. The relationship between mean travel length and peak excess unit stream power, for instance, is more similar to steep step-pool mountain streams than lower slope alluvial systems (Figure 3.15). Once mobilized, coarse particles also travelled farther relative to the median particle size compared to relations derived from alluvial gravel-bed rivers (Table 3.3). The effect is not thought to be due to initial transport effects, as the almost equal travel lengths amongst size classes are suggestive of well-mixed, partial transport (Wilcock, 1997) rather than 'unconstrained' transport expected of early events following seeding. Conceptually, the supply of coarse material directly to the stream bed is similar to colluvial inputs in high-energy mountain streams and it is perhaps for this reason that these observations tend to fit with what is observed in bedrock semi-

alluvial channels (Hodge et al., 2011). Bedload transport in the rural stream can be characterized as an 'episodic' regime, sharing several characteristics with alluvial gravel-bed rivers but driven by peak flows, and with longer travel lengths of mobilized particles.

A comparison of the urbanized creek (Wilket) with the rural creek (Ganatsekaigon) shows that watershed urbanization does not change the fundamental mechanisms of entrainment and displacement but does affect the frequency of bedload transport. Entrainment thresholds match with the rural system and alluvial channels, while event-based travel lengths and the primary control of peak flow on travel lengths are similarly unaffected (Table 3.3). In contrast to the rural stream, however, bedload transport is dominated by frequent events that mobilize larger fractions of the bed, equal mobility of coarse sediment (D_{50}–D_{90}), and short overall travel lengths relative to the median size class (Table 3.3), which was attributed by Plumb et al (2017) to the shortened duration of mobilizing flows in urban rivers. Accelerated downstream displacement rates of bed sediment (Table 3.3) are thus the result of the more frequent sediment mobilization. The equal mobility of coarse sediment during all magnitudes of transport events is evidence of an increases in the geomorphic significance of low-to-medium magnitude flood events (as suggested by Plumb et al., 2017), which combined with enhanced mobility of material up to the D_{90} (Table 3.3), is likely exceed the supply of coarse material from the underlying till. In this urban system, the bedload transport thus appears to have shifted from an episodic to a 'conveyor belt' regime in which significant movement of all particle sizes occurs several times a year, and channel enlargement and degradation are endemic.

The urban stream with SWM shares several characteristics with the rural stream, including entrainment thresholds and size-selective transport (Table 3.3). In particular, the reduced travel lengths of particles > D_{50} successfully decrease the downstream displacement rate of these coarse particles to pre-urban values (Table 3.3), which supports the idea that the SWM strategy is preventing some of the most damaging impacts of watershed urbanization. Several lines of evidence, however, suggest that the channel has shifted to a new bedload transport regime. First, peak flow magnitude exerts a smaller control on bedload transport (Table 3.3). Second, there is a reduction in fine material on the bed due to settling in the SWM ponds (Badelt, 1999), so that as fine material downstream of the ponds is flushed away, little sand and silt is available to replace it. The resulting bed armouring further suppresses the mobility of coarse sediment (Miwa & Parker, 2017; Venditti et al., 2010). Third, extreme excess shear stresses are reduced due to the attenuation of floods from the SWM infrastructure and the small channel dimensions. The small channel cross-section results in flow dissipating into the floodplain more often and dampening the increase in transport capacity with increasing discharge (Bledsoe and Watson, 2000). This shear stress reduction due to channel

geometry acts as a feedback; the altered flow and sediment supply regime from the SWM result in channel narrowing that, in turn, further reduce the extreme shear stresses. Channel narrowing and bed coarsening has also been observed downstream of dams that subdue flows and decrease sediment supply (Boix-Fayos et al., 2007; Brandt, 2000; Choi et al., 2005), while the interactions between altered hydraulic conditions and channel morphology have been demonstrated in urban systems through modelling (Amin et al., 2018). Finally, the lack of bars and the presence of large plane-bed features are indicative of a transition between supply-limited and competence-limited conditions (Montgomery & Buffington, 1997). Together, these changes in the morphology and sediment dynamics support the idea that the urban stream with SWM has shifted into a competence-limited bedload transport regime.

The findings in this study can be used to inform urban river management that aims to mitigate channel degradation. Hydrologic modification is a common strategy that attempts to suppress the increased competence of floods in urban watersheds. However, the design of SWM infrastructure is typically based on relatively rare events (e.g. 2-year or 10-year storm) (Doyle et al., 2000; Hawley & Vietz, 2016; Tillinghast et al., 2012), while our results suggest that even frequent events occurring several times a year contribute to morphologic change in urban systems. Moreover, these smaller magnitude events have been shown to be more significantly altered by urbanization (Konrad et al., 2005). Hydrologic approaches to urban river management might shift focus to these more frequent events, perhaps through increasing infiltration capacity with low-impact-development (LID) (Pomeroy et al., 2008; Rohrer & Roesner, 2006; Tillinghast et al., 2012), catchment-scale stormwater management strategies (e.g. Anim et al., 2019a), or through designing for threshold discharge rather than large-magnitude events with little geomorphic significance (Hawley & Vietz, 2016; Tillinghast et al., 2011). Traditional peak-shaving SWM has successfully mitigated channel enlargement in this study, but the lack of bedforms and static nature of the bed may have unintended ecological consequences. Bed complexity is recognized as important for instream habitat availability (Walsh et al., 2005), and dynamic channels have been shown to better support aquatic ecosystems (Beagle et al., 2015; Chin & Gregory, 2009; Clarke et al., 2003; Thorp et al., 2006). Improvements to the ecological integrity of streams with peak-shaving SWM may be possible if occasional large floods can pass through the system to replace fine material and develop/maintain bedforms. Such a strategy fits with the shift in focus from controlling high-magnitude events and may be attainable through LID strategies. Another common strategy to mitigate river degradation is bed coarsening. The addition of even small volumes of coarse material has been shown to promote bed stability (MacKenzie & Eaton, 2017). However, material exceeding the D_{90} (as suggested by MacKenzie & Eaton, 2017) would be

required in systems such as Wilket Creek, as even particles in this size class are mobilized frequently, highlighting the need for case-specific considerations. A final strategy to arrest river degradation is sediment augmentation to counteract the imbalance between increased competence and reduced sediment supply. This strategy has been proposed in rivers with a reduced sediment supply due to dams (e.g. Downs et al., 2016; Liedermann et al., 2013; Rinaldi et al., 2005; Rollet et al., 2014; Sklar et al., 2009), but its application to urban systems has not been thoroughly investigated. It is likely that the most successful urban river management strategies will require a combination of hydrologic measures to restore both hydrologic and morphologic processes of streams (Amin et al., 2019b).

Further research on several topics related to the current work can improve our understanding of bedload transport in urban systems. For instance, while a large range of flood events was captured in this study, bedload dispersion and morphodynamics over longer timescales remain to be described, particularly in the case of the rural stream where significant mobility of the coarse size fractions in this study occurred only during two floods. The rarity of transport in these systems requires longer durations than studies in urban systems, where dispersal rates are much higher. Future research should also aim at understanding the effects of altered hydrologic conditions from urbanization and SWM at larger spatial and temporal scales. Upstream and downstream effects may vary, and the range of approaches including the bedload transport dynamics in streams with LID remains to be explored. Morphological changes in this study were also affected by the presence of woody debris. Future research should include reaches containing large wood to investigate its effects on roughness and shear stress available for bedload transport and explore wood as a potential river restoration and management tool (Poelman et al., 2019).

3.6 Conclusions

This study presents an investigation into the bedload transport regimes of glacially-conditioned semi-alluvial rivers conditioned by urbanization and SWM. Three streams were chosen to represent a rural, an urban without SWM, and an urban with SWM hydrologic conditions. The major findings are:

1. Bedload sediment transport in the rural setting is episodic and driven by the magnitude of floods. The semi-alluvial nature of the bed does not change the mechanisms of sediment entrainment but may increase the travel distance of coarse sediment once mobile.
2. The stream in the urban setting with no SWM has shifted to a ‘conveyor belt’ bedload transport regime characterized by frequent mobilization of all sediment up to the D_{90},

resulting in accelerated downstream displacement rates. The ability of the stream to frequently transport large material can explain urban channel enlargement.

3. The SWM hydrologic setting has shifted the system into a competence-limited transport regime, where transport is driven by the increased duration of flow.

The characterization of grain-scale bedload transport dynamics in urban and SWM settings can inform management and restoration efforts that stem from a process-level understanding of modified sediment transport regimes. Efforts to mitigate urban river enlargement should focus on compensating for the accelerated displacement of coarse grains and the increased geomorphic significance of frequent, small-to-medium magnitude events. SWM designs should attempt to alleviate the homogenization and inactivity of downstream reaches to improve upon habitat availability by allowing occasional large events to pass through the system to maintain bedforms and channel complexity.

Transition B

Chapter 3 focused on understanding the effects of urbanization and SWM on bedload transport dynamics, and its relationship to channel morphology. Chapter 4 moves from the explanatory perspective (how are bedload transport processes changing in response to urbanization and SWM), to a predictive goal (can we predict bedload transport responses in urban and SWM settings). The goal of Chapter 4 is to answer the third research question of this thesis: How can bedload transport responses be predicted in environments with hydrology impacted by urbanization and stormwater management? Many bedload tracking studies have developed relationships between variables that describe tracer behaviour, and metrics that characterize the flow conditions. However, bedload tracking studies are inconsistent, with a large number of tracer variables and flow metrics developed, and no standard method set. Furthermore, these flow metrics are developed for rural or laboratory settings and have not been tested in streams with hydrographs altered by urbanization and SWM. Chapter 4 explores which of the flow metrics developed in the literature best predicts tracer displacements in the streams introduced in Chapter 3, and attempts to develop a common model that can be used in streams with a large range of hydrologic conditions. Considerations for proper tracer data management and model calibration are discussed with the intention of providing researchers with a guide that will facilitate a better comparison of results from bedload tracking studies. The model presented in Chapter 4 was developed with the intention that the needed data is easy to obtain so that it can be integrated into a decision support tool that is being developed for conservation authorities in Southern Ontario.

Chapter 4
Predicting Bedload Tracer Responses in Urban Streams

4.1 Introduction

Urbanization results in significant modifications to the hydrology of river systems, termed 'urban hydromodification'. The main drivers of urban hydromodification are the expansion of impervious surfaces and the introduction of efficient storm sewer systems (Booth et al., 2004; Hammer, 1972). The increased runoff and efficiency at which rainwater is delivered to rivers leads to an increase in peak flows and decreased lag times between rainfall and peak flows, resulting in characteristic 'flashy' hydrographs (Bledsoe and Watson, 2000; Chapuis et al., 2014a; Chin, 2006; Konrad et al., 2005; Ladson et al., 2006; Poff et al., 2006). The addition of peak-shaving stormwater management (SWM) infrastructure such as retention ponds further modifies urban hydrographs by reducing peak flows, but elongating falling limbs (Bledsoe, 2002; Bledsoe & Watson, 2001; Nehrke & Roesner, 2004; Rohrer & Roesner, 2006). Although the hydromodification of urban rivers has been well documented, its relevance for predicting and modelling other river processes remains unclear. One important fluvial process that has shown to respond to urban hydromodification is bedload sediment transport (Chin, 2006, Russell et al., 2017; Plumb et al., 2017). The ability to predict bedload transport responses to urban hydromodification is imperative for urban river management, as bedload transport is the driver of morphological adjustments in streams (MacKenzie et al., 2018) and provides a link between hydrologic and biological responses (Booth et al., 2004). However, bedload sediment transport models have been developed in rural and laboratory settings, and have not been extensively tested in streams with urban hydromodification.

Predicting bedload transport is a difficult task due to the complexity of flow and sediment interactions (Yager et al., 2018b). An alternative approach to measuring and predicting bulk transport rates is predicting the timing, extent, and rate of individual bed particle movements. Such an approach can lead to better predictions of channel change (Haschenburger and Church, 1998; Hassan et al., 2013), and can be used in conjunction with active layer depth to estimate bedload transport rates (e.g. Brenna et al., 2019; Haschenburger & Church, 1998; Mao et al., 2017; Wilcock, 1997). The relationship between flow and the fraction of mobile bed particles, their travel lengths, and their velocity, has been a central topic in bedload tracer studies. A large number of flow metrics have been developed to explore these relationships, with varying success and consistency. These metrics can be grouped into two categories; those calculated for the instantaneous peak flow, which is thought to exert a dominant control on tracer displacement (Hassan et

al., 1992), and cumulative metrics that integrate all values above the threshold for mobilization. Cumulative metrics capture both the magnitude and duration of mobilizing flows, and include cumulative excess shear stress (Klösch et al., 2017), excess stream power (Schneider at al., 2014), excess energy expenditure (Haschenburger, 2011; Papangelakis & Hassan, 2016), and excess velocity (MOE, 2003). Furthermore, several non-dimensional versions of parameters have been developed to improve comparison between systems and between different particle sizes, such as dimensionless stream power (Eaton & Church, 2011; Vazques-Tarrio et al., 2019; Vazquez-Tarrio & Batalla, 2019), and dimensionless impulse (Phillips et al., 2013; Phillips & Jerolmack, 2014). Given the importance of hydrograph shape on bed particle displacement and sorting processes (Hassan et al., 2006; Humphries et al., 2012; Klösch et al., 2017; Phillips et al., 2018), urban hydromodification and SWM are expected to be important for predicting bedload transport in urban environments. However, the performance of flow metrics developed in rural settings in predicting tracer behaviour in urban rivers has not been tested.

A challenge in building predictive models of bed particle behaviour is choosing the critical shear stress at which bedload transport begins. Many studies assign this value based on an assumed Shields parameter, also known as the critical dimensionless shear stress (commonly 0.047). However, estimates of the critical dimensionless shear stress from laboratory and field experiments have shown large variability in observed values (Buffington & Montgomery, 1997). Methods to calibrate the critical dimensionless shear stress include physical approaches, such as those based on data from sediment traps (e.g. Ferguson & Wathen, 1998) and scour indicators (Haschenburger & Church, 1998), and empirical estimations based on regressions of tracer displacements (e.g. Klösch et al., 2017; Phillips et al., 2013). The effect of grain size is vitally important in calibrating the critical shear stress, as different grain sizes are mobilized at different shear stresses. The interactions between particles of different sizes due to packing and structural arrangements further complicate the relationship between particle size and critical shear stress (Monslave et al., 2017; Parker & Klingeman, 1982; Wilcock, 1988; Yager et al., 2018a). Many bedload tracking studies, however, set a single mobilization threshold for the tracer population, regardless of whether a wide range of particle sizes is employed (e.g. Ferguson & Wathen, 1998; Ferguson et al., 2002; Gintz et al., 1996; Haschenburger & Church; Hassan et al., 1992; Papangelakis & Hassan, 2016; Phillips et al., 2013). Some studies have separated tracer particles size classes to achieve improved critical shear stress calibrations (e.g. Lenzi, 2004; Milan, 2013b; Klösch et al., 2017), but are done for only one tracer variable (mobility, travel length or virtual velocity). The discrepancy between using different tracer variables for model calibration has not been quantified, and the most appropriate method for model calibration remains to be explored.

The goal of this study is to calibrate and build predictive models of bed particle mobility and travel lengths in rivers with hydromodification resulting from watershed urbanization and SWM. Bedload tracer data used from three study streams in Southern Ontario with a rural, urban with no SWM, and urban with

extensive SWM watershed hydrology, are used. This study has the following specific objectives: (1) quantify the degree to which estimated critical shear stresses differ when considering different tracer variables for calibration, and determine the most appropriate method for tracer data applications; (2) assess which flow metrics perform best at predicting the mobility and travel length of tracers in streams with different hydrograph shapes; and (3) build the strongest model for predicting the mobility and travel length of bed particles for application to rivers with varying types of hydromodification. The aim is to assess the applicability of flow metrics developed in rural settings for predicting bedload transport in urban environments, and to provide recommendations for the application of such metrics to river management efforts.

4.2 Methods

4.2.1 Study Sites

Data collected from three streams in the Greater Toronto Area in Southern Ontario, Canada (Figure 3.1) were used to calibrate and build the models presented in this study. Details of the streams, including their hydrology, development history, and study reach descriptions can be found in Chapter 3 (Section 3.2). The similarities between study reaches allows for direct comparison of bedload transport responses in rivers with different hydrograph shapes resulting from urbanization (Wilket Creek) and SWM (Morningside Creek) (Figure 3.4), while controlling for other variables that influence bedload transport, such as slope, geology, and drainage area (Table 3.1). The streams have evolved to have different dimensions, which influences the distribution of erosive flows experienced in each stream (Section 3.4.1). However, in this study flow metrics are calculated directly from measured water level hydrographs, so that the distribution of flows will not influence the results of this analysis.

4.2.2 Bedload sediment tracking

Bedload transport was characterized using RFID tracer stones. Detailed descriptions of the tracer stone creation, sample size, and seeding methodology can be found in Chapter 3 (Section 3.3.3). Following the methods described in Chapter 3, three variables were calculated for each recovery. The first is the fraction of tracer stones that moved in each size class (i) since the last recovery (f_{mi}) (Equation 3.5). The second variable calculated was the geometric mean travel distance of mobile tracers in each size class (L_i, m). The final variable used in this study to characterize tracer displacement is the weighted mean travel length ($\tilde{L}_i$, m), calculated as the product of the mobility and mean travel length ($\tilde{L}_i = f_{mi} \times L_i$). This variable accounts for immobile particles, providing a metric representative of the overall displacement of the entire tracer

population. The models built in this study attempt to predict these three variables based on inputted water level measurements. Particular emphasis is placed on $\tilde{L}_i$ in this study due to its ability to quantify the mobility and the travel length of bed particles in one variable, both of which are important for translating tracer data to bulk sediment transport rates.

A total of 10, 12, and 13 recoveries took place in Ganatsekaigon, Wilket, and Morningside Creeks, respectively. For this study, tracking periods over the winter seasons (December – March) were excluded from the analysis due to the complexity of characterizing winter hydrographs that include combinations of snowmelt, rain-on-snow, and rainfall events (see Table A.1 for winter period recovery dates). One additional recovery in Morningside Creek was excluded from the analysis presented in this Chapter because the flow hydrograph corresponding to the maximum precipitation event was not recorded due to a pressure transducer malfunction (see Table A.1). After winter periods were removed, 7 recoveries were used from Ganatsekaigon Creek, and 9 recoveries from Wilket and Morningside Creeks. Given the three size classes in each stream, these recoveries lead to 21 tracer variables calculated in Ganatsekaigon Creek, and 27 calculated in Wilket and Morningside Creeks. Recovery rates ranged between 86 – 100%, including tracers whose positions were not recorded in the field but could be inferred from subsequent surveys that confirmed they had not moved (Table A.1).

4.2.3 Flow Metrics

Flow metrics used to predict the three tracer variables (f_{mi}, L_i, and $\tilde{L}_i$) were calculated from water level measurements, the cross-sectional geometry at each gauge, the mean channel slope of the study reach, and an assigned roughness parameter. The flow metrics are derived from four base parameters that were calculated for each water level time step (t): shear stress (τ_t), mean velocity (V_t), discharge (Q_t), and specific stream power (ω_t) (Table 4.1). Two categories of flow metrics were calculated: peak flow metrics, calculated for the maximum water level measured during the entire time between tracking periods, and cumulative metrics, which are summed over the duration the hydrograph was above the threshold for sediment mobilization. This process is the numerical approximation of the integral under the hydrograph curve of each metric for the time it is above the set threshold (Figure 4.2). In cases of tracking periods with more than one event exceeding threshold, the metrics calculated for each event were summed to obtain a total for the entire period between tracer surveys. Given that the threshold for mobilization varied by tracer size class, and some flow metric formulas include the sediment diameter (Table 4.1), flow metrics were calculated independently for each tracer size class.

Table 4.1. Formulas of flow metrics used in this study. Cumulative flow metrics are in the form of $\sum_{E_1}^{E_n}\sum_{t_s}^{t_e}(F)\Delta t$, where E_i denotes each mobilizing event, t_s and t_e denote the start and end of each mobilizing event, respectively, and (F) is listed in the table. B is the channel bed width, and the subscript 'ci' denotes the threshold for mobilization of size class i.

Peak Metrics	Formula	Units	Source
Shear stress (τ_p)	$\tau_p - \tau_{ci}$	Pa	
Dimensionless shear stress (τ_p^*)	$\tau_p^* - \tau_{ci}^*$	-	
Discharge (Q_p)	$Q_p - Q_{ci}$	m^3/s	
Specific stream power (ω_p)	$\omega_p - \omega_{ci} = \frac{\rho g S(Q_p - Q_{ci})}{B}$	W/m^2	Hassan et al., 1992
Dimensionless specific stream power (ω_p^*)	$\frac{(\omega_p - \omega_{ci})}{\rho_w \left(\frac{g D_i(\rho_s - \rho)}{\rho_s}\right)^{3/2}}$	-	Eaton & Church, 2011
Cumulative Metrics	(F)	Units	Source
Time of exceedance (*TE*)	-	h	
Excess shear stress (*CESS*)	$(\tau_t - \tau_{ci})$	Pa·s	
Excess dimensionless shear stress (*CEDSS*)	$(\tau_t^* - \tau_{ci}^*)$	s	
Specific bedload transport rate (q_b)	$2.66 D_i(\tau_t^* - \tau_{ci}^*)^{1.5}\sqrt{\frac{g D_i(\rho_s - \rho_w)}{\rho_s}}$	m^2	Wong & Parker, 2006
Bedload transport rate (Q_b)	$q_b B$	m^3	Wong & Parker, 2006
Excess impulse (*CI*)	$(u_{*t} - u_{*i}) = \left(\sqrt{\frac{\tau_t}{\rho_w}} - \sqrt{\frac{\tau_{ci}}{\rho_w}}\right)$	m	Phillips et al., 2013
Excess dimensionless impulse (*CDI*)	$\frac{1}{D_i}(u_{*t} - u_{*ci})$	-	Phillips et al., 2013
Excess velocity (*CEV*)	$(V_t - V_{ci})$	m	MOE, 2003
Excess discharge (*CEQ*)	$(Q_t - Q_{ci})$	m^3	
Excess energy expenditure (Ω)	$\rho_w g S(Q_t - Q_{ci})$	N	Haschenburger, 2011
Excess specific stream power (*CESP*)	$(\omega_t - \omega_{ci})$	N/m	Schneider et al., 2014
Work index (*WI*)	$(\tau_t - \tau_{ci})\, V_t$	J/m^2	CVC, 2012

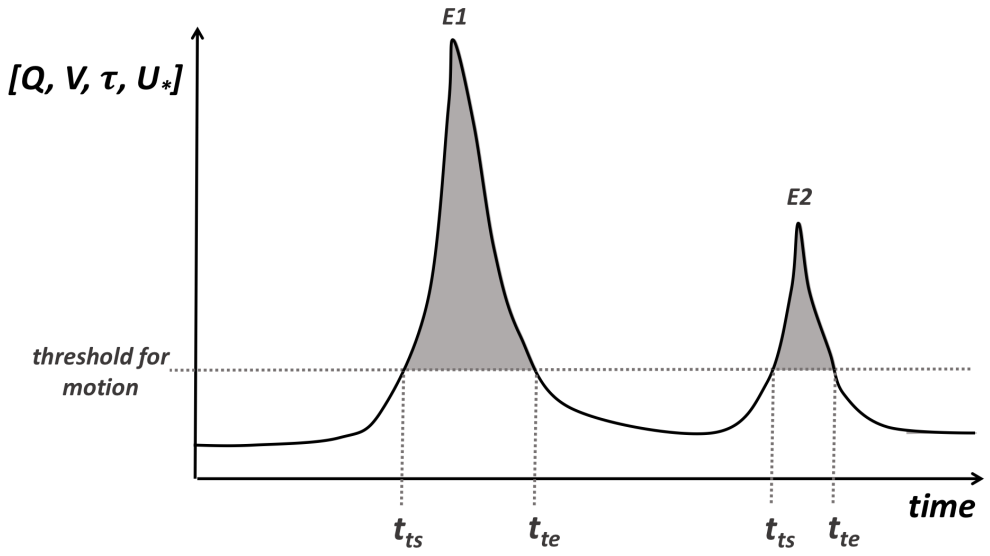

Figure 4.1. Conceptual figure of flow metric calculations. Y-axis can represent any flow variable (e.g. discharge, velocity, shear stress, shear velocity, etc.). Cumulative parameters are equal to the area under the hydrograph curve that exceeds the threshold for tracer mobilization (shown in grey).

Continuous water level measurements were recorded from gauges installed each study reach between July 2015 and July 2018 (Figure 3.3). Raw pressure recorded from pressure transducers (HOBO-U20 Water Level Data Logger, Onset; ± 0.05 m error) was converted to a water surface elevation after a barometric compensation using atmospheric pressure data collected at each site. Measurements were recorded at 2-minute intervals between April and November, and at 7-minute intervals between December and March of each year. The high temporal resolution of the water level data allows for the adequate capture of flashy hydrographs in Wilket Creek, which often go from baseflow to peak discharge within 20 minutes (Figure 3.5).

The channel slope (S) and cross section geometry at the gauge were obtained through total station surveys (Sokkia SET530R, ± 2 mm error). For the purposes of building predictive models in this study, channel slope and cross-sectional geometry were set constant over the three-year study period since repeated surveys show only minor differences in channel geometry between survey dates. The reference bed elevation above which flow parameters were calculated was set as the minimum bed elevation of the gauge cross section, excluding deep pools that were not seeded with tracers. Water level inputs and channel cross section surveys were used to calculate the wetted cross-sectional area (A_t) and wetted perimeter (P_t) at each time step (t). The hydraulic radius (R_{ht}, m) was then calculated as:

$$R_{ht} = \frac{A_t}{P_t} \tag{4.1}$$

Using the surveyed bed slope, shear stress (τ_t, Pa) was then calculated at each time step:

$$\tau_t = \rho_w g R_{ht} S \quad (4.2)$$

where ρ_w is the density of water (1000 kg/m^3), and g is the gravitational acceleration (9.81 m/s^2).

Flow velocity (m/s) was calculated at each time step using the Keulegan equation:

$$V_t = 5.75 \log\left(\frac{12.2R_{ht}}{k_s'}\right)\sqrt{gSR_{ht}} \quad (4.3)$$

where V_t is the velocity at each time step, and k_s' (m) is the roughness parameter. The Keulegan equation was chosen over the more commonly-used Mannings equation because of its applicability when relative roughness $\frac{h}{D_{50}} < 10$ (where h is the mean flow depth) (Julien, 2002). At smaller relative roughness, the two equations collapse (Julien, 2002). Since channels in this study had relative roughness between 13 (Morningside Creek) and 28 (Wilket Creek) at top-of-bank flows, the Keulegan equation was deemed more appropriate for capturing the full range of flows captured in this study. The k_s' values were chosen to be $4D_{84}$, as suggested by Ferguson (2007) for gravel-bed rivers. The chosen k_s' values were verified using field measurements of flow velocity from a handheld radar gun (Surface Velocity Radar, Decatur Electronics Inc.). From the calculated velocity, the discharge (m^3/s) was calculated at each time step:

$$Q_t = V_t \times A_t \quad (4.4)$$

Finally, the specific stream power was calculated at each time step following:

$$\omega_t = \frac{\rho_w g Q_t S}{B} \quad (4.5)$$

where B is the mean channel bed width of each study reach (m).

4.2.3.1 Threshold for tracer mobilization

The threshold for tracer mobilization is fundamental for this analysis since it sets the value above which metrics are summed to obtain cumulative metrics. Thresholds for mobilization were set using the critical shear stress of each tracer size class (τ_{ci}) because it is a measure of the frictional force acting on the bed, and therefore responsible for sediment entrainment. The critical values of mean velocity (V_{ci}), discharge (Q_{ci}), and specific stream power (ω_{ci}) were calculated at the water level that corresponds to the τ_{ci}.

The critical shear stress for mobilizing sediment is notoriously difficult to estimate because it involves many complex processes, and several different, and often conflicting, methods have been developed to calibrate it (Buffington & Montgometry, 1997; Yager et al., 2018b). As the prediction of tracer behaviour is the focus of this study, regression of tracer data was used to calibrate τ_{ci} here. The threshold shear stress was calibrated for each tracer size class (i) by plotting peak shear stress versus each tracer variable ($f_{mi}, L_i, \tilde{L}_i$) and fitting a regression to determine the value of the intercept. Both linear and power regressions were fitted to determine the calibration with the highest goodness-of-fit based on the R^2 of the regression. Three estimates of τ_{ci} were determined this way to assess the range in critical shear stress

estimated from using different tracer variables. Next, the dimensionless critical shear stress (τ^*_{ci}) was determined for each τ_{ci} by rearranging the Shields equation:

$$\tau^*_{ci} = \frac{\tau_{ci}}{(\rho_s - \rho_w) g D_i} \tag{4.6}$$

where ρ_s is the mean density of the tracer stones (2700 kg/m^3), and D_i is the median tracer b-axis diameter (mm) of size class *i*. It has been shown that due to the geometry of interlocking particles on the stream bed in mixed-size sediment, τ^*_{ci} values vary based on the relative size of the particles to the median size class (D_{50}) of the bed following a hiding function of the form (Parker & Klingeman, 1982; Wilcock, 1988):

$$\frac{\tau^*_{ci}}{\tau^*_{cD50}} = \frac{\tau_{ci}}{\tau_{cD50}} = \left[\frac{D_i}{D_{50}}\right]^b \tag{4.7}$$

To assess whether the hiding function varies between field sites, and determine a common hiding function for applications in these streams, the parameter *b* was calibrated using the τ^*_{ci} determined through the regression analysis for all field sites together.

4.2.4 Model Building

4.2.4.1 Single Variable Regressions

To explore which flow metric best predicts tracer displacement variables (f_{mi}, L_i, $\tilde{L}_i$), single variable regressions were performed with each flow metric. Linear ($y = \beta_o + \beta_1 x$), power ($y = \alpha x^{\beta}$), and exponential ($y = \alpha\beta^x$) regression models were fit to the data using the ordinary least-squares method. These models were fit for each study site separately, as well as for all study sites together. The residual standard error of the regression (RSE) was used as a goodness-of-fit measure to compare between fitted models, defined as the square root of the sum of squares of the residuals divided by the residual degrees of freedom. The common R^2 parameter used as a goodness-of-fit measure was not applicable in this instance, as it is not appropriate for non-linear models that cannot be linearized, and can therefore not be calculated for exponential regressions (Sapra, 2014). Once the strongest regression was determined using the RSE, the R^2 was reported if the best model fit was linear or power.

4.2.4.2 Multiple Linear Regressions

To explore the possibility of improving models by considering multiple flow metrics together, multiple linear regressions were considered between each tracer variable and the flow metrics. Multiple linear regression used to build models to predict tracer movement has been proposed in other studies with success (Vazquez-Tarrio & Batalla, 2019). Multiple linear regression takes the form:

$$y = \beta_o + \beta_1 x_1 + \beta_2 x_2 + \ldots \beta_n x_n \tag{4.8}$$

where y is the tracer variable considered, $x_1 - x_n$ are the flow metrics, and $\beta_o - \beta_n$ are the fitted coefficients.

A fundamental assumption of multiple linear regression is the absence of perfect multicollinearity between the predictor variables (i.e. the flow metrics). Using predictor variables that are closely correlated in the same multiple linear regression should be avoided, as it artificially inflates the goodness-of-fit of the regression without strengthening the predicting power of the model (Zuur et al., 2010). The variance inflation factor (VIF) is a measure of the severity of multicollinearity between predictor variables (Craney & Surles, 2002). The threshold VIF is set for each application, but VIF > 10 is typically chosen as the cut-off, while values > 5 are taken with caution (Craney & Surles, 2002). To avoid multicollinearity in the multiple linear regression model, predictor variables that produce high VIF values should be removed from the model (Craney & Surles, 2002; Zuur et al., 2010). A VIF > 10 between two predictor variables corresponds to a Pearson Correlation Coefficient (r) = 0.9, so that the correlation between two predictor variables is a good first step to assess collinearity (Craney & Surles, 2002). To assess correlations between the calculated flow metrics, a correlation matrix was first built using data from all recoveries, and flow metrics with $r \geq 0.9$ were not used together in the multiple linear regression. Of the remaining flow metrics, a both-direction stepwise regression was performed to select the best subset of flow metrics for the model. An Akaike Information Criterion (AIC) was used within the stepwise regression as an estimator of the relative quality of the models tested (Cavanaugh & Neath, 2019).

4.3 Results

4.3.1 Observed tracer slowdown in Wilket Creek

Preliminary data exploration revealed significant tracer slowdown in the urban stream, Wilket Creek. Early events at Wilket Creek produce higher values of f_{mi}, L_i, and $\tilde{L}_i$ in relation to flow metrics. Figure 4.2 shows examples of tracer slowdown in relation to both peak metrics with peak shear stress (τ_p) (Figure 4.2a), and cumulative metrics, with specific bedload transport rate (q_b) (Figure 4.2b). Separation of early events was done by progressively adding data from the first event in order, and fitting linear regressions until the R^2 of the regression dropped to ≤ 0.5. Almost all combinations of tracer variables and flow metrics produced this drop in R^2 following the addition of the eighth recovery of the study, which occurred on June 20, 2017 (Table A.1), with the only exception being L_i versus q_b (Figure 4.2b). This recovery took place after a long rainfall event between May 3–5, 2017 that produced unusually long-duration hydrographs in Wilket Creek that were not typical of the characteristic flashy hydrographs. The regressions demonstrate the difference in the relationships between tracer variables and flow metrics as the tracer study progresses. Tracer slowdown over multiple mobilizing events has been documented in other studies and has been attributed to tracer burial

and vertical mixing of tracers into the bed (Ferguson & Hoey, 2002; Ferguson et al., 2002). The higher number of mobilizing events in Wilket Creek makes the tracer slowdown more evident in this stream than the other two study streams (see Appendix Table A.1). Given that Ganatsekaigon Creek and Morningside Creek experienced fewer than eight events with significant mobility ($f_m \geq 0.1$) (Table A.1), it is expected that tracer behaviour in these systems matches more closely with the early events at Wilket Creek. For this reason, all subsequent analyses are performed using only the early event data from Wilket Creek (recoveries 1–7, Table A.1) to allow meaningful comparison with the other systems. The data from Wilket Creek demonstrates the need for predictive models of tracer mobility and dispersion to account for tracer slowdown.

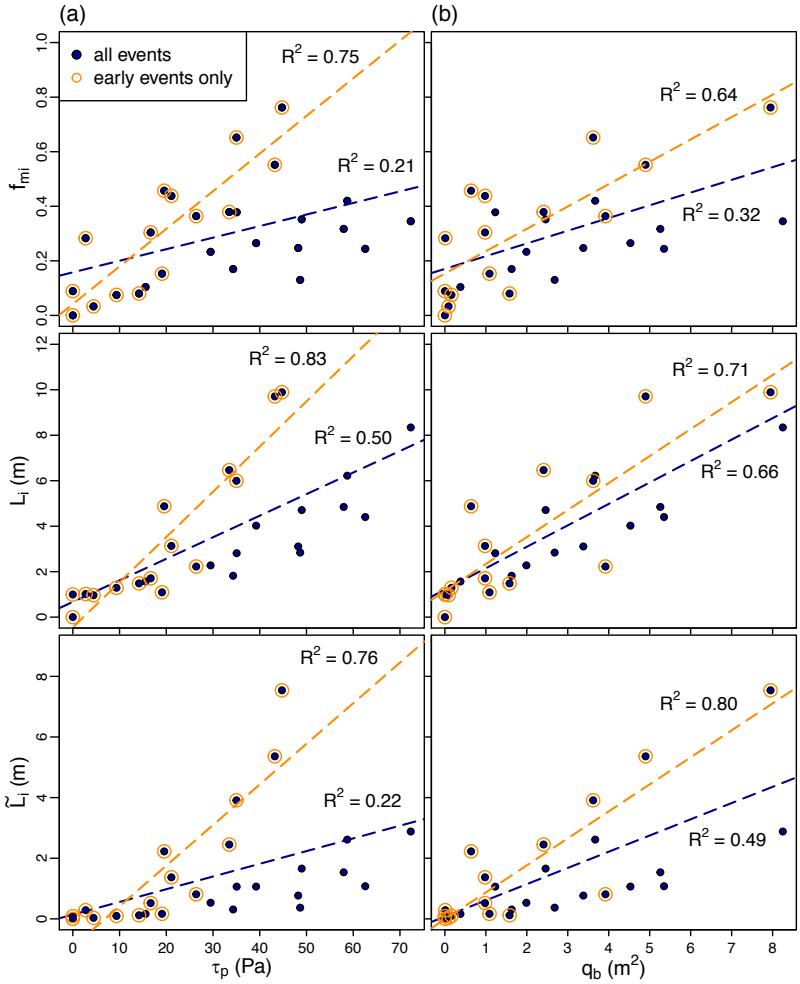

Figure 4.2. Tracer slowdown in Wilket Creek shown through regression models of f_{mi}, L_i, and $\tilde{L}_i$ versus (a): peak shear stress (τ_p), and (b): the specific bedload transport rate (q_b).

4.3.2 Critical shear stress calibration

Calibration of τ^*_{cD50} using the three tracer variables results in very large ranges of values depending on which tracer variable is used for calibration (Table 4.2). Most calibrated values fall within the range of observed values in other studies that fall between 0.03 and 0.086 (Buffington & Montgomery, 1997), although many fall near the outside limits of the range. Values at Wilket Creek were higher than those calibrated in the other two streams using all three tracer variables, and fall near the limits of values reported in other studies (Buffington & Montgomery, 1997). A likely explanation is that the gauge at Wilket Creek where the flow metrics are calculated is located ~100 m upstream of the tracer seeding location, whereas at the other two streams the gauge is installed directly on one of the two seeding riffles. The considerable variability in Wilket Creek cross-sectional geometry (Figure 3.3b) means that shear stresses calculated at the gauge may not reflect the shear stresses experienced at the tracer locations. The calibration of the τ^*_{cD50} based on observed tracer displacements allows for these values to be used in the models developed here, regardless of whether they are the true shear stress experienced by the tracers. Variability in calibrated values between sites is introduced due to the sensitivity of this method to tracer data and its dependence on parameters such as the number and magnitude of events captured and local hydraulic conditions. It is important to note that linear and power models produced stronger regressions for different variables and in different study sites (Table 4.2). Combined, these results highlight the need to calibrate τ^*_{cD50} depending on which tracer variable is of interest and the importance of site-specific calibration. Given the usefulness of $\tilde{L}_i$ in capturing both the mobility and travel length of tracers as an overall variable of tracer behaviour, the τ^*_{cD50} calibrated using $\tilde{L}_i$ was used for the subsequent model building presented in this study.

Table 4.2. Best model fit, calibrated τ^*_{cD50} values, and regression R^2 determined using f_{mi}, L_i, and $\tilde{L}_i$.

	Ganatsekaigon			**Wilket**			**Morningside**		
	Model	τ^*_{cD50}	R^2	Model	τ^*_{cD50}	R^2	Model	τ^*_{cD50}	R^2
f_{mi}	linear	0.026	0.94	linear	0.064	0.94	linear	0.038	0.91
L_i	linear	0.035	0.82	power	0.070	0.92	power	0.043	0.89
$\tilde{L}_i$	power	0.085	0.85	power	0.090	0.99	power	0.070	0.91

Although the calibrations produce high R^2 values (Table 4.2), considerable scatter exists in the data, particularly in the regression of the D_{75} and D_{90} size classes (Figure 4.3). This error is built into the uncertainty of the calibrated τ^*_{cD50}, and must be considered when producing predictive models of tracer displacement. Uncertainty in τ^*_{cD50} is expected, given the complexity of sediment entrainment and the high spatial and temporal variability in local shear stresses produced by local roughness elements and small-

scale turbulence (Yager et al., 2018a), as well as effects of historical flows (Masteller et al., 2019). Results of the threshold shear stress calibration demonstrate the inherent error in field calibrated τ^*_{cD50} values, and the need for site-specific calibration and considerations.

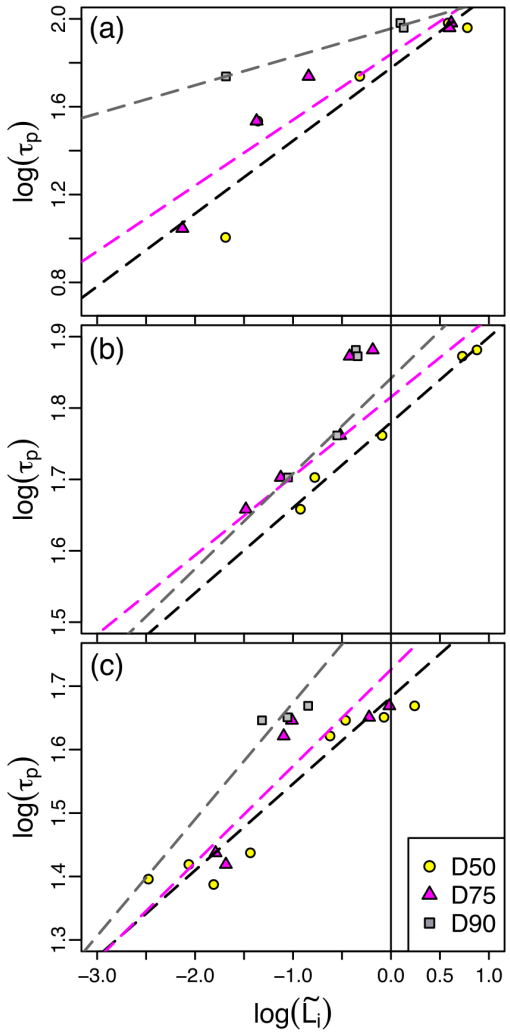

Figure 4.3 Calibration of τ_{ci} using regressions of the $\tilde{L}_i$ of the tracer particles in each size class for (a): Ganatsekaigon Creek, (b): Wilket Creek, and (c): Morningside Creek.

The final step in calibrating the critical shear stress was the application of a hiding function to allow for the calculation of the τ^*_{ci} of tracers outside the D_{50} size class without the need to perform the calibration for each size class individually, or for calculating flow metrics for size classes outside the range of the tracers. The τ_{ci} values determined from the regression calibration using $\tilde{L}_i$ (Table 4.2) were used to calibrate the general form of the hiding function (Equation 4.7). All three study streams fell close to the same relationship, providing an exponent $b = -0.8 = -\frac{4}{5}$ (Figure 4.4). The high confidence of the hiding function allows for the τ^*_{cD50} in each stream to be set to the values calibrated using $\tilde{L}_i$, and the τ^*_{ci} values of the other

tracer size classes to be calculated through the hiding function, rather than calibrated individually. The determined exponent (b) value is < 1, which indicates partial mobility and is expected of streams with mixed-size bedload (Parker & Klingeman, 1982; Wilcock, 1988). The similarity in the relationship between and in the three streams suggests that coarse particle interactions due to mixed particle sizes are similar in the three streams, an expected result given the similarity in the coarse tail of their grain size distributions (Figure 3.2).

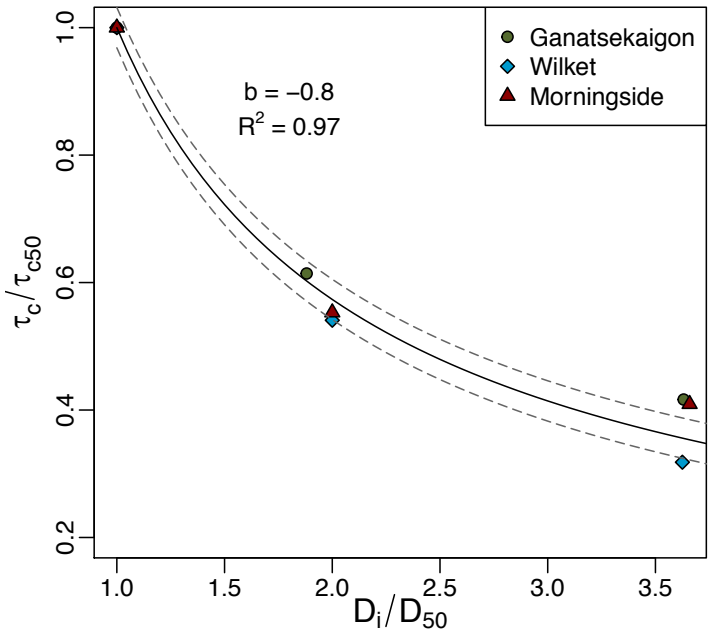

Figure 4.4. Calibration of the hiding function (Equation 4.7).

4.3.3 Regression models

The single variable regressions yielded strong relations between the tracer variables and the flow metrics. For all flow variables, linear regressions produced the strongest goodness-of-fit (i.e. lowest RSE), and dimensional versions of metrics outperformed their non-dimensional counterparts. Regressions were strongest in Ganatsekaigon Creek, and lowest in Wilket Creek (Figure 4.5), revealing higher variability in tracer behaviour in Wilket Creek even after separating early events (Figure 4.2). The flow metrics that produced the strongest regression was not consistent between streams, but some trends can be observed. In all three streams, peak flow metrics had the strongest relationship to f_{mi}, suggesting the maximum flow conditions have the strongest influence on the mobility of bed particles. In contrast, cumulative flow metrics had the strongest relation to L_i in Ganatsekaigon and Morningside Creeks, but peak unit stream power (ω_p) had the strongest relation in Wilket Creek. This difference may be a consequence of the short duration of floods in Wilket Creek making the magnitude of flow, rather than the sustained duration of flows. Finally,

cumulative flow metrics consistently had the strongest relation to $\tilde{L}_i$ in all three streams (Figure 4.5), highlighting the influence of both flow magnitude and duration exert influence on overall tracer displacements. Plotting f_{mi} and L_i reveals that flow metrics of zero (i.e. no flow above threshold) result in mobility of up to almost 0.4 (Figure 4.5a), while mean travel lengths reach up to 5 m (Figure 4.5b). This discrepancy is due to the calibration of τ^*_{cD50} based on $\tilde{L}_i$, which is higher than estimates using f_{mi} and L_i (Table 4.2). The effect is improved when considering the $\tilde{L}_i$ relations (Figure 4.5c), although some variation continues, particularly in Morningside Creek, where values of $\tilde{L}_i$ up to almost 2 m persist when *CI* is equal to zero. The Morningside Creek regression is particularly difficult to assess, as only one event exceeding τ^*_{cD50} was recorded, and so the relation is based on only 3 data points. These results demonstrate how the choice of τ^*_{cD50} calibration affects models of tracer displacement and the need to capture several mobilizing events to produce more confident models.

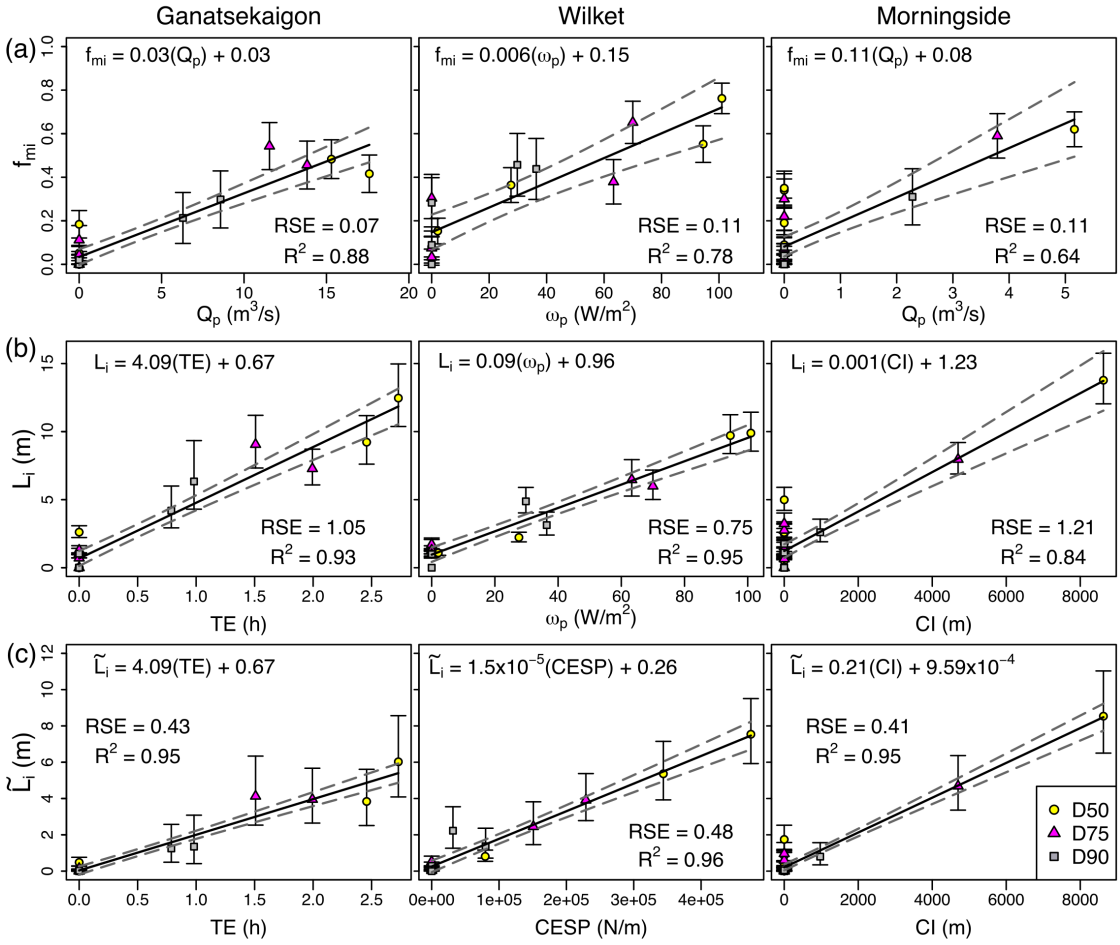

Figure 4.5. Strongest single variable regression for (a): mobility (f_{mi}), (b): mean travel length (L_i), and (c): weighted travel length ($\tilde{L}_i$).

Regressions using tracer data from all three sites together tests the ability to produce a single model that predicts tracer behaviour in streams with different hydrograph characteristics. The strongest fits for all tracer variables were linear, counter to other studies that fit power models to tracer displacements (e.g. Hassan et al., 1992; Schneider et al., 2014). Although f_{mi} and L_i had the strongest relation to peak flow metrics, $\tilde{L}_i$ has the strongest relation to cumulative excess discharge (*CEQ*), a cumulative flow metric (Figure 4.6). This result further confirms the importance of both flow magnitude and duration in overall tracer displacement. Normalizing L_i and $\tilde{L}_i$ by the mean channel width (*B*) of each stream can be used to incorporate the influence of channel morphology on tracer travel lengths and improve comparison between streams (Pyrce & Ashmore, 2003a), as was explored in Chapter 3 (Section 3.4.4 and Section 3.4.5). Using the normalized L_i appears to reduce some of the scatter in the data, but does not improve the goodness-of-fit of the regression (Figure 4.6b versus Figure 4.6d). However, using normalized $\tilde{L}_i$ collapses the scatter in the data, and improves the goodness-of-fit of the regression to a value of $R^2 = 0.92$ (Figure 4.6c versus Figure 4.6e). The strong relations between the tracer variables and flow metrics using data from all three streams combined, particularly between *CEQ* and normalized $\tilde{L}_i$, suggest a universal model can be used to predict tracer displacements in streams with different hydrograph characteristics. These results also highlight the importance of considering flow magnitude, flow duration, and channel morphology in predicting bedload particle behaviour.

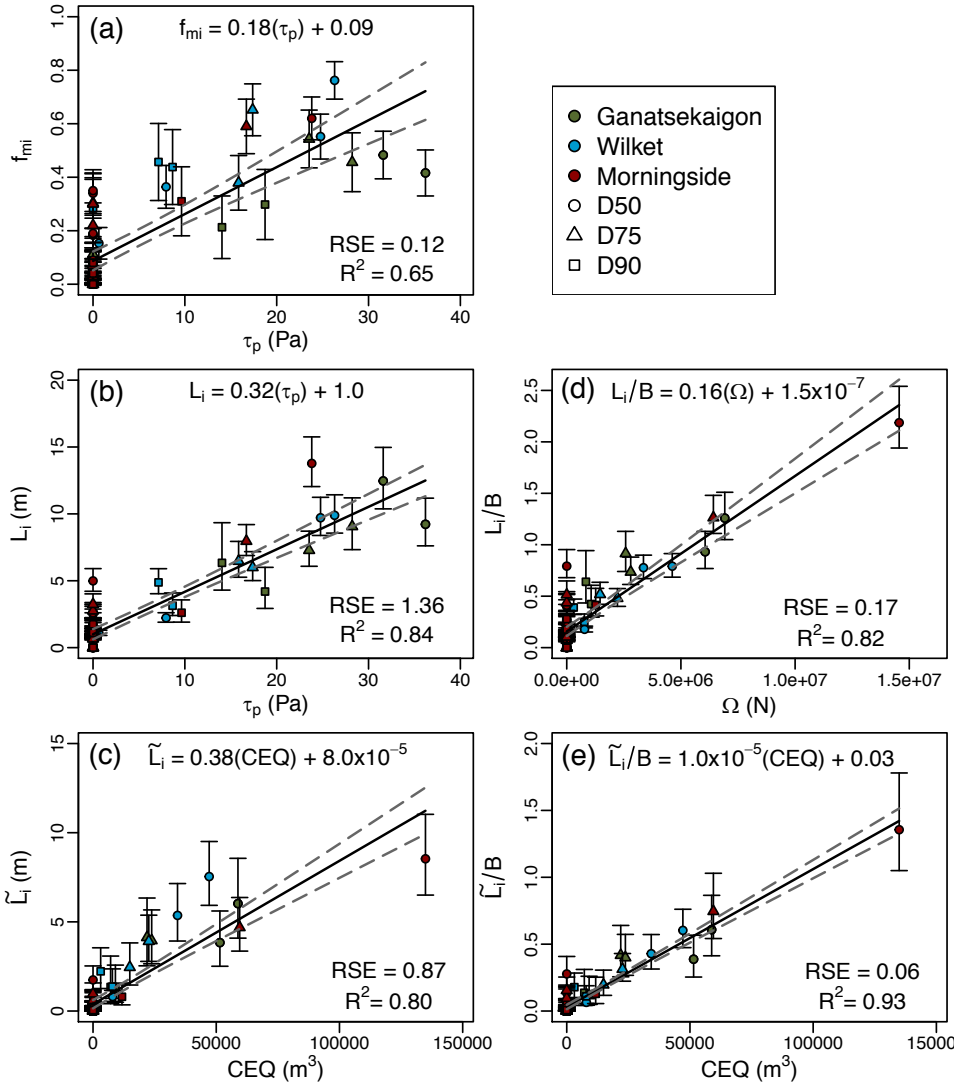

Figure 4.6. Strongest single regression model for all study streams combined for (a): mobility (f_{mi}), (b): mean travel length (L_i), (c): weighted mean travel length ($\tilde{L}_i$), (d): the mean travel length scaled by the mean channel width (B), and (e): the weighted mean travel length scaled by the mean channel width.

The correlation matrix of the calculated flow metrics indicates high collinearity (Figure 4.7). This result is unsurprising, as several metrics are mathematically related. For example, specific bedload transport rate (q_b) and bedload transport rate (Q_b) are identical save for a multiplier of channel width (Table 4.1), which is a constant at high flow. The peak flow parameters were all highly correlated, with $r \geq 0.84$. In fact, the dimensional versions of τ_p and ω_p^* were perfectly correlated (r = 1), as were their non-dimensional versions (r = 0.99) (Figure 4.7). The dimensional and non-dimensional versions of the metrics were slightly less correlated, but the possibility of multicollinearity when using them in together in conjunction with other flow metrics still exists, and needs to be verified by calculating the VIF. Similarly, the cumulative flow metrics were also highly correlated ($r \geq 0.8$), except for *TE*. The strong collinearity between flow

metrics means that using more than one in the same model (e.g. as in a multiple linear regression) will lead to an inflation of the goodness-of-fit parameter, obscuring whether the model truly predicts the tracer variables better. Given the high *r* values between certain flow metrics and the results of the single variable regressions, only the following were chosen for the multiple linear regression analysis: the strongest peak metric, non-dimensional peak metric, and cumulative metric from the single variable regressions, and *TE*. A list of the chosen variables for the multiple linear regressions can be found in the Appendix (Table A.3). The VIF between these chosen flow metrics was calculated before conducting the stepwise regression. In cases where VIF > 10, all combinations of subsets of these flow metrics that had a VIF < 10 were run through the stepwise regression.

The multiple linear regression performed on each stream separately did not significantly improve the strength of the models. Only the regression for f_{mi} at Ganatsekaigon Creek produced a higher goodness-of-fit than the single variable regression. In this case, $Q_p + \tau_p^*$ produced a RSE = 0.06 and $R^2 = 0.90$ (VIF = 7.27), which is a small improvement from the single variable regression (Figure 4.5). The VIF exceeds the caution limit of 5, suggesting some inflation of the goodness-of-fit due to the collinearity between Q_p and τ_p^* (Figure 4.7). In all other cases, the multicollinearity between flow metrics limited the combinations of metrics that could be used in the multiple linear regression. Of the variable combinations attempted, the stepwise regression yielded the strongest relation with the single variables outlined in Figure 4.5. This result is beneficial, as it suggests that the addition of more metrics in more complicated models does not significantly improve model predictions. With each additional flow metric added to the model, additional uncertainty and error are also introduced, as each metric has its own associated uncertainty given measurement and calibration error. Therefore, the use of a single variable to predict tracer displacement minimizes the uncertainty, without significantly impacting the strength of the model.

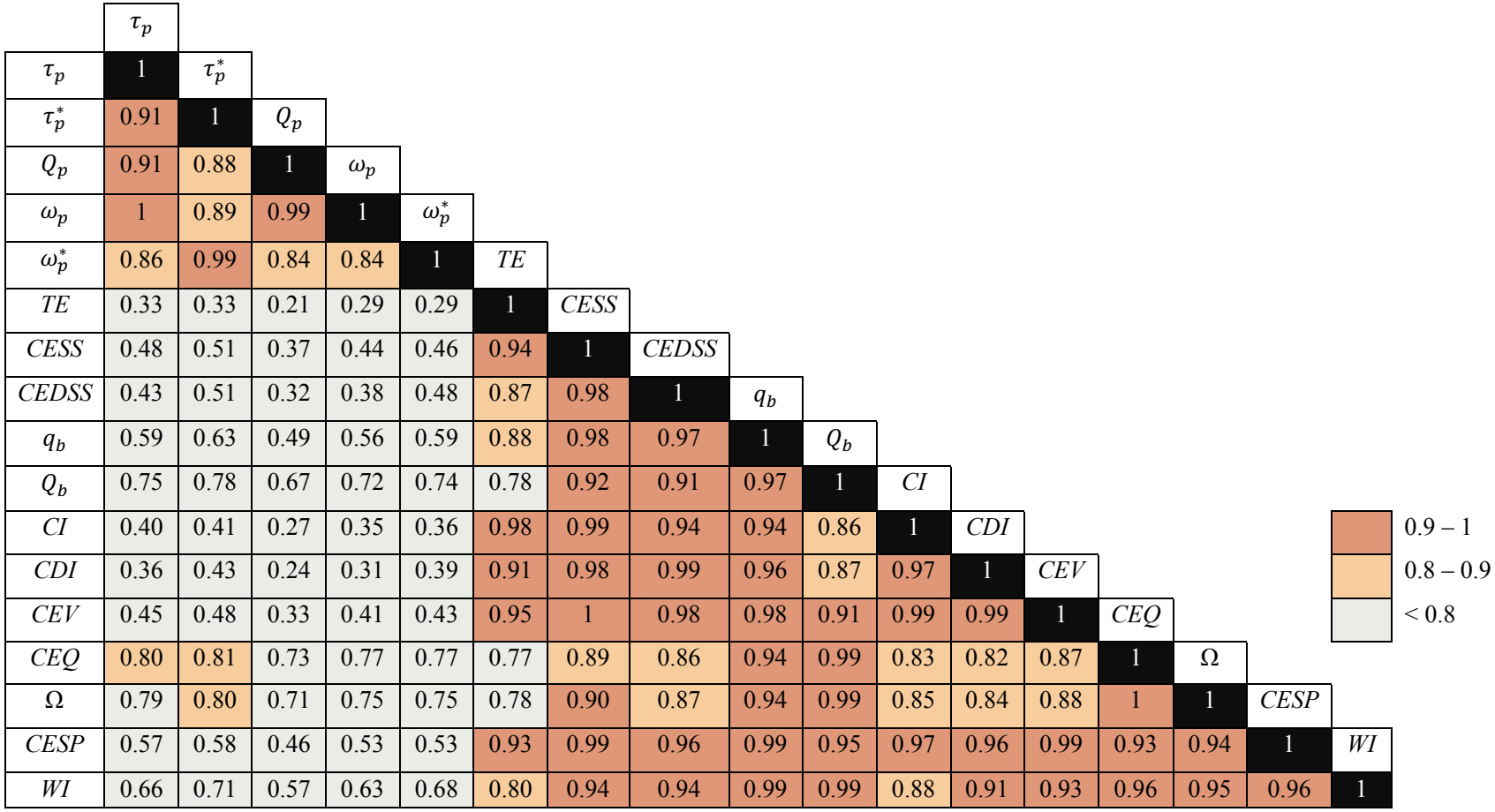

Figure 4.7. Correlation matrix of calculated flow metrics showing multicollinearity.

The multiple linear regression moderately improved the model strength when considering all streams together. Results of the stepwise regression showing the strongest model are summarized in Table 4.3. The goodness-of-fit of the models was higher than those with the single variable regression (Figure 4.6), but not consistently. Although the R^2 of the regressions were improved for all tracer variables except scaled weighted mean travel length ($\frac{\tilde{L}_i}{B}$), the RSE was sometimes larger, indicating larger deviations of residuals from predicted values. The stepwise regression yielded the strongest regression with combinations of flow metrics that include both peak and cumulative metrics, suggesting that both flow magnitude and duration play a role in tracer displacement. Overall, the slight improvements in goodness-of-fit of the multiple linear regression models where they exist may not be enough to offset the increased uncertainty and error associated with including additional flow metrics. For example, the strong relation between peak metrics and both f_{mi} and L_i in the single variable regressions (Figure 4.5) allows for the error associated with calibration of τ^*_{cD50} to be avoided, as τ_p can be calculated as an absolute value independent of the critical shear stress.

Table 4.3 Flow metrics, RSE and R^2 of strongest multiple linear regressions performed on all streams together.

	Single Variable Regression			Multiple Regression		
	Metric	RSE	R^2	Metrics	RSE	R^2
f_{mi}	τ_p	0.12	0.65	τ_p+ *TE*	0.12	0.68
L_i	τ_p	1.36	0.84	τ_p+ Ω	1.13	0.89
$\tilde{L}_i$	*CEQ*	0.87	0.80	τ_p+ *CEQ*	0.62	0.90
$\frac{L_i}{B}$	Ω	0.17	0.82	τ_p+ τ^*_p + Ω	0.15	0.86
$\frac{\tilde{L}_i}{B}$	*CEQ*	0.06	0.93	τ_p+ τ^*_p + *CEQ*	0.06	0.94

4.4 Discussion

Bedload tracer data and detailed water level measurements were used to develop models for predicting tracer displacements in streams with different hydrograph characteristics resulting from urbanization and SWM. Objectives were to determine the most appropriate critical shear stress calibration method for tracer data applications, assess which flow metrics perform best at predicting the mobility and travel length of tracers in streams with different hydrograph characteristics resulting from urbanization and SWM, and build

the strongest model for predicting the mobility and travel length of bed particles for application to urban rivers. Several flow metrics proposed in the literature for relating to tracer data were tested, and considerations for building models of tracer displacements were explored. The weighted mean tracer travel length ($\tilde{L}_i$) is introduced for the improved application of tracers in riverine settings.

This study revealed several challenges in building predictive models of tracer behaviour in riverine environments. Firstly, the slowdown of tracers over several mobilizing events due to burial is a significant limitation of RFID tracer technologies, and has been documented in other studies (Ferguson & Hoey, 2002; Ferguson et al., 2002). Careful consideration must be placed on identifying shifts in tracer behaviour as the study progresses. A method to rectify this would be to split the data, and perform analyses separately for early and later events, as was done in this study. Such a method is appropriate when the goal is to compare tracer dynamics between systems, and the difference between unconstrained versus well-mixed particles must be accounted for. Another strategy would be to re-seed waves of tracers in intervals to counteract burial rates (e.g. Biron et al., 2012; MacVicar & Roy, 2011; Schneider et al., 2014). Both these methods, however, do not allow for information of vertical mixing processes to be collected. Given the importance of vertical mixing in bedload transport (Hassan et al., 2013; Mao et al., 2017; Parker et al., 2000; Wong et al., 2007), a method to obtain burial depths (e.g. Papangelakis et al., 2019) would allow for more detailed information on bedload transport processes to be explored. Another important consideration in building predictive models of bedload transport is calibration of the critical shear stress. The determination of the critical shear stress is a topic of great discussion due to the range of methods used, and its inherent spatial and temporal variability (Montgomery & Buffington, 1997; Yager et al., 2018b). This study supports the need to carefully estimate the critical shear stress separately for each system and for each application (Montgometry & Buffington, 1997), as well as to set different critical shear stresses for each tracer size class separately either through individual calibration (Wilcock, 1997; Milan, 2013b).

Regression models built in this study can be used to assess the dominant controls on bedload transport, and provide insight into the effects of urban hydromodification on tracer dynamics. For example, tracer mobility was most strongly related to peak flows, demonstrating the importance of flow magnitude on bedload mobilization (Hassan et al., 1992). Mean travel lengths were less consistent, having stronger relationships to cumulative metrics in Ganatsekaigon Creek and Morningside Creek, but with peak metrics in Wilket Creek. The importance of both flow magnitude and duration on tracer travel lengths has been demonstrated in other undeveloped systems (Papangelakis & Hassan, 2016; Phillips et al., 2013; Schneider et al., 2014), suggesting the strong relationship between peak excess shear stress and mean travel length is a consequence of the urban hydromodification leading to shorter duration, flashy hydrographs. However, the weighted mean travel length, which considers both mobility and travel lengths ($\tilde{L}_i$) consistently had the strongest relationship with cumulative metrics in all systems, highlighting the importance of considering

both flow magnitude and duration in urban river management. The weighted mean travel length is useful for bedload sediment monitoring applications as it considers both the mobility and travel length of tracers and is, therefore, more representative of the overall behaviour of the bedload material.

The strong relationship between flow metrics and tracer variables when considering all three streams together links to some of the long-term tracer dynamics explored in Chapter 3; the collapse of all three systems onto the same regression line supports that the fundamental processes of bedload transport are not altered between streams, confirming that the increased long-term displacement in Wilket Creek is a result of more frequent bed mobilization, rather than an increase in bedload transport for events of a given magnitude (as concluded in Chapter 3). Furthermore, the collapse of the data on a single regression line supports that bedload transport in Morningside Creek is driven by the increased duration of mobilizing flows; the elongated falling hydrograph falling limbs from the peak-shaving SWM result in higher values of cumulative flow metrics. At the same time, the smaller channel width in Morningside Creek results in higher weighted mean travel lengths when normalized by channel width.

The strongest model between flow metrics and tracer variables across systems was the regression model between the cumulative excess discharge (CEQ) and scaled $\tilde{L}_i$ (Figure 4.6). The high goodness-of-fit of the model means that a single model can be used across systems, regardless of differences in hydrograph shape due to urbanization and SWM. The weighted mean travel length and its relationship to cumulative excess discharge provides a tool that can be used to design, monitor, and assess the impact of SWM and urban stream restoration on bedload sediment transport. For example, SWM and restoration efforts can focus on mimicking pre-urban event-based cumulative excess discharge, rather than attenuating peak flows or artificially increasing roughness. Catchment-scale stormwater management efforts that attempt to match pre-urban hydraulic conditions, such as low impact development (LID), can be used to achieve such goals, and are more likely to have ecological benefits (Anim et al., 2019a). Models have also shown that alterations to the channel form (e.g. widening, coarsening, grade control) can also achieve changes to the local hydraulics that can change the distribution of mobilizing forces (Anim et al., 2019c), and therefore the cumulative excess discharge.

Several limitations to the model presented in this study exist. Firstly, the number of events that resulted in significant tracer displacement was limited, particularly at Morningside Creek. A larger number of mobilizing events would help verify and strengthen the relationships presented, but the issue of tracer slowdown must be adequately addressed. Second, the model presented here is based on only three stream systems. Data from a larger array of streams with different geologic, morphologic and hydrologic settings would allow for the model to be tested in a larger variety of environments. Although several studies using bedload tracers exist (see Vazquez-Tarrio et al., 2019), inconsistencies between study methodologies make a direct comparison of relationships between tracer variables and flow metrics difficult. Many tracer studies

calculate flow metrics based on a single threshold for mobilization for the entire tracer population, despite using a wide range of tracer sizes (e.g. Gintz et al., 1996; Haschenburger & Church, 1998; Haschenburger, 2013; Hassan et al., 1992; Liébault et al., 2012; Mao et al., 2017; Papangelakis & Hassan, 2016; Schneider et al., 2014). There are also discrepancies in how the mean travel length is defined. Some studies report the mean travel length of only mobile tracers (e.g. Bradley & Tucker, 2012; Chapuis et al., 2015; Phillips et al., 2013; Schneider et al., 2014), while others of the entire tracer population, including immobile tracers (e.g. Liébault et al., 2012; Liedermann et al., 2013; Papangelakis & Hassan, 2016). Most tracer studies also calculate the arithmetic mean travel lengths, rather than the geometric mean, despite the reported skewness in tracer travel length distributions (e.g. Bradley & Tucker, 2012; Gintz et al., 1996; Liébault et al., 2012; MacVicar & Roy, 2011; Papangelakis & Hassan, 2016; Phillips et al., 2013; Phillips & Jerolmack, 2014; Schneider et al., 2014). The final limitation of this study is the incorporation of uncertainty analysis in the calculation of flow metrics. Next research steps should include complete sensitivity analysis for the input parameters (e.g. critical shear stress, roughness parameter), to identify the uncertainty in the presented models and assess how to best minimize it for applications.

4.5 Conclusions

The aim of this study was to build predictive models of tracer mobility and travel lengths from storm hydrographs in streams impacted by urban hydromodification and SWM. We introduce the weighted mean travel length as a useful variable for quantifying tracer displacements. Results from this study highlight several important considerations when building models of tracer behaviour: the need to assess and account for tracer slowdown, the importance of choosing the appropriate tracer variable (i.e. mobility, mean travel length, weighted mean travel length) for calibrating the mobilization threshold based on the intended model application, and the importance of setting separate thresholds for each tracer size class. Linear, single variable regressions performed the best at predicting tracer mobility, mean travel lengths, and weighted mean travel lengths in each stream separately, and for all streams combined. Multiple linear regressions did not significantly improve the performance of models, avoiding the need for additional complexity and uncertainty in models. Of the large number of flow metrics from the literature tested, there was inconsistency in which performed best in predicting tracer variables in each stream, reflecting the shifts in controls of bedload transport in each system (Chapter 3). A single model to predict the weighted mean travel length normalized by mean stream width based on the cumulative excess discharge is presented with a very high goodness-of-fit. The ability to predict bedload transport processes with a single model in streams with different hydrograph characteristics has applications for urban river management, providing a tool that can be used for decision making and SWM design.

Transition C

Chapters 3 and 4 focused on comparing and predicting bedload transport dynamics of streams with rural, urban, and SWM hydrologic settings. In-stream restoration is another popular management strategy for improving degraded urban river systems that focuses on addressing local channel degradation. Chapter 5 examines constructed riffle-pool channels to answer the fourth research question of the thesis: How can bedload transport and morphological monitoring be used to assess the performance of in-stream restoration projects from a geomorphic process perspective? Although there is increasing consensus that river restoration should focus on restoring processes rather than form, proven techniques to design and monitor projects for sediment transport processes are lacking (Wilcock, 2012). Most in-stream restoration designs do not explicitly design for the transport of bed sediment, but rather focus on goals related to structural stability (Chapuis et al., 2014a). The transport of sediment is, however, an important process for both maintaining dynamic equilibrium in natural stable systems (Sear, 1994), and ecologic health. Furthermore, the consequences of spatially isolated restoration projects on the larger sediment connectivity at the network or catchment scale are unknown. Chapter 5 monitors bedload transport and channel morphology in adjacent unrestored and restored reaches of Wilket Creek to compare bedload transport regimes, assess the stability and self-maintenance of constructed riffle-pool sequences, and evaluate the impact of the project on sediment continuity in the creek. Assessment of the performance of the restoration project shifts depending on whether static or process-bed criteria of 'success' are considered. Chapter 5 demonstrates how bedload tracking and morphological surveys can be used to assess river restoration projects, and highlights the importance of incorporating coarse sediment connectivity into restoration design and monitoring.

Chapter 5

Process-Based Assessment of Success and Failure in a Riffle-Pool River Restoration Project

This chapter is based on the following manuscript under review:

Papangelakis, E., & MacVicar, B. (*under review*). Process-based assessment of success and failure in a riffle-pool river restoration project. *River Research and Applications.*

Data presented in the figures and tables of this chapter can be downloaded from:

Papangelakis, E., MacVicar, B., (2019). Bedload sediment transport and morphologic data in an unrestored and restored reach of Wilket Creek, Toronto, Canada [Dataset]. https://dx.doi.org/10.20383/101.0179

5.1 Introduction

Urban river management increasingly focuses on treating symptoms of stream degradation through river restoration (Bernhardt et al., 2007; Pasternack, 2013). Constructed riffle-pool sequences are especially popular designs because of their perceived stability and benefits for aquatic ecology (Bernhardt et al., 2005; Wohl et al., 2005). There has been increasing attention on process-based restoration, which aims to restore natural hydrologic and geomorphic processes in order to improve the functionality of river ecosystems (Anim et al., 2019b; Beechie et al., 2010; Diaz-Redondo et al., 2018; Elosegi et al., 2010; Formann et al., 2014; Grabowski et al., 2014; Poppe et al., 2016; Vaughan et al., 2009; Whipple & Viers, 2019). Bedload sediment transport is an important geomorphic process that lies at the nexus of channel morphology, hydrology, and ecology. Incorporating bedload transport processes in restoration efforts has been proposed, primarily through the addition of coarse sediment to counteract diminishing sediment supply in large, regulated rivers (Arnaud et al., 2017; Liedermann et al., 2013), and in urban environments (Vietz et al., 2015). Despite increasing focus on bedload transport as an important river process for river management (Wohl et al., 2015a), tools for incorporating bedload transport processes into constructed riffle-pool design are lacking (Wilcock, 2012; Wohl et al., 2015b), and the effects of current design strategies on sediment dynamics is poorly understood (Biron et al., 2012).

Effective post-construction monitoring of in-stream restoration projects is lacking (Bernhardt et al., 2007; Miller & Kochel, 2009; Morandi et al., 2014; Poppe et al., 2016). Assessment of

restoration project performance is often done through hydraulic simulations and predictive models (e.g. Khosronejad et al., 2013; Khosronejad et al., 2014; Krapesch et al., 2009; MacWilliams et al., 2010; Nardini & Pavan, 2012). Field assessments of project performance typically involve methods to evaluate the stability of the designs, such as measuring geomorphic change (e.g. Bouska & Stoebner, 2015), or monitoring the structural integrity of constructed features (e.g. Buchanan et al., 2014; Miller & Kochel, 2009; Roni et al., 2002). However, focusing on bed stability as a goal of river restoration is counter to geomorphic principles of dynamic equilibrium (Sear, 1994), leads to reduced long-term project success (Thompson, 2002), and ignores evidence that dynamic channels better support aquatic ecosystems (Beagle et al., 2015; Chin & Gregory, 2009; Clarke et al., 2003; Thorp et al., 2006). As river restoration increasingly moves towards process-based designs, it is necessary to build complementary methodologies to evaluate project success through monitoring dynamic processes. Such methodologies have been developed for assessing hydrologic, morphodynamic and ecological processes in restored channels (e.g. Diaz-Redondo et al., 2017; Formann et al., 2014; Gurnell et al., 2016; Habersack et al., 2016; Schwindt et al., 2019), as well as for assessing responses in bedload sediment dynamics in regulated rivers (e.g. Arnaud et al., 2017; Liedermann et al., 2018). Analogous methodologies for evaluating bedload transport dynamics through constructed riffle-pool restoration projects are yet to be developed.

Current river restoration practices are typically spatially isolated to small reaches of the stream, rather than designed with the entire watershed or river network in mind (Bernhardt & Palmer, 2011; Wohl et al., 2005). Longitudinal sediment connectivity (also referred to as sediment continuity) has been defined as the degree to which sediment is able to be transferred between river reaches (Heckmann et al., 2018; Hooke, 2003; Wohl, 2017). Constructed riffle-pool channels may lead to a disruption of longitudinal sediment connectivity by locally altering the hydraulic forces due to changes in slope, roughness, and channel dimensions (Heckmann et al., 2018; Kondolf et al., 2006). Locations with low sediment connectivity within a channel network have been linked to areas of significant geomorphic change (Czuba & Foufoula-Georgiou, 2015). Increased morphologic change has also been documented downstream of weirs and dams that impede sediment longitudinal sediment mobility (e.g. Fremion et al., 2016; Habersack et al., 2016; Jordan et al., 2010; Sindelar et al., 2017; Yoshimura & Shinya, 2018). Therefore, even if a restored reach demonstrates local stability, disruptions to the coarse sediment connectivity may result in unintended geomorphic changes upstream or downstream of the constructed reach. Reach-scale river management efforts that lack context of the greater river network are therefore unlikely to be successful (Wohl et al., 2015b). An ideal method for assessing restoration designs should consider the local construction within the

context of a continuous river system.

Tracking the movement of individual grains has become a popular approach for gravel-bed river research (Vazquez-Tarrio et al., 2019). Bedload transport in gravel-bed rivers often occurs as partial mobility, where only a fraction of bed particles is mobile during transport (Wilcock & McArdell, 1997). The fraction of mobile particles and their travel lengths decrease with size (Church & Hassan, 1992; Ferguson & Wathen, 1998), and increase with flow magnitude (Ashworth & Ferguson, 1989). The virtual velocity of bed particles is defined as the average rate of travel (Hassan et al., 1992), and may be calculated either over single transport events (e.g. Brenna et al., 2019), or over several years (e.g. Houbrechts et al., 2015). When defined in the latter way, it can be used to quantify the mean long-term velocity of bedload sediment through the system (Houbrechts et al., 2015). A recent study comparing the virtual velocity of riverine tracer particles showed that bed particles move farther downstream per year in rivers with urbanized watersheds (see Chapter 3). The increase in the virtual velocity of bed particles and an increase in mobility of the coarsest fractions was linked to the different hydrologic conditions observed (see Chapter 3). A reasonable goal of urban river restoration could therefore be to decrease the virtual velocity of bed sediment particles to match those measured in relatively stable non-urban rivers. Bedload tracking can be used to assess the performance of constructed riffles and pools in relation to what has been observed in natural analogs (e.g. Chapuis et al., 2015; MacVicar & Roy, 2011; Milan, 2013a). Such process-based definitions of success would help support restoration approaches that reduce undesirable channel degradation and provide a more natural sediment transport regime in the channel.

This research aims to assess the performance of a constructed riffle-pool restoration project. The objectives of the current study are to: (1) compare how coarse sediment is being transported through a rural, an un-restored urban and a restored urban channel reach, (2) evaluate whether the restoration project meets goals of stability and self-maintenance, and (3) assess how the local restoration project is affecting sediment continuity in the larger river corridor. The study uses the same site and follows from that of MacVicar et al. (2015), who demonstrated the feasibility of particle tracking using Radio Frequency Identification (RFID) transponders for assessing the performance of a constructed riffle-pool. However, this earlier work used a limited number of tracer particles spread over a wide range of size classes and captured only three transport events. For the current study, the control site in a rural catchment is added for comparison, two waves of sediment tracers are followed, and morphologic adjustments are tracked over 5 years to get a better perspective on the processes that may lead to success or failure for this project.

5.2 Methods

5.2.1 Study site

Wilket Creek is a tributary of the Don River in the City of Toronto, Canada with a watershed area of 14.9 km^2. Additional details of the Wilket Creek watershed, including its location and surficial geology, is outlined in Chapter 3. The Wilket Creek watershed is highly urbanized, with 68% impervious cover and predominantly suburban residential with some commercial land use. Rapid urbanization began in the 1950s, with the watershed fully developed by the mid-1970s (Barr, 2017). The road network is sewered, and roof leaders/foundation drains are typically connected to storm sewers (D'andrea et al., 2004). The majority of development occurred in the early 1960s, before the appreciation for the need for stormwater management (TRCA, 2015). Consequently, there is no stormwater control infrastructure in the watershed to dampen flood magnitudes (TRCA, 2015), resulting in frequent flooding, increased discharges, and flashy hydrographs (Bevan et al., 2018; Barr, 2017; MacVicar et al., 2015). The upstream portions of the creek and most tributaries are buried in pipes, leaving only the downstream 6 km of the main channel above ground. Wilket Creek has experienced significant channel enlargement since watershed development. Between 1958 and 2016, the average channel width increased by 75%, while the average depth increased by about 50% (Bevan et al., 2018). Several attempts at erosion control have been employed in locations along the length of the creek, including gabion baskets, rip rap, and armour stone (Barr, 2017). Large floods in 2005 and 2008 resulting in extensive damage to park infrastructure prompted the Wilket Creek Rehabilitation Project in 2009, a plan to restore reaches of the channel identified as areas of risk to infrastructure and public safety (Parish Geomorphic, 2011; TRCA, 2015). Under the Wilket Creek Rehabilitation Project, several downstream reaches of the channel have undergone complete channel reconstruction.

This study monitored a 180 m long un-restored reach of Wilket Creek and a 360 m restored reach directly downstream between its completion in 2013 and 2018 (Figure 5.1a). The un-restored reach has a mean bed slope of 1.00 %, a mean top of bank (TOB) width of 12.45 m, and a mean TOB depth of 1.4 m. The morphology of the un-restored reach is a meandering riffle-pool channel (Figure 5.1b), and a D_{50} of 40 mm (Figure 5.1a). The design of the restoration was focused on minimizing perceive erosion problems in the channel, and therefore the design was made to focus on reduced channel mobility and bank stability. The restored reach consists of a constructed riffle-pool sequence through an irregularly meandering channel with a mean bed slope of 1.12%. The higher bed slope of the restored reach compared to the un-restored reach is a consequence of the artificial straightening of the meanders and decrease in the sinuosity from 1.8 in the un-restored reach to 1.5 in the restored

reach post-construction. The choice of a riffle-pool design was to follow the existing riffle-pool morphology of the un-restored channel. The dimensions of the restored channel were designed based on the critical velocity for a stable channel accounting for modelled urban flood magnitudes in Wilket Creek (AECOM, 2011; Parish Geomorphic, 2011). The mean TOB width is larger than that of the un-restored channel at 18.8 m, while the mean TOB depth is smaller at 1.3 m (Figure 5.1c). Grain size analysis conducted by Parish Geomorphic (2011) indicates that the grain size distribution of the restored reach pre-construction matched that of the un-restored reach monitored in this study (Figure 5.2a). The D_{50} of the restored reach was increased from 48 mm to 91 mm post-construction (Figure 5.2a). The constructed riffles are particularly coarse and angular, having large boulders > 1 m diameter to provide riffle stability and fixed bed elevations at sanitary sewer crossings (Figure 5.2a). To provide bank protection from erosion, the coarse banks of the restored reach are lined with dense vegetation, primarily willows and red osier dogwood (Figure 5.1c).

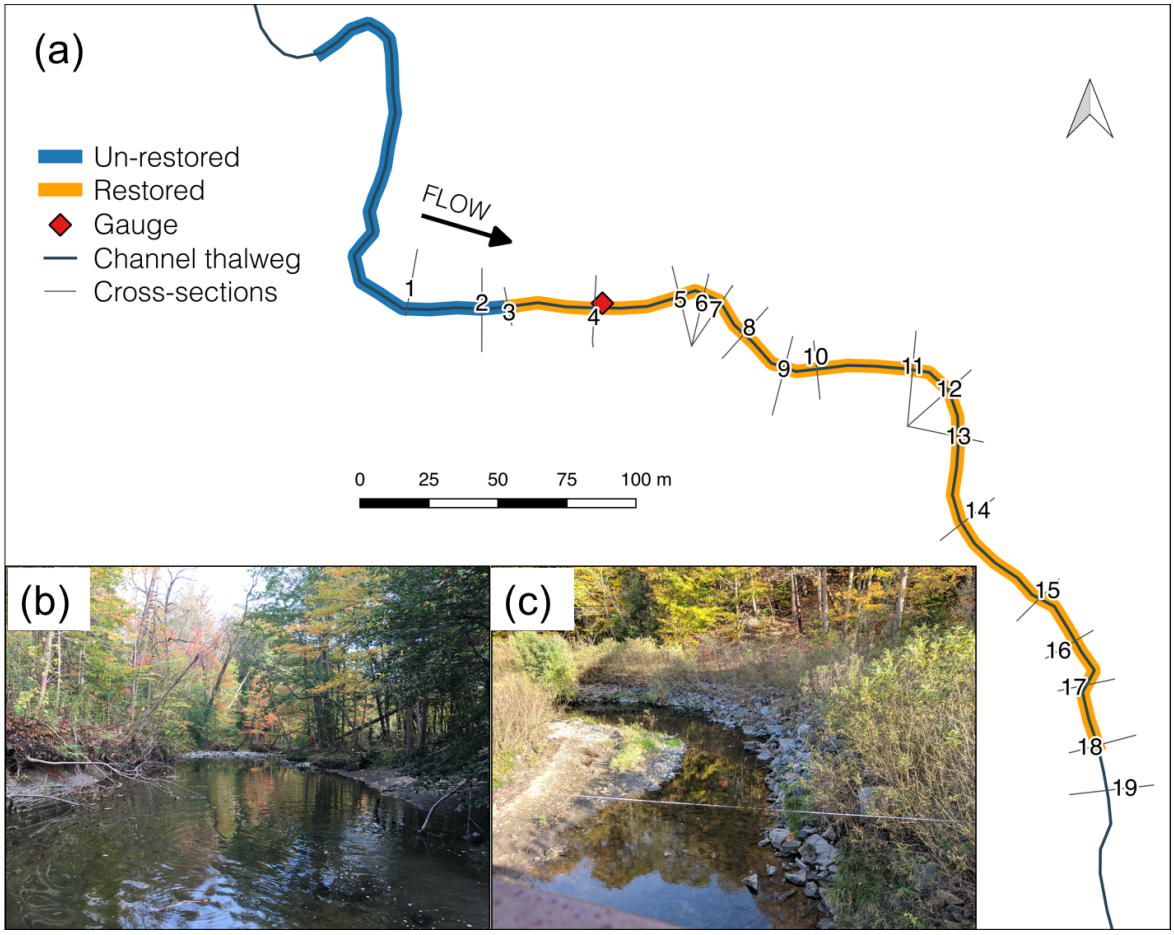

Figure 5.1. (a): Map of the study reaches, (b): photo at the upstream end of the unrestored, and (c): photo of the restored reach at cross-section 13.

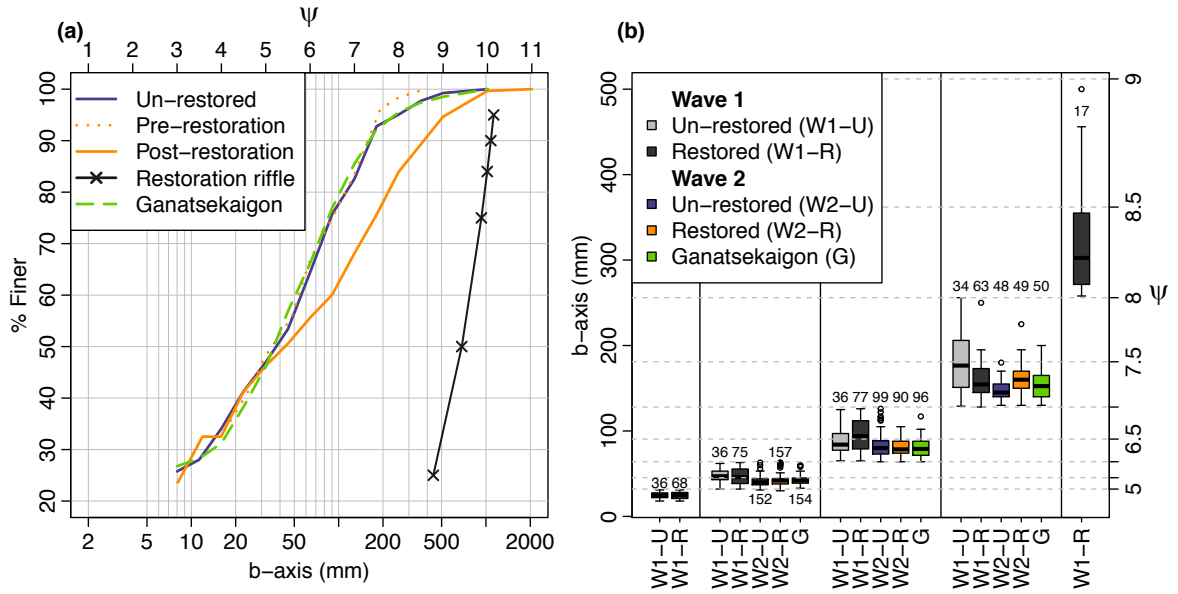

Figure 5.2. (a): Grain size distribution of study reaches and tracers and (b): boxplots of tracer b-axis diameters within each tracer size class for each seeded reach and tracer wave. Numbers above each boxplot report the total number of tracers in that size class. Pre-construction grain size distribution of restored reach and riffle design grain size distribution is from Parish Geomorphic (2011).

To compare Wilket Creek with a rural watershed, bedload sediment transport data from Ganatsekaigon Creek was used. The Ganatsekaigon Creek study reach and data collection is described in more detail in Chapter 3. The similarities between the sites on Wilket and Ganatsekaigon Creeks allow a space-for-time substitution between the two creeks, with Ganatsekaigon serving as the analog for what the pre-urban Wilket Creek might have looked like.

5.2.2 Water level

Continuous water level data was recorded from pressure transducers (HOBO-U20 Water Level Data Logger, Onset) gauges located at the upstream end of each reach in Wilket Creek (Figure 5.1a). The gauge in the restored reach was installed in June 2013, while the gauge in the un-restored site was installed in August 2015 and is located ~ 100 m upstream of the upstream limit of the un-restored reach. Measurements were taken every 1–5 minutes during the field season (April–November), and every 7–10 minutes during the winter season (December–March) to avoid frequent gauge downloads when the creek was frozen. Raw pressure was converted to water surface elevation after barometric compensation using atmospheric pressure collected from a local gauge. Shear stress is the force of friction induced by the flow on the channel bed and is therefore responsible for the entrainment and

transport of bed sediment. Shear stress was calculated using the water level data and a detailed cross-section at the gauge by:

$$\tau = \rho_w g R_h S \quad (5.1)$$

where $\rho_w$is the density of water (1000 kg/m^3), g is the acceleration due to gravity (9.81 m/s^2), R_h is the hydraulic radius (m), and S is the reach-averaged slope.

Sensor depth from the Wilket Creek gauge was converted to discharge using measurements from a handheld surface velocity radar gun (Surface Velocity Radar 2, Decatur Electronics Inc.). Mean flow velocity was calculated as 0.8 times the surface velocity and multiplied by the cross-sectional area of flow to obtain discharge. The rating curve includes discharges from 1.6–12 m^3/s and extrapolated for higher discharges. Estimates of discharge using the Keulegan flow resistance equation was used to verify the quality of the extrapolated rating curve discharge predictions.

5.2.3 Bedload sediment tracking

Coarse bedload sediment was monitored in this study because of its fundamental role in channel morphodynamics and stability (MacKenzie et al., 2018). Radio Frequency Identification (RFID) transponders are frequently used to monitor bedload particles in riverine applications due to their robustness, low cost, battery-free operation, and high detection rates compared to other tracer technologies (Hassan & Bradley, 2017; Hassan & Roy, 2016; Lamarre et al., 2005). Two waves of RFID tracers were seeded in the restored and un-restored reaches of Wilket Creek. The second wave corresponds to the tracers seeded in Wilket Creek and Ganatsekaigon Creek described in Chapter 3 (Section 3.3.3). The second wave of tracers was designed to improve upon several limitations observed by MacVicar et al. (2015) using the first tracer wave. First, the second tracer wave used HDX (half-duplex) tags, which are less susceptible to background noise than the FDX (full-duplex) tags used in the first wave, resulting in improved recovery rates. Second, MacVicar et al. (2015) showed that the small number of tracers in each size class and the wide range of tracer sizes in each group made it difficult to discern differences between reaches and between size classes at a high level of statistical significance. The second wave of tracers had a narrower range of particle sizes in each size class and a smaller number of size classes each with a larger population, allowing for more statistically rigorous comparison of tracer mobility and dispersion between reaches and between size classes (Ferguson & Hoey, 2002; MacVicar et al., 2015).

The first tracer wave had a total of 143 and 299 tracers in the un-restored and restored reach, respectively, spanning 5 size classes of particles with b-axes between 4–5 ψ and 8–9 ψ (Figure 5.2b). Tracers were made by collecting stones from each reach and transporting them back to the lab where

they were drilled, an RFID tag placed inside, and sealed them with masonry caulking. Large angular stones (> 7ψ) in the restoration riffles were tagged in-situ in the field. 12 mm tags (# TRPGR30TGC), 23 mm tags (# RI-TRP-WR3P), and 32 mm tags (# RI-TRP-WR2B) were used in the < 5 ψ, 5–6 ψ, and > 6 ψ size classes, respectively. The second tracer wave had three size classes with median particle b-axes that matched the half-phi size class of the D_{50}, D_{75}, and D_{90} of upstream reach, corresponding to 5–5.5 ψ, 6–6.5 ψ, and 7–7.5 ψ, respectively (Figure 5.2b). In this way, we monitored the effect of the restoration on the presumed sediment supply through the reach, rather than on the transport of the artificially coarse material added for stabilization purposes.

The first tracer wave was seeded in August 2013. Tracers in the un-restored reach were all seeded on a single riffle, while tracers in the restored reach were seeded across two riffle-pool sequences and point bar. Stones were seeded on the surface, with approximately 10 tracers spaced 1 m apart along each channel cross-section. Tracers were randomized in each cross-section based on size. An attempt was made to recover tracer positions after major mobilizing flood events, although the close succession of floods in the summer months made it difficult to isolate all floods, leading to some recovery periods capturing multiple events. Tracers in the first wave were located using a loop antenna (Aquartis Ltd.) with a 0.05–0.41 m detection radius, depending on the size and orientation of the RFID tag. The seeding and recovery procedures of the second tracer wave are outlined in Chapter 3 (Section 3.3.3)

Throughout the study, a large number of tracer recoveries were completed, capturing bedload transport under varying flow conditions. A total of 10 and 12 tracer recoveries were completed in Wilket Creek of the first and second wave of tracers, respectively, with recovery rates ranging between 72–100%. A complete summary of the tracer recoveries in the un-restored and restored reaches of Wilket Creek can be found in the Appendix (Table A.4). Recoveries of the two reaches were completed together so that direct event-scale comparisons can be made. A total of 10 recoveries were completed in Ganatsekaigon Creek. Event-scale dynamics in Ganatsekaigon Creek are described in Chapter 3, but are not part of the current paper because of differences in the flood histories and recovery dates with Wilket Creek. Instead, transport dynamics over the entire duration of the study are examined in Ganatsekaigon creek in this study, which had a recovery rate of 80%. Peak discharges of recovery periods ranged between 7.8–34.7 m^3/s in Wilket Creek, and between 1.6–19.2 m^3/s in Ganatsekaigon Creek.

5.2.4 Bedload transport analysis

To relate tracer results to hydraulic forcing, the critical shear stress (τ_c) required to mobilize each tracer size class was calculated:

$$\tau_{ci} = \tau^*_{ci}(\rho_s - \rho_w)gD_i \quad (5.2)$$

where ρ_s is the mean tracer stone density (2700 kg/m^3), and τ^*_{ci} is the critical dimensionless shear stress, which was chosen based on the tracer data following the method described in Chapter 3 (Section 3.3.3). The number, magnitude, and duration of events exceeding the critical shear stress of each tracer size class were compared between study reaches. The shear stress analysis was conducted between August 2015 and May 2018 for which there is data from gauges in both reaches.

For each recovery, the fraction of mobile tracers and their travel lengths along the thalweg direction were calculated. For the first tracer wave, a travel length of 1 m was used as the threshold for a tracer to be considered to have moved. This threshold was chosen as a conservative value to account for the antenna precision (MacVicar et al., 2015). The same tracer variables calculated in the two previous chapters were calculated for this study. The fraction tracers that moved was calculated ($F_{m(i)}$, Equation 3.5) over the entire duration of the study, and for each recovery ($f_{m(i)}$) both for the entire tracer population and by tracer size class (i). The geometric mean travel length of mobile tracers for each recovery period was also calculated for the entire tracer population (L), as well as by size class (L_i). The weighted mean travel length ($\tilde{L}_{(i)}$) was then calculated as the product of mobility and mean travel length ($\tilde{L}_{(i)} = f_{m(i)} \times L_{(i)}$), which accounts for the immobile particles.

Finally, the virtual velocities of tracers over the entire length of the study (in m/year) were calculated to quantify the yearly downstream travel rate of bed particles (Houbrechts et al., 2015). Virtual velocity was calculated for each size class by dividing the mean overall travel lengths of tracers (including immobile tracers) by the total duration of the study, which was 2.8 and 2.6 years for the un-restored and restored reach of the first wave, respectively, and 2.8 years for the second wave in all reaches monitored. Immobile tracers were included in the virtual velocity calculation to capture the fraction of mobility in the long-term downstream displacement rate.

5.2.5 Morphological surveys

Morphological changes in the restoration reach of Wilket Creek were measured through repeated cross-section surveys. A total of 19 cross-sections were established in February 2013 over the restoration reach and including short distances up- and down-stream (Figure 5.1a). Cross-sections were surveyed between 4 and 6 times over the study period, with a final survey in July of 2018. A summary of cross-section descriptions and survey dates can be found in the Appendix (Table A.5).

Cross-sections XS-15 to XS-19 could not be surveyed in 2018 due to the beginning of the construction of a new restoration reach immediately downstream of the study site that began in May 2018. Surveys were conducted using an automatic level or a total station. Point density varied between 0.5–1 m on the banks, and 0.2–0.3 m in the channel. Monumented rebar pins were used to ensure surveys were conducted at the same location each year. Some sections were adjusted in post-processing to match non-eroded bank lines and other prominent topographical features where either the right or left rebar pin was not found. For each survey, the cross-sectional area and thalweg position were determined and used to calculate the total change in cross-sectional area (ΔA), as well as lateral (Δx) and vertical (Δy) changes in thalweg position between surveys. The estimated survey error is 0.01 m for distance and 0.008 m for elevation (see Chapter 3, Section 3.3.2 for details).

5.3 Results

5.3.1 Shear stress

Shear stress thresholds were estimated by assuming the peak shear stress of events with low mobility approximates the critical shear stress, following the process outlined in Chapter 3 (Section 3.4.1). This method was used because similarly to Chapter 3, the interest in shear stress in this Chapter is to compare relative distributions of shear stress, rather than build predictive models of sediment transport.

The study reaches in Wilket Creek and Ganatsekaigon Creek had different critical shear stresses for mobilizing tracer stones, and different frequencies and durations of mobilizing events. For the un-restored reach of Wilket Creek and Ganatsekaigon Creek, the critical dimensionless shear stress of the median particle size class (D_{50} = 5–6 ψ) was determined using Equation (5.2) to be $\tau^*_{c(5-6\,\psi)}$ = 0.047 (see Chapter 3, Section 3.4.1), which is in accordance with other gravel-bed rivers and for this particle size (Buffington & Montgomery, 1997). Due to the coarse material added for stabilization, critical shear stresses for all particle sizes in the restored reach of Wilket Creek are 1.5 times higher than those in the un-restored reach. Tracers in this reach are smaller than the median bed material, particularly the coarse riffles, meaning the pocket geometry works to increase the shear stress required for entrainment, as calculated from the Egiazaroff (1965) hiding function (Equation 3.8). The restoration therefore reduced the number of mobilizing events for the 5–6 ψ size class by more than half in comparison with the un-restored reach, though mobilization was still more frequent than in the rural analog (Table 5.1). A large proportion of events exceeding the $\tau_{c(5-6\,\psi)}$ also exceed

the $\tau_{c(6-7\,\psi)}$ and $\tau_{c(7-8\,\psi)}$ in the restored reach, however, so that the number of events exceeding these thresholds is similar between the two reaches at Wilket Creek and much greater than in Ganatsekaigon Creek (Table 5.1). The duration of mobilizing events is also decreased in the restored reach for events exceeding the $\tau_{c(5-6\,\psi)}$, but not events exceeding the $\tau_{c(6-7\,\psi)}$ or $\tau_{c(7-8\,\psi)}$ (Table 5.1). Event durations remain much smaller compared to the rural stream that experiences less flashy hydrographs (See Chapter 3, Figure 3.4).

Table 5.1. Summary of critical shear stresses and mobilizing events in the Wilket Creek reaches and in Ganatsekaigon Creek.

	Un-Restored	Restored	Ganatsekaigon
Dimensionless critical shear stress (τ_c^*)			
5-6 ψ	0.047	0.105	0.047
6-7 ψ	0.031	0.061	0.032
7-8 ψ	0.023	0.037	0.023
Critical shear stress (τ_c) (Pa)			
5-6 ψ	31.4	73.5	32.9
6-7 ψ	49.1	79	42.0
7-8 ψ	55.0	99.3	57.8
Number of events > τ_c			
5-6 ψ	81	36	18
6-7 ψ	29	28	9
7-8 ψ	13	9	2
Mean events duration > τ_c			
5-6 ψ	2.1	1.5	6.7
6-7 ψ	1.4	1.3	5.4
7-8 ψ	0.9	0.8	2.8

The coarser substrate and larger channel geometry of the restored reach leads to different distributions of measured exceed shear stresses for the same discharges. Plotting the exceedance probability of shear stresses exceeding the τ_{cD50} of the sediment supply (i.e. 5–6 ψ) reveals that although fewer events mobilizing the tracer size classes occur in the restored reach, their relative magnitude is increased (Figure 5.3). Relative frequencies of mobilizing flows are similar between the un-restored reach of Wilket Creek and Ganatsekaigon Creek (Figure 5.3), despite differences in watershed urbanization (Chapter 3, Section 3.4.1). However, fewer extreme values exceeding 35 Pa above the $\tau_{c(5-6\,\psi)}$ occur in the restored reach compared to both the un-restored reach and Ganatsekaigon Creek.

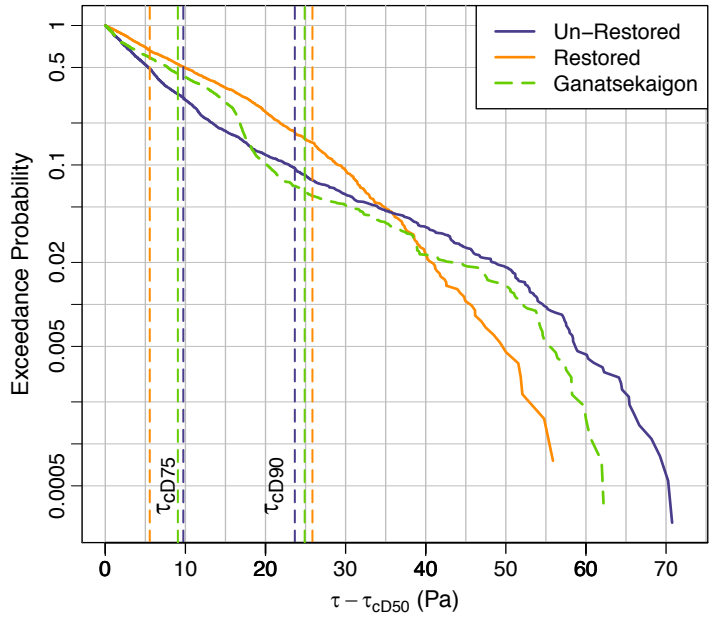

Figure 5.3. Exceedance probability of events exceeding the critical shear stress of the sediment supply D_{50} (5-6 ψ) size class in reach. Vertical dotted lines indicate the critical shear stress of the sediment supply D_{75} (6-7 ψ) and D_{90} (8-9 ψ) size classes in the respective reaches.

5.3.2 Bedload transport

5.3.2.1 Event-scale tracer dynamics

A comparison of bedload transport metrics between the two reaches at Wilket Creek reveals that the restoration is successful at reducing the mobility and travel length of bed particles (Figure 5.4). A larger fraction of tracers was mobile (Figure 5.4a), and travel lengths were longer (Figure 5.4b), more often in the un-restored reach compared to the restored reach. The fraction of tracers that moved (f_m) was higher in the un-restored reach than the restored reach for 18 of 22 recoveries (82%), while mean travel lengths (L) were higher in the un-restored reach than the restored reach for 17 of 22 recoveries (77%). Weighted mean travel lengths ($\tilde{L} = f_m \times L$) are higher in the un-restored reach 18 of the 22 recoveries similar to f_m, but collapse closer to the 1:1 line at low values (Figure 5.4c), suggesting differences between reaches become larger during higher transport events.

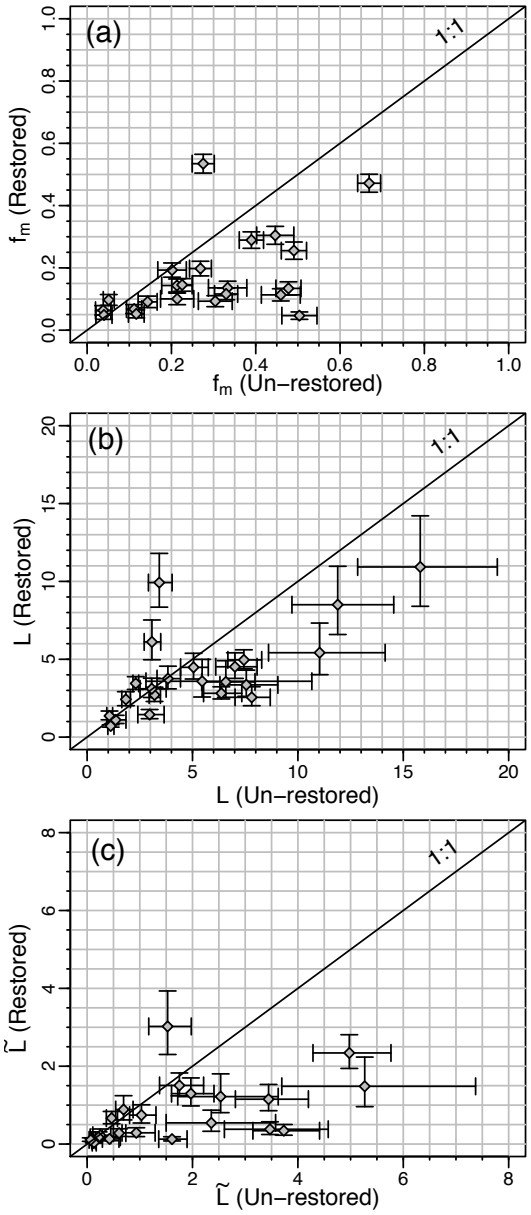

Figure 5.4. Event-based (a): f_m, (b): L, and (c): $\tilde{L}$ of the entire tracer population in the un-restored and restored reaches of Wilket Creek.

Given the importance of particle size on mobility and travel distance, $\tilde{L}_i$ was also calculated for each event and tracer size class for Wave 2 in Wilket Creek. For comparison, Figure 5.5 shows the difference in $\tilde{L}_i$ between the two reaches:

$$\Delta\tilde{L}_i = \tilde{L}_{(un-restored)} - \tilde{L}_{(restored)} \tag{5.3}$$

Values of $\Delta\tilde{L}_i$ are positive for most events and most tracer size classes, confirming higher values in the un-restored reach compared to the restored reach (Figure 5.5). Differences between reaches are

larger for the 5–6 and 6–7 ψ size classes compared to the largest tracer size class. Furthermore, events with discharges between ~15–27 m^3/s produce larger differences between reaches ($\Delta\tilde{L}_i$ up to ~ 6 m) compared to events with lower or higher discharges ($\Delta\tilde{L}_i$ ~ 0 m). Interestingly, the decrease in $\Delta\tilde{L}_i$ occurs at discharges greater than the top-of-bank discharge of the un-restored reach, suggesting the effect is related to the entrenchment of the channel. Only one event is an outlier to this trend for the 5–6 and 6–7 ψ size classes. This result suggests that the decrease in tracer mobility and travel lengths of all tracer size classes are driven by these medium-magnitude events with peak discharges when flow is within the channel in the un-restored reach.

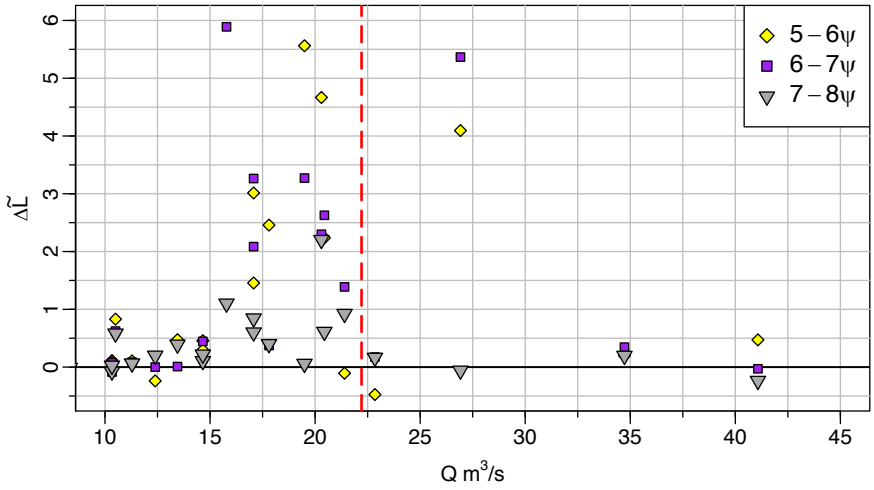

Figure 5.5. Difference in event-based $\tilde{L}_i$ values between the un-restored and restored reach by peak event discharge. Dotted red line indicates the top-of-bank discharge in the un-restored reach.

5.3.2.2 Long-term tracer dynamics

The long-term mobility of tracer size classes over the entire duration of the study (F_{mi}) are only moderately affected by the restoration. The un-restored reach has high overall mobility (> 80%) for all size classes and in both tracer waves (Figure 5.6). This result is expected given the ongoing erosion problems in the channel that lead to the downstream stabilization project. The mobility of all three size classes, and particularly the largest size class, also exceeds that measured in Ganatsekaigon Creek, demonstrating the shift in bedload transport occurring because of urbanization (see Chapter 3, Section 3.4.3). Comparison between the restored and un-restored reaches of Wilket Creek provides some evidence that the restoration is effective at reducing the mobility of coarse size fractions (≥ 7–8 ψ). The mobility of tracers in the 7–8 ψ size class of the first wave was reduced by half compared to the un-restored reach, and both the 7–8 ψ and 8–9 ψ size classes had mobility significantly lower

(95% CI) than the 4–5 ψ size class (Figure 5.6). Wave 2 also shows some decrease in the mobility of traces in the 7–8 ψ size class, although differences are not significant (95% CI) when comparing to other size classes and to the un-restored reach. Results from tracer Wave 2 are more robust, as sample sizes were more carefully designed for this type of test. The lack of significant difference in the mobility indicates that material up to the D_{90} of the sediment supply (7–8 ψ) entering the restored reach does not exhibit differences in mobility related to particle size over long timescales. This result does not encompass the very coarse material added to the riffles and banks for stabilization as part of the restoration.

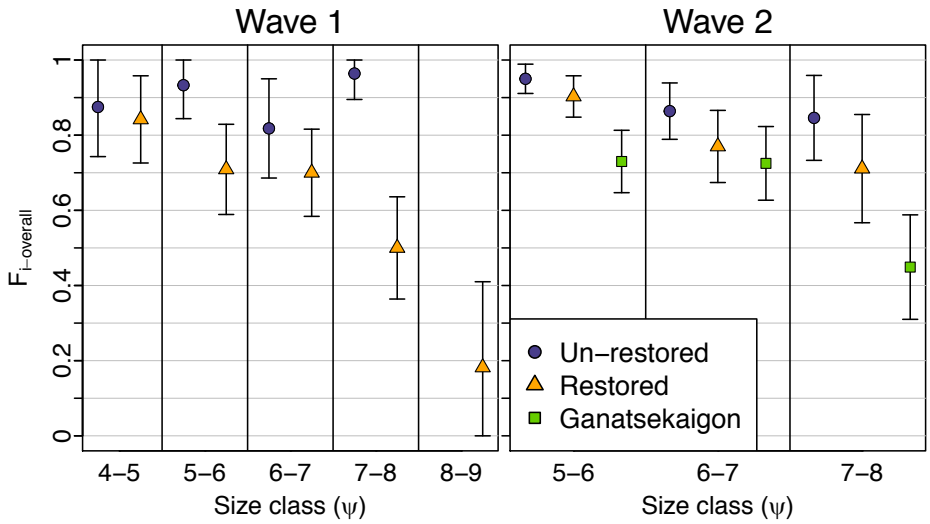

Figure 5.6. Fraction of stones in Wave 1 and Wave 2 that were mobile over the entire duration of the study separated by size class.

The effectiveness of the restoration in reducing long-term particle travel lengths thus appears to vary with particle size. Exceedance probabilities of tracer travel lengths (ℓ) over the entire duration of the study were calculated and plotted on a log-log scale following other studies (Hassan et al., 2013; Papangelakis and Hassan, 2016; Phillips and Jerolmack, 2014) (Figure 5.7). The distribution of travel lengths of all tracers show tracers travelled long distances over the duration of the study, exceeding 200 m in both reaches (Figure 5.7a). The distributions are similar, with tracers in Wave 1 travelling slightly shorter distances in the restored reach compared to the un-restored reach. Travel distances decrease with increasing size in both reaches, but the difference between the two reaches increases with tracer size (Figure 5.7b-c). A smaller number of tracers in the 5–6 ψ size class of Wave 1 travelled up to ~ 100 m, but a similar number of tracers travelled > 100 m (Figure 5.7b). The travel distance distributions of Wave 2 overlap, indicating tracers travelled similar distances in the two

reaches. The larger number of tracers in the 5–6 ψ size class of Wave 2 means that the travel distance distribution of this size class dominated the distribution of the entire tracer population (Figure 5.7a). The 6–7 ψ size class travelled shorter distances in the restored reach compared to the un-restored reach in both waves (Figure 5.7c). Finally, the 7–8 ψ size class shows the largest difference between reaches in Wave 2, with shorter travel distances in the restored reach compared to the unrestored reach (Figure 5.7d). The distribution of the two reaches overlap between 10–20 m, and more tracers travelled > 20 m in the restored reach. The longer travel distances in the restored reach may be an effect of tracers in this size class being smaller than those in the un-restored reach (Figure 5.2b). The travel distance distributions suggest that over the duration of study, the restored reach decreased the dispersion of larger bed sediment (> D_{50} size class of the sediment supply) more than smaller sediment.

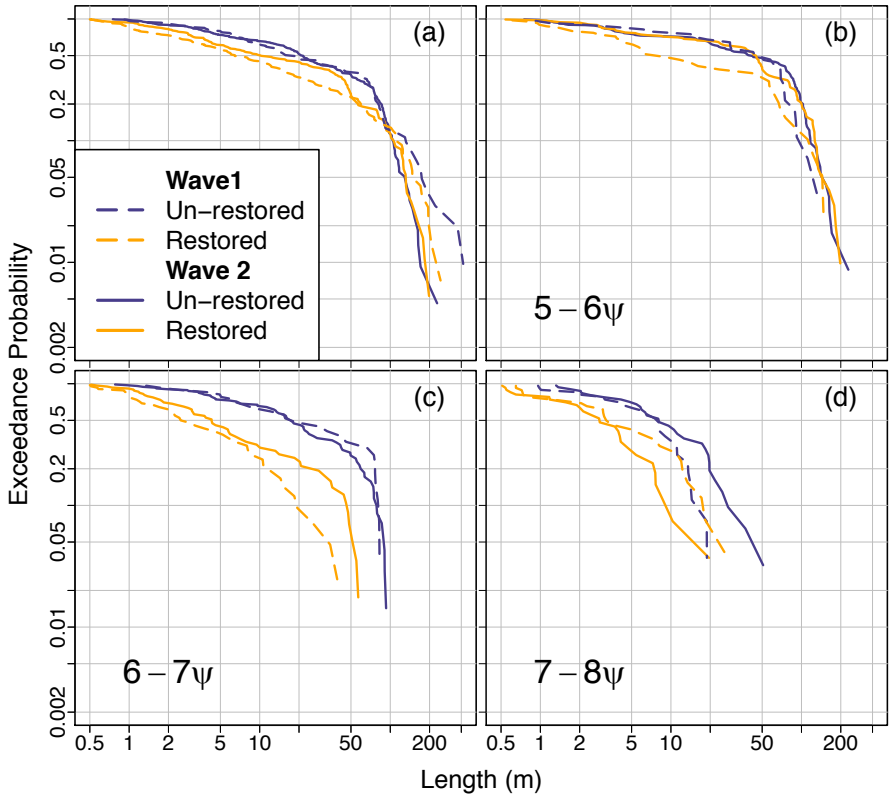

Figure 5.7. Tracer travel length distributions of mobile tracers over the entire duration of the study of (a): the entire tracer population, (b): tracers in the 5–6 ψ size class (c): tracers in the 6–7 ψ size class, and (d): tracers in the 7–8 ψ size class.

The virtual velocity of tracers over the duration of the study shows that the restoration is effective at slowing down the transport of coarse sediment through Wilket Creek. Significant

differences are observed in the virtual velocities of particles in the restored and un-restored reach for both tracer waves where $D \geq \sim 2D_{50}$ (Figure 5.8). A comparison with results from Ganatsekaigon Creek shows that virtual velocities in the restored reach are comparable to the rural site for these particle sizes. Such a result demonstrates the effectiveness of instream channel restorations in reducing overall bed degradation. For particles closer to the D_{50}, however, the difference between the restored and un-restored reach is not significant. With the exception of the first wave of particles, the virtual velocities are many times higher than what was observed in the rural site. The low virtual velocity seen in the restored reach in Wave 1 around the D_{50} may be attributed to the large range of tracer sizes in this class; tracers in this size class have a median particle size of 6.5–7 ψ, compared to the particles in Wave 2 that had a mean size within 6–6.5 ψ. Results of Wave 2, which had improved sample sizes and more targeted tracer sizes, are unable to distinguish between the restored and un-restored reached for this particle size. The sharp decrease in virtual velocity for particles just slightly greater than the D_{50} suggests that there is a discontinuity in the virtual velocity and particle size relations, with the restoration helping to reduce the transport of particles greater than a threshold size, but below which it seems to have little influence on transport velocities. The reduction in virtual velocity of size classes $\geq 2D_{50}$ can be attributed to decrease in travel lengths of coarse sediment over long timescales, as the long-term mobility of tracers in the restored reach not being significantly reduced.

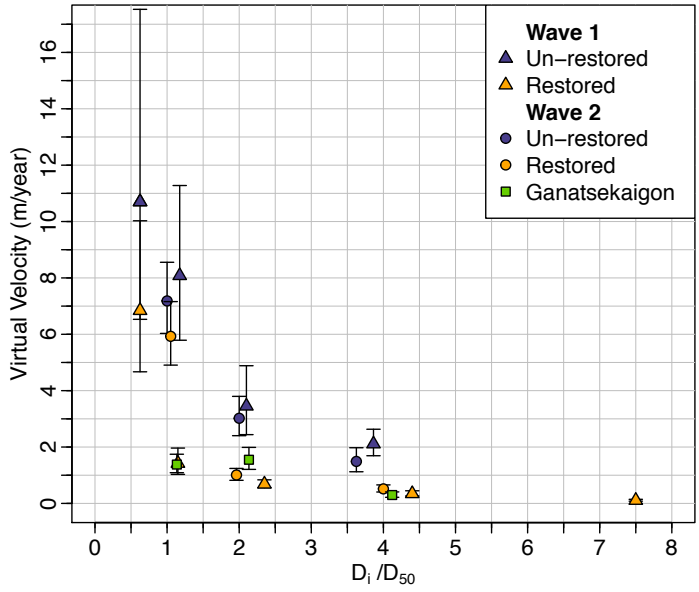

Figure 5.8. Virtual velocity of the Wilket Creek tracers by normalized size.

5.3.3 Morphodynamics

To examine spatial trends of erosion and deposition, the seeding section of the restored reach is isolated and straight-line paths of tracer displacements are shown for three recovery periods in Figure 5.9. Tracers from the upstream riffle tend to travel towards the outside of pool bend bed, but the majority remain within the riffle or deposit at the head of the first pool. Occasional particles move from one riffle to the next, or are deposited on the margin of the point bar or on the tail of the pool. Some lateral movement is also notable, with particles generally moving towards the pool through the riffle sections, but then away from the deep centre of the pool so that they are deposited on the margins of the bar or on the next riffle. Patterns of preferential particle paths are consistent with increasing magnitude of transport events, but become more pronounced as f_m increases. Tracer paths observed in the resorted reach of Wilket Creek support the sediment routing hypothesis for riffle-pool maintenance proposed by Milan (2013a) developed in natural riffle-pool sequences. In this model, coarse sediment is preferentially routed along the point bar edge, similar to observations in the Wilket Creek restoration, suggesting that point bars are zones of maximum transport (Dietrich & Smith, 1984). The maintenance of pools through the scour at pool heads and deposition at the tail or head of the next riffle has been described as a mechanism for pool maintenance in several studies of naturally-occurring riffle-pool channels (MacVicar & Roy, 2011; Petit, 1987; Sear, 1996; Thompson et al., 1996).

Travel paths of tracer particles can be linked to the evolution of the channel morphology. The erosion of particles from the middle of the pool and deposition of particles on the bar is reflected in the evolution of XS-5 and XS-6, which show a deepening of the pool and aggradation of the bar on the right-bank side over the surveys (Figure 5.9). XS-7 also shows deepening of the pool, but the bar migrated laterally to the right rather aggraded significantly vertically. In contrast, tracers in riffles tended to move shorter distances and remain within the unit, supporting the overall stability seen in XS-10 and XS-8 throughout the study. The significant erosion at XS-8 is lateral erosion of the left bank, which is not captured by the tracers. The evolution of XS-9 reflects patterns of lateral tracer movement, as the inside bend of the pool (left bank) showed aggradation over the study period, while the thalweg moved down and to the right. The coarsened banks of the pools do not allow for erosion of the outside bends. Lateral migration of material is thus occurring without much bank retreat, so banks are getting higher and steeper, introducing a threat of over-steeping.

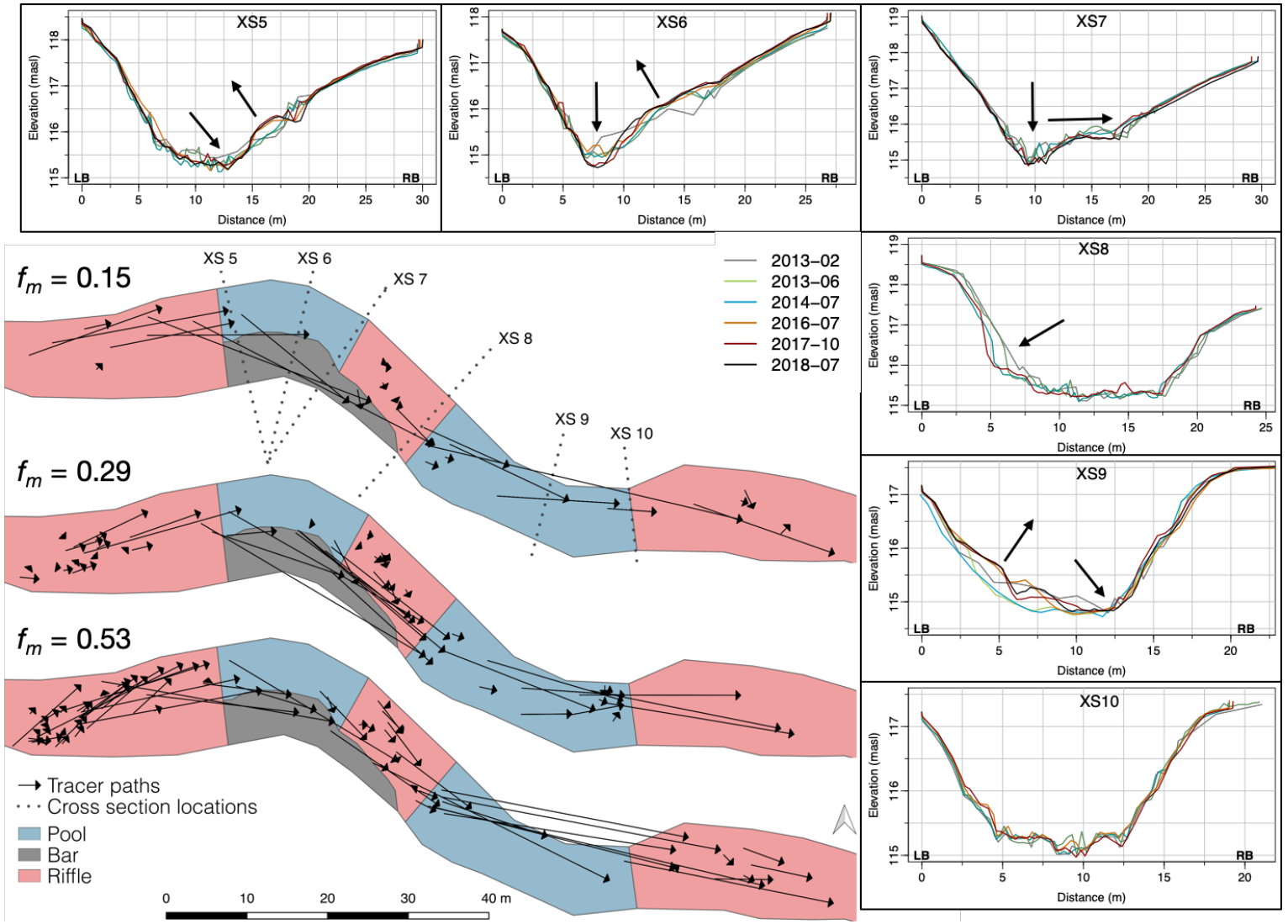

Figure 5.9. Paths of tracers under different conditions, and the evolution of cross sections.

Changes in cross-sectional area and thalweg position show that riffle and pool features experienced different morphologic trends over the duration of the study. Within the limits of the restoration (sections 3-17), most cross-sections show only small net changes in cross-sectional area between 2013 and 2018 (Figure 5.10a). Considering the right and left side of each cross section separately (relatively to the thalweg), most cross sections show a balance of erosion and deposition (Figure 5.10b), which indicates that the channel is laterally migrating. Exceptions are sections 5 and 12, both located in pools, which show erosion on both sides of the thalweg and overall channel enlargement. Changes in the lateral position of the thalweg (Δx) also confirm lateral migration within the restored reach was ≤ 2 m over the duration of the study (Figure 5.10c). Vertical changes in the thalweg position (Δy) show deepening of the pools (sections 5-6, 11-12, and 16) and aggradation or no change in the riffles (sections 3-4, 7-8, 10, and 13-15) (Figure 5.10d). Overall, the restoration appears to have stable riffle features, while pools are self-maintaining or enlarging through scour with minimal lateral translation across the floodplain.

Changes in cross-sections located up- and down-stream of the restoration limits show larger morphological changes than within the restoration. At the upstream end, both ($-\Delta A$) and (Δy) values indicate aggradation. Conversely, XS-18 and XS-19 located at the downstream limits of the restoration show enlargement, lateral migration of ~ 8 m, and degradation (Figure 5.11). The overall vertical aggradation upstream and erosion downstream result in an increase in slope through the restoration. The large cross-section changes at XS-18 can be attributed to the eventual bank failure of the left bank. The combination of increased slope through the restoration and the greater reduction of transport of coarse sediment compared to finer sediment leads to increasing flow forces but finer substrate at the downstream end. This increase in erosion potential may exacerbate channel erosion downstream of the limits of the constructed channel.

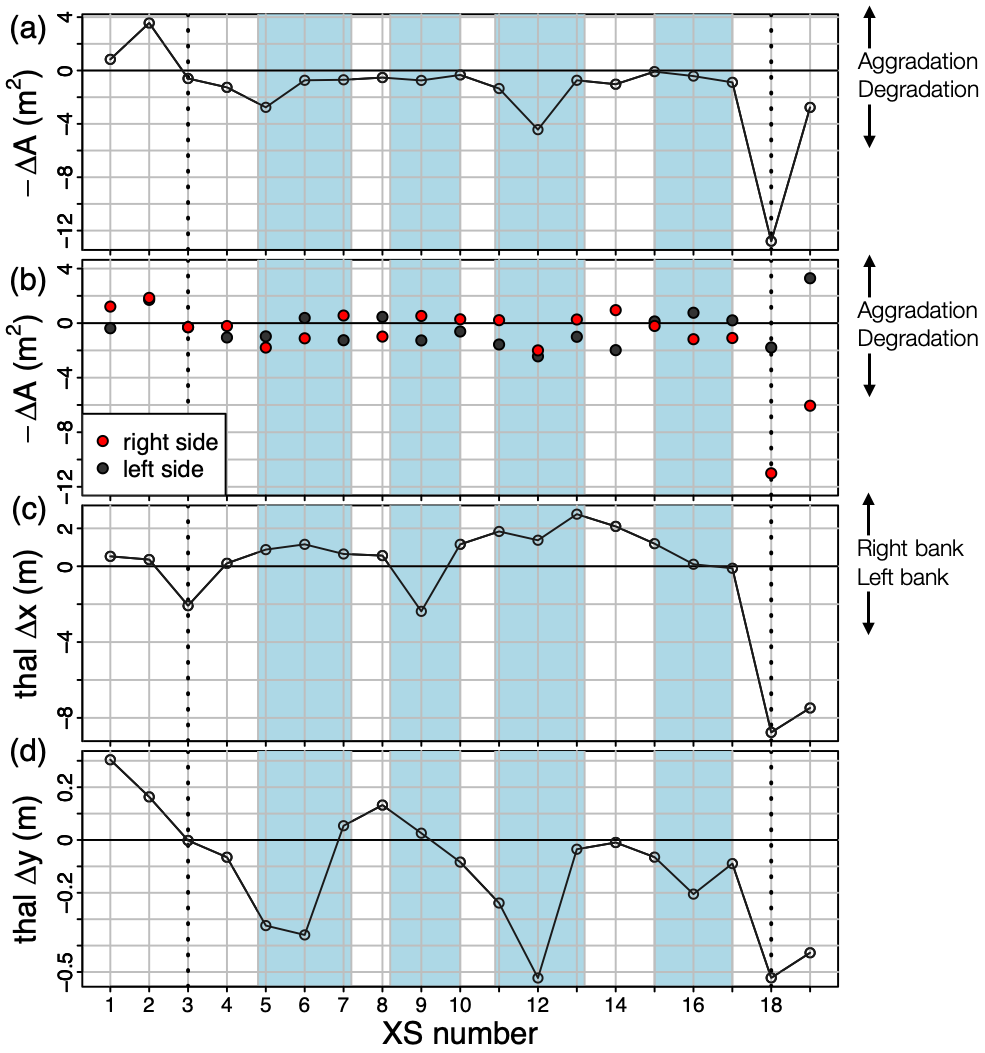

Figure 5.10. Overall changes in cross sections between 2013 and 2018 showing (a): net change in cross-sectional area, (b): net change in cross-sectional area of the left and right half of the cross section, (c): lateral change in thalweg position, and (d): vertical change in thalweg position. Shaded blue areas indicate pool locations. Dotted vertical lines indicate the up- and down-stream limits of the constructed channel.

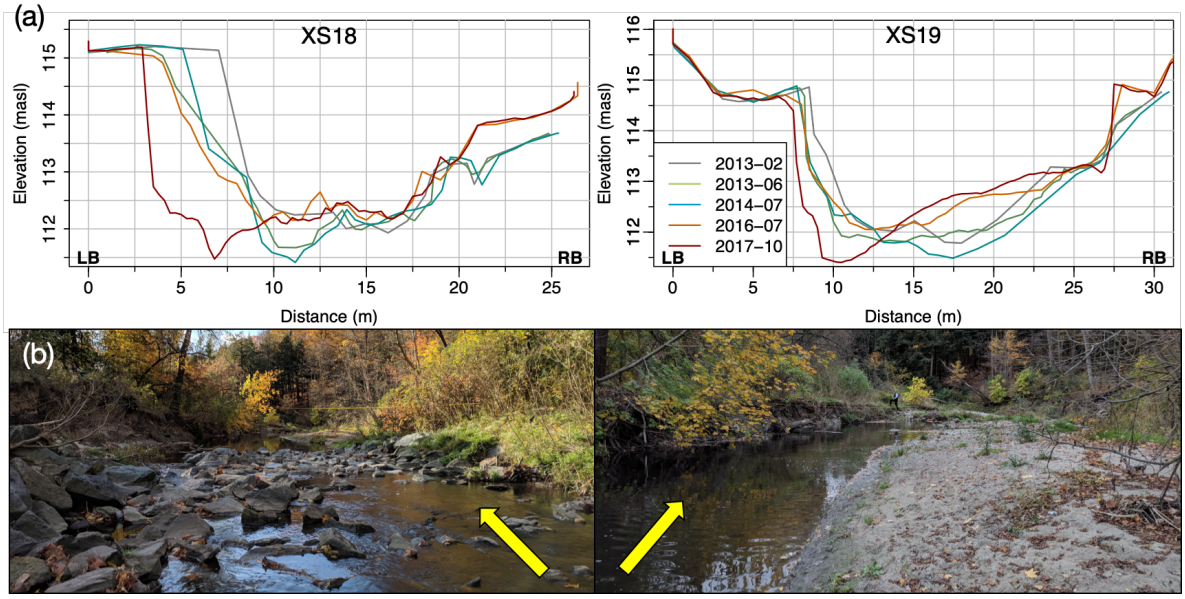

Figure 5.11. (a): Cross-section surveys plotted from left bank (LB) to right bank (RB), and (b): field photos of XS-18 and XS-19. Arrows indicate the direction of flow.

5.4 Discussion

Bedload sediment transport and morphological change was monitored over five years in an un-restored and restored reach of an urbanized river. The objectives of the study were to compare bedload transport dynamics between the two reaches and with a rural analog, assess the stability of the constructed features, and evaluate the effects of restoration project in the context of sediment connectivity in the channel network. The large number and range of mobilizing events captured in combination with direct comparison to un-restored reaches of the channel and paired rural reach provide a unique opportunity to examine the success or failure of a riffle-pool restoration project at the process-level.

Results from particle tracking reveal differences in bedload transport between the two reaches. At the event scale, the restoration affects bedload transport primarily during medium-magnitude events. The restoration successfully reduced the downstream velocity of coarse particles > D_{50} to values observed in rural analog, which can be attributed to a reduction in the travel lengths of these particles over long timescales, rather than their mobility. The hydraulic forcing experienced by the two reaches can explain this result. The critical shear stress to mobilize sediment is higher in the restored reach, leading to a smaller number of events exceeding the mobilizing threshold of the sediment supply D_{50}. However, the restored reach experiences a higher relative frequency of excess shear stress, so that the D_{50} is exposed to higher shear stresses more often during these events, while

the number of events mobilizing the D_{75} and the D_{90} are unchanged. This difference in how the two reaches experience mobilizing flows in terms of shear stress explains the lack of significant difference in long-term mobility of coarse sediment. The observed reduction in the travel length of coarse tracers > D_{50} in the restored reach cannot be explained by a reduction in the duration of mobilizing flows, which has been suggested as an important control on particle travel lengths (Church & Hassan, 1992; Hassan et al., 1992; Haschenburger & Church, 1998), and is likely due to the presence of the large angular sediment added for bed stabilization that traps smaller material and impedes tracer displacement. Mackenzie and Eaton (2017) demonstrate how adding a small volume of coarse grains can significantly improve channel stability and decrease in transport rates, even if mean bed shear stresses are increased. A smaller change to the proportion of coarse grains on the bed may therefore attain similar results in the restored reach of Wilket Creek, which can benefit the integrity of aquatic communities that rely on specific sedimentary conditions (e.g. Jowett, 2003; Rempel et al., 2000; Rice et al., 2001; Sarriquet et al., 2007).

The 'success' or 'failure' of the restoration project is dependent on whether the immediate reconstructed channel is assessed, or whether the channel beyond the limits of the project is considered. The constructed riffle-pool sequences showed stability of riffles and scouring in pools, indicating 'success' in terms of structural criteria. The scouring of pools has been measured in other restored channels, and is associated with the self-maintenance of bedforms (Biron et al., 2012), boding well for the longevity of the constructed morphology. Furthermore, tracer paths provide additional evidence that the artificially constructed riffle and pool features follow similar grain-scale maintenance processes as natural stable riffle-pool sequences. Evidence from the tracer dynamics and morphological surveys up- and down-stream of the project limits, however, suggests that the restored reach introduces a discontinuity to the sediment transport regime of Wilket Creek. In the Wilket Creek restoration, the decrease in downstream bedload displacement is driven by the increased trapping capacity of the artificially coarse sediment. In this way, the constructed channel acts to slow down coarse sediment and impede its downstream displacement, analogous to the effects of a weir or dam and similar to other channels where a decrease in the channel transport capacity leads to a disruption of coarse sediment connectivity (Wohl et al., 2017). At the same time, the altered channel dimensions and increased bed slope and decreased sinuosity through the restored channel results in increasing shear stress at the downstream limit of the constructed channel. The combination of coarse sediment slowdown and increased shear stress through the restoration produce an energy imbalance, which contributes to the local bank failure and increased instability downstream of the construction limits. Increased channel instability because of infrastructure that disrupts sediment continuity has

been observed in other urban environments (Jordan et al., 2010; Simon & Darby, 2002). The interplay between flow and channel morphology in modified channels has been recognized as an important consideration for successful channel restoration through hydraulic modelling (Anim et al., 2018, 2019c), highlighting the need to carefully design channels to account for both the watershed hydrologic and local hydraulic conditions.

Results from this study highlight coarse sediment connectivity as a useful tool for river restoration. Sediment connectivity is rarely a focus of river restoration, and explicit goals with respect to sediment connectivity are not defined. A possible goal may be to ensure full throughput of supplied material to reduce long-term changes to the channel. In such cases, sediment augmentation or coarse sediment transfer has been proposed as a method to reduce channel degradation downstream of infrastructure that disrupts sediment connectivity such as dams (e.g. Arnaud et al., 2017; Rollet et al., 2014; Liedermann et al., 2013; Surian et al., 2009). In contrast, restoration projects focused on channel stability may be designed to encourage coarse sediment slow-down to combat erosion and degradation, as is the case in Wilket Creek. Alternatively, strategies might include reducing designed channel dimensions to restore flood access to the floodplains (Anim et al., 2019c; Jordan et al., 2010). An added benefit of such a strategy is that floodplain access during high flows has been shown is considered beneficial for ecological processes as well (McMillan & Noe, 2017; Roley et al., 2014). In these cases, results from this study support the need to analyse and design restoration projects in the context of the entire channel corridor (Kondolf et al., 2006; Doyle & Harbor, 2000; Shields et al., 2003; Jordan et al., 2010), and that monitoring of restoration projects should extend beyond the limits of the construction (Surian et al., 2009). Although restoring coarse sediment connectivity should not be the sole objective of restoration projects (Frings et al., 2018), it is an important geomorphic process that should be included in restoration design. Taking a catchment-scale approach to managing coarse sediment supply and transport in urban rivers can lead to urban river management strategies with increased chances of positively affecting channels (Vietz et al., 2015).

5.5 Conclusions

This study aimed to assess the performance of a constructed riffle-pool channel by monitoring geomorphic process. Direct comparison of tracer displacement characteristics between an un-restored and restored reach of the channel shows that the restoration is successful at slowing down the dispersion of coarse sediment ($> D_{50}$) but does not significantly affect the movement of particles $\leq D_{50}$. The repeated cross-section surveys indicate the restored reach has stable riffles, and that pools

are self-maintaining through scour but deepening. Links between tracer paths and morphological adjustments show that particles rarely deposit or move through the pool, which support the sediment routing hypothesis of riffle-pool maintenance and indicates that sediment transport is occurring in much the same way as it would in natural sequences. Coarsening of the banks however introduce a risk of bank over-steeping. Finally, although the restored reach shows local 'success' in terms of stability and self-maintenance, the overall measured increase in slope and slowdown of coarse sediment through the reach results in severe bank failure increased instability downstream of the construction. Results from this study highlight the need to incorporate analysis over longer spatial and temporal scales and to include processes coarse sediment connectivity in restoration design and monitoring.

Transition D

The previous three chapters focused on the grain-scale bedload transport dynamics in urban rivers, revealing small-scale processes and their relationship to channel morphology. A large limitation of the RFID tracer technology employed in this study is the absence of burial depth data. Vertical mixing is a very important component in understanding long-term bedload transport processes. For example, bedload tracer data can be translated into bulk transport rates if the active layer thickness is known (Wilcock, 1997). Studies that estimate bedload transport rates using RFID tracers need to employ secondary methods to obtain the active layer depth (e.g. scour pins), or require each tracer stone to be dug up and its burial depth manually measured, a process that resource intensive, prone to error, and artificially disturbs the bed. The lack of vertical tracer data was also highlighted as a limitation in building predictive models of long-term tracer behavior in Chapter 4. Building upon these limitations, Chapter 6 focuses on the final research question of this thesis: How can limitations of current bedload transport monitoring technology be improved? In this Chapter, new synthetic tracer stones are introduced that provide the ability to obtain burial depth information without disturbing the bed, and promising lab performance tests are presented. Since the development of the 'Wobblestones', additional steps have been taken to improve upon the design and test their performance in real bedload tracking applications. Muirhead (2018) worked on creating a process to mass-produce the synthetic tracer stone, and field tests were performed by Cain (2019), who tested the accuracy of the burial depth estimation method, and explored considerations for the manufacturing and tracking procedures in field settings.

Chapter 6

New Synthetic Radio Frequency Identification (RFID) Tracer Stone for Burial Depth Estimation

This chapter is based on the following published manuscript:

Papangelakis, E., Muirhead, C., Schneider, A., & MacVicar, B. (2019). New synthetic Radio Frequency Identification (RFID) tracer stone for burial depth estimation. *Journal of Hydraulic Engineering, 145*(12), 06019014. DOI: 10.1061/(ASCE)HY.1943-7900.0001650

Data presented in this chapter can found at:

Papangelakis, E. (2019). Data for: Synthetic Radio Frequency Identification tracer stones with weighted inner ball for burial depth estimation [Dataset]. https://doi.org/10.5683/SP2/O9XJPF

6.1 Introduction

Particle tracking is a method for studying bedload transport that follows the movement of individual tracer sediment particles. Passive radio frequency identification (RFID) tags have become popular for bedload tracking applications due their low cost, battery-free nature, robustness, and high recovery rates as compared to other tracer technologies (Cassel et al., 2016; MacVicar et al., 2015; Tsakiris et al., 2015; Lamarre et al., 2005). The most common type of RFID tags used in sediment tracking applications are low-frequency cylindrical glass transponders known as Passive Integrated Transponder (PIT) tags. Tracer stones with embedded PIT tags have been successfully employed in a variety of river environments to track coarse sediment movement (e.g. Phillips & Jerolmack, 2014; Schneider et al., 2014; Bradley & Tucker, 2012; Liébault et al., 2012). A limitation of RFID tracers is that the shape of the detection field is highly dependent on the transponder orientation relative to the antenna (Arnaud et al., 2015; Chapuis et al., 2014b). Transponders oriented horizontally relative to the antenna detection plane show a 26–76% reduction in their detection distance compared to vertically-oriented transponders (Tsakiris et al., 2015). As tracer stones are transported, the variability in the shape of the detection zone increases uncertainty in particle position and can shield particles from detection, particularly when smaller transponders are used and where multiple tags are within the detection field of the antenna (Cassel et al., 2016; Chapuis et al., 2014b). A second limitation of current RFID tracer stones is that they do not offer the possibility of determining the burial depth of detected particles without disturbing the bed. This limitation is significant because vertical mixing of

the active layer is of fundamental importance for understanding tracer mobility and dispersion processes (Hassan et al., 2013; Mao et al., 2017; Parker et al., 2000; Wong et al., 2007).

To address challenges associated with variable detection fields, Lauth and Papanicolaou (2009) designed 'anti-collision' tracers in which two PIT tags oriented at 90 degrees are embedded in the tracer stone. However, the practicality and application of the technique in larger field experiments has not been tested. Hufnagel and MacVicar (2017) developed an automated laboratory system for tracking RFID-tagged stones in a flume. Performance tests indicated that signal interference from closely located tags led to an increase in zones of non-detection, and fixed-orientation tracer stones were recommended for flume applications. Dziadak et al. (2009) developed a methodology to estimate the burial depth of vertical buried PIT tags using the known detection field shape and measuring the distance above the surface at which it is detected. Previous laboratory and field tests have shown that the shape of the detection field of vertically-oriented transponders is unaffected by dry sediment, while saturated sediments result in only a 10–15% reduction in the detection zone (Chapuis et al., 2014b). Therefore, if the orientation of the transponder is known to be vertical, it would be possible to infer the burial depth of the tracer stone from the distance above the surface at which it is first detected when approached with an antenna from above. The application of such a method in sediment tracking is currently not possible due to the variability in transponder orientation. Finally, Tsakiris et al. (2015) developed a different method to infer the distance between the antenna and RFID transponder by analyzing the voltage of the return signal received by the antenna. This method requires the orientation of the transponder relative to the antenna to be known (Tsakiris et al., 2015), and is therefore not practical for sediment tracking applications with existing RFID tracer designs. A tracer stone with a vertically-fixed RFID transponder can offer a solution to problems associated with signal interference, as well as provide opportunities for burial depth estimation.

The goal of the current study is to develop a synthetic tracer stone in which the RFID transponder remains vertical regardless of the stone orientation. This paper presents two prototypes of the 'Wobblestone' and the results from a series of performance tests. Tracer density, resistance to impact and resistance to freezing were tested. Performance tests were conducted to confirm transponders maintain a vertical orientation following tracer rotation and the utility of the tracers for estimating burial depth in a sedimentary bed. It is anticipated that these new tracers can be used to improve sediment transport measurements in flumes and real rivers through increased precision of tracer positioning data and new non-intrusive measurements of the vertical position of buried tracers.

6.2 Synthetic stone design

The conceptual 'Wobblestone' design features an outer stone shell with an embedded weighted inner ball containing the transponder tag (Figure 6.1). With this design, the inner ball is free to rotate under the force of gravity to a position where the tag is oriented vertically regardless of the stone orientation. Two prototypes were created with this concept using different assembly procedures. The first prototype is inexpensive and can be created from readily available components, but takes longer to assemble and produces higher variability in performance between tracers. The second prototype was made to enhanced performance, reduce variability between tracers, and speed-up the assembly process by mass-production of the rotating component of the tracer. Assembly of the inner sphere of the second prototype is reliant on a key custom-built part.

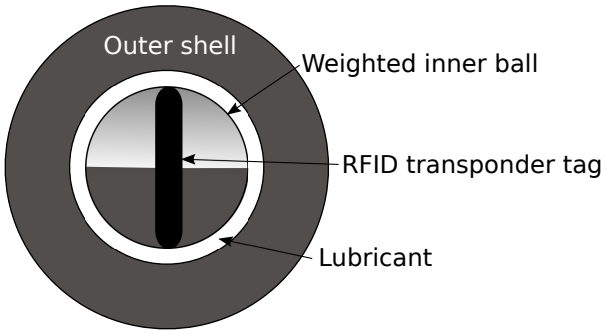

Figure 6.1. Conceptual design of the synthetic tracer stone.

The material used to create the outer shell was the same for both prototypes and largely followed the recommendations of Cassel et al. (2016). The outer shell material needed to meet five criteria including: moldability, non-toxicity, resistance to cracking and degradation, non-interference with the RFID signals, and density matching with natural gravels. Cassel et al. (2016) tested a mixture of a polyurethane plastic resin and corundum powder (Al_2O_3; density = 3.95–4.10 g/cm^3) to create synthetic tracing stones that met the above criteria. The lower density of their synthetic stones (~2.2 g/cm^3) as compared to natural stones was not observed to systematically affect particle transport in their experiments (Cassel et al., 2016). Furthermore, abrasion tests conducted by Cassel et al. (2016) showed that 95% of the synthetic stones survived the test with no damage, with the remaining 5% showing only minor splinter losses, demonstrating the durability of the material for sediment transport research applications.

The resin used for the prototypes described here is a high density polyurethane plastic resin manufactured by Smooth-On (Smooth-Cast® 380) with a density of 1.74 g/cm^3 and a Shore hardness of 82D. The resin was mixed at a 1:2 ratio with corundum powder based on a series of tests to achieve the identified criteria. At this ratio, the mixture is dry but easily moldable and, once hardened (~ one hour), has a density of 3.02 g/cm^3.

6.2.1 Prototype 1

The inner ball of the first prototype stone contains a 12 mm RFID HDX PIT tag (Oregon RFID; ISO 11784/11785) inside a 20 mm hollow plastic sphere ordered from a plastic ball manufacturer (CIC Ball Company; #PPH07870N). To create the inner weighted ball, a hole with diameter slightly larger than that of the transponder was first drilled into the hollow plastic sphere. The sphere was then half filled with a 1:1 resin-corundum powder mixture using a syringe. The resin-corundum mixture flows more easily at this ratio, which allowed it to be pushed through the syringe. Before the resin mixture hardened, the transponder tag was inserted into the hole so that it was completely in the ball, but not pushed through all the way so that it remained vertical during the hardening time (Figure 6.2a). Once hardened, the portion of the inner ball filled with the resin-corundum mixture was heavy enough that it always rotated to the bottom, which maintained the tag in the vertical position.

The lubricant used to facilitate the rotation of the inner ball needed to be non-toxic, in case of leakage to the environment, and have a low freezing temperature to avoid stone breakage in cold environments. Additionally, the lubricant should be of high viscosity so that the inner sphere rotates slowly in comparison to movements of the tracer stone to minimize the effect of its rotation on the rotational inertia of the tracer. Based on these criteria, a solution of 70% glycerin and 30% water was used, resulting in a liquid lubricant with a freezing temperature of –38 °C. The viscosity of the glycerin solution ranges between 0.13 Ns/m^3 at 0 °C and 0.035 Ns/m^3 at 20 °C (Cheng, 2008).

The mould for the outer shell of the tracer stone was made from Mold Star® 15 SLOW; a platinum silicone rubber manufactured by Smooth-On specifically for use with polyurethane plastic resins without the need of a release agent. The mould for the first prototype was made using a golf ball (diameter = 42.7 mm) and was created by first placing the golf ball on top of a silicone platform in a disposable container. The container was then filled with the silicon mixture to cover the entire ball. Once the silicone rubber hardened (~ 4 hours), it was cut into two halves (Figure 6.2b). A golf ball was used to create the outer shell of Prototype 1 for simplicity, as the purpose was to test the feasibility and performance of ball-within-a-ball design. For sediment transport applications, the

procedure for creating the outer shell mould may be replicated using natural stones to create tracers with a variability of shape and size reflective of natural gravel.

The final step was to cast the outer shell of the synthetic stone. Each half of the mould was filled with the 1:2 resin-corundum powder mixture. The cavity in which the inner ball sat needed to be a smooth round indent with a diameter slightly larger than the inner ball. String tied to nails inserted into the mould edge was used as visual markers to ensure the cavity was centered in each half of the outer shell (Figure 6.2c). The cavity was made by rolling the inner ball into the resin-corundum powder mixture. The dry, sandy nature of the resin-corundum powder mixture allowed for the cavity to hold its shape during the hardening process. Once the two halves of the outer shell hardened, the inner ball and lubricant were placed into one half (Figure 6.2d), and the two halves were sealed together using excess resin-corundum powder mixture.

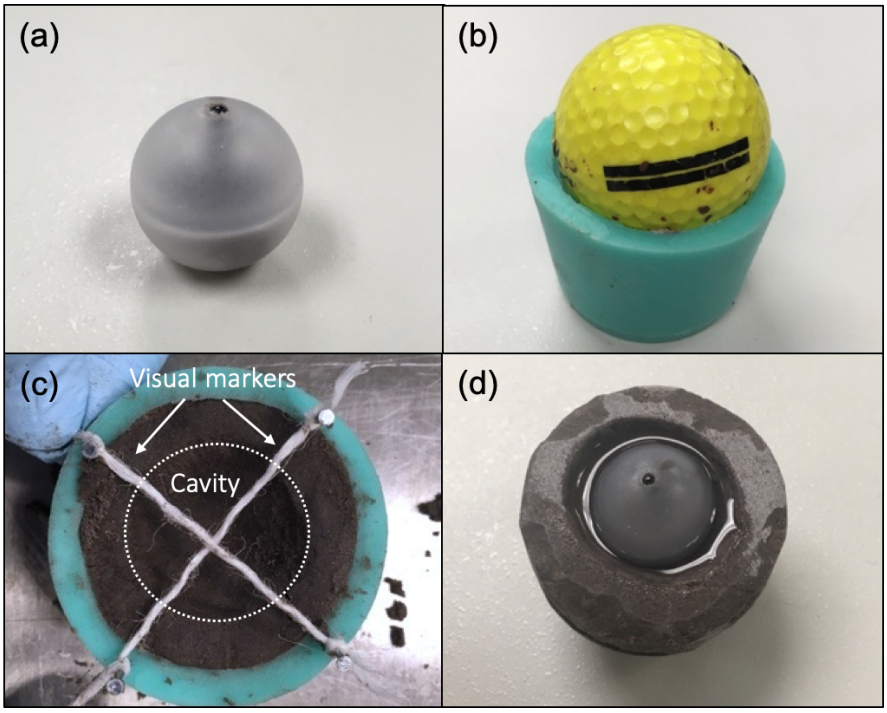

Figure 6.2. Procedure for the first 'Wobblestone' prototype assembly: (a) weighted inner ball, (b) silicone mould for outer shell cut in half, (c) creation of the outer shell cavity, and (d) inner ball within the outer shell with lubricant.

6.2.2 Prototype 2

The second prototype follows the same design concept (Figure 6.1) as the first, but uses a custom ball-within-a-ball insert to hold the RFID transponder (Figure 6.3). This procedure accelerates tracer

assembly for mass production, and ensures a more consistent cavity for smooth rotation of the weighted inner ball. The custom insert is made from a high density polyethylene plastic and includes an outer ball (diameter = 16 mm), and a smaller inner ball (diameter = 12 mm) designed to hold a 12 mm RFID HDX PIT tag (Figure 6.3a). Each of the balls are moulded in two halves and feature a ribbing edge for precise assembly and sealing (Figure 6.3a). The four plastic pieces of the insert are fabricated using injection moulding with a custom mould (Figure 6.3b).

To construct the insert, one half of the inner ball is filled with the 1:2 resin-corundum powder mixture, and the transponder is placed vertically in the holder of the inner insert ball (Figure 6.3a). As the resin hardens, the second half of the inner ball is connected to the first with the ribbing edge and glued. Once dry, the inner ball is placed within one half of the outer ball along with the same water-glycerin solution used in the first prototype. The second half of the outer ball is then connected with the ribbing edge and the two halves are glued in place to create the insert (Figure 6.3c). The outer shell of the second prototype was made using the same materials and procedure as the first prototype, but the mould was made from a natural stone (b-axis = 32 mm) rather than a golf ball. The result is a synthetic replica of the original stone that contains the ball-within-a-ball insert (Figure 3d). The custom-made insert allows for the two halves of the outer shell to be sealed while the resin mixture is still wet, ensuring a better bond between them.

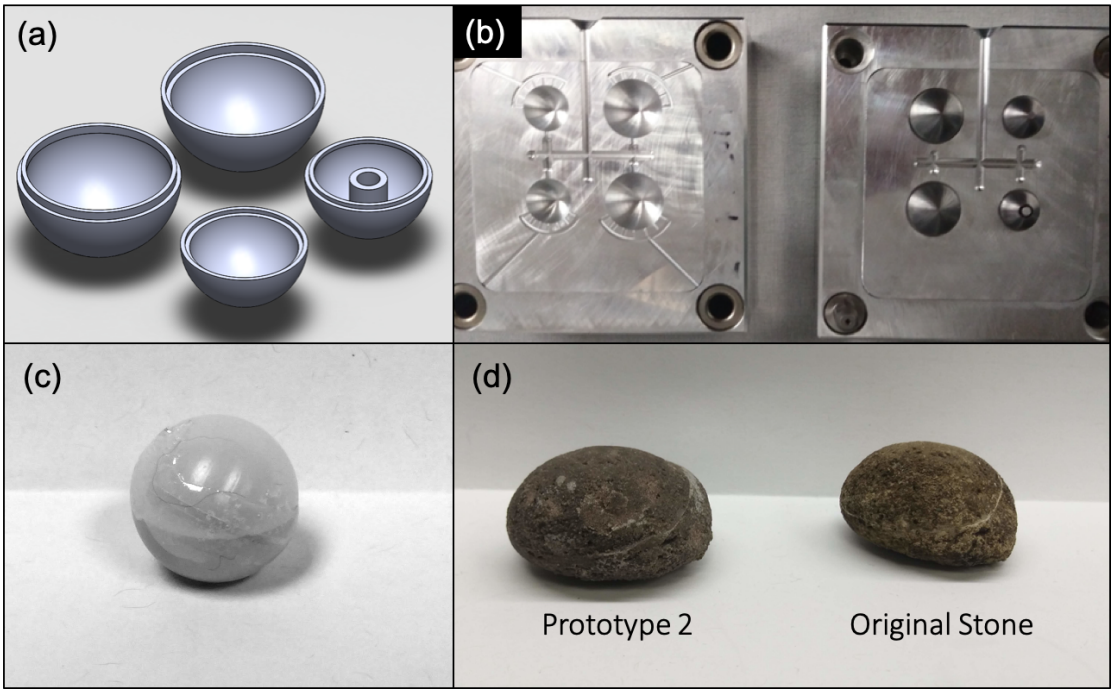

Figure 6.3. Procedure for the second 'Wobblestone' prototype assembly: (a) design drawings of plastic injection parts, (b) injection mould, and (c) completed inner ball.

6.3 Performance and durability tests

A series of four tests were completed on the two prototypes to assess density, durability, rotation of the inner ball, and the utility of the tags for the determination of burial depth. All of the tests were performed in the lab.

The first test measured the density of the two prototypes to ensure that the synthetic stones were within an acceptable range for bedload transport research applications. The first prototype has a total density of 2.39 ± 0.04 g/cm^3 and a diameter of 45 mm. The second prototype has a total density of 2.30 ±0.06 g/ cm^3, and a b-axis of 33 mm. These densities are slightly higher than what was achieved by Cassel et al. (2016) using similar materials (~2.2 g/cm^3). Compared with natural sediments the synthetic particles are less dense than granite (2.63–2.75 g/cm^3), within the range of limestone (1.76–2.56 g/cm^3), and within the 95% range of variability of approximately 1,500 randomly sampled stones from creeks in Ontario, Canada that are part of an ongoing study.

The second test was a simple drop test and repeated freezing and thawing cycles to confirm the durability of the synthetic tracers. Both prototypes survived being dropped from chest height 5 times onto a concrete floor without breakage or chipping. These simple impact tests support results from lab transport tests on synthetic stones by Cassel et al. (2016). Prototype 1 also underwent two cycles of freeze-thaw of approximately 24 hours at –16 °C with no damage, demonstrating the suitability of the chosen lubricant material.

The third test was a detection zone shape test to verify that the weighted inner ball rotated successfully and the transponder remained vertical regardless of the stone orientation. Previous tests in laboratory and field environments have shown that vertically oriented transponders have a circular detection zone centered around the transponder location, while horizontal transponders produce a double-lobed detection zone extending from the ends of the tag (Chapuis et al., 2014b). Transponder orientations that fall between vertical and horizontal produce a variety of irregular detection zone shapes (Arnaud et al., 2015). For the current study, the detection zone of a vertically-oriented transponder was verified by pressing a 12 mm PIT tag into a small clay ball at the center of a large cardboard board and approaching it with a stick antenna (AEA580 antenna with a DataTracer II FDX/HDX Reader from Oregon RFID Inc.) from 12 equally spaced directions along the board surface. A stick antenna was chosen for this test for its higher precision and simpler detection field shape as compared to more commonly used loop antennas (Chapuis et al., 2014b), allowing for more accurate determination of detection zone shapes in this test. Once the antenna detected the tag, a mark was placed on the cardboard, forming an outline of the detection zone shape. The process was repeated for a horizontal transponder and for each prototype placed at a randomly chosen orientations.

Totals of 15 and 20 repetitions were completed for prototype 1 and prototype 2, respectively. The results confirm that the shape of the detection zone for the tracers is consistent regardless of stone orientation and that it matches the detection zone shape of vertically oriented tags (Figure 6.4). The circular detection zone shape of a vertical transponder also enables the position of the tracer stone to be reliably inferred as the centroid of the detection zone in the horizontal plane.

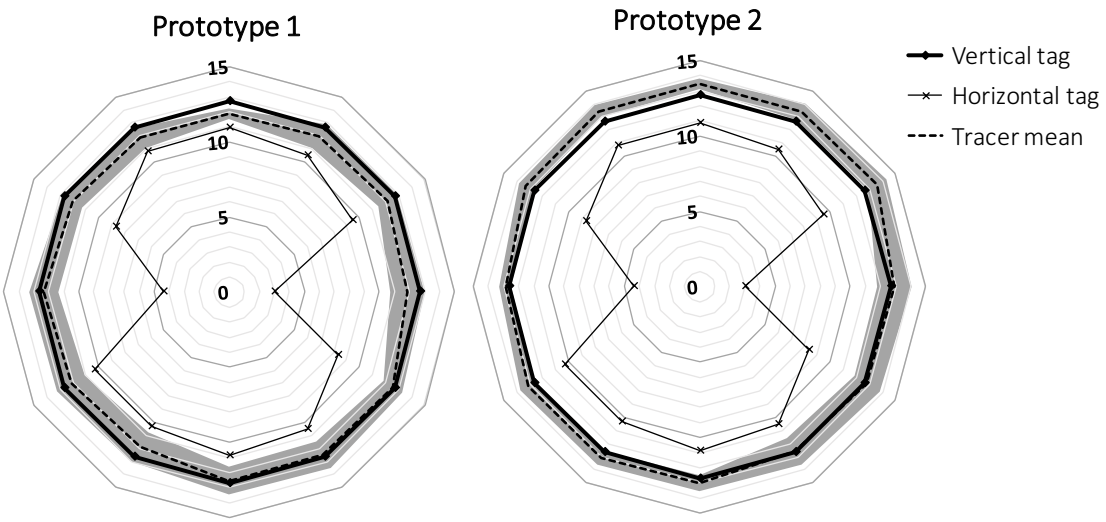

Figure 6.4. Results of the performance tests showing the detection zone shapes of horizontal and vertical RFID tags, and both 'Wobblestone' prototypes. Scale is in centimeters (cm).

The fourth test was a laboratory burial test to confirm that a tracer with a vertically oriented transponder can be used to determine the vertical position of the tracer relative to the surface of the channel bed, i.e. the burial depth. To demonstrate this application, the second 'Wobblestone' prototype was buried to different depths beneath coarse sand and approached with the antenna from the vertical direction. Ten repetitions of the test were completed to estimate the uncertainty. As expected from the results of Chapuis et al. (2014b), burial did not affect the total distance between the antenna and the tag at the first detection (Figure 6.5). Burial depth can therefore be estimated (± 1 cm) as the difference between the height of the antenna above the bed at the first detection and the average height of the detection zone for a tracer on the surface (12.2 cm). The variability in tracer detection distance with different antenna types (Dziadak et al., 2009) means that such a method would require calibration for each antenna. The reduction in detection zone with saturation (Chapuis et al., 2014b) would also require independent calibration for dry and saturated conditions prior to field applications. Furthermore, the tracers presented here could also be used with the methods developed by Tsakiris et al. (2015) to calculate the position of the tracer from the return signal voltage. Tests are

ongoing with a moderate number (300) of the second prototype of the tracers to assess the effect of the self-righting mechanism on the accuracy of estimated tracer position and burial depth in field applications.

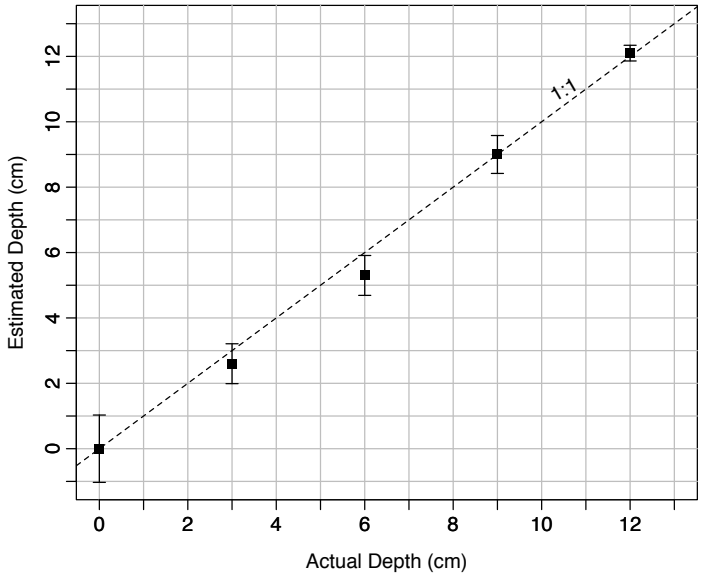

Figure 6.5. Results of the burial depth tests. Error bars represent one standard deviation of repeated measurements.

6.4 Conclusions

This paper presents the conceptual design and two successful prototypes of a synthetic tracer stone that allow for the orientation of the RFID transponder to remain vertical even as the tracer stone is rotated on any axis. The design uses a weighted inner ball that is free to rotate under gravity to a position with the transponder in a vertical orientation. This new design of tracer stone provides several advantages when used for sediment tracking experiments. A vertically oriented transponder produces a simple and known detection zone shape, which should reduce signal interference from closely located tracers and increase precision in locating tracers. The consistent height of the detection zone allows tracer burial depth to be estimated, which represents significant new information about transported tracers that will allow vertical mixing processes to be easily assessed in field studies. Studies are ongoing to demonstrate these advantages in field applications, as well as the practicability of the assembly procedures for making large sample sizes of tracers.

Chapter 7
General Conclusions

This thesis explores how bedload sediment transport in gravel-bed streams is impacted by watershed urbanization and two common river management strategies, SWM and in-stream restoration. The overarching goals of the project were to add to the scientific understanding of how bedload transport processes are affected by urbanization, provide tools that can be used by engineers and river managing authorities to improve urban river management and improve bedload transport monitoring technology. Results from this thesis are summarized in this Chapter, and limitations and future research directions are discussed.

7.1 Summary of results and contributions

A key contribution of this project is a large dataset of bedload transport data in urban environments. The rarity of bedload sediment data in rivers, and particularly in urban rivers, is a contributing factor in the knowledge gap that exists on the human influences on bedload transport processes (Wohl et al., 2015b; Wilcock, 2012). The dataset collected is archived in open online repositories to encourage and facilitate future research and collaboration.

The objective of Chapter 3 was to gain an understanding of how urbanization and SWM affect bedload transport regimes of rivers and their relationship to morphologic adjustments. A space-for-time substitution was employed so that bedload transport and morphodynamics measured in three similar streams with different watershed settings: rural, urban with no SWM, and urban with SWM. Bedload displacement of particles up to the D_{90} is accelerated in the urban river, driven by more frequent mobilizing events rather than an increase in travel lengths during floods. Frequent mobilization of coarse sediment can explain trends of channel enlargement. SWM decreases the mobility and travel lengths of coarse particles that, in combination with channel narrowing, bed armouring, and loss bedforms, suggests the stream is moving towards a competence-limited transport regime. Although the bulk sediment transport rates of urban rivers have been modelled or measured, this study presents empirical evidence of shifts in the grain-scale dynamics of urban rivers. Recommendations for process-based urban river management strategies based on the results of this study are presented, including a shift in focus to frequent small-to-medium magnitude events, rather than designs based on rare large-magnitude events. SWM designs that attempt to alleviate the

homogenization and inactivity of downstream reaches by more closely matching pre-urbanization hydraulics are likely to improve the ecologic conditions of streams.

The objective of Chapter 4 was to build predictive models of tracer displacements in rivers with hydrographs altered by urban hydromodification and SWM. Tracer data from the same three streams introduced in Chapter 3 were used. Results demonstrated the dependence of model results on considerations of tracer slowdown and model calibration techniques. The weighted mean travel length ($\tilde{L}$, m) is introduced as a useful variable that captures both the mobility and travel length of tracers Despite differences in hydrograph characteristics between streams in this study, the cumulative excess discharge (CEQ, m^3) (Haschenburger, 2011) can be used to reliably predict the weighted mean travel length scaled of tracers scaled by mean channel width. Such a model has applications for urban river management, SWM design, and in-stream restoration design by providing a tool that can be linked with hydrologic models to predict bedload transport responses to future watershed development decisions. The hope is to implement the model presented in this study in a scenario-testing tool as part of a decision-making tool aimed at watershed conservation authorities.

The objective of Chapter 5 was to assess the performance of an in-stream riffle-pool restoration project from a process-based perspective. Bedload sediment transport and morphologic change were monitored in adjacent unrestored and restored reaches of an urban channel, and compared to a rural analog. The channel reconstruction slows down the virtual velocity of particles (the mean distance travelled per year) in the D_{75} and D_{90} size classes but does not significantly change the virtual velocity of particles in the D_{50} size class or smaller. Surveys show that riffle features remain stable and that pool depths are maintained or deepened, while tracer paths match with what has been observed in natural riffle-pools. However, the slowdown of coarse sediment and increase in channel slope may lead to future failures related to the over-steepening of the banks and a disruption in the continuity of sediment transport in the creek. This study demonstrates how bedload tracking and morphological surveys can be used to assess river restoration projects and highlights the importance of incorporating coarse sediment connectivity into restoration design and monitoring.

Finally, the objective of Chapter 6 was to improve the limitation of RFID tracking technology that does not allow for particle burial depth to be determined. The 'Wobblestone' design was introduced, and the performance of two prototypes was presented, demonstrating the ability to ensure the PIT tag remains vertical regardless of particle orientation. Although field tests of burial depth estimation using the 'Wobblestone' are ongoing, the design shows promise based on a series of laboratory testing. The ability to monitor the burial depth of bedload particles will improve bedload tracking studies by allowing for vertical mixing to be measured using RFID technology, providing

new opportunities to study these processes and allow easier translation of tracer data into bulk transport rates.

7.2 Revisiting the urban stream syndrome

The drivers of the urban stream syndrome can be revisited with new insights revealed in this study. As discussed in Chapter 2, the urban stream syndrome is complex, involving many hydrologic, geomorphic and ecologic processes that affect one another through many mechanisms. As such, the urban stream syndrome is a multi-dimensional problem that can only be fully understood by investigating every component of the urban fluvial system and the interactions between them. Bedload sediment transport is a key geomorphic process that is not well-understood or measured in the context of urbanization and river management. The results of this study improve understanding of how bedload transport is affected by urbanization and SWM that may contribute to the understanding of the degradation of urban river ecology.

A shift in the bedload transport regime of urban rivers was observed, characterized by an increase in the frequency of bedload mobilization and a consequent increase in the geomorphic significance of small-to-medium-magnitude events. As bedload provides the building blocks of aquatic habitat for invertebrates, and spawning material for fish, an increase in the frequency of bed disturbance is likely to have negative effects on riverine organisms. Although episodic bed disturbance is important for the maintenance of bedforms and optimal grain size distributions on the streambed, a large increase in the frequency of this disturbance may have negative consequences. The timing of this disturbance is also altered with urbanization, as the geomorphic significance of flood events shifts from seasonally-dominant springtime events to frequent summertime flashy storms. Considering the lifecycle and adaptations of riverine organisms, such stressors are likely to impact the ecologic resilience. Finally, the flashy nature of urban storms leads to high flow accelerations from baseflow to peak flow, which may exceed the flow accelerations that aquatic organisms have been adapted to survive.

Peak-shaving SWM approaches also changed the bedload transport regimes of rivers measured in this study. The increased duration of flood events in streams with this type of SWM is likely to put stress on aquatic organisms, as the duration of high-intensity flows are elongated. Furthermore, the shift of the transport regime towards a competence-limited transport regime in this study led to a static and armoured bed absent of bars and prominent bedforms. The inactivity of the bed does not promote bedform maintenance and the bed complexity required to sustain aquatic

habitats. Furthermore, severe bed armouring leads to changes in the bed material texture that may not be suitable for native species.

Ecological studies to examine these stressors are required to confirm these hypotheses of how changes to the bedload transport regime may impact aquatic ecosystems. The ongoing ecological study carried out by the School of Environment, Resources and Sustainability at the University of Waterloo is designed to complement this study aim to explore these connections to gain a better process-level understanding of the urban stream syndrome. Collaborative research into links between the physical and ecological processes of urban rivers will greatly benefit the future management of urban rivers.

7.3 Future research

Results from this study reveal directions for future bedload sediment transport and urban river management research. The conclusions drawn from the results presented in Chapter 3 are constrained to the geographic region of Southern Ontario. This region has a unique glacial legacy that leads to semi-alluvial rivers that may behave differently than rivers in other settings. For example, the bedload tracking in this study revealed that the displacement characteristics of bed particles may be different compared to those in fully alluvial settings. Applying methods presented in Chapter 3 across a wider range of environments with different climatic and geologic settings will further test the generalizability of the results. The limited duration of the study is also not able to capture the full range of hydrologic conditions that may occur in this setting. Longer duration studies are required to adequately capture the range of precipitation events that occur in Southern Ontario.

Another important limitation of this study is that only three rivers were examined at one stage of channel evolution. Future research should explore the bedload transport dynamics of rivers at different stages of channel evolution, to understand how transport dynamics change at different stages towards a new dynamic equilibrium. This is particularly important for uncovering feedback relationships between hydraulic and morphologic changes (e.g. Anim et al., 2019c). Although the channel evolution of rivers in response to urbanization occurs over very long timescales (e.g. Bevan et al., 2018), the grain-scale dynamics are likely to adjust in tandem with hydrologic changes that are likely to occur quickly after paving or construction of SWM structures. Bedload sediment tracking can, therefore, provide a method to investigate the effects of urbanization and management strategies on rivers as hydrologic changes occur.

The model built in Chapter 4 is limited by the small number of rivers and mobilizing events captured in this project. Ideally, data from a larger variety of rivers and over multiple mobilizing

events should be used to validate the model and assess its wider applicability. Although a large number of particle tracking studies exist in the literature, the inconsistency in how data is interpreted and presented leads to difficulties in testing models across datasets. Future research using bedload particle tracking should focus on setting standardized data analysis techniques to allow for the generalizability of tracer behaviour models to be more rigorously tested. Another important direction for future research in predictive models of bedload transport is an investigation into model uncertainties and sensitivity analyses to determine sources of error and ways to minimize them. The usefulness of a model lies within the balance of maximizing predictive power and minimizing uncertainty in results. A full sensitivity analysis of the calculation of flow metrics using data from this project is planned.

Chapter 5 focused on a riffle-pool restoration project. Although these designs are common, many other restoration strategies are used to restore urban rivers. An important direction for future research is to monitor bedload transport dynamics in a variety of river restoration designs and geographic settings. There is also a need to study the effects of river restoration projects at longer timescales. While the restoration at Wilket Creek was now completed six years ago, morphologic adjustment may occur over several decades. In fact, the question of how long it takes for 'success' or 'failure' to manifest is important to assess (Buchanan et al., 2014; Morandi et al., 2014). Continued monitoring of restoration projects is resource-intensive, which is a large barrier to adequate monitoring programs, but imperative for understanding the long-term consequences of current restoration practices. Bedload sediment tracking offers a process-based view of the effects of restoration projects, which can be used in conjunction with morphologic and ecologic monitoring to assess the performance of in-stream restoration designs. Such research would be helpful in improving restoration design and developing recommendations for urban river management that moved towards process-based solutions and adaptive management.

A final limitation of the work presented in this thesis is the focus on coarse bed sediment ($\geq D_{50}$ of the surface material). Given the resources needed for fieldwork data collection, this was a conscious choice, as coarse bed material plays a dominant role in channel stability and morphodynamics (McKenzie et al., 2018). However, the importance of fine sediment for many river geomorphic and ecologic processes warrants complementary investigations of the effects of urbanization and river management practices on fine sediment dynamics. This is particularly important in the glacially-conditioned context of Southern Ontario, where an abundance of sand and silt-sized material is supplied to the channels.

Despite the inherent limitations of this study, results add to the growing body of literature exploring the effects of anthropogenic activities on landscape processes and ecologic health. This thesis provides one piece of the large puzzle, which can only be understood through examining process-level shifts in geomorphic process, as well as the links between geomorphic dimensions of natural systems and other important aspects such as hydrology and ecology. Collaborations with research teams from the School of Environment, Resources and Sustainability at the University of Waterloo, and the Department of Geography at Western University to address some of these topics are ongoing, with the hope of providing interdisciplinary perspectives for urban river management. Results from this thesis add to the growing knowledge of the effects of urbanization and current river management strategies on river processes and open new avenues for future research.

References

AECOM (2011). *Wilket Creek Rehabilitation Project Master Plan – Hydraulic Analysis*. Retrieved from: http://www.trca.on.ca/dotAsset/201894.pdf

Ahmad, Z., Singh, U. K., Kumar, A. (2017). Incipient motion for gravel particles in clay-silt-gravel cohesive mixtures. *Journal of Soils and Sediments*, *42*, 1–12. DOI: 10.1007/s11368-017-1869-z

Andrews, E. D. (1983). Entrainment of gravel from naturally sorted riverbed material. *Geological Society of America Bulletin*, *94*(10), 1225–1231. DOI: 10.1130/0016-7606(1983)94<1225:EOGFNS>2.0.CO;2

Anim, D. O., Fletcher, T. D., Pasternack, G. B., Vietz, G. J., Duncan, H. P., Burns, M. J. (2019a). Can catchment-scale urban stormwater management measures benefit the stream hydraulic environment? *Journal of Environmental Management*, *233*, 1–11. DOI: 10.1016/j.jenvman.2018.12.023

Anim, D. O., Fletcher, T. D., Vietz, G. J., Burns, M. J., Pasternack, G. B. (2019b). How alternative urban stream channel designs influence ecohydraulic conditions. *Journal of Environmental Management*, *247*, 242–252. DOI: 10.1016/j.jenvman.2019.06.095

Anim, D. O., Fletcher, T. D., Vietz, G. J., Pasternack, G. B., Burns, M. J. (2018). Effect of urbanization on stream hydraulics. *River Research and Applications*, *34*(7), 661–674. DOI: 10.1002/rra.3293

Anim, D. O., Fletcher, T. D., Vietz, G. J., Pasternack, G. B., Burns, M. J. (2019c). Restoring in-stream habitat in urban catchments: Modify flow or the channel? *Ecohydrology*, *12*(1). DOI: 10.1002/eco.2050

Annable, W. K., Lounder, V. G., Watson, C. C. (2011). Estimating channel-forming discharge in urban watercourses. *River Research and Applications*, *27*(6), 738–753. DOI: 10.1002/rra.1391

Annable, W. K., Watson, C. C., Thompson, P. J. (2012). Quasi-equilibrium conditions of urban gravel-bed stream channels in Southern Ontario, Canada. *River Research and Applications*, *28*(3), 302–325. DOI: 10.1002/rra.1457

Arnaud, F., Piégay, H., Beal, D., Collery, P., Vaudor, L., Rollet, A.-J. (2017). Monitoring gravel augmentation in a large regulated river and implications for process-based restoration. *Earth Surface Processes and Landforms*, *42*(13), 2147–2166. DOI: 10.1002/esp.4161

Arnaud, F., Piégay, H., Vaudor, L., Bultingaire, L., Fantino, G. (2015). Technical specifications of low-frequency radio identification bedload tracking from field experiments: Differences in antennas, tags and operators. *Geomorphology*, *238*, 37–46. DOI: 10.1016/j.geomorph.2015.02.029

Ashworth, P. J., Ferguson, R. I. (1989). Size-selective entrainment of bed load in gravel bed streams. *Water Resources Research*, *25*(4), 627–634. DOI: 10.1029/WR025i004p00627

Badelt, B. (1999). *Change in channel morphology due to urbanization in Morningside Creek, Ontario* (Master's thesis). University of Guelph, Guelph, ON. Retrieved from Library and Archives Canada: https://central.bac-lac.gc.ca/.item?id=MQ47305&op=pdf&app=Library

Bagnold, R. A. (1966). An approach to the sediment transport problem from general physics. United States Geological Survey Professional Paper, 4221.

Barr, D. (2017). *Wilket Creek: urbanization, geomorphology, policy, and design* (Master's thesis). Western University, London, ON. Retrieved from the Electronic Thesis and Dissertation Repository (4578): https://ir.lib.uwo.ca/etd/4578

Baker, D. W., Pomeroy, C. A., Annable, W. K., MacBroom, J. G., Schwartz, J. S., Gracie, J. (2008). Evaluating the effects of urbanization on stream flow and channel stability — state of practice (pp. 1–10). *Proceedings of the World Environmental and Water Resources Congress 2008: Ahupua'a*, Honolulu, HI: American Society of Civil Engineers.

Beagle, J. R., Kondolf, G. M., Adams, R. M., Marcus, L. (2015). Anticipatory management for instream habitat: Application to Carneros Creek, California. *River Research and Applications*, *32*(3), 280–294. DOI: 10.1002/rra.2863

Beechie, T. J., Sear, D. A., Olden, J. D., Pess, G. R., Buffington, J. M., Moir, H., et al. (2010). Process-based principles for restoring river ecosystems. *BioScience*, *60*(3), 209–222. DOI: 10.1525/bio.2010.60.3.7

Bernhardt, E. S., Palmer, M. A. (2007). Restoring streams in an urbanizing world. *Freshwater Biology*, *52*(4), 738–751. DOI: 10.1111/j.1365-2427.2006.01718.x

Bernhardt, E. S., Palmer, M. A. (2011). Evaluating river restoration. *Ecological Applications*, *21*(6), 1925–1925. DOI: 10.1890/11-0644.1

Bernhardt, E. S., Palmer, M., Allan, J. D. (2005). Synthesizing US river restoration efforts. *Science*, *308*(5722), 636–637.

Bernhardt, E. S., Sudduth, E. B., Palmer, M. A., Allan, J. D., Meyer, J. L., Alexander, G., et al. (2007). Restoring rivers one reach at a time: Results from a survey of U.S. river restoration Practitioners. *Restoration Ecology*, *15*(3), 482–493. DOI: 10.1111/j.1526-100X.2007.00244.x

Bevan, V., MacVicar, B., Chapuis, M., Ghunowa, K., Papangelakis, E., Parish, J., Snodgrass, W. (2018). Enlargement and evolution of a semi-alluvial creek in response to urbanization. *Earth Surface Processes and Landforms*, *43*(11), 2295–2312. DOI: 10.1002/esp.4391

Biron, P. M., Carver, R. B., Carré, D. M. (2012). Sediment transport and flow dynamics around a restored pool in a fish habitat rehabilitation project: Field and 3D numerical modelling experiments. *River Research and Applications*, *28*(7), 926–939. DOI: 10.1002/rra.1488

Bledsoe, B. P. (2002). Stream erosion potential and stormwater management strategies. *Journal of Water Resources Planning and Management*, *128*(6), 451–455. DOI: 10.1061/(ASCE)0733-9496(2002)128:6(451)

Bledsoe, B. P., Watson, C. C. (2000). Observed thresholds of stream ecosystem degradation in urbanizing areas: A process-based geomorphic view (pp. 1–10). *Proceedings of the Watershed Management and Operations Management Conferences 2000*, Fort Collins, CO: American Society of Civil Engineers. DOI: 10.1061/40499(2000)96

Bledsoe, B. P., Watson, C. C. (2001). Effects of urbanization on channel instability. *JAWRA Journal of the American Water Resources Association*, *37*(2), 255–270. DOI: 10.1111/j.1752-1688.2001.tb00966.x

Boix-Fayos, C., Barberá, G. G., López-Bermúdez, F., Castillo, V. M. (2007). Effects of check dams, reforestation and land-use changes on river channel morphology: Case study of the Rogativa catchment (Murcia, Spain). *Geomorphology*, *91*, 103–123. DOI: 10.1016/j.geomorph.2007.02.003

Booth, D. B. (1990). Stream-channel incision following drainage-basin urbanization. *Water Resources Bulletin*, *26*(3), 407–417. https://doi.org/10.1111/j.1752-1688.1990.tb01380.x

Booth, D. B. (1991). Urbanization and the natural drainage system - Impacts, solutions, and prognoses. *Northwest Environmental Journal*, *7*(1), 93–118. Retrieved from: http://hdl.handle.net/1773/17032

Booth, D. B., Fischenich, C. J. (2015). A channel evolution model to guide sustainable urban stream restoration. *Area*, *47*(4), 408–421. DOI: 10.1111/area.12180

Booth, D. B., Jackson, C. R. (1997). Urbanization of aquatic systems: Degradation thresholds, stormwater detection, and the limits of mitigation. *JAWRA Journal of the American Water Resources Association*, *33*(5), 1077–1090. https://doi.org/10.1111/j.1752-1688.1997.tb04126.x

Booth, D. B., Karr, J. R., Schauman, S., Konrad, C. P., Morley, S. A., Larson, M. G., Burges, S. J. (2004). Reviving urban streams: Land use, hydrology, biology and human behavior. *Journal of the American Water Resources Association*, *40*(5), 1351–1364. DOI: 10.1111/j.1752-1688.2004.tb01591.x

Booth, D. B., Roy, A. H., Smith, B., Capps, K. A. (2015). Global perspectives on the urban stream syndrome. *Freshwater Science*, *35*(1), 412–420. DOI: 10.1086/684940

Bouska, K. L., Stoebner, T. J. (2015). Characterizing geomorphic change from anthropogenic disturbances to inform restoration in the Upper Cache River, Illinois. *Journal of the American Water Resources Association*, *51*(3), 734–745. DOI: 10.1111/jawr.12266

Bradley, N. D., Tucker, G. E. (2012). Measuring gravel transport and dispersion in a mountain river using passive radio tracers. *Earth Surface Processes and Landforms*, *37*(10), 1034–1045. DOI: 10.1002/esp.3223

Brandt, S. A. (2000). Classification of geomorphological effects downstream of dams. *Catena*, *40*(4), 375–401. DOI: 10.1016/S0341-8162(00)00093-X

Brayshaw, A. C. (1985). Bed microtopography and entrainment thresholds in gravel-bed rivers. *Geological Society of America Bulletin*, *96*(2), 218–223. DOI: 10.1130/0016-7606(1985)96<218:BMAETI>2.0.CO;2

Brenna, A., Surian, N., Mao, L. (2019). Virtual velocity approach for estimating bed material transport in gravel-bed rivers: Key factors and significance. *Water Resources Research, 55*(2), 1651-1674. DOI: 10.1029/2018WR023556

Buchanan, B. P., Nagle, G. N., Walter, M. T. (2014). Long-term monitoring and assessment of a stream restoration project in Central New York. *River Research and Applications*, *30*(2), 245–258. DOI: 10.1002/rra.2639

Buffington, J. M., Montgomery, D. R. (1997). A systematic analysis of eight decades of incipient motion studies, with special reference to gravel-bedded rivers. *Water Resources Research*, *33*(8), 1993–2029. DOI: 10.1029/96WR03190

Cain, A. (2019). *High precision sediment tracking for characterization of sediment transport of a rural stream in Southern Ontario conditioned by glacial legacy deposits* (Master's thesis). University of Waterloo, Waterloo, Canada. Retrieved from UWSpace: http://hdl.handle.net/10012/15188

Cassel, M., Piégay, H., Lavé, J. (2016). Effects of transport and insertion of radio frequency identification (RFID) transponders on resistance and shape of natural and synthetic pebbles: Applications for riverine and coastal bedload tracking. *Earth Surface Processes and Landforms*, *42*(3), 399–413. DOI: 10.1002/esp.3989

Cavanaugh, J. E., Neath, A. A. (2019). The Akaike information criterion: Background, derivation, properties, application, interpretation, and refinements. *WIREs Computational Statistics, 11*(3), e1460. https://doi.org/10.1002/wics.1460

Chapuis, M., Bevan, V., MacVicar, B., Roy, A. (2014a). Sediment transport and morphodynamics in an urbanized river: The effect of restoration on sediment fluxes (pp. 2119–2126). *Proceedings of the River Flow International Conference on Fluvial Hydraulics*, Lausanne, Switzerland: Taylor Francis Group.

Chapuis, M., Bright, C. J., Hufnagel, J., MacVicar, B. (2014b). Detection ranges and uncertainty of passive Radio Frequency Identification (RFID) transponders for sediment tracking in gravel rivers and coastal environments. *Earth Surface Processes and Landforms, 39*(15), 2109–2120. DOI: 10.1002/esp.3620

Chapuis, M., Dufour, S., Provansal, M., Couvert, B., de Linares, M. (2015). Coupling channel evolution monitoring and RFID tracking in a large, wandering, gravel-bed river: Insights into sediment routing on geomorphic continuity through a riffle-pool sequence. *Geomorphology*, *231*, 258–269. DOI: 10.1016/j.geomorph.2014.12.013

Cheng, N. S. (2008). Formula for the viscosity of a glycerol-water mixture. *Industrial and Engineering Chemistry Research, 47*(9), 3285–3288. https://doi.org/10.1021/ie071349z

Chin, A. (2006). Urban transformation of river landscapes in a global context. *Geomorphology*, *79*(3-4), 460–487. DOI: 10.1016/j.geomorph.2006.06.033

Chin, A., Gregory, K. (2009). From research to application: Management implications from studies of urban river channel adjustment. *Geography Compass*, *3*(1), 297–328. DOI: 10.1111/j.1749-8198.2008.00193.x

Chin, A., Gregory, K. J. (2005). Managing urban river channel adjustments. *Geomorphology*, *69*, 28–45. DOI: 10.1016/j.geomorph.2004.10.009

Chin, A., O'Dowd, A. P., Gregory, K. J. (2013). Urbanization and river channels. In J. Shroder E. Wohl, (Eds.), *Treatise on Geomorphology* (vol. 9, pp. 809–827). Academic Press, San Diego, CA: Elsevier. DOI: 10.1016/B978-0-12-374739-6.00266-9

Choi, S. U., Yoon, B., Woo, H. (2005). Effects of dam-induced flow regime change on downstream river morphology and vegetation cover in the Hwang River, Korea. *River Research and Applications*, *21*(2-3), 315–325. DOI: 10.1002/rra.849

Church, M., Hassan, M. A. (1992). Size and distance of travel of unconstrained clasts on a streambed. *Water Resources Research*, *28*(1), 299–303. DOI: 10.1029/91WR02523

Church, M., Hassan, M. A. (2002). Mobility of bed material in Harris Creek. *Water Resources Research*, *38*(11), 1237. DOI: 10.1029/2001WR000753

Clarke, S. J., Bruce-Burgess, L., Wharton, G. (2003). Linking form and function: towards an eco-hydromorphic approach to sustainable river restoration. *Aquatic Conservation: Marine and Freshwater Ecosystems*, *13*(5), 439–450. DOI: 10.1002/aqc.591

Craney, T. A., Surles, J. G. (2002). Model-dependent Variance Inflation Factor cutoff values. *Quality Engineering, 14*(3), 391–403. https://doi.org/10.1081/QEN-120001878

Czuba, J. A., Foufoula-Georgiou, E. (2015). Dynamic connectivity in a fluvial network for identifying hotspots of geomorphic change. *Water Resources Research*, *51*(3), 1401–1421. DOI: 10.1002/2014WR016139

d'Andrea M, Snodgrass W, Chessie P. (2004). City of Toronto wet weather flow management master plan. In: J. Marsalek, D. Sztruhar, M. Giulianelli, B. Urbonas (Eds.) *Enhancing urban environment by environmental upgrading and restoration* (vol. 43). Nato Science Series: IV: Earth and Environmental Sciences, Springer, Dordrecht.

Diaz-Redondo, M., Egger, G., Marchamalo, M., Damm, C., de Oliveira, R. P., Schmitt, L. (2018). Targeting lateral connectivity and morphodynamics in a large river-floodplain system: The upper Rhine River. *River Research and Applications*, *34*(7), 734–744. DOI: 10.1002/rra.3287

Downs, P. W., Bithell, C., Keele, V. E., Gilvear, D. J. (2016). Dispersal of augmented gravel in a steep, boulder-bedded reach: Early implications for restoring salmonid habitat (pp. 380–387). *11th International Symposium on Ecohydraulics (ISE 2016)*. Barton, ACT: Engineers Australia.

Downs, P. W., Dusterhoff, S. R., Leverich, G. T., Soar, P. J., Napolitano, M. B. (2018). Fluvial system dynamics derived from distributed sediment budgets: Perspectives from an uncertainty-bounded application. *Earth Surface Processes and Landforms, 43*(6), 1335–1354. DOI: 10.1002/esp.4319

Downs, P. W., Piégay, H. (2019). Catchment-scale cumulative impact of human activities on river channels in the late Anthropocene: Implications, limitations, prospect. *Geomorphology*, *338*, 88–104. DOI: 10.1016/j.geomorph.2019.03.021

Doyle, M. W., Harbor, J. M., Rich, C. F., Spacie, A. (2000). Examining the effects of urbanization on streams using indicators of geomorphic stability. *Physical Geography*, *21*(2), 155–181.

Dufour, S., Piégay, H. (2009). From the myth of a lost paradise to targeted river restoration: forget natural references and focus on human benefits. *River Research and Applications*, *25*(5), 568–581. DOI: 10.1002/rra.1239

Dziadak, K., Kumar, B., Sommerville, J. (2009). Model for the 3D location of buried assets based on RFID Technology. *Journal of Computing in Civil Engineering*, *23*(3), 148–159. DOI: 10.1061/(ASCE)0887-3801(2009)23:3(148)

Eaton, B. C., Church, M. (2011). A rational sediment transport scaling relation based on dimensionless stream power. *Earth Surface Processes and Landforms*, *36*(7), 901–910. DOI: 10.1002/esp.2120

Eaton, B., Hassan, M., Phillips, J. C. (2008). A method for using magnetic tracer stones to monitor changes in stream channel dynamics. *Streamline*, *12*(1), 22–27. DOI: 10.1002/hyp.10232/full

Ebisa Fola, M., Rennie, C. D. (2010). Downstream hydraulic geometry of clay-dominated cohesive bed rivers. *Journal of Hydraulic Engineering*, *136*(8), 524–527. DOI: 10.1061/(ASCE)HY.1943-7900.0000199

Egiazaroff, I. V. (1965). Calculation of nonuniform sediment concentrations. *Journal of Hydraulic Division - American Society of Civil Engineers, 91*(4), 225–247.

Einstein, H. A. (1950). The bed-load function for sediment transportation in open channel flows. *United States Department of Agriculture Soil Conservation Service Techical Bulletin*, *1026*.

Elgueta-Astaburuaga, M. A., Hassan, M. A., Saletti, M., Clarke, G. K. C. (2018). The effect of episodic sediment supply on bedload variability and sediment mobility. *Water Resources Research*, *74*(6), 11302. DOI: 10.1029/2017WR022280

Elosegi, A., Diez, J., Mutz, M. (2010). Effects of hydromorphological integrity on biodiversity and functioning of river ecosystems. *Hydrobiologia*, *657*(1), 199–215. DOI: 10.1007/s10750-009-0083-4

Ferguson, R. (2007). Flow resistance equations for gravel- and boulder-bed streams. *Water Resources Research*, *43*(5). DOI: 10.1029/2006WR005422

Ferguson, R. I. (2005). Estimating critical stream power for bedload transport calculations in gravel-bed rivers. *Geomorphology*, *70*, 33–41. DOI: 10.1016/j.geomorph.2005.03.009

Ferguson, R. I., Hoey, T. B. (2002). Long-term slowdown of river tracer pebbles: Generic models and implications for interpreting short-term tracer studies. *Water Resources Research*, *38*(8), 1142. DOI: 10.1029/2001WR000637

Ferguson, R. I., Wathen, S. J. (1998). Tracer-pebble movement along a concave river profile: Virtual velocity in relation to grain size and shear stress. *Water Resources Research*, *34*(8), 2031–2038. DOI: 10.1029/98WR01283

Ferguson, R. I., Bloomer, D. J., Hoey, T. B., Werritty, A. (2002). Mobility of river tracer pebbles over different timescales. *Water Resources Research*, *38*(5), 3–1–3–8. DOI: 10.1029/2001WR000254

Formann, E., Egger, G., Hauer, C., Habersack, H. (2014). Dynamic disturbance regime approach in river restoration: Concept development and application. *Landscape and Ecological Engineering*, *10*(2), 323–337. DOI: 10.1007/s11355-013-0228-5

Fremion, F., Bordas, F., Mourier, B., Lenain, J.-F., Kestens, T., Courtin-Nomade, A. (2016). Influence of dams on sediment continuity: A study case of a natural metallic contamination. *Science of the Total Environment*, *547*, 282–294. DOI: 10.1016/j.scitotenv.2016.01.023

Frings, R. M., Maass, A.L. (2018). Sediment continuity as a guiding principle for river basin management - are we on the right track? *Hydrologie Und Wasserbewirtschaftung*, *62*(4), 257–270. DOI: 10.5675/HyWa_2018,4_3

Galster, J. C., Pazzaglia, F. J., Germanoski, D. (2008). Measuring the impact of urbanization on channel widths using historic aerial photographs and modern surveys. *JAWRA Journal of the American Water Resources Association*, *44*(4), 948–960. DOI: 10.1111/j.1752-1688.2008.00193.x

Ganti, V., Meerschaert, M. M., Foufoula-Georgiou, E., Viparelli, E., Parker, G. (2010). Normal and anomalous diffusion of gravel tracer particles in rivers. *Journal of Geophysical Research*, *115*(F2), F00A12. DOI: 10.1029/2008JF001222

Gintz, D., Hassan, M. A., Schmidt, K. H. (1996). Frequency and magnitude of bedload transport in a mountain river. *Earth Surface Processes and Landforms*, *21*(5), 433–445. DOI: 10.1002/(SICI)1096-9837(199605)21:5<433::AID-ESP580>3.0.CO;2-P

Grabowski, R. C., Surian, N., Gurnell, A. M. (2014). Characterizing geomorphological change to support sustainable river restoration and management. *Wiley Interdisciplinary Reviews-Water*, *1*(5), 483–512. DOI: 10.1002/wat2.1037

Gregory, K. J., Davis, R. J., Downs, P. W. (1992). Identification of river channel change to due to urbanization. *Applied Geography*, *12*(4), 299–318.

Gurnell, A. M., Corenblit, D., Garcia De Jalon, D., Gonzalez Del Tanago, M., Grabowski, R. C., O'Hare, M. T., Szewczyk, M. (2016). A conceptual model of vegetation-hydrogeomorphology interactions within River corridors. *River Research and Applications*, *32*(2), 142–163. DOI: 10.1002/rra.2928

Habersack, H. M. (2001). Radio-tracking gravel particles in a large braided river in New Zealand: A field test of the stochastic theory of bed load transport proposed by Einstein. *Hydrological Processes*, *15*(3), 377–391. DOI: 10.1002/hyp.147

Habersack, H., Hein, T., Stanica, A., Liska, I., Mair, R., Jaeger, E., et al. (2016). Challenges of river basin management: Current status of, and prospects for, the River Danube from a river engineering perspective. *Science of the Total Environment*, *543*(Part A), 828–845. DOI: 10.1016/j.scitotenv.2015.10.123

Hammer, T. R. (1972). Stream channel enlargement due to urbanization. *Water Resources Research*, *8*(6), 1530–1540.

Haschenburger, J. K. (2011). The rate of fluvial gravel dispersion. *Geophysical Research Letters*, *38*(24), L24403. DOI: 10.1029/2011GL049928

Haschenburger, J. K. (2013). Tracing river gravels: Insights into dispersion from a long-term field experiment. *Geomorphology*, *200*, 121–131. DOI: 10.1016/j.geomorph.2013.03.033

Haschenburger, J. K., Church, M. (1998). Bed material transport estimated from the virtual velocity of sediment. *Earth Surface Processes and Landforms*, *23*(9), 791–808. DOI: 10.1002/(SICI)1096-9837(199809)23:9<791::AID-ESP888>3.0.CO;2-X

Haschenburger, J. K., Wilcock, P. R. (2003). Partial transport in a natural gravel bed channel. *Water Resources Research*, *39*(1), 1020. DOI: 10.1029/2002WR001532

Hassan, M. A. (1992). Structural controls of the mobility of coarse material in gravel-bed channels. *Israel Journal of Earth-Sciences*, *41*(2-4), 105–122.

Hassan, M. A., Bradley, D. N. (2017). Geomorphic controls on tracer particle dispersion in gravel-bed rivers. In D. Tsutsumi, J. Laronne (Eds.), *Gravel-Bed Rivers: Processes and Disasters* (pp. 159-184). Chichester, UK: Wiley-Blackwell.

Hassan, M. A., Ergenzinger, P. (2005). Use of tracers in fluvial geomorphology. In H. Piégay G. M. Kondolf (Eds.), *Tools in Fluvial Geomorphology*. Chichester, UK: John Wiley Sons.

Hassan, M. A., Church, M., Ashworth, P. J. (1992). Virtual rate and mean distance of travel of individual clasts in gravel-bed channels. *Earth Surface Processes and Landforms*, *17*(6), 617–627. DOI: 10.1002/esp.3290170607

Hassan, M. A., Church, M., Schick, A. P. (1991). Distance of movement of coarse particles in gravel bed streams. *Water Resources Research*, *27*(4), 503–511. DOI: 10.1029/90WR02762

Hassan, M. A., Church, M., Lisle, T. E., Brardinoni, F., Benda, L. (2005). Sediment transport and channel morphology of small, forested streams. *JAWRA Journal of the American Water Resources Association*, *41*(4), 853–876. DOI: 10.1111/j.1752-1688.2005.tb03774.x

Hassan, M., Voepel, H., Schumer, R., Parker, G., Fraccarollo, L. (2013). Displacement characteristics of coarse fluvial bed sediment. *Journal of Geophysical Research: Earth Surface*, *118*(1), 155–165. DOI: 10.1029/2012JF002374

Hawley, R. J., Bledsoe, B. P. (2013). Channel enlargement in semiarid suburbanizing watersheds: A southern California case study. *Journal of Hydrology*, *496*, 17–30.

Hawley, R. J., Vietz, G. J. (2016). Addressing the urban stream disturbance regime. *Freshwater Science, 35*, 278–292. DOI: 10.1086/684647

Hawley, R. J., MacMannis, K. R., Wooten, M. S. (2013). Bed coarsening, riffle shortening, and channel enlargement in urbanizing watersheds, northern Kentucky, USA. *Geomorphology*, *201*, 111–126. DOI: 10.1016/j.geomorph.2013.06.013

Heckmann, T., Cavalli, M., Cerdan, O., Foerster, S., Javaux, M., Lode, E., et al. (2018). Indices of sediment connectivity: Opportunities, challenges and limitations. *Earth-Science Reviews*, *187*, 77–108. DOI: 10.1016/j.earscirev.2018.08.004

Henshaw, P. C., Booth, D. B. (2000). Natural restabilization of stream channels in urban watersheds. *Journal of the American Water Resources Association*, *36*(6), 1219–1236. DOI: 10.1111/j.1752-1688.2000.tb05722.x

Heritage, G. L., Milan, D. J., Large, A. R. G., Fuller, I. C. (2009). Influence of survey strategy and interpolation model on DEM quality. *Geomorphology*, *112*, 334–344. DOI: 10.1016/j.geomorph.2009.06.024

Hill, K. M., DellAngelo, L., Meerschaert, M. M. (2010). Heavy-tailed travel distance in gravel bed transport: An exploratory enquiry. *Journal of Geophysical Research: Earth Surface*, *115*, F00A14. DOI: 10.1029/2009JF001276

Hodge, R. A., Hoey, T. B., Sklar, L. S. (2011). Bed load transport in bedrock rivers: The role of sediment cover in grain entrainment, translation, and deposition. *Journal of Geophysical Research*, *116*(F4), F04028. DOI: 10.1029/2011JF002032

Hollis, G. E. (1975). The effect of urbanization on floods of different recurrence interval. *Water Resources Research*, *11*(3), 431–435. DOI: 10.1029/WR011i003p00431

Hooke, J. (2003). Coarse sediment connectivity in river channel systems: A conceptual framework and methodology. *Geomorphology*, *56*, 79–94. DOI: 10.1016/S0169-555X(03)00047-3

Houbrechts, G., Levecq, Y., Peeters, A., Hallot, E., Van Campenhout, J., Denis, A. C., Petit, F. (2015). Evaluation of long-term bedload virtual velocity in gravel-bed rivers (Ardenne, Belgium). *Geomorphology*, *251*, 6–19. DOI: 10.1016/j.geomorph.2015.05.012

Hubbell, D. W., Sayre, W. W. (1964). Sand transport studies with radioactive tracers. *Journal of the Hydraulics Division – American Society of Civil Engineers, 90*(3), 39-68.

Hufnagel, J., MacVicar, B. (2017). Design and performance of a radio frequency identification scanning system for sediment tracking in a purpose-built experimental channel. *Journal of Hydraulic Engineering*, *144*(2). DOI: 10.1061/(ASCE)HY.1943-7900.0001412

Humphries, R., Venditti, J. G., Sklar, L. S., Wooster, J. K. (2012). Experimental evidence for the effect of hydrographs on sediment pulse dynamics in gravel-bedded rivers. *Water Resources Research*, *48*(1), W01533. DOI: 10.1029/2011WR010419

Jordan, B. A., Annable, W. K., Watson, C. C., Sen, D. (2010). Contrasting stream stability characteristics in adjacent urban watersheds: Santa Clara Valley, California. *River Research and Applications*, *26*(10), 1281–1297. DOI: 10.1002/rra.1333

Jowett, I. G. (2003). Hydraulic constraints on habitat suitability for benthic invertebrates in gravel-bed rivers. *River Research and Applications*, *19*(5-6), 495–507. DOI: 10.1002/rra.734

Julien, P. Y. (2002). *River Mechanics*. Cambridge University Press, Cambridge, UK.

Kasprak, A., Wheaton, J. M., Ashmore, P. E., Hensleigh, J. W., Peirce, S. (2015). The relationship between particle travel distance and channel morphology: Results from physical models of braided rivers. *Journal of Geophysical Research: Earth Surface*, *120*(1), 55–74. DOI: 10.1002/2014JF003310

Keller, E. A., Melhorn, W. N. (1978). Rhythmic spacing and origin of pools and riffles. *Geological Society of America Bulletin*, *89*(5), 723–730. DOI: 10.1130/0016-7606(1978)89<723:RSAOOP>2.0.CO;2

Khosronejad, A., Hill, C., Kang, S., Sotiropoulos, F. (2013). Computational and experimental investigation of scour past laboratory models of stream restoration rock structures. *Advances in Water Resources*, *54*, 191–207. DOI: 10.1016/j.advwatres.2013.01.008

Khosronejad, A., Kozarek, J. L., Sotiropoulos, F. (2014). Simulation-based approach for stream restoration structure design: Model development and validation. *Journal of Hydraulic Engineering*, *140*(9). DOI: 10.1061/(ASCE)HY.1943-7900.0000904

Klösch, M., Habersack, H. (2017). Deriving formulas for an unsteady virtual velocity of bedload tracers. *Earth Surface Processes and Landforms, 43*(7). DOI: 10.1002/esp.4326

Kondolf, G. M., Boulton, A. J., O'Daniel, S., Poole, G. C., Rachel, F. J., Stanley, E. H., et al. (2006). Process-based ecological river restoration: Visualizing three-dimensional connectivity and dynamic vectors to recover lost linkages. *Ecology and Society*, *11*(2). DOI: 10.5751/ES-01747-110205

Konrad, C. P., Booth, D. B., Burges, S. J. (2005). Effects of urban development in the Puget Lowland, Washington, on interannual streamflow patterns: Consequences for channel form and streambed disturbance. *Water Resources Research*, *41*(7), W07009. DOI: 10.1029/2005WR004097

Krapesch, G., Tritthart, M., Habersack, H. (2009). A model-based analysis of meander restoration. *River Research and Applications*, *25*(5), 593–606. DOI: 10.1002/rra.1236

Ladson, A. R., Walsh, C. J., Fletcher, T. D. (2006). Improving stream health in urban areas by reducing runoff frequency from impervious surfaces. *Australian Journal of Water Resources*, *10*(1), 23–34. DOI: 10.1080/13241583.2006.11465279

Lague, D. (2014). The stream power river incision model: Evidence, theory and beyond. *Earth Surface Processes and Landforms*, *39*(1), 38–61. DOI: 10.1002/esp.3462

Lamarre, H., Roy, A. G. (2008). The role of morphology on the displacement of particles in a step–pool river system. *Geomorphology*, *99*, 270–279. DOI: 10.1016/j.geomorph.2007.11.005

Lamarre, H., MacVicar, B., Roy, A. G. (2005). Using passive integrated transponder (PIT) tags to investigate sediment transport in gravel-bed rivers. *Journal of Sedimentary Research*, *75*(736-741). DOI: 10.2110/jsr.2005.059

Lane, E. W. (1955). Importance of fluvial morphology in hydraulic engineering (vol. 81). *Proceedings of the American Society of Civil Engineers, 81*(7), 1–71.

Laronne, J. B., Carson, M. A. (1976). Interrelationships between bed morphology and bed-material transport for a small, gravel-bed channel. *Sedimentology*, *23*(1), 67–85. DOI: 10.1111/j.1365-3091.1976.tb00039.x

Lauth, T. J., Papanicolaou, A. N. (2009). Application of radio frequency tracers to individual and group particle displacement within a laboratory (vol. 342, pp. 2264–2271). *Proceedings of World Environmental and Water Resources Congress 2009: Great Rivers*. Kansas City, MO: American Society of Civil Engineers. DOI: 10.1061/41036(342)225

Lenzi, M. A. (2004). Displacement and transport of marked pebbles, cobbles and boulders during floods in a steep mountain stream. *Hydrological Processes*, *18*(10), 1899–1914. DOI: 10.1002/hyp.1456

Leopold, L. B. (1956). Land use and sediment yield (pp. 639–647). *Proceedings of Man's role in changing the face of the Earth: Second annual Wenner-Gren Symposium*. Chicago, IL: University of Chicago Press.

Leopold, L. B. (1968). Hydrology for urban land planning - A guidebook on the hydrologic effects of urban land use. In *Geological Survey Circular 554*. Washington, DC: United States Department of the Interior. DOI: 10.1007/978-3-662-24715-0

Leopold, L. B., Wolman, M. G., Miller, J. P. (1964). *Fluvial processes in geomorphology*. San Francisco, CA: WH Freeman and Co.

Li, C., Fletcher, T. D., Duncan, H. P., Burns, M. J. (2017). Can stormwater control measures restore altered urban flow regimes at the catchment scale? *Journal of Hydrology*, *549*, 631–653. DOI: 10.1016/j.jhydrol.2017.03.037

Liedermann, M., Gmeiner, P., Kreisler, A., Tritthart, M., Habersack, H. (2018). Insights into bedload transport processes of a large regulated gravel-bed river. *Earth Surface Processes and Landforms*, *43*(2), 514–523. DOI: 10.1002/esp.4253

Liedermann, M., Tritthart, M., Habersack, H. (2013). Particle path characteristics at the large gravel-bed river Danube: Results from a tracer study and numerical modelling. *Earth Surface Processes and Landforms*, *38*(5), 512–522. DOI: 10.1002/esp.3338

Liébault, F., Bellot, H., Chapuis, M., Klotz, S., Deschâtres, M. (2012). Bedload tracing in a high-sediment-load mountain stream. *Earth Surface Processes and Landforms*, *37*(4), 385–399. DOI: 10.1002/esp.2245

Little, W. C., Meyer, P. G. (1976). Stability of channel beds by armoring. *Journal of the Hydraulics Division-American Society of Civil Engineers*, *102*(11), 1647–1661.

Lub, B. G., Baker, D. W., Bledsoe, B. P., Palmer, M. A. (2012). Range of variability of channel complexity in urban, restored and forested reference streams. *Freshwater Biology*, *57*(5), 1076–1095. DOI: 10.1111/j.1365-2427.2012.02763.x

MacKenzie, L. G., Eaton, B. C. (2017). Large grains matter: contrasting bed stability and morphodynamics during two nearly identical experiments. *Earth Surface Processes and Landforms*, *42*(8), 1287–1295. DOI: 10.1002/esp.4122

MacKenzie, L. G., Eaton, B. C., Church, M. (2018). Breaking from the average: Why large grains matter in gravel-bed streams. *Earth Surface Processes and Landforms*, *43*(15), 3190–3196. DOI: 10.1002/esp.4465

Mackin, J. H. (1948). Concept of the graded river. *Geological Society of America Bulletin*, *59*(5), 463–511. DOI: 10.1130/0016-7606(1948)59[463:COTGR]2.0.CO;2

MacRae, C. R. (1991). *A procedure for the design of storage facilities for instream erosion control in urban streams* (PhD thesis). University of Ottawa, Ottawa, Canada.

MacRae, C. R. (1997). Experience from morphological research on Canadian streams: Is the control of the two-year frequency runoff event the best basis for stream channel protection? In L. A. Roesner (Ed.), *Effects of watershed development and management for aquatic ecosystems* (pp. 144–162). Reston, VA: American Society of Civil Engineers.

MacVicar, B. J., Roy, A. G. (2011). Sediment mobility in a forced riffle-pool. *Geomorphology*, *125*, 445–456. DOI: 10.1016/j.geomorph.2010.10.031

MacVicar, B., Chapuis, M., Buckrell, E., Roy, A. (2015). Assessing the performance of In-stream restoration projects using Radio Frequency Identification (RFID) transponders. *Water*, *7*(10), 5566–5591. DOI: 10.3390/w7105566

MacWilliams, M. L. J., Tompkins, M. R., Street, R. L., Kondolf, G. M., Kitanidis, P. K. (2010). Assessment of the effectiveness of a constructed compound channel river restoration project on an incised stream. *Journal of Hydraulic Engineering*, *136*(12), 1042–1052. DOI: 10.1061/(ASCE)HY.1943-7900.0000196

Mao, L., Picco, L., Lenzi, M. A., Surian, N. (2017). Bed material transport estimate in large gravel-bed rivers using the virtual velocity approach. *Earth Surface Processes and Landforms*, *42*(2), 595–611. DOI: 10.1002/esp.4000

Masteller, C.C., Finnegan, N. J., Turowski, J. M., Yager, E. M., Rickenmann, D. (2019). History-dependent threshold for motion revealed by continuous bedload transport measurements in a steep mountain stream. *Geophysical Research Letters, 46*(5), 2583–2591. DOI: 10.1029/2018GL081325

McClintock, K., Harbor, J. M. (2013). Modeling potential impacts of land development on sediment yields. *Physical Geography*, *16*(5), 359–370.

McCuen, R. H., Molgen, G. E. (1988). Multicriterion stormwater management methods. *Journal of Water Resources Planning and Management*, *114*(4), 414–431.

McMillan, S. K., Noe, G. B. (2017). Increasing floodplain connectivity through urban stream restoration increases nutrient and sediment retention. *Ecological Engineering*, *108*, 284–295. DOI: 10.1016/j.ecoleng.2017.08.006

Meyer-Peter, E., and R. Muller (1948), Formulas for bed-load transport (pp. 39-64). *Proceedings of the IAHSR 2nd Meeting*. Stockholm, Sweden: International Association of Hydraulic Research.

Meyer, J. L., Paul, M. J., Taulbee, W. K. (2005). Stream ecosystem function in urbanizing landscapes. *Journal of the North American Benthological Society*, *24*(3), 602–612. DOI: 10.1899/04-021.1

Milan, D. J. (2013a). Sediment routing hypothesis for pool-riffle maintenance. *Earth Surface Processes and Landforms*, *38*(14), 1623–1641. DOI: 10.1002/esp.3395

Milan, D. J. (2013b). Virtual velocity of tracers in a gravel-bed river using size-based competence duration. *Geomorphology*, *198*, 107–114. DOI: 10.1016/j.geomorph.2013.05.018

Miller, J. R., Kochel, R. C. (2009). Assessment of channel dynamics, in-stream structures and post-project channel adjustments in North Carolina and its implications to effective stream restoration. *Environmental Earth Sciences*, *59*(8), 1681–1692. DOI: 10.1007/s12665-009-0150-1

Miwa, H., Parker, G. (2017). Effects of sand content on initial gravel motion in gravel-bed rivers. *Earth Surface Processes and Landforms*, *42*(9), 1355–1364. DOI: 10.1002/esp.4119

Monsalve, A., Yager, E. M., Schmeeckle, M. W. (2017). Effects of bed forms and large protruding grains on near-bed flow hydraulics in low relative submergence conditions. *Journal of Geophysical Research: Earth Surface*, *122*(10), 1845–1866. DOI: 10.1002/2016JF004152

Montgomery, D. R., Buffington, J. M. (1997). Channel-reach morphology in mountain drainage basins. *Geological Society of America Bulletin*, *109*(5), 596–611. DOI: 10.1130/0016-7606(1997)109<0596:CRMIMD>2.3.CO;2

Morandi, B., Piégay, H., Lamouroux, N., Vaudor, L. (2014). How is success or failure in river restoration projects evaluated? Feedback from French restoration projects. *Journal of Environmental Management*, *137*, 178–188. http://dx.doi.org/10.1016/j.jenvman.2014.02.010

Muirhead, C. (2018). *Advances in river bedload tracking technology: Self-righting Radio Frequency Identification tracers and an in-stream automated station.* University of Waterloo, Waterloo, Canada. Retrieved from UW Space: http://hdl.handle.net/10012/13929

Nardini, A., Pavan, S. (2012). What river morphology after restoration? The methodology VALURI. *International Journal of River Basin Management*, *10*(1), 29–47. DOI: 10.1080/15715124.2011.640637

Nehrke, S. M., Roesner, L. A. (2004). Effects of design practice for flood control and best management practices on the flow-frequency curve. *Journal of Water Resources Planning and Management*, *130*(2), 131–139. DOI: 10.1061/(ASCE)0733-9496(2004)130:2(131)

Newson, M. D. (2002). Geomorphological concepts and tools for sustainable river ecosystem management. *Aquatic Conservation: Marine and Freshwater Ecosystems*, *12*(4), 365–379. DOI: 10.1002/aqc.532

Niezgoda, S. L., Johnson, P. A. (2005). Improving the urban stream restoration effort: Identifying critical form and processes relationships. *Environmental Management*, *35*(5), 579–592. DOI: 10.1007/s00267-004-0088-8

O'Driscoll, M. A., Soban, J. R., Lecce, S. A. (2009). Stream Channel Enlargement Response to Urban Land Cover in Small Coastal Plain Watersheds, North Carolina. *Physical Geography, 30*(6), 528-555. DOI: 10.2747/0272-3646.30.6.528

Olinde, L., Johnson, J. P. L. (2015). Using RFID and accelerometer-embedded tracers to measure probabilities of bed load transport, step lengths, and rest times in a mountain stream. *Water Resources Research*, *51*(9), 7572–7589. DOI: 10.1002/2014WR016120

Ontario Ministry of the Environment (MOE) (2003). *Stormwater Management Planning and Design Manual.* Toronto, Canada: Queen's Printer for Ontario.

Paintal, A. S. (1971). A stochastic model of bed load transport. *Journal of Hydraulic Research*, *9*(4), 527–554.

Palmer, M. A., Bernhardt, E. S. (2006). Hydroecology and river restoration: Ripe for research and synthesis. *Water Resources Research*, *42*(3). DOI: 10.1029/2005WR004354

Palmer, M. A., Bernhardt, E. S., Allan, J. D., Lake, P. S., Alexander, G., Brooks, S., Carr, J., Clayton, S., Dahm, C. N., Follstad Shah, J., Galat, D., L., Loss, S. G., Goodwin, P., Hart, D. D., Hassett, B., Jenkinson, R., Kondolf, G. M., Lave, R., Meyer, J. L., O'Donnell, T. K., Pagano, L., Sudduth, E. (2005). Standards for ecologically successful river restoration. *Journal of Applied Ecology*, *42*(2), 208–217. DOI: 10.1111/j.1365-2664.2005.01004.x

Palmer, M. A., Filoso, S., Fanelli, R. M. (2014). From ecosystems to ecosystem services: Stream restoration as ecological engineering. *Ecological Engineering*, *65*, 62–70.DOI: 10.1016/j.ecoleng.2013.07.059

Palmer, M. A., Menninger, H. L., Bernhardt, E. (2010). River restoration, habitat heterogeneity and biodiversity: A failure of theory or practice? *Freshwater Biology*, *55*(s1), 205–222. DOI: 10.1111/j.1365-2427.2009.02372.x

Papangelakis, E., Hassan, M. A. (2016). The role of channel morphology on the mobility and dispersion of bed sediment in a small gravel-bed stream. *Earth Surface Processes and Landforms*, *41*(15), 2191–2206. DOI: 10.1002/esp.3980

Papangelakis E., Muirhead C., Schneider A., MacVicar B. (2019). Synthetic Radio Frequency Identification tracer stones with weighted inner ball for burial depth estimation. *Journal of Hydraulic Engineering, 145*(12), 06019014. DOI: 10.1061/(ASCE)HY.1943-7900.0001650

Parish Geomorphic (2011). *TRCA Wilket Creek Emergency Works (Sites 6&7) – Technical Design Brief.*

Parker, G., Klingeman, P. C. (1982). On why gravel bed streams are paved. *Water Resources Research*, *18*(5), 1409–1423. DOI: 10.1029/WR018i005p01409

Parker, G., Toro-Escobar, C. M. (2002). Equal mobility of gravel in streams: The remains of the day. *Water Resources Research*, *38*(11), 461–468.DOI: 10.1029/2001WR000669

Parker, G., Paola, C., Leclair, S. (2000). Probabilistic Exner sediment continuity equation for mixtures with no active layer. *Journal of Hydraulic Engineering*, *126*(11), 818–826. DOI: 10.1061/(ASCE)0733-9429(2000)126:11(818)

Pasternack, G. B. (2013). Geomorphologist's guide to participating in river rehabilitation. In J. Shroder E. Wohl, (Eds.), *Treatise on Geomorphology* (vol. 9, pp. 843–860). Academic Press, San Diego, CA: Elsevier. DOI: 10.1016/B978-0-12-374739-6.00268-2

Paul, M. J., Meyer, J. L. (2001). Streams in the urban landscape. *Annual Review of Ecology and Systematics*, *32*, 333–365. DOI: 10.1007/978-0-387-73412-5_12

Petit, F. (1987). The relationship between sher-stress and the shaping of the bed of a pebble-loaded river Larulles Ardenne, *Catena, 14*(5), 453–468.

Phillips, C. B., Jerolmack, D. J. (2014). Dynamics and mechanics of tracer particles. *Earth Surface Dynamics Discussions*, *2*(1), 429–476. DOI: 10.5194/esurfd-2-429-2014

Phillips, C. B., Martin, R. L., Jerolmack, D. J. (2013). Impulse framework for unsteady flows reveals superdiffusive bed load transport. *Geophysical Research Letters*, *40*(7), 1328–1333. DOI: 10.1002/grl.50323

Phillips, R. T. J., Desloges, J. R. (2014). Glacially conditioned specific stream powers in low-relief river catchments of the southern Laurentian Great Lakes. *Geomorphology*, *206*, 271–287. DOI: 10.1016/j.geomorph.2013.09.030

Phillips, R. T. J., Desloges, J. R. (2015a). Alluvial floodplain classification by multivariate clustering and discriminant analysis for low- relief glacially conditioned river catchments. *Earth Surface Processes and Landforms, 40*(6), 756–770. DOI: 10.1002/esp.3681

Phillips, R. T. J., Desloges, J. R. (2015b). Glacial legacy effects on river landforms of the southern Laurentian Great Lakes. *Journal of Great Lakes Research, 41*(4), 951–964. DOI: 10.1016/j.jglr.2015.09.005

Pike, L., Gaskin, S., Ashmore, P. (2018). Flume tests on fluvial erosion mechanisms in till-bed channels. *Earth Surface Processes and Landforms*, *43*(1), 259–270. DOI: 10.1002/esp.4240

Pizzuto, J. E., Hession, W. C., McBride, M. (2000). Comparing gravel-bed rivers in paired urban and rural catchments of southeastern Pennsylvania. *Geology*, *28*(1), 79–82. DOI: 10.1130/0091-7613(2000)028<0079:CGRIPU>2.0.CO;2

Plumb, B. D., Annable, W. K., Thompson, P. J., Hassan, M. A. (2017). The impact of urbanization on temporal changes in sediment transport in a gravel-bed channel in Soutern Ontario, Canada. *Water Resources Research*, *53*(10), 8443–8458. DOI: 10.1002/2016WR020288

Poelman, J. Y., Hoitink, A. J. F., de Ruijsscher, T. V. (2019). Flow and bed morphology response to the introduction of wood logs for sediment management. *Advances in Water Resources*, *130*, 1–11. DOI: 10.1016/j.advwatres.2019.05.023

Poff, N. L., Bledsoe, B. P., Cuhaciyan, C. O. (2006). Hydrologic variation with land use across the contiguous United States: Geomorphic and ecological consequences for stream ecosystems. *Geomorphology*, *79*, 264–285. DOI: 10.1016/j.geomorph.2006.06.032

Pomeroy, C. A., Postel, N. A., O'Neill, P. A., Roesner, L. A. (2008). Development of storm-water management design criteria to maintain geomorphic stability in Kansas City Metropolitan Area streams. *Journal of Irrigation and Drainage Engineering*, *134*(5), 562–566. DOI: 10.1061/(ASCE)0733-9437(2008)134:5(562)

Poppe, M., Kail, J., Aroviita, J., Stelmaszczyk, M., Gielczewski, M., Muhar, S. (2016). Assessing restoration effects on hydromorphology in European mid-sized rivers by key hydromorphological parameters. *Hydrobiologia*, *769*(1), 21–40. DOI: 10.1007/s10750-015-2468-x

Pyrce, R. S., Ashmore, P. E. (2003a). Particle path length distributions in meandering gravel-bed streams: Results from physical models. *Earth Surface Processes and Landforms*, *28*(9), 951–966. DOI: 10.1002/esp.498

Pyrce, R. S., Ashmore, P. E. (2003b). The relation between particle path length distributions and channel morphology in gravel-bed streams: A synthesis. *Geomorphology*, *56*, 167–187. DOI: 10.1016/S0169-555X(03)00077-1

Pyrce, R. S., Ashmore, P. E. (2005). Bedload path length and point bar development in gravel-bed river models. *Sedimentology*, *52*(4), 839–857. DOI: 10.1111/j.1365-3091.2005.00714.x

Raso, T. (2017). *The impacts of stormwater management on hydromodification and bedload sediment transport in a gravel-bed Stream* (Master's thesis). University of Waterloo, Waterloo, Canada. Retrieved from UW Space: http://hdl.handle.net/10012/12489

Reid, I., Frostick, L. E., Layman, J. T. (1985). The incidence and nature of bedload transport during flood flows in coarse-grained alluvial channels. *Earth Surface Processes and Landforms*, *10*(1), 33–44. DOI: 10.1002/esp.3290100107

Reid, I. Laronne, J. B. (1995). Bed load sediment transport in an ephemeral stream and a comparison with seasonal and perennial counterparts. *Water Resources Research*, *31*(3), 773–781. https://doi.org/10.1029/94WR02233

Rempel, L. L., Richardson, J. S., Healey, M. C. (2000). Macroinvertebrate community structure along gradients of hydraulic and sedimentary conditions in a large gravel-bed river. *Freshwater Biology*, *45*(1), 57–73. DOI: 10.1046/j.1365-2427.2000.00617.x

Rice, S. P., Greenwood, M. T., Joyce, C. B. (2001). Macroinvertebrate community changes at coarse sediment recruitment points along two gravel bed rivers. *Water Resources Research*, *37*(11), 2793–2803. DOI: 10.1029/2000WR000079

Rinaldi, M., Wyżga, B., Surian, N. (2005). Sediment mining in alluvial channels: physical effects and management perspectives. *River Research and Applications*, *21*(7), 805–828.DOI: 10.1002/rra.884

Rohrer, C. A., Roesner, L. A. (2006). Matching the critical portion of the flow duration curve to minimise changes in modelled excess shear. *Water Science and Technology*, *54*(6-7), 347–354. DOI: 10.2166/wst.2006.590

Roley, S. S., Tank, J. L., Griffiths, N. A., Hall, R. O. J., Davis, R. T. (2014). The influence of floodplain restoration on whole-stream metabolism in an agricultural stream: Insights from a 5-year continuous data set. *Freshwater Science*, *33*(4), 1043–1059. DOI: 10.1086/677767

Rollet, A. J., Piégay, H., Dufour, S., Bornette, G., Persat, H. (2014). Assessment of consequences of sediment deficit on a gravel river bed downstream of dams in restoration perspectives: Applications of a multicriteria, heirarchical and spatially explicit diagnosis. *River Research and Applications*, *30*(8), 939–953. DOI: 10.1002/rra.2689

Roni, P., Beechie, T. J., Bilby, R. E., Leonetti, F. E., Pollock, M. M., Pess, G. R. (2002). A review of stream restoration techniques and a hierarchical strategy for prioritizing restoration in Pacific northwest watersheds. *North American Journal of Fisheries Management*, *22*(1), 1–20. DOI: 10.1577/1548-8675(2002)022<0001:AROSRT>2.0.CO;2

Roni, P., Hanson, K., Beechie, T. (2008). Global review of the physical and biological effectiveness of stream habitat rehabilitation techniques. *North American Journal of Fisheries Management*, *28*(3), 856–890. DOI: 10.1577/M06-169.1

Rosgen, D. L., 1996. *Applied River Morphology*. Pagosa Springs, CO: Wildland Hydrology.

Russell, K. L., Vietz, G. J., Fletcher, T. D. (2017). Global sediment yields from urban and urbanizing watersheds. *Earth-Science Reviews*, *168*, 73–80. DOI: 10.1016/j.earscirev.2017.04.001

Russell, K. L., Vietz, G. J., Fletcher, T. D. (2018). Urban catchment runoff increases bedload sediment yield and particle size in stream channels. *Anthropocene*, *23*, 53–66. DOI: 10.1016/j.ancene.2018.09.001

Sapra, R.L. (2014). Using R^2 with caution. *Current Medicine Research and Practice, 4*(3), 130-134. https://doi.org/10.1016/j.cmrp.2014.06.002

Sarriquet, P. E., Bordenave, P., Marmonier, P. (2007). Effects of bottom sediment restoration on interstitial habitat characteristics and benthic macroinvertebrate assemblages in a headwater stream. *River Research and Applications*, *23*(8), 815–828. DOI: 10.1002/rra.1013

Schneider, J. M., Turowski, J. M., Rickenmann, D., Hegglin, R., Arrigo, S., Mao, L., Kirchner, J. W. (2014). Scaling relationships between bed load volumes, transport distances, and stream power in steep mountain channels. *Journal of Geophysical Research: Earth Surface*, *119*(3), 533–549. DOI: 10.1002/2013JF002874

Schumm, S. A. (1977). *The fluvial system.* New York, NY: John Wiley Sons.

Schumm, S. A., Harvey, M. D., Watson, C. C. (1984). *Incised channels: Morphology, dynamics and control*. Littleton, CO: Water Resources Publications.

Schwartz, J. S., Niezgoda, S. L., Slate, L. O., Carpenter, D. D., Annable, W. K., Wynn, T. M., et al. (2009). A monitoring and assessment framework to evaluate stream restoration needs in urbanizing watersheds (pp. 1–11). *Proceedings of World Environmental and Water Resources Congress 2009: Great Rivers*. Kansas City, MO: American Society of Civil Engineers.

Schwindt, S., Pasternack, G. B., Bratovich, P. M., Rabone, G., Simodynes, D. (2019). Hydro-morphological parameters generate lifespan maps for stream restoration management. *Journal of Environmental Management*, *232*, 475–489. DOI: 10.1016/j.jenvman.2018.11.010

Sear, D. A. (1994). River restoration and geomorphology. *Aquatic Conservation: Marine and Freshwater Ecosystems*, *4*(2), 169–177. DOI: 10.1002/aqc.3270040207

Sear, D. A. (1996). Sediment transport processes in pool-riffle sequences. *Earth Surface Processes and Landforms*, *21*(3), 241–262. DOI: 10.1002/(SICI)1096-9837(199603)21:3<241::AID-ESP623>3.0.CO;2-1

Segura, C., Booth, D. B. (2010). Effects of geomorphic setting and urbanization on wood, pools, sediment storage, and bank erosion in Puget Sound streams. *JAWRA Journal of the American Water Resources Association*, *46*(5), 972–986. DOI: 10.1111/j.1752-1688.2010.00470.x

Sharpe, D. A., Barnett P. J., Brennand, T. A., Finley, D., Gorrell, G., Russell, H. A. J., Stacey, P. (1997). Surficial geology of the Greater Toronto Area and Oak Ridges Moraine area. Canada Geological Society: Southern Ontario Open File 3062.

Shields, A. (1936). Anwendung der Aehnlichkeitsmechaniuknd der Turbu-lenzforschung auf die Geschiebebewegun. Mitteilungen der Preussischen Versuchsanstalt fur Wasserbau und Schiffbau, Berlin. (English translation by W. P. Ott and J. C. van Uchelen), U.S. Department of Agriculture, Soil Conservation Service Cooperative Laboratory, California Institute of Technology, Pasadena, California.

Shields, F. D. J. (2009). Do we know enough about controlling sediment to mitigate damage to stream ecosystems? *Ecological Engineering*, *35*(12), 1727–1733. DOI: 10.1016/j.ecoleng.2009.07.004

Shields, F. D., Copeland, R. R., Klingeman, P. C., Doyle, M. W., Simon, A. (2003). Design for stream restoration. *Journal of Hydraulic Engineering*, *129*(8), 575–584. DOI: 10.1061/(ASCE)0733-9429(2003)129:8(575)

Simon, A. (1989). A model of channel response in disturbed alluvial channels. *Earth Surface Processes and Landforms, 14*(1), 11–26. DOI: 10.1002/esp.3290140103

Simon, A., Darby, S. E. (2002). Effectiveness of grade-control structures in reducing erosion along incised river channels: the case of Hotophia Creek, Mississippi. *Geomorphology*, *42*, 229–254. DOI: 10.1016/S0169-555X(01)00088-5

Simon, A., Hupp, C. R. (1986). Channel widening characteristics and bank slope development along a reach of Cane Creek, west Tennessee. *US Geological Survey Water Supply Paper*, *2290*, 113–126.

Simon, A., Rinaldi, M. (2006). Disturbance, stream incision, and channel evolution: The roles of excess transport capacity and boundary materials in controlling channel response. *Geomorphology*, *79*, 361–383. DOI: 10.1016/j.geomorph.2006.06.037

Sindelar, C., Schobesberger, J., Habersack, H. (2017). Effects of weir height and reservoir widening on sediment continuity at run-of-river hydropower plants in gravel bed rivers. *Geomorphology*, *291*, 106–115. DOI: 10.1016/j.geomorph.2016.07.007

Sklar, L. S., Fadde, J., Venditti, J. G., Nelson, P., Wydzga, M. A., Cui, Y., Dietrich, W. E. (2009). Translation and dispersion of sediment pulses in flume experiments simulating gravel augmentation below dams. *Water Resources Research, 45*(8), W08439. DOI: 10.1029/2008WR007346

Solari, L., Parker, G. (2000). The curious case of mobility reversal in sediment mixtures. *Journal of Hydraulic Engineering*, *126*(3), 185–197. https://doi.org/10.1061/(ASCE)0733-9429(2000)126:3(185)

Surian, N., Ziliani, L., Comiti, F., Lenzi, M. A., Mao, L. (2009). Channel adjustments and alteration of sediment fluxes in gravel-bed rivers of North-Eastern Italy: Potentials and limitations for channel recovery. *River Research and Applications*, *25*(5), 551–567. DOI: 10.1002/rra.1231

Thayer, J. B., Ashmore, P. (2016). Floodplain morphology, sedimentology, and development processes of a partially alluvial channel. *Geomorphology*, *269*, 160–174. DOI: 10.1016/j.geomorph.2016.06.040

Thayer, J. B., Phillips, R. T. J., Desloges, J. R. (2016). Downstream channel adjustment in a low-relief, glacially conditioned watershed. *Geomorphology*, *262*, 101–111. DOI: 10.1016/j.geomorph.2016.03.019

Thompson, D. M. (2002). Long-term effect of instream habitat-improvement structures on channel morphology along the Blackledge and Salmon rivers, Connecticut, USA. *Environmental Management*, *29*(2), 250–265. DOI: 10.1007/s00267-001-0069-0

Thompson, D. M., Wohl, E. E., Jarrett, R. D. (1996). Revised velocity-reversal and sediment-sorting model for a high-gradient, pool-riffle stream. *Physical Geography*, *17*(2), 142–156. DOI: 10.1080/02723646.1996.10642578

Thorp, J. H., Thoms, M. C., Delong, M. D. (2006). The riverine ecosystem synthesis: Biocomplexity in river networks across space and time. *River Research and Applications*, *22*(2), 123–147. DOI:10.1002 /rra.901

Tillinghast, E. D., Hunt, W. F., Jennings, G. D. (2011). Stormwater control measure (SCM) design standards to limit stream erosion for Piedmont North Carolina. *Journal of Hydrology*, *411*(3-4), 185–196. DOI: 10.1016/j.jhydrol.2011.09.027

Tillinghast, E. D., Hunt, W. F., Jennings, G. D., Jenning, D'Arconte, P. (2012). Increasing stream geomorphic stability using storm water control measured in a densely urbanized watershed. *Journal of Irrigation and Drainage Engineering*, *17*(12), 1381–1388. DOI: 10.1061/(ASCE)0733-9437(2008)134:5(562)

Toronto and Region Conservation Authority. (2015). *Wilket Creek Rehabilitation Project*. Retrieved from: https://trca.ca/conservation/erosion-risk-management/restore/wilket-creek-rehabilitation-project/

Trimble, S. W. (1997). Contribution of Stream Channel Erosion to Sediment Yield from an Urbanizing Watershed. *Science*, *278*(5342), 1442–1444. DOI: 10.1126/science.278.5342.1442

Trudeau, M. P., Richardson, M. (2015). Change in event-scale hydrologic response in two urbanizing watersheds of the Great Lakes St Lawrence Basin 1969-2010. *Journal of Hydrology*, *527*, 1174–1188. DOI: 10.1016/j.jhydrol.2015.04.031

Trudeau, M. P., Richardson, M. (2016). Empirical assessment of effects of urbanization on event flow hydrology in watersheds of Canada's Great Lakes-St Lawrence basin. *Journal of Hydrology*, *541*, 1456–1474. DOI: 10.1016/j.jhydrol.2016.08.051

Tsakiris, A. G., Papanicolaou, A. N. T., Moustakidis, I. V. D., Abban, B. K. (2015). Identification of the burial depth of Radio Frequency Identification transponders in riverine applications. *Journal of Hydraulic Engineering*, *141*(6), 04015007. DOI: 10.1061/(ASCE)HY.1943-7900.0001001

van den Berg, J. H. (1995). Prediction of alluvial channel pattern of perennial rivers. *Geomorphology*, *12*(4), 259–279. DOI: 10.1016/0169-555X(95)00014-V

Vaughan, I. P., Diamond, M., Gurnell, A. M., Hall, K. A., Jenkins, A., Milner, N. J., et al. (2009). Integrating ecology with hydromorphology: A priority for river science and management. *Aquatic Conservation: Marine and Freshwater Ecosystems*, *19*(1), 113–125. DOI: 10.1002/aqc.895

Vazquez-Tarrio, D., Batalla, R. J. (2019). Assessing controls on the displacement of tracers in gravel-bed rivers. *Water*, *11*(8), 1598. DOI: 10.3390/w11081598

Vazquez-Tarrio, D., Recking, A., Liébault, F., Tal, M., Menendez-Duarte, R. (2019). Particle transport in gravel-bed rivers: Revisiting passive tracer data. *Earth Surface Processes and Landforms*, *44*(1), 112–128. DOI: 10.1002/esp.4484

Venditti, J. G., Dietrich, W. E., Nelson, P. A., Wydzga, M. A., Fadde, J., Sklar, L. (2010). Effect of sediment pulse grain size on sediment transport rates and bed mobility in gravel bed rivers. *Journal of Geophysical Research: Earth Surface*, *115*(3), 43. DOI: 10.1029/2009JF001418

Vietz, G. J., Walsh, C. J., Fletcher, T. D. (2015). Urban hydrogeomorphology and the urban stream syndrome: Treating the symptoms and causes of geomorphic change. *Progress in Physical Geography*, *40*(3), 480–492. DOI: 10.1177/0309133315605048

Violin, C. R., Cada, P., Sudduth, E. B., Hassett, B. A., Penrose, D. L., Bernhardt, E. S. (2011). Effects of urbanization and urban stream restoration on the physical and biological structure of stream ecosystems. *Ecological Applications*, *21*(6), 1932–1949. DOI: 10.1890/10-1551.1

Walsh, C. J., Roy, A. H., Feminella, J. W., Cottingham, P. D., Groffman, P. M., Morgan, R. P., II. (2005). The urban stream syndrome: current knowledge and the search for a cure. *Journal of the American Benthological Society*, *24*(3), 706–723. DOI: 10.1899/04-028.1

Whipple, A. A., Viers, J. H. (2019). Coupling landscapes and river flows to restore highly modified rivers. *Water Resources Research*, *55*(6), 4512–4532. DOI: 10.1029/2018WR022783

Wilcock, P. R. (1988). Methods for estimating the critical shear-stress of individual fractions in mixed-size sediment. *Water Resources Research*, *24*(7), 1127–1135. DOI: 10.1029/WR024i007p01127

Wilcock, P. R. (1997). Entrainment, displacement and transport of tracer gravels. *Earth Surface Processes and Landforms*, *22*(12), 1125–1138. https://doi.org/10.1002/(SICI)1096-9837(199712)22:12<1125::AID-ESP811>3.0.CO;2-V

Wilcock, P. R. (2012). Stream restoration in gravel-bed rivers. In M. Church, P. M. Biron A. G. Roy (Eds.) *Gravel-Bed Rivers: Processes, Tools, Environments* (pp. 135–149). Chichester, UK: John Wiley Sons. DOI: 10.1002/9781119952497.ch12

Wilcock, P. R., Crowe, J. C. (2003). Surface-based transport model for mixed-size sediment. *Journal of Hydraulic Engineering*, *129*(2), 120–128. DOI: 10.1061/(ASCE)0733-9429(2003)129:2(120)

Wilcock, P. R., Kenworthy, S. T. (2002). A two-fraction model for the transport of sand/gravel mixtures. *Water Resources Research*, *38*(10), 1194. DOI: 10.1029/2001WR000684

Wilcock, P. R., McArdell, B. W. (1993). Surface-based fractional transport rates: Mobilization thresholds and partial transport of a sand-gravel sediment. *Water Resources Research*, *29*(4), 1297–1312. DOI: 10.1029/92WR02748

Wilcock, P. R., McArdell, B. W. (1997). Partial transport of a sand/gravel sediment. *Water Resources Research*, *33*(1), 235–245. DOI: 10.1029/96WR02672

Wohl, E. (2017). Connectivity in rivers. *Progress in Physical Geography*, *41*(3), 345–362. DOI: 10.1177/0309133317714972

Wohl, E., Angermeier, P. L., Bledsoe, B., Kondolf, G. M., MacDonnell, L., Merritt, D. M., et al. (2005). River restoration. *Water Resources Research*, *41*(10), W10301. DOI: 10.1029/2005WR003985

Wohl, E., Bledsoe, B. P., Jacobson, R. B., Poff, N. L., Rathburn, S. L., Walters, D. M., Wilcox, A. C. (2015a). The natural sediment regime in rivers: Broadening the foundation for ecosystem management. *BioScience*, *65*(4), 358–371. DOI: 10.1093/biosci/biv002

Wohl, E., Lane, S. N., Wilcox, A. C. (2015b). The science and practice of river restoration. *Water Resources Research*, *51*(8), 5974–5997. DOI: 10.1002/2014WR016874

Wong, M., Parker, G. (2006). One-dimensional modeling of bed evolution in a gravel bed river subject to a cycled flood hydrograph. *Journal of Geophysical Research*, *111*(F3), F03018. DOI: 10.1029/2006JF000478

Wong, M., Parker, G., DeVries, P., Brown, T. M., Burges, S. J. (2007). Experiments on dispersion of tracer stones under lower-regime plane-bed equilibrium bed load transport. *Water Resources Research*, *43*(3), W03440. DOI: 10.1029/2006WR005172

Yager, E. M., Schott, H. E. (2013). The initiation of sediment motion and formation of armor layers. In J. Shroder E. Wohl (Eds.), *Treatise on Geomorphology* (vol. 9, pp. 87–102). Academic Press, San Diego, CA: Elsevier. DOI: 10.1016/B978-0-12-374739-6.00232-3

Yager, E. M., Schmeeckle, M. W., Badoux, A. (2018a). Resistance is not futile: Grain resistance controls on observed critical Shields stress variations. *Journal of Geophysical Research: Earth Surface*, *123*(12), 3308–3322. DOI: 10.1029/2018JF004817

Yager, E. M., Venditti, J. G., Smith, H. J., Schmeeckle, M. W. (2018b). The trouble with shear stress. *Geomorphology*, *323*, 41–50. DOI: 10.1016/j.geomorph.2018.09.008

Yoshimura, T., Shinya, H. (2018). Environmental impact assessment plan due to sediment sluicing at dams along Mimikawa river system. *Journal of Disaster Research*, *13*(4), 709–719. DOI: 10.20965/jdr.2018.p0709

Zuur, A. F., Ineo, E. N., Elphick, C. S. (2010). A protocol for data exploration to avoid common statistical problems. *Methods in Ecology and Evolution, 1*(1), 3–14. DOI: 0.1111/j.2041-210X.2009.00001.x

Appendix

Table A.1. Summary of tracer recoveries. dates and recovery rates, as well as mobility (f_m) and mean travel lengths (L) of all tracers. Recoveries used in Chapter 4 for comparison are (a): $F_{mt} \approx 0.05$, (b): $F_{mt} \approx 0.13$, (c): $F_{mt} \approx 0.40$, and (d): $F_{mt} \geq 0.45$. Winter periods are highlighted in grey. **Notes:** *Period between Aug. 25 – Nov. 15, 2015 removed from discharge analysis due to beaver dam. Peak flow verified to correspond to maximum precipitation event. † Flow hydrograph corresponding to maximum precipitation event on May 25, 2017 was not captured due to a malfunctioning pressure transducer. Data from this recovery is excluded from peak flow analyses.

Creek	Recovery ID	Date	Q_p	Recovery (%)	f_m	L (m)
Ganatsekiagon	1	2015-10-26	0.05	100	0	0
	2	2015-11-11[a]	1.6	99.7	0.04	0.89
	3	2016-05-02	3.9	98.7	0.11	1.43
	4	2016-06-17	0.04	100	0.01	1.02
	5	2016-08-18	0.2	100	0	0
	6	2017-04-13	3.2	98.7	0.08	1.57
	7	2017-05-10[b]	4.5	97.3	0.13	2.12
	9	2017-07-05[c]	19.2	86	0.41	8.22
	10	2017-08-02[d]	17.7	88.3	0.45	9.5
	12	2018-05-07	3.3	80	0.14	1.26
Wilket	1	2015-10-20	22.3	94.7	0.67	7.44
	2	2015-11-03	13.5	97.7	0.33	1.84
	3	2016-05-09	10.2	97.7	0.33	1.06
	4	2016-06-07	10.6	95.7	0.12	1.12
	5	2016-08-23[d]	21.5	93	0.48	7.81
	6	2017-04-18	27.6	93.3	0.49	7.01
	7	2017-05-16[a]	8.9	95.3	0.05	1.35
	8	2017-06-20[c]	30.5	95.3	0.39	5.05
	9	2017-06-28	19.4	98.6	0.23	3.07
	10	2017-07-25	30.0	96.9	0.27	3.83
	11	2017-08-09	39.8	98.3	0.28	6.36
	12	2018-05-14[b]	11.0	79.9	0.14	2.96
Morningside	1	2015-10-25	1.7	96.7	0.26	2.46
	2	2015-11-10[d]	3.0	97	0.56	9.74
	3	2016-05-03	1.4	99.7	0.16	1.8
	4	2016-06-22	0.9	99.7	0.03	0.8
	5	2016-08-19	0.9	99.7	0.01	0.78
	6	2017-04-12	1.5	100	0.08	1.38
	7	2017-05-11	1.7	98	0.29	4.09
	8	2017-06-21	0.9	95.3	0.07	1.24
	9	2017-07-04[a]	1.5	99.3	0.06	2.26
	10	2017-07-24	0.6	99.3	0	0.51
	11	2017-09-13	0.8	98.7	0.01	0.77
	12	2018-05-02[c]	1.8	93	0.37	5.32
	13	2018-07-19[b]	1.7	88.7	0.13	1.64

Table A.2. Summary of river characteristics from previous tracking studies used for comparison in Chapter 4.

Source	River	DA (km^2)	Slope	Mean width (m)	$D_{50\text{-surface}}$ (mm)	Tracer Size (mm)
Haschenburger and Church (1998)	Carnation Creek	11	0.012	15	47	16 - 180
Houbrechts et al., (2012)	Aisne	186	0.0047	13.6	92	0.75 - 1.25 D_{50}
	Berwinne	123	0.0044	10	49	
Gintz et al. (1996)	Lienbach	15.6	0.02	10	57.5	30 - 170
Lenzi (2004)	Rio Cordon	5	0.13	5.7	90	40 - 160
Plumb et al. (2017)	Mimico	73.8	0.004	13	48	35 - 230
Schneider et al. (2014)	Erlenbach	0.7	0.17	3.5	64	28 - 100

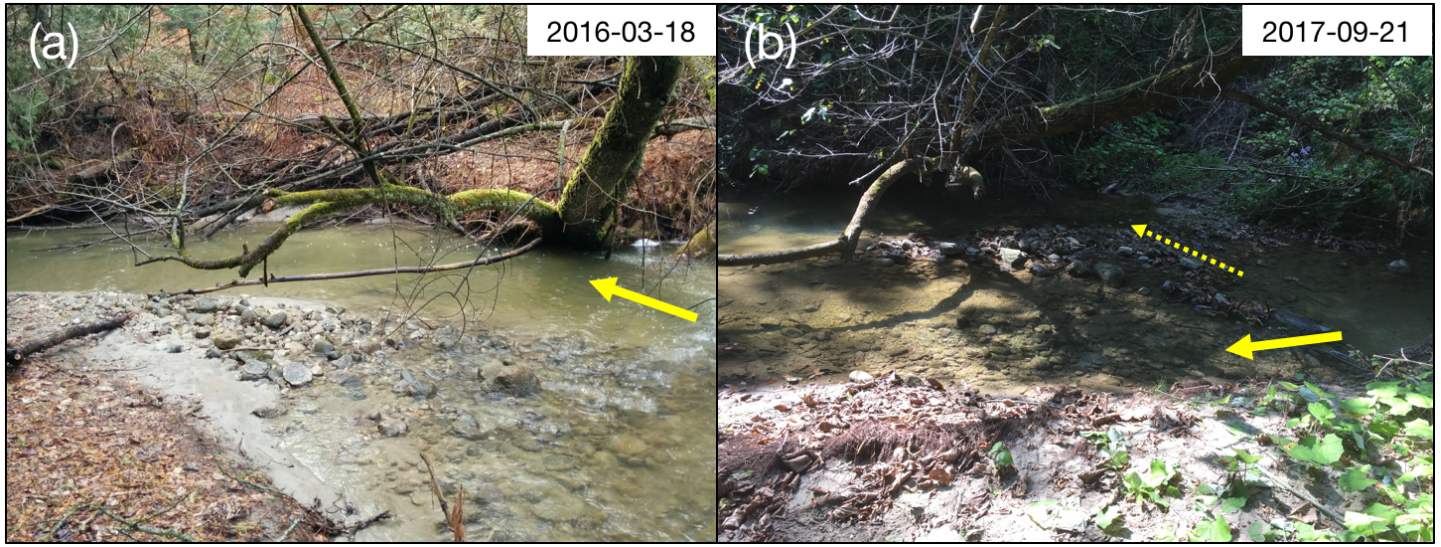

Figure A.1. Photos of the small avulsion at the upstream end of the Ganatsekiagon Creek reach showing the position of the thalweg with yellow arrows (a): before, and (b): after the summer of 2017 floods. Dotted yellow arrow shows direction of thalweg in 2016.

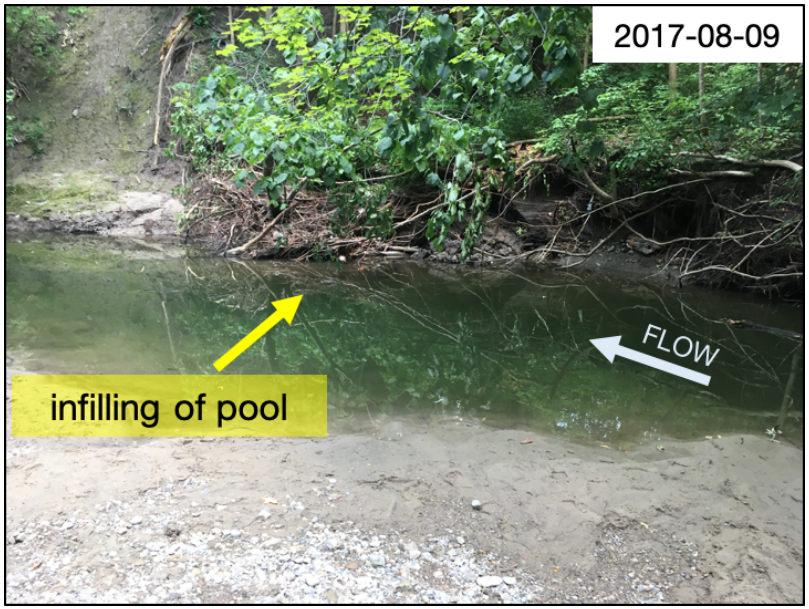

Figure A.2. Photos from Wilket Creek showing infilling of downstream pool upstream of woody debris accumulation.

Table A.3. Summary of strongest regressions used in the multiple linear regression analysis. Best single variable regressions are highlighted in grey.

	Strongest peak metric			Strongest dimensionless peak metric			Strongest cumulative metric		
	Metrics	RSE	R2	Metrics	RSE	R2	Metrics	RSE	R2
Ganatsekaigon									
f_{mi}	Q_p	0.07	0.88	τ_c^*	0.11	0.66	*CI*	0.08	0.81
L_i	τ_p	1.15	0.91	τ_c^*	1.76	0.80	*CI*	1.16	0.91
$\tilde{L}_i$	Q_p	0.59	0.90	τ_c^*	0.78	0.82	*CI*	0.44	0.94
Wilket									
f_{mi}	ω_p	0.11	0.78	τ_c^*	0.16	0.60	*CI*	0.13	0.74
L_i	ω_p	0.75	0.95	τ_c^*	1.34	0.84	*CESP*	1.18	0.88
$\tilde{L}_i$	τ_p	0.67	0.92	τ_c^*	0.82	0.88	*CESP*	0.48	0.96
Morningside									
f_{mi}	Q_p	0.11	0.64	τ_c^*	0.13	0.52	*CI*	0.12	0.58
L_i	τ_p	1.40	0.78	τ_c^*	1.29	0.82	*CI*	1.21	0.84
$\tilde{L}_i$	τ_p	0.66	0.87	τ_c^*	0.51	0.93	*CI*	0.41	0.95
All Together									
f_{mi}	τ_p	0.12	0.65	τ_c^*	0.14	0.53	*CEQ*	0.15	0.48
L_i	τ_p	1.36	0.84	τ_c^*	1.58	0.78	Ω	1.76	0.72
$\tilde{L}_i$	τ_p	0.92	0.78	τ_c^*	0.91	0.78	*CEQ*	0.87	0.80
$\frac{L_i}{B}$	τ_p	0.25	0.61	τ_c^*	0.26	0.58	Ω	0.17	0.82
$\frac{\tilde{L}_i}{B}$	τ_p	0.15	0.60	τ_c^*	0.15	0.61	*CEQ*	0.06	0.93

Table A.4. Summary of tracer stone recoveries in the restored and un-restored reaches of Wilket Creek. Gauging of the un-restored reach began on 2015-08-08.

			Un-Restored				Restored			
Tracer Wave	Date	Max Q (m^3/s)	Max τ	Recovery (%)	f_m	L(m)	Max τ	Recovery (%)	f_m	L(m)
1	2013-11-14	7.72		95.8	0.50	3.20	77.66	100.0	0.05	2.71
	2013-12-06	12.39		94.4	0.20	2.31	91.15	95	0.19	3.45
	2014-05-22	10.50		88.1	0.30	3.07	86.28	87.0	0.09	3.10
	2014-07-25	19.50		92.3	0.45	3.42	105.39	88.3	0.30	9.92
	2014-08-21	17.81		91.3	0.21	11.89	102.43	91.5	0.14	8.50
	2015-06-02	15.78		83.2	0.46	7.55	98.58	80.7	0.11	3.36
	2015-07-09	26.92		83.5	0.33	15.81	116.35	86.2	0.14	10.93
	2015-10-20	17.07	77.15	83.1	0.21	11.03	101.08	81.8	0.10	5.42
	2015-11-03	14.66	57.55	85.2	0.04	6.58	96.28	82.0	0.06	3.54
	2016-05-09	10.33	49.05	81.1	0.04	5.46	85.80	72.2	0.05	3.59
2	2015-10-20	17.07	77.15	94.7	0.67	7.44	101.08	95.0	0.47	4.96
	2015-11-03	14.66	57.55	97.7	0.33	1.84	96.28	99.0	0.12	2.43
	2016-05-09	10.33	49.05	97.7	0.11	1.06	85.80	99.7	0.07	1.37
	2016-06-07	11.29	50.15	95.7	0.12	1.12	88.39	96.3	0.05	0.71
	2016-08-23	20.30	75.25	93	0.48	7.81	106.72	82.9	0.13	2.55
	2017-04-18	20.44	86.25	93.3	0.49	7.01	106.96	92.3	0.26	4.52
	2017-05-16	8.33	44.95	95.3	0.05	1.35	79.71	95.0	0.10	1.11
	2017-06-20	21.40	91.85	95.3	0.39	5.05	108.48	95.1	0.29	4.48
	2017-06-28	22.85	71.35	98.6	0.23	3.07	110.69	96.8	0.15	6.11
	2017-07-25	34.72	90.95	96.9	0.27	3.83	125.55	89.0	0.20	3.76
	2017-08-09	41.08	98.15	98.3	0.28	6.37	131.87	93.5	0.53	2.81
	2018-05-14	13.45	51.05	79.9	0.14	2.96	93.63	73.6	0.09	1.45

Table A.5. Description and survey dates of cross sections.

Cross-Section	Location	Number of Surveys	Survey Dates
1	Beginning of restoration; pool	4	(2013-02-01) (2013-07-25) (2016-07-20) (2017-10-20)
2	End of riffle	5	(2013-02-01) (2013-07-25) (2014-07-15) (2016-07-20) (2017-10-02)
3	Under foot bridge; middle of pool	5	(2013-02-01) (2013-07-25) (2014-07-15) (2016-07-20) (2017-10-02)
4	Middle of riffle	3	(2013-02-01) (2016-07-20) (2017-10-20)
5	Start of pool	6	(2013-02-01) (2013-07-25) (2014-07-15) (2016-07-20) (2017-10-02) (2018-07-11)
6	Middle of pool	6	(2013-02-01) (2013-07-25) (2014-07-15) (2016-07-20) (2017-10-02) (2018-07-11)
7	End of pool	6	(2013-02-01) (2013-07-25) (2014-07-15) (2016-07-20) (2017-10-02) (2018-07-11)
8	Middle of riffle	4	(2013-02-01) (2013-07-25) (2014-07-15) (2017-10-02)
9	Middle of pool	6	(2013-02-01) (2013-07-25) (2014-07-15) (2016-07-20) (2017-10-02) (2018-07-11)
10	Start of riffle	5	(2013-02-01) (2013-07-25) (2014-07-15) (2017-10-02) (2018-07-11)
11	Start of pool	6	(2013-02-01) (2013-07-25) (2014-07-15) (2016-07-20) (2017-10-02) (2018-07-11)
12	Middle of pool	6	(2013-02-01) (2013-07-25) (2014-07-15) (2016-07-20) (2017-10-02) (2018-07-11)
13	End of pool	6	(2013-02-01) (2013-07-25) (2014-07-15) (2016-07-20) (2017-10-02) (2018-07-11)
14	End of riffle	6	(2013-02-01) (2013-07-25) (2014-07-15) (2016-07-20) (2017-10-02) (2018-07-11)
15	End of riffle	5	(2013-02-01) (2013-07-25) (2014-07-15) (2016-07-20) (2017-10-02)
16	Middle of pool	5	(2013-02-01) (2013-07-25) (2014-07-15) (2016-07-20) (2017-10-02)
17	End of pool	5	(2013-02-01) (2013-07-25) (2014-07-15) (2016-07-20) (2017-10-02)
18	End of restoration; end of riffle	5	(2013-02-01) (2013-07-25) (2014-07-15) (2016-07-20) (2017-10-02)
19	Downstream of restoration; pool	5	(2013-02-01) (2013-07-25) (2014-07-15) (2016-07-20) (2017-10-02)